THE HONG KONG POLYTECHNIC UNIVERSITY

INSTITUTE OF TEXTILES AND CLOTHING

BREAST SIZING AND DEVELOPMENT OF 3D SEAMLESS BRA

ZHENG RONG

A thesis submitted in partial fulfillment of the requirements for the Degree of Doctor of Philosophy

December 2006

CERTIFICATE OF ORIGINALITY

I hereby declare that this thesis is my own work and that, to the best of my knowledge and belief, it reproduces no material previously published or written, nor material that has been accepted for the award of any other degree or diploma, except where due acknowledgement has been made in the text.

____________________ (Signed)

ZHENG Rong (Name of student)

DEDICATION

This thesis is dedicated to my family

for their love, encouragement, and support

ABSTRACT

In intimate apparel, sizing and fit are two most important issues. The current bra sizing system has been based on bust girth and underbust girth and was developed in 1935. However, the woman's breast is a very complex 3D geometry; the existing sizing system is inappropriate to categorize breast sizes, and thus it is difficult for women to find their correct bra size. One of the purposes of this project is to develop a new bra sizing system to fit Chinese women’s breast shapes and sizes.

Based on the 3D nude breast measurements of 456 Chinese women subjects aged between 20 and 39, an improved bra sizing system was developed through principal components factor analysis and K-means cluster analysis of the data. The new system uses “underbust girth” and “breast depth width ratio” as the classifying parameters, which were identified as the two most critical parameters out of 103 measurements.

The new bra sizing system was compared with the existing bra system in terms of accommodation (coverage) rate, efficiency of classifying the breast shape, and fit performance for the covered individuals. The study showed that, although both deploy two classifying parameters, the new bra sizing system is more efficient. It covers 97.4% of the population, provides better fit to the accommodated individuals, while maintaining a clear structure and keeping the same number of size categories.

Another objective of the project is to develop seamless knitted bras with improved fitting. Based on the understanding of the breast dimensions and shapes, seamless knitted bras

were developed with proper underband tension and sufficient cup strain. The key knitting parameters, including loop density, elastic yarn tension, cover yarn tension and Nylon yarn tension were investigated using factorial experimental design. It was found that the underband tension is mainly affected by the loop density and elastic yarn tension, whereas the most important factor affecting the cup strain is the loop density. Empirical prediction equations are also established for specific experimental conditions.

To hold the breast shape in a natural manner, a soft 3D supporting wire prototype was designed based on the average shape of breast root of the 49 women subjects sized 75B* in the new bra sizing system.

Seamless knitting is becoming popular, but existing seamless knitted bras have many problems. Therefore, we made three new seamless bra styles. Fifteen test bra samples of these 3 styles were developed using two key knitting parameters – loop density and elastic yarn tension. To test the fitting performances of the newly developed seamless knitted bras and four commercial bras (2 cut and sewn and 2 seamless knitted bras), evaluations were made of objective pressure, subjective comfort & pressure sensation and 3D breast shape on six subjects with a bra size of 75B*. The results indicated that the 3D supporting wires could provide definite support to the breasts and improve the breast vertical-sectional profiles, especially for those seamless knitted bras which have relatively larger value of loop density. Empirical equations were established to predict two pressure points at the apex and at the side of the bottomband.

The research results add to our knowledge base for the development of bra sizing systems and its application to seamless knitted bra development.

PUBLICATIONS ARISING FROM THIS THESIS

REFEREED JOURNAL ARTICLE

1. **Zheng, R**., Yu, W., & Fan, J. (2007). Development of a new Chinese bra sizing system based on breast anthropometric measurements. *International Journal of Industrial Ergonomics*, **37**, 697-705.

BOOK CHAPTERS IN RESEARCH MONOGRAPHY

1. **Zheng, R.**, Yu, W., & Fan, J. (2006). Breast measurement and sizing, Chapter 2. In W. Yu, J. Fan, S. C. Harlock & S. P. Ng (Eds.), *Innovation and Technology of Women's Intimate Apparel*. Boca Raton, Fla: CRC press; Cambridge: Woodhead Publishing. ISBN-13: 978-1-84569-046-5; ISBN-10: 1-84569-046-X.
2. Lim, N. Y., **Zheng, R.**, Yu, W., & Fan, J. (2006). Assessment of women's body beauty, Chapter 1. In W. Yu, J. Fan, S. C. Harlock & S. P. Ng (Eds.), *Innovation and Technology of Women's Intimate Apparel*. Boca Raton, Fla: CRC press; Cambridge: Woodhead Publishing. ISBN-13: 978-1-84569-046-5; ISBN-10: 1-84569-046-X.
3. Yu, W., Ng, S. P., **Zheng, R.**, & Yip, J. (2006). Process innovations of seamless intimate apparel, Chapter 10. In W. Yu, J. Fan, S. C. Harlock & S. P. Ng (Eds.), *Innovation and Technology of Women's Intimate Apparel*. Boca Raton, Fla: CRC press; Cambridge: Woodhead Publishing. ISBN-13: 978-1-84569-046-5; ISBN-10: 1-84569-046-X.

CONFERENCES

1. **Zheng, R.**, Yu, W. & Fan, J. (2006). Development of a new bra sizing system. In *Proceedings of the International Fiber Conference 2006*, (pp. 477-478).
2. **Zheng, R.**, Yu, W. & Fan, J. (2006). Prediction of underband tension of seamless knitted bra from loop density and yarn tension. In *Proceedings of the International Fiber Conference 2006*, (pp. 727-728).

PATENT

1. Yu, W., Fan, J., & **Zheng, R.**, Underwire assembly for brassiere, brassiere using the same, and process for producing and wearing the brassiere, US patent application number 11/452,424.

SUBMISSIONS TO REFEREED JOURNALS

1. **Rong Zheng**, Winnie Yu & Jintu Fan, Prediction of stretch tension for 3D seamless knitted bras, Fiber and Polymers. [Submitted in May 2007]
2. **Rong Zheng**, Winnie Yu & Jintu Fan, Pressure Evaluation of 3D Seamless Knitted Bras and Conventional Wired Bras, Fiber and Polymers. [Submitted in May 2007]

ACKNOWLEDGEMENTS

I would like to express special gratitude to my Chief supervisor, Dr. Winnie Yu, Associate Professor of the Institute of Textiles & Clothing, The Hong Kong Polytechnic University, for her professional guidance, valuable academic advice and strong support throughout the whole research period and the writing of this thesis.

I would also like to forward the deepest gratitude to my Co-supervisor, Prof. Jintu Fan, Professor of the Institute of Textiles & Clothing, The Hong Kong Polytechnic University, for his invaluable guidance, expert suggestions and timely support in the whole project and writing the thesis.

I wish to appreciate the funding support from the ITF project account ITS/028/03 "Development of innovative apparel products and evaluation technology". I also acknowledge the 3D body scanning data provided by AIMER HEC-BICT (Aimer Human Engineering Research Centre of the Beijing Institute of Clothing Technology), and thank to those female subjects.

I am full of gratitude to Dr. G. A. V. Leaf, formerly reader of the Department of Textile Industries, The University of Leeds, for his academic comments and valuable advice. I am also grateful to Dr. Simon Harlock, the Textile and Apparel Development Manager of Media Innovation Ltd., for his valuable suggestion on the seamless knitted bra development.

I acknowledge the technical support from the Chemtax Industrial Co., LTD., Hong Kong and material support from the ACE Style Group. Specially, I am grateful to Mr. Stone Tsang, Chief Service Engineer of Chemtax Industrial Co., LTD.; Dr. Jimmy Lam, Lecturer and Mr. Jinyun Zhou, Scientific Officer of the Institute of Textiles & Clothing, The Hong Kong Polytechnic University; Mr. Ivan Tang, Mr. Yiu Choi Lee, and Mr. Tak wai Zheung, in the Chemtax Industrial Co., LTD., for their valuable advice and kindly assistance on the development of seamless knitted bras.

I would express my sincere thanks to my old friends, Jackie, Seabridge, Juana, Jean Xiaodai, in AIMER HEC-BICT, for their friendship and kind assistance. I also appreciate Prof. Ping Zhao, Professor of the Beijing Institute of Clothing Technology, and Mr. Rongming Zhang, the president of the Aimer Intimate Apparel Group for their warm encouragement and support.

I would like to thank all my team members of ITS/028/03 project, for their strong assistance and support. I also thank my roommates in X105 for their friendship and kind support.

Importantly, I would like to give special recognition to my husband, Hao, and my daughter, Ruoxi, for their constant love, understanding, support and patience. I also wish to express my deepest gratitude to my parents and Hao's parents, for their constant understanding and support.

This study could not have been completed without the assistance and support of every one of these special people.

TABLE OF CONTENTS

CHAPTER 2 LITERATURE REVIEW

CHAPTER 4 DEVELOPMENT OF A NEW BRA SIZING SYSTEM

CHAPTER 5 FUNDAMENTAL EXPERIMENT FOR SEAMLESS BRA DESIGN

CHAPTER 6 DEVELOPMENT OF A 3D SOFT SUPPORTING WIRE

CHAPTER 7 SEAMLESS KNITTED BRA DEVELOPMENT AND FITTING EVALUATION

CHAPTER 8 CONCLUSIONS AND RECOMMENDATIONS

LIST OF FIGURES

LIST OF TABLES

CHAPTER 1

INTRODUCTION

1.1 Background

Sizing systems present a range of sizes designed to fit subgroups of the population, based on demographic anthropometric data (Winks, 1997; Ashdown, 2003). In the apparel industry, various studies on body shape have been conducted to establish standards for clothing design (Armstrong, 1987). However, very limited research has been carried out to explore the breast shape in the intimate apparel industry. Conventionally, breast sizing has been classified using only two measurements of bust girth and underbust girth since 1935. A more scientific method to identify the 3D shape and dimensions of women's breasts is necessary.

Victoria's Secret stated (Williamson, 2000) that seamless underwear was a fast growing sector that would affect the normal intimate apparel business. A special report written by CIRFS (Comité International de la Rayonne et des Fibres Synthétiques) also revealed that the seamless garment knitting technology on circular knitting machines would change the bodywear industry significantly during the first decade of the 21st century (Morris, 2003).

The capabilities of the latest seamless circular knitting technology have given designers the opportunities to develop innovative seamless knitted bras, in creative colors, jacquard patterns, surface dimensions and new styles (Powell, 2003). They have no seams to cause irritation, so are as comfortable as a second skin, and give a clean and smooth look under tight fitting garments. There are several reasons why a customer chooses to purchase seamless garments. They include: (1) individualized fit to each consumer, (2) invisibility and comfort, (3) natural softness, and (4) a smooth, streamlined and sleek shape (Cajah web, 2005).

Although the seamless knitted bra, as one important type of seamless garments, has good growth prospects in the intimate apparel market, a number of existing problems limit its development.

1) The sizing chart for seamless knitted bras, developed from the general bra sizing system, makes it difficult for customers to find their correct sizes in the commercial market. The existing sizing system does not accommodate the actual shape of the breast (Morris et al., 2002).
2) The women’s breasts tend to be compressed when wearing seamless bras due to the lack of extensibility or lack of flexibility of cup strain.
3) The existing styles of seamless knitted bras cannot provide sufficient cup volume for full-figures of D cup sizes or larger. Furthermore, insufficient cup volume and lack of extensibility of a seamless bra cause a large gore gap between a wearer and the garment.
4) The commercial seamless knitted bras are generally designed from a fashion perspective rather than to provide functional support to the breast. Even though different knitting structures have been used to improve the support of the existing

seamless bras, these provide less support to the breasts than those designed with the traditional underwire.

5) Developing a new bra using a seamless knitting system is a complex time consuming process due to lack of understanding of how the yarn properties and fabric physical performance affect the breast shape and the bra fitting effect.

1.2 Objectives and Scope of Current Study

The overall aim of the current research is to develop a new bra sizing system to accommodate the full range of Chinese women's breast shapes and sizes, and to develop seamless knitted bras with a 3D support wire to improve comfort and provide natural support.

Specific objectives are:

1) To examine the validity of the existing bra sizing system and propose methods to develop a new one.
2) To investigate the effects of knitting factors, such as loop density and yarn tension, on the size and fit of seamless knitted bra designs.
3) To develop a 3D soft underwire prototype that provides natural and comfortable support to the breast shape.
4) To evaluate the fitting performance of the newly developed seamless bras.

1.3 Research Methodology

In order to achieve the objectives of this study, the following research methodologies were performed:

1.3.1 Breast Data Collection by 3D Body Scanning and Manual Measurement

The sample used in this study consisted of 456 Chinese female subjects aged between 20 and 39. The distribution of their height, weight, bust girth and underbust girth is representative of the sample used to create the existing bra sizing system. Their basic breast dimensions were collected using the VOXELAN 3D laser body scanner and Martin’s anthropometer. To accurately describe the breast shape, five manual measurements were taken, and additionally ninety-eight 3D body scan measurements were obtained from 3D body scan data using the measurement software 3D-Rugle, Shapeline-3D and Rapidform. Measurements taken included circumference, height, width, thickness, angle, surface distance, volume and curvature, which were extracted from the cross-section, side view profile, vertical-section, breast bottom curve and the whole body.

Descriptive statistics and One-way ANOVA were employed in the data analysis.

1.3.2 Evaluation of the Existing Bra Sizing System

The accommodation (coverage) rate of the existing bra sizing system was evaluated using probability density. For the 75B subgroups classified by the existing bra sizing system, “distance measure” was used to investigate the difference between individual’s “bust-underbust” shape.

1.3.3 Multivariate Analysis for Developing a New Bra Sizing System

Principal components factor analysis was used to identify the significant parameters to be included in the new sizing system that was established by using layered k-means cluster analysis. The efficiency of the new bra sizing system was evaluated based on the dissimilarity measures of the factor scores and the aggregate fit loss function (McCulloch et al., 1998; Ashdown, 1998) between the existing system and the new one.

1.3.4 Factorial Design of the Experiment for Identifying Key Knitting Parameters

The development of a 3D seamless knitted bra is an application study based on the new bra sizing system. In order to investigate the relationships among the fabric strength, loop density and yarn tension, factorial designs were used to conduct experiments on knitting seamless underbands and cups. A SANTONI 14 inches SM8-Top2 circular machine was used. Yarns of Nylon 78/68/1, 20 core 20/10/1 cover Lycra and 210D bare Lycra were employed. MINITAB Statistical Software was used to analyze the experimental data, and the key knitting parameters were identified for the development of seamless knitted bras.

1.3.5 3D Soft Underwire Development Based on Determination of the Breast Root

A 3D soft supporting underwire prototype for a medium breast size of the new bra sizing system was developed, based on the curvature of the breast root. The 3D coordinates of 14 key points along the breast root were connected to build a structure to support the breasts. With the aim of providing natural shape and comfortable support, Stereolithography (SLA) was used to produce the prototype fabrication. Finally, the 3D soft supporting wire was created using polyurethane (PU) in the shape of the prototype to enhance surface quality and material performance.

1.3.6 Seamless Knitted Bra Development and Fitting Evaluation

Using the results of the study of the relationships between the body parameters and knitting parameters investigated above, three new styles of seamless knitted bras were designed and developed. The new products were evaluated objectively and subjectively by comparing them with selected conventional bras and commercial seamless bras. For this comparative study, pressure magnitude measurements and evaluation of the fitting effect were conducted on medium breast size human subjects. The best match between breast shape parameters and seamless knitting parameters for seamless knitted bra design was developed.

1.4 Significance of the Study

This study is significant in the following respects:

1) The existing bra (breast) sizing system was designed more than 70 years ago. It was developed based on the size of the underbust girth and the difference between the bust girth and underbust girth. Obviously, these two factors alone cannot portray the 3D shapes of the breasts completely. Significant key parameters, identified for closely fitted ladies' wear using principal component factor analysis, are useful for a

better understanding of the breast. This is the first time that a bra sizing system has been proposed based on 3D breast characteristics. Apart from its application in the intimate apparel industry, the new breast (bra) sizing system can be applied in the Chinese medical field to identify the breast size and shape for use in breast reduction and enlargement procedures.

2) Many knitting factors influence the seamless knitted bra design. However, it is not clear which factors are the major parameters related to the breast shapes. This study improves our knowledge of the relationships between the body shape and knitting parameters, and develops knitting equations for predicting the underband tension and cup strain based on common commercial yarns.
3) Existing seamless knitted bras provide limited support to the breasts. A new 3D soft supporting underwire prototype is a novel approach to characterize the breast root and support individual customer's breasts in a natural shape. This will be a breakthrough technology that can enhance the performance of the traditional 2D underwire, especially for seamless knitted bras.
4) This study improves our understanding of how to evaluate the fit of seamless knitted bras, and provides guidelines for seamless knitted bra design and production development.

1.5 Outlines of the thesis

The research study is presented in eight chapters. Chapter 1, Introduction, describes the research purposes as well as the general research background. The significance of the study is stated with specific objectives and research methodology.

Chapter 2, Literature review, emphasizes the past research work relevant to the current study. The breast structure & technologies for breast measurements, breast shape analyses, breasts sizing system & fit issues, and development of circular seamless knitted bras are reviewed. Also the research gaps in the areas are described.

Chapter 3, Acquisition of 3D breast anthropometric data, describes the sampling method in the current study, which is comparable to the random sample size of 5507 subjects used for establishing the existing Chinese bra sizing system. 3D breast data collection procedures, data analysis & results are also presented.

Chapter 4, Development of a new bra sizing system, reports the research approaches, methods and results relevant to building a new bra sizing system for Chinese women based on 3D breast anthropometric data. The efficiency comparisons of the new bra sizing system and the existing bra sizing system are also portrayed.

Chapter 5, Fundamental experiment for seamless bra design, reports the methods and results of the seamless knitting experiments based on the findings of the new bra sizing system.

Chapter 6, Development of a 3D soft supporting wire, describes the development of a 3D soft supporting underwire that is used in seamless knitted bras to provide natural support.

Chapter 7, Seamless knitted bra development and fitting evaluation, presents experiments to develop new styles of seamless knitted bras, and their fitting evaluations are compared with the commercial bras.

Chapter 8, Conclusions and recommendations, provides a general summary of the whole project, including the limitations of the research and recommendations for future work.

Appendices present detailed results of the data analysis relevant to the principle factor analysis in chapter 4, and a series of questionnaires related to the bra fitting evaluation in chapter 7.

CHAPTER 2

LITERATURE REVIEW

2.1 Introduction

The current study is focused on building relationships among seamless knitted bra design, breast shape classification and knitted bra fitting. Therefore, the review of literature in this chapter presents the publications in this area or studies relevant to this research. It consists of the following four sections: (1) Breast structure and technologies for breast measurements, (2) Breast shape analysis, (3) Breast sizing systems and fit issues, (4) Development of circular seamless knitted bras.

2.2 Breast Structure and Technologies for Breast Measurements

The technical understanding of intimate apparel requires in-depth knowledge of breast structure, human anthropometry and sizing. To achieve accurate fit of second-skin intimate apparel, in particular bras, detailed body measurements are necessary to define the body shape, curve profile and dimensions of the torso, especially for the breast region.

In order to obtain accurate measurements for the body and the breasts, it is important to control the human subject’s posture, clothing and to correctly choose and identify body landmarks, as well as carefully selecting the measuring devices and relevant measurement items.

2.2.1 Breast Structure of Female Adult

The female adult's breasts are situated on the chest wall between the 2nd and 6th intercostal cartilage in the vertical plane. The breasts cover the area from the mid-axillary line to the sternum and overlay the anterior serratus and pectoralis major muscles. As shown in Figure 2.1, the breast's posterior boundary is marked by the deep layer of the fascia, whereas its anterior boundary is marked by the superficial portion of the fascia (Lawrence, 1980).

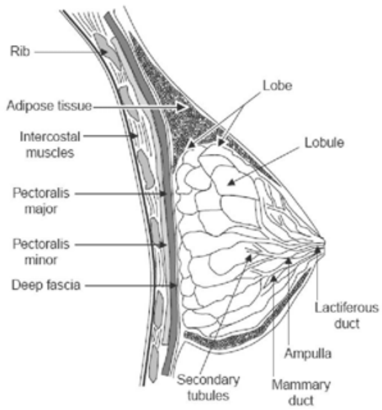

Figure 2.1 Structure of the female adult's breast from a sagittal section (Page & Steele, 1999)

There are three major structural components within a female's breasts: the skin, the subcutaneous tissue and the corpus mammae (Lawrence, 1980). Corpus mammae is the functional section of the breast which can be further broken down into 2 subcomponents: the parenchyma and the stroma. The parenchyma consists of ductular, lobular and alveolar structures, whereas the stroma is composed of connective tissue, lymphatics, fat tissue, blood vessels and nerves (Read, 1993). Since the breasts have no muscle tissue to provide support, the ligaments and fibrous tissues became internal anatomical support for the breast (Gehlsen & Stoner, 1987).

According to the previous studies, we know that the breasts are supported mainly by the skin, ligaments and tissues (Page & Steele, 1999), contain no muscle except in the nipple area (Costantakos & Watkins, 1982), and are approximately composed with two-thirds of breast tissue, one-third of superficial fascia (fat) tissue (Starr et al., 2005). Due to the lack of intrinsic structural breast support, the breasts require some external support, such as a bra that can hold the breasts and reduce their movements.

Every woman's breast size and shape is unique. It has been reported that most the majority of western women's breasts measure 10 to 12cm in diameter and 5 to 7cm in a central thickness. It has also been stated that each adult female breast contains 90% water and weighs approximately 200g. Differences in breast size and shape can probably be attributed to the variations in the amount of adipose tissue in the breast. The breast's size is also affected by hormonal changes associated with other factors including menstruation, pregnancy, oral contraceptives and the menopause (Lawrence, 1980).

Since breast shape and size varies among individuals, it is important to measure the breast dimensions in detail and define representative measurements of the population for further bra design.

2.2.2 General Control of Body Measurements

2.2.2.1 Measuring Posture and Measuring Clothing

The accuracy of body measurements is affected by the clothing worn by the human subject, her breathing and posture. The international standard of body dimensions, ISO 8559 (1989), suggests measuring over a well-fit unpadded and thin brassiere with minimum accessories and support. ISO 7250 (1996) specifies body measuring procedures based on a nude subject who is wearing minimal clothing and no shoes, standing fully erect with feet together, head in the Frankfurt plane[1] and shoulders relaxed with arms hanging freely during the standing position measurements. ISO/DIS 20685 (2004) recommends three standing positions for various 3D body scanners to obtain reliable data. It was suggested that during 3D body scanning, measurements should be taken during the subject’s quiet respiration; the shoulders should be straight, being natural with relaxed muscles.

2.2.2.2 Body Landmarks

In the collection of anthropometric data, the identification of body landmarks is the first key step to prevent operational errors in handling the measuring device and determination of the body position. By definition, a body landmark is an anatomical feature used as a point of reference to locate body features for measurements (Merriam-Webster Online Dictionary, 2005). International Standards only identify the common anthropometric measurement points and lines for the sizing of general clothing, but more detailed points and lines are needed for meaningful measurements of the breast size and shape.

45- 13

[1] Standard horizontal plane at the level of the upper edge of the opening of the external auditory meatus (external ear opening) and the lower border of the orbital margin (lower edge of the eye socket), when the median plane of the head is held vertically (ISO 7250, 2.2.8).

Before taking actual manual breast measurements, all the anthropometric measurement points should be marked on the skin with a non-smearing pencil (O'Brien & Shelton, 1941) or skin-safe washable ink (Roebuck, 1995). Furthermore, for 3D scanning purposes it is recommended that special raised stickers (Robinette & Daanen, 2003) be used to mark the key landmark locations on the subject to ensure that the measuring points can be found. In the application of 3D body scanners, it is also important to establish landmarks so that the data automatically obtained and calculated can be widely understood and used by various industries. Simmons and Istook (2003) compared the common body-scanners [TC][2], Cyberware, and SYMCAD with traditional manual anthropometric methods. They found that measuring techniques varied among the different scanners. It was impossible to use the current standards to determine the optional measuring process in 3D scanning. Using such non-contact methods, absolute identification of landmarks could not be achieved well automatically.

In the CAESAR anthropometric survey, Robinette and Daanen (2003) found that the automatic landmarking methods for 3D body scanners did not work consistently enough on all body types. Even when using neural networks or other automated recognition packages to identify the landmark location of the stickers, the success rate was only 70% of the measurements. The authors considered that manual intervention for validation and verification of the landmark locations on all subjects was still required.

Tailors and researchers normally use tape measures to record the body circumference at a specific body height. In order to ensure data accuracy, Miyoshi (1970) developed a sliding gauge method to draw women's cross-sections based on the determined measurement points. Using a similar concept but much simpler mechanical design, Yu et al. (Zheng, Yu & Fan, 2006) have developed a laser device to determine four body points respectively at the four body directions of front, back, left and right on the skin, exactly at the same height level.

2.2.3 Traditional Measurements: Manual Measurements

Measuring a breast using manual methods can be very embarrassing (Westreich, 1997) and difficult to ensure accuracy although there is a good set of measuring tools for this purpose called the Martin measurement tools (Martin, 1957). Figure 2.2 shows typical Martin style measuring tools. Even though measurers are usually trained to reliably measure subjects for a study, the manual measurement process is still very difficult to perform and time consuming (Simmons, 2001). For example, in a 1988 anthropometric survey of US Army personnel, four hours were required to physically landmark, measure, and record the data for one subject (Paquette, 1996).

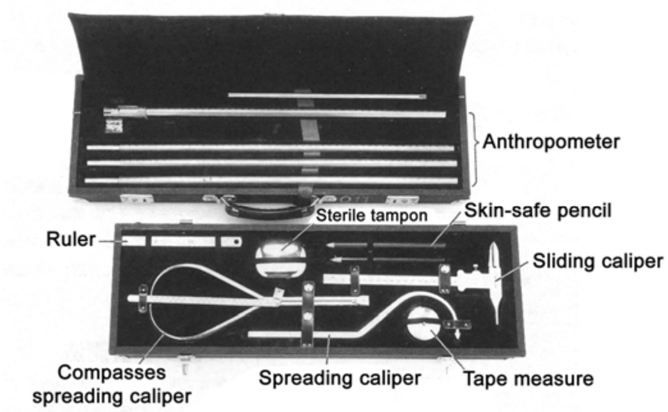

Figure 2.2 The Martin measurement tools (Miyoshi, 2001)

Before the development of 2D and 3D measurement methods, researchers in the apparel industry and in the medical field analyzed the dimensions of the female breast exhaustively using manual measurements. In order to establish a standard of aesthetically perfect breasts for breast reduction, Penn (1955) measured the breasts of 150 healthy volunteers in a standing position using 12 measurements, and selected 20 subjects as being aesthetically perfect. Penn stated that the triangle between the clavicular point and the two nipple points, and the distance from the mid-clavicular point to the nipple point were key measurements for breast assessment.

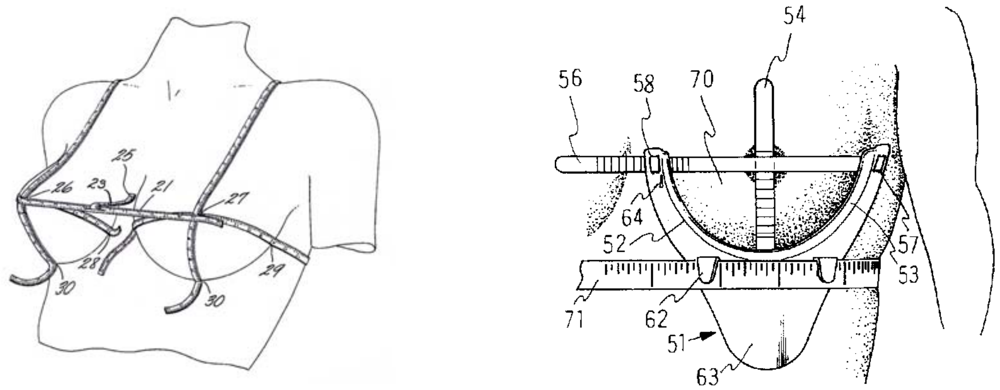

(a) The measuring device invented by Gittelson (1960)

(b) The measuring device invented by Shiraiwa (1994)

Figure 2.3 The breasts measuring devices

In order to determine the breast cup size accurately, Van Graf (1949, 1953) and Kirianoff (1975) developed devices that could be placed around the breasts similar to the conventional bra. For the purpose of obtaining accurate sizes and shapes of breasts, Gittelson (1960) invented a multi-planar tape measure consist of a flexible bust band having a calibrated free end section in the front portion, and two shoulder bands located from the back to the bust point and passing through the breasts to their base (see Figure

2.3 (a)). Ellenbogen (1978) also described a method for breast cup size judgment by using a commercial bra sizer. Later, Shiraiwa and Kusakabe (1994, 1996) invented a breast measuring device (see Figure 2.3 (b)), which could measure underbust girth and the breast circumference in detail.

Manual measurement has been used in national sizing surveys as an indicator of body dimension and health status (Marks et al., 1989) for many years.

Throughout the development of anthropometric technology, assessment of data reliability has been a big topic of research (Martorell et al., 1975; Bray et al., 1978; Foster et al., 1980; Kouchi et al., 1996). Mueller and Martorell (1988) defined the reliability of measurement data by defining two components, precision and dependability, and emphasized that precision was the most important factor. Gordon and Bradtmiller (1992) also mentioned that observer error was the most troublesome source of manual measurement error, and included imprecision in landmark location, subject position, and instrument application. Although the observers were trained by the same individual (Jamison & Zegura, 1974; Utermohle & Zegura, 1982; Utermohle et al., 1983; Bennett & Osborne, 1986), and error limits were usually monitored in the process of data collection (Johnston & Martorell, 1988; Himes, 1989), observer errors in anthropometry were not random and not unusual (Bennett & Osborne, 1986; Gordon & Bradtmiller, 1992). Therefore, various non-contact methods based on 2D photo silhouette imaging and 3D body scanning have been developed which provide more reliable data (Miyoshi, 2001).

2.2.4 2D Measurements

To compensate for the complicated and time-consuming body measurements, especially in the torso region, Miyoshi et al. have reported the use of a horizontal sliding gauge and a vertical sliding gauge to obtain 2D profiles of cross-sections and vertical-sections of a woman's body (Miyoshi & Nakahon, 1983).

Douty (1968) developed a graphic somatometry (*soma* means body and *metry* means measurements) method to measure the body visually in 1963. She photographed bodies of subjects in back and side views on a grid to study body shape and posture. Later, many researchers have used this method to study bodies and their relationships to clothing. Brinson (1977) evaluated the body characteristics of posture, general mass, proportion, contour, balance and symmetry of similar body parts by using angle measurements. Farrell-Beck and Pouliot (1983) also added body angles and body proportions mathematically, in addition to body length and circumference measurements.

Using optical methods, Makabe (1977) and Nakai et al. (1976) employed 2D photo silhouette imaging using a camera or silhouette analyzer to classify the posture and the figure of adult women in Japan.

Gazzuolo et al. (1992) further proposed a photographic method using video capture and automated measurement of frontal and lateral view photographs, which they claimed was useful in determining pattern dimensions for the upper torso of the female body form.

For commercial purposes, Wacoal designed a 2D profile analyzer based on the use of a television camera in 1984 (Wacoal Crop, 1995; Fontanel, 1997). This system was used in Wacoal's monopolistic shop so that the customer could see her front and side profiles on the screen and understood how different underwear would correct her anatomical profile.

Fan and Yu's research team has developed a system for individual users to assess their body beauty between the nude body and the clothed body (Zheng, Yu & Fan, 2006). This system captured two body images of a female from the front and side views, retrieved the silhouettes, and determined body beauty with reference to the beauty parameters such as the angle of the breast and the smoothness of the body side view profile.

Using a CCD camera, Zheng's team (2004) has also developed an automatic 2D shape anthropometric system. It measured the body shape angles, height, width and thickness from 2D photo imaging, and compared the whole body shape from different silhouettes, especially the breasts and upper torso. According to the 2D photogrammetry system of AIMER HEC-BICT, there are at least 11 data items of breast detail measurements that can be obtained from the side view silhouette of the body.

2.2.5 3D Body Scanning Measurements

In traditional manual measurements, the subject is no longer available after finishing her/ his measuring process (Paquette, 1996). However, once the subject is scanned by a 3D body scanner, her/his 3D data and image can be effectively further used for body measurements and virtual try-on of garments. Since 3D body scanning technology was introduced to the apparel industry in the early 1990s, it has made significant contributions to several sizing surveys (Devarajan & Istook, 2004) including Size Japan (1992-1994), CAESAR (1997-2001), SizeUK (2000-2001), SizeUSA (2002-2003), and Lands End (2000).

Several studies have been conducted concerning 3D body scanning technology. Istook and Hwang (2000), and Yu (2004) reviewed all the 3D body scanning systems generally available in the apparel industry and explained the underlying principles that allow these systems to work. By comparing the specifications of each system, Istook and Hwang (2000) also provided some direction in the integration of these systems with current apparel CAD pattern design or pattern generation technologies for further research. McKinnon and Istook (2001) conducted a comparative study between $[TC]^2$ scanner models 2T4 and 3T6. Simmons and Istook (2003) compared 3D body scanning and anthropometric methods for apparel application based on 21 identified measurements using three different scanners.

3D body scanning is not new to the apparel industry (Loker et al., 2004), it has significant potential for use in the lingerie industry in particular. Wacoal pioneered the use of 3D scanning technology to obtain a large quantity of measurement data (Wacoal, 2005) for the breast in order to assess breast shape characteristics.

Using 3D measuring technologies, in addition to general data that can be acquired using manual measurement methods, more information can be reliably obtained from 3D surface point clouds. Based on 3D scanning technique, Lee et al. demonstrated a folding line method (Lee et al., 2004) to find a continuous and natural boundary for the breasts so that the breasts base and volume could be measured more accurately. They asked the subjects to push their breasts up and inward extremely, then the upper and inner boundaries of the breasts were marked using flat landmarks. To identify the most useful parameter of breast shape for the design of bra, comprehensive measurements were put into investigation. They include the breast's volume, surface area, base, nipple height, surface distance, curvature of breast bottom curve (BBC), inner breast curve (IBC) and outer breast curve (OBC). The results of cluster analysis showed that the BBC was a useful and simple parameter for the characterizations of the breast root.

In addition, 3D body scanning technology can be used for bra pattern design. AGMS-3D (Asahikasei AGMS Corporation, 2005) created bra patterns to fit the three-dimensional shapes of the breasts based on the 3D body model.. CAD systems such as Gerber Technology's V-stitcher (GERBER Technology, 2005) can virtually stitch up a bra automatically and visualize the stress distributions of the virtual bra on a virtual body form.

2.2.6 Medical Research on Breast Volume Measurement

In addition to the apparel industry, a number of medical research projects have been carried out to assess breast volume measurements for asymmetry analysis or breast surgery considerations (Bouman, 1970; Campaigne et al., 1979; Grossman & Roudner, 1980; Ellenbogen, 1978). In the medical field, mammograms, magnetic resonance imaging, thermoplastic sheet moulding methods (Figure 2.4), Archimedes measurement principles and anatomical measurements are often used to assess the breast volume (Bulstrode et al., 2001). However, it was found that the results from these five different techniques were not comparable.

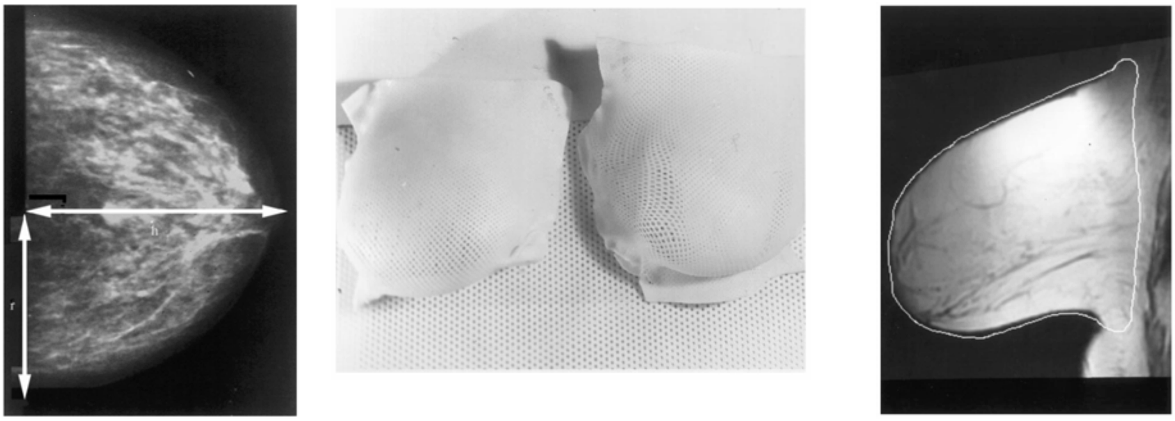

(a) Mammograms (b) Thermoplastic sheet moulding method (c) Magnetic resonance imaging

Figure 2.4 Medical methods for the breast volume measurements (Bulstrode et al., 2001)

Grossman & Roudner (1980) developed an adjustable geometrical conical device that could be used to determine the breast volume for breast surgery. The sliding surface of the form allowed a wide range for volume measurements, and the breast volume could be directly read from the graduated scale on the surface of the device.

Katariya et al. (1974) demonstrated a method to calculate the breast volume by taking measurements from a mammogram. He assumed the breast shape to be a regular cone, so the formula for the volume is $1/3 \pi r^2 h$, where r is half-length of the base of the breast and h is the distance from the nipple to base.

Malini et al. (1985) used ultrasound to scan the breast in 1cm longitudinal and transverse slices and calculated the volume using an integrated sum.

Campaigne et al. (1979) performed an analysis of the breast volume by making a gypsum cast of the subject’s chest and then measuring the volume of sand that filled the mold. Smith et al. (1986) also determined the breast volumes of 55 volunteers using this chest wall casting technique. It was found that the mean of the breast volumes of the volunteers was 275.46 cc, and there was no significant difference between the right breast and the left breast.

Loughry et al. (1987, 1989) used biostereometric analysis to study the right and left breast volumes of 248 subjects in 1987 and 598 subjects in 1989. They used close-range stereophotogrammetry to analyze the breast shape (Figure 2.5). The generally accepted clinical impression of left breast volume dominance was confirmed in the study of 1989. In both studies, no significant relationships were found between age, handedness, menstrual status and the breast volume.

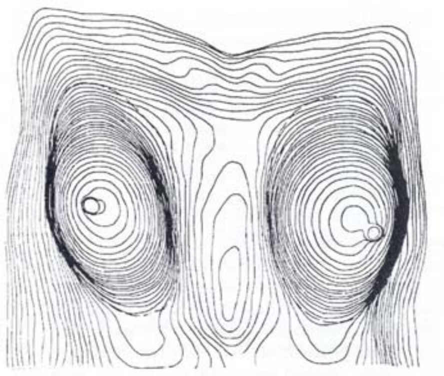

Figure 2.5 Contour mammogram with the breast boundary for volume measurements (Loughry et al.,1987)

Fowler et al. (1990) utilized magnetic resonance imaging to assess changes in breast volume and composition during the menstrual cycle.

Edsander-Nord et al. (1996) produced a negative replica of the breast using a perforated 2mm thermoplastic sheet; the volume was then measured by laying cling film into the mould to block the perforations and calculating the volume of water that filled the mould.

In order to measure the increase in breast volume from the end of one breastfeed to the beginning of the next, Cox et al. (1998) developed a Computerized Breast Measurement (CBM) system capable of quantifying changes in breast volume using Moiré techniques.

In addition, another method, using the Archimedes principle and involving the use of a calibrated container, has been generally used (Bulstrode et al., 2001; Bounman, 1970). The patient was asked to put her breast into the container filled with water at body temperature. Then the volume of the water displaced was measured. After repeating this procedure three times, an average volume for each breast could be obtained.

2.3 Breast Shape Analysis

A great number of research projects relevant to body shape classification have been carried out in the apparel industry. However, very limited research has been conducted in the area of intimate apparel, especially breast assessment.

Using the breast curve line observed from the side view, Martin (1957) classified the breast shape into four types (Figure 2.6). The definition of these four types is as follows:

1) Flat breast: the breast height measurement ranges from 3cm to 5cm, which is shorter than the radius of the breast root circle.
2) Hemisphere breast: the breast height measurement ranges from 5cm to 6cm, which is approximately equal to the radius of the breast root circle.
3) Conic breast: the breast height measurement is 6cm or larger, which is greater than the radius of the breast root circle.
4) Goat-breast: the proportions of this type are very similar to the conic breast, but the angle of breast to the chest wall is smaller.

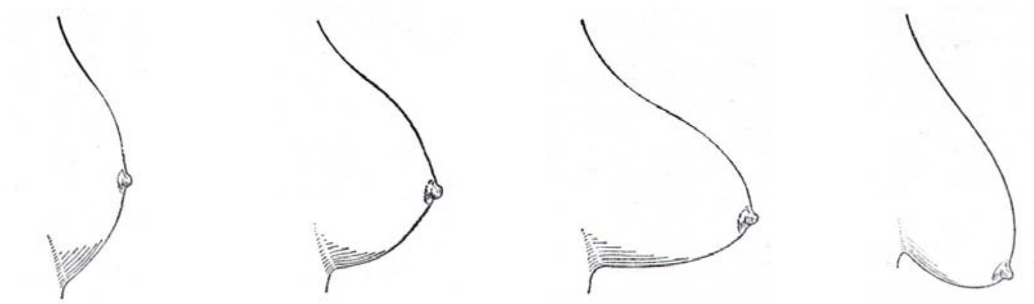

(a) Flat breast (b) Hemisphere breast (c) Conic breast (d) Goat-breast

Figure 2.6 Categorization of the breast shape (Martin, 1957)

In order to incorporate the concepts of beauty, comfort and wellness into intimate apparel product design, the Human Science Research Centre of Wacoal has been observing individual women for over 40 years (Wacoal Corp., 2005). In 1994, the centre investigated 1115 Japanese women by measuring their body size and asking 6 judges to assess their body beauty (Wacoal Corp., 1995). Based on both manual measurement and 3-dimensional (3D) data, they found 6 key parameters strongly related to the judges' assessment of a female's body beauty as follows:

1) Girth balance of BWH (bust, waist and hip): the relationships among bust girth, waist girth and hip girth. The proportions are calculated as B/W and H/W. Waist girths ranging from 64cm to 70cm were regarded as beautiful.
2) Ratio balance of the torso (see Figure 2.7): this was assessed based on the width and thickness of the torso. As viewed from the front, the width of waist was defined as 1; the ratio of front torso was determined by evaluating the relative width ratio of shoulder width, bust point width and hip width. A similar method was used to assess the balance of relative thickness ratio and the height proportion of the torso segments as viewed from the side.
3) Dimensional balance of the breast: the breast base shapes and the orientation of the breasts in relation to the torso were two major factors which determined the assessment of 3D breast balance. As shown in Figure 2.8, the researchers in Wacoal (1995) used contour slice lines to evaluate the different breast shapes. It was discovered that the breasts of females judged to be attractive tended to have orbicular base shapes and very limited departure from the centre of the body (the white dots in Figure 2.8)
4) Dimensional balance of the hip: the hip base shapes and the orientation of the hips were the two key parameters that were used to evaluate hip balance.
5) Balance between whole height & weight: this proportion related to the identification of a healthy image.

6) Proportion balance of overall height: the proportion of the whole body assessed as most beautiful was defined as 7.5 times the total head height, with a leg height of about 0.47 times the whole body height.

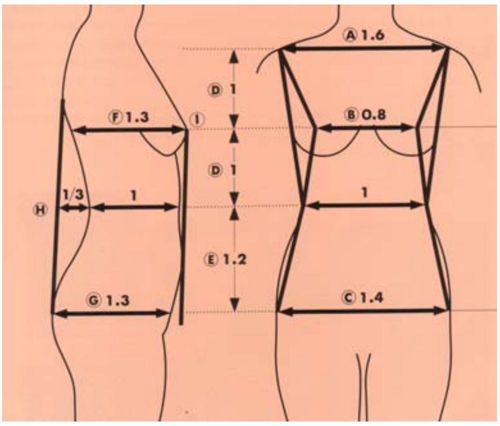

Figure 2.7 The ratio balance of torso from Wacoal's golden canon (Wacoal Corp., 1995)

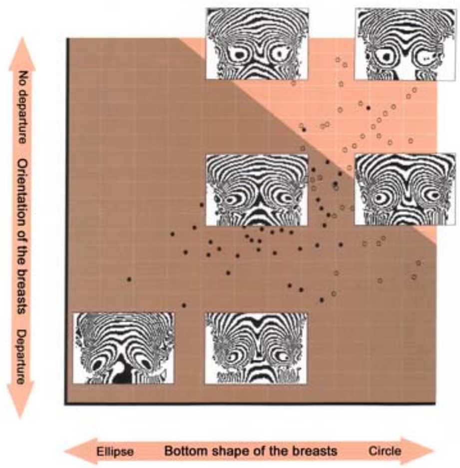

Figure 2.8 Two major factors influencing the assessment of 3D breasts' balance (Wacoal Corp., 1995)

Based on their research findings, Wacoal categorized the body types of women from a combination of front view and side view images (The human science research center of Wacoal, 2000). They included 7 types: VV, AV, AA, VA, HA, II and NI, where the first letter represented the figure type of the front view image and the second letter indicated the categorization of the side profile. In their study, it was very important to draw a framework connecting dots at the extreme points of the left and right shoulders and waist and hip on the front view of a subject's body image. The difference among the widths of bust, waist and hip were calculated. The definition of these seven body types can be described as follows:

1) VV: the shoulder width is obviously broader than the hip width as viewed from both front and side.
2) AV: the hip is much wider than shoulder with an indented waist from the front view, and the bust width is larger than the hip width as viewed from the side.
3) AA: the overall body proportions show an indented waist and an extreme hip in both front and side views.
4) VA: the proportions show a wider shoulder in the front view and an indented waist in the side view.
5) HA: the shoulder width is approximately equal to the hip width with little waist indentation.
6) II: the overall body silhouette is slim.
7) NI: the ratios of the bust-to-waist and the hip-to-waist arc balanced.

2.4 Breast Sizing System and Fit Issues

2.4.1 General Bra and Breast Sizing System

According to the history on record (Morris et al., 2002), the fundamentals of the current bra sizing systems were founded as early as 1926. Its original intent was to classify breast shapes into analogous types. Berlei Underwear Company in Australia first carried out a size survey to study women's figures between 1926 and 1928. It primarily used the circumference of the women's chest, bust and underbust (also known as the ribcage) to identify the bra size.

Ida Rosenthal, who was a founder of Maidenform, introduced cup sizes for bras in 1928 (Marples, 2004). Later in 1935, Warner in America realized that, in addition to the full bust measurement, it was necessary to incorporate the volume of breasts into the bra size specification. It first advertised the alphabet bras as A cup = youthful, B cup = average, C cup = large and D cup = heavy (Bressler et al., 1998) and such a system became the basic modern bra sizing standard (Figure 2.9).

Figure 2.9 Warner's alphabetic bra (Bressler et al., 1998)

For commercial and marketing considerations, intimate apparel designers and manufacturers of different brands usually have their own distinctive bra size charts (Richards, 2001). The size charts are varied because the process of developing such size charts is to modify patterns until the bra fits nicely on the body figures of the brand's live fitting models. As different brands use different fitting models, a customer may find herself having a better fit with one brand rather than another even though the size of the two bras is nominally the same.

The 3D shape and dimensions of women’s breasts are complex and variable. Conventional linear measurements are probably not sufficient to present the breast size that best describes the fit of a bra. However, a simple standard is necessary for communication between customers and retailers, designers and manufacturers. The Imperial system (Table 2.1) and the Metric system (Table 2.2) are two major breast sizing systems that have been universally used for more than 70 years since Warner’s introduction of the alphabetic bra size in 1935.

Table 2.1 Imperial bra sizing system (Zheng, Yu & Fan, 2006)

Bra size	**30B**	**32B**	**34B**	**36B**	**38B**	**40B**	**42B**	**44B**
Underbust girth (inches)	25-26	27-28	29-30	31-32	33-34	35-36	37-38	39-40
Bust girth (inches)	31	33	35	37	39	41	43	45
Bra size	**34AA**	**34A**	**34B**	**34C**	**34D**	**34DD**	**34E**	**34F**
Underbust girth (inches)	29-30	29-30	29-30	29-30	29-30	29-30	29-30	29-30
Bust girth (inches)	33	34	35	36	37	38	39	40

Table 2.2 Metric bra sizing system (Zheng, Yu & Fan, 2006)

Bra size	**65A**	**70A**	**75B**	**80B**	**85B**	**90B**	**95B**	**100B**
Underbust girth (cm)	65	70	75	80	85	90	95	100
Bust girth (cm)	75	80	87.5	92.5	97.5	102.5	107.5	112.5
Bra size	**75AA**	**75A**	**75B**	**75C**	**75D**	**75DD**	**75E**	**75F**
Underbust girth (cm)	75	75	75	75	75	75	75	75
Bust girth (cm)	82.5	85	87.5	90	92.5	95	97.5	100

ISO DIS 4416 (ISO 4416, 1981; Winks, 1997) suggests preferred size scales for women’s foundation garments based on bust girth and cup size as shown in Table 2.3.

Table 2.3 Preferred sizes scales from ISO 4416 (ISO 4416, 1981; Winks, 1997)

	Underbust girth (cm)												
	64	68	72	76	80	84	88	92	96	100	104	108	112
Bust girth (cm)													
Cup A	76	80	84	88	92	96	100	104	108	112	116	120	124
Cup B	80	84	88	92	96	100	104	108	112	116	120	124	128
Cup C	84	88	92	96	100	104	108	112	116	120	124	128	132

It needs to be mentioned that compared to traditional bras, the sizing charts for seamless knitted bras are simpler. Some manufacturers just use A, B, C, D to describe the cup size. Alternatively, others use S, M, L to identify the production size.

Based on the conventional definition of Imperial bra sizes, Wright (2002) described the procedures for defining the band size mathematically by giving equations (2.1) and (2.2),

$$X = 2[([x+1/2]+5)/2], \tag{2.1}$$

$$Y = [y+1/2]-2[([x+1/2]+5)/2], \tag{2.2}$$

where [x+1/2] is the rounded underbust girth and [y+1/2] is the rounded bust girth. The integer X is the resulting band size and integer Y is converted into the corresponding cup size letter as in Table 2.4. The mapping of common band sizes and cup sizes are given in a graphical presentation as shown in Figure 2.10 (a).

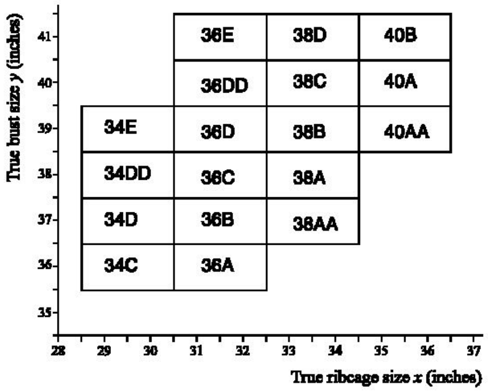

(a) Domain map for common calculating procedure

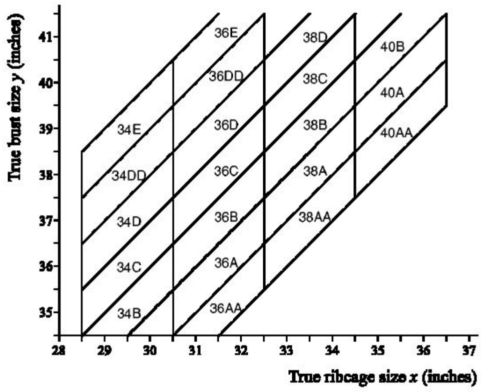

(b) Mapping of bra sizes from modified imperial system

Figure 2.10 Bra sizes calculating procedure comparison (Wright, 2002)

Table 2.4 Determination of bra cup size letters

Bust girth – band size	-1"	0"	1"	2"	3"	4"	5"	6"	7"
Cup size	AA	A	B	C	D	DD	E	F	G

Wright explains that in common bra sizing practice, each size occupies a 2” x 1” rectangular domain in (x, y) space and that this system creates anomalies. For example, a small error in x, y could cause the resulting size to cross the diagonal boundary between domains, and change a predicted size from an A-cup to a D-cup. He also pointed out that in equation (2.1), the band size X is rounded twice - firstly when x is rounded ±1½” and secondly when it is made even by ±1”. The cup size Y is the difference between two rounded values, which allows the rounding errors to accumulate and leads to an accumulated error of ±1½”, corresponding to a 3” size range.

In order to remove the error, Wright revised equation (2.2) to a new formula as given in equation (2.3) and presented a new domain map of bra sizes in Figure 2.10 (b).

$$Y = [y-x+1]-5, \qquad (2.3)$$

The equation (2.3) proposed to make a simple deduction of the full bust girth (y) by the underbust girth (x) for the determination of cup size letter Y. This new formula coincidentally matches the concept used in the Metric bra sizing system, where the cup size is derived from the calculated difference between the full bust girth and the underbust girth.

In the medical field, Pechter (1998) complained that the traditional breast sizing system was frequently inaccurate and useless. Particularly for the practice of plastic surgery, he stressed the importance of direct measurement of the mammary hemi-circumference in the determination of cup size. He measured the boundary of the unclothed breast from the lateral breast crease to the anterior breast crease, and proposed that a mammary hemi-circumference of 7” corresponded to an "A" cup, 8” to a "B" cup, 9” to a "C" cup, with each 1” increment or decrease determining a cup size up or down (see Figure 2.11).

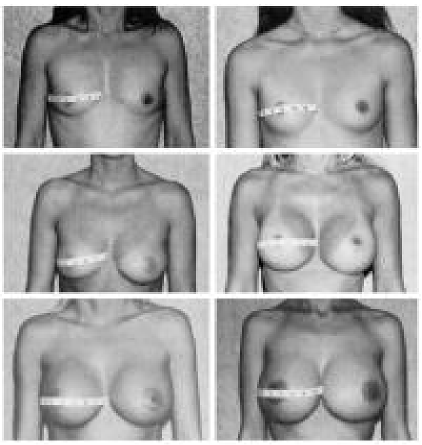

Figure 2.11 The breast size from AA cup to DD cup based on Pechter’s method (Pechter, 1998)

Kanhai and Hage (1999) however added that this formula is only valid for a 34 band size. The size and volume of a B cup on a small ribcage is different from that on a large chest. The same 8” mammary hemi-circumference corresponds not only to a 34B, but sometimes also to a 32C or 36A.

Although some research projects have been carried out to propose new breast size assessment methods and sizing systems, most of the measurement processes are based on 2D measurements and can not define 3D breast and ribcage shapes. By measuring and classifying 50 breast root shapes and dimensions, Morris et al. (2002) proposed a method for calibrating 3D female breast sizes by modelling the breast in its ideal position and shape on the chest wall. They claimed that the development of a range of perhaps 18 standard cup shapes would answer a massive commercial problem and allow important medical projects to classify patient’s breast sizes.

2.4.2 Fit Issues of Bra

“Fit” is generally defined as “to be of the right size or shape for” in Merriam-Webster’s Dictionary (Online, 2005) and “to be the right measure, shape and size for” in the Oxford Dictionary (2001).

It is believed by designers and production experts that the fit of a garment is one of the most important factors in producing satisfying garments for individual customers (Minott, 1978). In the apparel industry, fit has been defined as: “Directly related to the anatomy of the human body and most of the fitting problems are created by the bulges of the human body” (Gain, 1950). Furthermore, Laing and Sleivert (2000) proposed that static fit was the relationship between garment size and body size, and dynamic fit had to respect a garment’s performance, which allowed the body to do its usual tasks without garment interference and resistance. They suggested that fit could be evaluated using some coarse scales such as visual evaluation and perception of pressure on the body of the wearer.

Many people think bra fitting is more important than outerwear fitting since it is regarded as the second skin of the body. However, many articles (Lipton, 1996; Boyes, 1996; Young, 1995) have reported that 70% of the UK female population, especially large-breasted women, wore the wrong size bra. Pechter (1998) surveyed 100 women and found that they were wearing the wrong-sized bra 77% of the time. Greenbaum et al. (2003) studied 102 women, and all of their claimed bra sizes did not match with the manufacturers recommended size for their measurements. All wore an undersized band and oversized cups. The more obese they were, the more marked the disparity between the recommended and actual band size. It is especially sad to note that women who most need supportive bras were the least likely to get accurately fitted bras. This may significantly affect their physical health and quality of life. The approximation involved in the sizing formula is probably the root cause.

According to Thomas (1995), and Elam (1997), several key points were suggested for the essential perfect fit bra, as listed below.

1) The cup should fit smoothly and comfortably snug around the body, with the breasts filling the cups completely--no excess fabric in the cups, and no breast tissue spilling out of the cup at the top, side, or bottom.
2) The bridge of bra should very nearly touch the breastbone.

3) The shoulder strap should lie flat against the skin without slipping or digging into the shoulders.
4) The bra band should not ride up at the back, and stay comfortably under the shoulder blades.
5) Ideally, the bust level is about halfway between elbow and shoulder, although this may not be practical for a heavy-busted woman.

2.4.3 Bra Underwire for Support

Although the underwire appeared as early as 1934, it only became common until after World War II (Wohleber, 2003). The wire was originally designed to increase support for large-breasted women, but it quickly became a tool for molding the body into a certain shape. Customers and manufacturers found that the rigidity of the underwire could enhance the tissues of small-breasted women by pushing them up to new heights (Pederson, 2004; Wohleber, 2003). In the design area, the underwires play very important roles to accentuate the bust in focus defined as “pushups”. Some famous bras such as the Wonderbra and the Miracle Bra were designed with a primary reliance on underwires, despite the additional material and manufacturing variables (Wohleber, 2003).

In order to support the breast comfortably, some manufacturers have developed some new underwires for traditional bras. As early as 1993, Wacoal (1993) created a curved underwire based on changing the curvature of the normal underwire using steel or shape memory alloy. Compared with the traditional 2D plane underwire, this underwire was design using a curved shape, which had a 1~3mm raise at the forepart, a 2~3mm raise at the back-end and a 1~3mm raise at the midway of the underwire from the horizontal plane. They claimed that the shape memory alloy could help the underwire prevent shape changing or could resume to its original shape after shape changing. Later, Wacoal (2001) developed a curvilinear underwire by using nickel-Ti alloy and a stainless steel underwire, which changes the cross-section into an elliptical shape.

In 2003, Wacoal (2003) invented a cup padding material which could be used for the cup part of women's bodywear. It was stated that this padding material could be applied as a band plate, which the thickness was 0.2-0.4 mm and the width could be set as 3-7 mm. In order to enhance the performance of this band plate, the middle part was constructed in a three-dimensional form as an inclined surface. They also claimed that the shape of the padding could be recovered after distortion or transformation during the washing process.

Fildan and Wanzenbock (2001) proposed a spoon shaped underwire. It was stated that, relying on a swiveling tail, this underwire could be used in a brassiere-type garment to let the spoon fit the outer side of the breast well.

Seymour and Powell created a revolutionary Bioform bra (Figure 2.12) for large breasted women to support the weight of the bosom ("Designing the perfect bra?," 2002). The essential structure of the Bioform was a 2-shot moulding form where the inner core is made by infusing a softer polymer. This inner core could be used to replace the function of the underwire to hold and shape the breasts. Furthermore, the cup was made from a soft, body-forming polypropylene TPE, specially formulated by Krailburg, supported by a high isotactic polypropylene homopolymer from Solvay. It was claimed that the Bioform bra could fit all the requirements of support, comfort and washability.

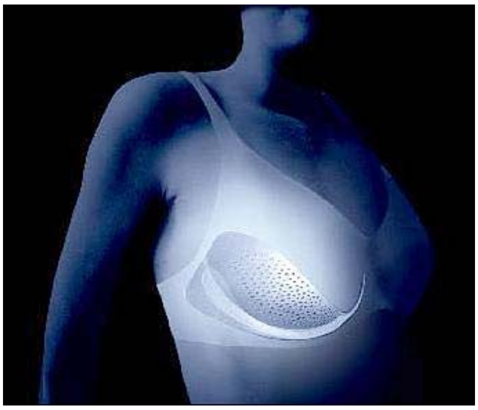

Figure 2.12 The Bioform bra invented by Seymour and Powell ("Designing the perfect bra?," 2002)

Because the above inventions are focused on underwire innovation, they are probably unsuitable for seamless knitted bras because of their rigidity and hard support.

2.5 Development of Circular Seamless Knitted Bras

2.5.1 Review of Knitting Fundamentals

Knitting is defined as "a process of forming a fabric by the intermeshing of loops of yarn" (McIntyre & Daniels, 1997) or "the technique of constructing textile structures by forming a continuous length of yarn into columns of vertically intermeshed loops" (Spencer, 1983/2001). Knitting manufacturing technologies include five main types: circular knitting, fully-fashioned knitting, hosiery knitting, warp knitting and speciality knitting. These knitting methods are generally used to make tubular or flat form fabrics, garments and components (Morris, 2003).

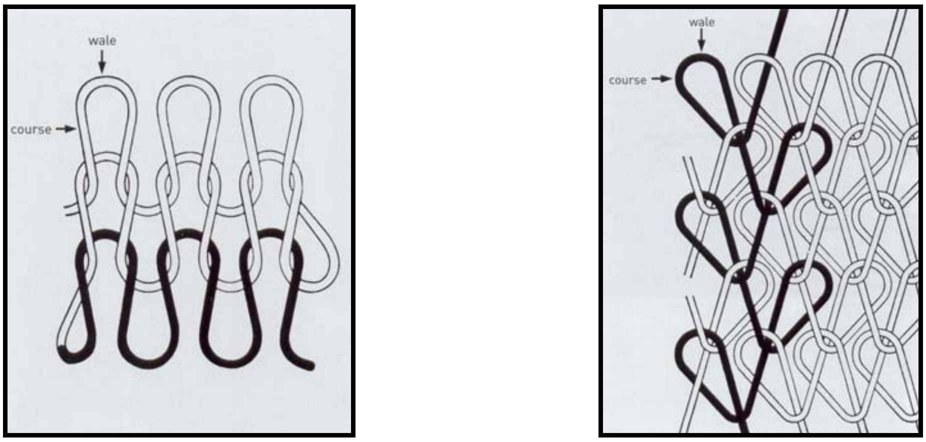

(a) Weft knitting (b) Warp knitting

Figure 2.13 Comparison between weft knitting and warp knitting (Black, 2002)

Knitted products can be divided into two main types: weft knitting and warp knitting (see Figure 2.13). Weft knitting is a process in which the fabric is made up of loops intermeshed in horizontal rows knitted sequentially by a single thread or a small number of threads passing a cross of the fabric from one side to the other. Conversely, warp knitting is a process in which multiple threads running the length of fabric are simultaneously formed into vertical chains of stitches from the beginning to the end of the fabric (Black, 2002). Compared with warp knitting, weft knitting is more diverse, more open, and tends to be distorted easily and recover easily under tension. Contrariwise, warp knitting has more cover, is less resilient, and is lighter weight and allows higher productivity (Choi & Powell, 2005).

Seamless knitting technology has been under development on weft knitting machines including electronic circular body-size knitting machines and V-bed flat machines. A variety of products can be knitted based on permutations of basic technologies, including variables such as knitting types, loop forming mechanisms, stitch types, needle bed configurations, and fabric structures. In electronic circular body-size machines, needles are held in one or more circular beds, whereas in V-bed flat machines, needles are arranged in a flat bed. The latch needles of both circular and V-bed flat machines can be selected to knit, tuck or miss to create patterns (Morris, 2003). This also facilitates the production of garment parts constructed as 3D shapes on the knitting machine. With the development of electro-magnetic selectors, a variety of seamless garments with ever more complex and sophisticated designs have been manufactured.

Compared to flat knitting machines, electronic circular body-size knitting machines may provide more rapid production speeds and greater fineness of gauge, i.e. the number of needles per unit length. In addition, electronic circular body-size knitting machines are more attractive to some manufacturers because of their versatility, related to low total capital costs, small floor space requirements, quick pattern changing facilities, and the potential for short production runs (Spencer, 1983/2001).

2.5.2 Contributions to the Development of Seamless Knitting

Seamless knitting is not a new concept, being as old as knitting itself (Black, 2002). Maitre Bertram’s painting (Figure 2.14) of Mary knitting Christ’s seamless garment is the earliest recorded illustration of a hand-knitted garment, which is dated to just before 1400 (Spencer, 1983/2001).

Figure 2.14 Mary knitting Christ's seamless garment - The earliest recorded illustration of a knitted garment. Part of a church architectural painting by Maitre Bertram (1345–1415) (Spencer, 1983/2001)

In 1558, the first knitting machine, a stocking hand frame, was invented by William Lee in England. An anonymous writer (Anon, 1994) depicts this advance, which represent complex hand movements at a single stroke by mechanising them, as 150–200 years in advance of its time. Lee's original invention was not economically viable since it needed two men to operate it. Later, in 1620, improvements were carried out by Aston, a former apprentice of Lee. By arranging the sinkers into alternating sets, several new features were obtained, including "better uniformity of loop length, finer machine gauges (24 gauge) and easier operation of a frame consisting of 2000 parts" (Spencer, 1983/2001).

Circular machines are classified as all those weft knitting machines "whose needle beds are arranged in circular cylinders and/or dials, including latch, bearded, or compound needle machinery, knitting a wide range of fabric structures, garments, hosiery and other articles in a variety of diameters" (Spencer, 1983/2001). Although Decroix patented the first circular frame in 1798, Marc Brunel's 'tricoteur' of 1816 has been considered to be probably the first practical working example of such a frame. In 1855, Matthew Townsend patented uses for the latch needle. This invention paved the way for electronically controlled individual needle selection both on circular and V-bed machines (Black, 2002). During the last 200 years, numbers of inventors have pushed the development of circular weft knitting technology towards the direction of more sophistication and diversity (Schwabe, 1989).

Circular garment-length machines include both body size and larger circular machines that have a cylinder and dial arrangement, with single or double cylinder, but also consist of small diameter machines for hosiery. The first small-diameter, revolving-cylinder machine appeared about 1907 but its technology was not good enough to produce high quality knitted articles consistently.

Electronic needle section and computer control was introduced to the whole of the hosiery and knitting industry in the 1960’s and 1970’s (“Revolution in seamless underwear and outerwear manufacture,” 2000). In the later twentieth century, the ability to knit in the round without seams was employed by electronic circular machines to knit a variety of three-dimensional seamless garments and components (Black, 2002).

In the past few years, Santoni of Italy have successfully developed fully electronic machines that are able to produce whole ready-made garments, and has created and produced 14 different types of sophisticated electronic circular knitting machines for “Seamless wear” production (“Seamless revolution: An Italian knitting machine builder offers a technique for the future,” 2000; Santoni, 2005). Based on the knowledge gained from the development of a hosiery and tights machinery, Santoni has taken several steps forward by providing a complete elasticated welt and comprehensive patterning, and incorporating spliced areas and figure-control by using step-motor-controlled stitch cams (“Revolution in seamless underwear and outerwear manufacture,” 2000; Spencer, 1983/2001). Recently, the Santoni group patented a new revolutionary 4-FEED single jersey electronic circular machine - SM4-TL2. It is designed with reciprocal movement, 2 selection points per feed and per rotation sense. The seamless garments knitted on this new machine can be sewn without any cutting processes being needed (Santoni, 2005).

Apart from Santoni, many knitting machine builders have been entering the electronic circular seamless knitting field, including Sangiacomo’s “Jumbo” in Italy, Okuma in Japan, whose machine is sold internationally by another Japanese firm named Nagata Seiki, Orizio with its BS machine, and the German company Merz with its MBS (“Revolution in seamless underwear and outerwear manufacture,” 2000, “Technology spurs seamless growth,” 2004b). Matec, another machine manufacturer in the Lonati Group has also developed revolutionary 6 to 10 inch diameter machines with jacquard capability, which can produce simple ‘bodysized’ children’s garments with patterned fabrics and minimal seams (Black, 2002).

Most of these developing machines’ specifications are very similar, including: (1) fine gauge single cylinder or double cylinder bodywear models, (2) all-electronic needle selection plus striping to give versatile patterning for both openwork and color patterns, (3) the ability to knit a single or double elastic waist, making them especially suitable for underwear (“Revolution in seamless underwear and outerwear manufacture,” 2000).

Many developments are focused on improving productivity, quality, and environmental friendliness (Morris, 2003).

2.5.3 Development of Seamless Knitting Techniques

2.5.3.1 Structural Design of Seamless knitted Bra

As smaller diameter machines become more popular, it becomes possible for circular machines to knit "body-size" side-seam-free body panels, integral waistbands and integral shoulder straps to enhance the innovation of seamless garments (Morris, 2003). As consumers demand aesthetic styles and comfort from bras, the seamless knitted bra is receiving the attention of an increasing number of intimate apparel manufacturers. Many brands have been using Body-Size machines to innovate their distinctive seamless knitted underwear – Jockey, Victoria's Secret, Wolford, Nike, Reebok, Adidas, Dior, Banana Republic, Donna Karen, Calvin Klein and many others ("Seamless revolution: An Italian knitting machine builder offers a technique for the future," 2000).

It is claimed that seamless technology could shorten manufacturing process, reduce material wastage, and offer greater comfort and better fit to wearers (Lam, 2005). Based on these features, various styles and patterns of seamless bras have been created by manufacturers.

In 1985, a knitted bra was invented using a cylindrical tube knitted from a circular weft knitting machine (Richards, 1985). As shown in Figure 2.15, the knitting structure used for the centre panel of the bra was constructed using combinations of plain stitches and float stitches. In order to generate different sizes of the garment, the yarn was held in either a float or a missed stitch for a multiplicity of courses, ranging from 3 to 22 in number. Side panels were constructed using a similar method. The bra cups were thus defined between the centre panel and the two side panels. After cutting and sewing, the cylindrical blank could produce an integral garment having straps, bra cups and a welt band.

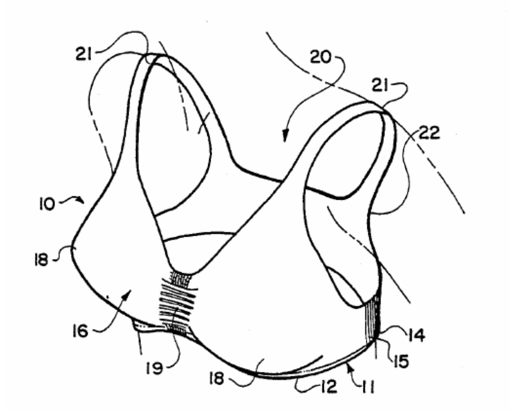

Figure 2.15 Seamless knitted bra invented by Richards in 1985 (Richards, 1985)

The Russell Group patented a knitted brassiere blank which had integral seamless elasticated contours defining the bra cup borders (Albright & Rockingham, 1998). A circular knitting machine equipped with a computerized electronic needle selection system was used to design a sports bra without cutting and sewing operations in the cup area. The blank (see Figure 2.16) could be cut into two pieces to produce two separate bras.

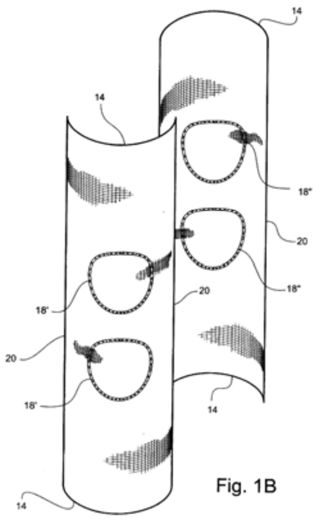

Figure 2.16 Separate panels of the bra blank (Albright & Rockingham, 1998)

Alba Waldensian patented a circular seamless knit technology for making seamless brassieres (Osborne & Boomer, 1999) as is shown in Figure 2.17. It was proposed that a tubular blank could be knitted on a circular knitting machine, with walewise longitudinal openings forming the torso and neck openings of the brassiere along opposite sides of the blank. It was claimed that this ‘knit-in-one’ bra could support the breast and offer the same figure-flattering look as an underwire brassiere without the discomfort of pads, wires, hooks and snaps (Osborne & Boomer, 1999; “Intimate Apparel and Shapewear,” 1997).

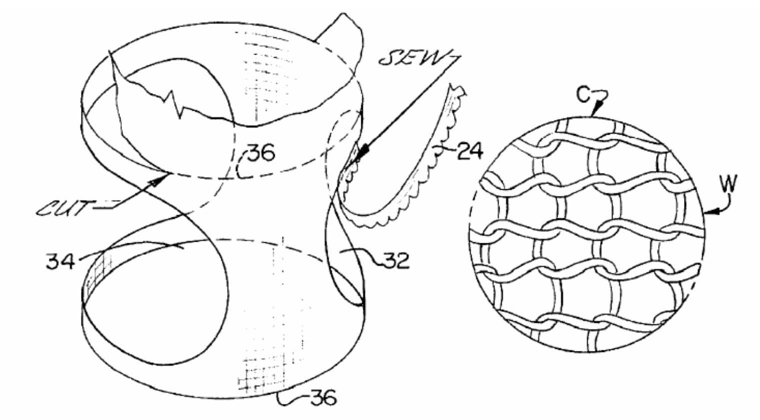

Figure 2.17 Front elevation view of the blank with enlarged sectional view (Osborne & Boomer, 1999)

Browder (2000) invented a circular knitted bra formed of an inner fabric and an outer fabric that were connected to each other through the welt band (Figure 2.18). The bra is completed by sewing up the straps and fixing the outer and inner fabrics together. The patent proposed that the outer fabric was preferably knitted from flat nylon yarn, or combinations of nylon and cotton to provide strength, support, or aesthetic properties in specific areas. For the inner layer, it was suggested that it should be knitted with yarns selected for their softness, comfort, and moisture properties.

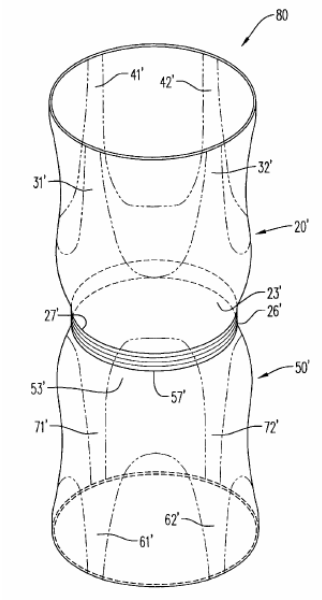

Figure 2.18 Perspective view of the cylindrical blank (Browder, 2000)

For the development of a seamless sports bra using circular knitting technology, Yeung et al. (2002) applied for a new patent, which is disclosed as having a unique double-layered construction that can provide sufficient support for the breast during moderately strenuous physical activity. Furthermore, they claimed that the invention could also provide nonabrasive comfort and style to consumers.

Most recently, an invention of a seamless circular knitted bra (Mitchell, 2005) was developed giving varying degrees of stretchability in different cup areas. Each bra cup is formed using a plain jersey stitch. As shown in Figure 2.19, each bra cup has three distinct areas of different stitch density which can enhance the supporting and shaping effect for the wearer's breasts. The stitch density was designed to be most dense at the bottom of the cup and gradually decreased towards the top of the cup. This design feature was achieved by using specific yarn tension control devices that can regulate the stitch construction configuration throughout the bra.

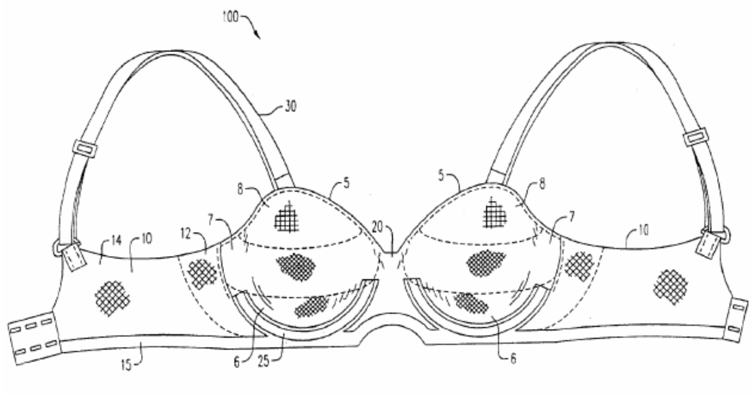

Figure 2.19 Top view of the bra (Mitchell, 2005)

A similar patent to US patent 6,899,591 B2, filed by Mitchell and Waitz (2004), also focuses on changing the extensibility of different areas of the bra. Compared with the core region, tighter stitches with shorter stitch lengths are used in the cup areas for supporting the weight of the breasts. Conversely, looser stitches with longer stitch lengths are used in each side wing to provide more comfort and flexibility.

Seamless tubular garment blanks with an integral complete band or welt have been widely used to produce bras, underwear and other apparel items. This integral knitted band can provide better comfort to the wearer than cut-and-sewn bras. However, they have an “unshaped” appearance when compared with those bras with preformed cup shapes. Mitchell et al. (2005) invented seamless shaped bands to improve the benefits of normal complete bands. As shown in Figure 2.20, the breast cup areas are designed to extend to the underband regions. Therefore, the seamless interface of the underband and body portion is created along the region of underband into the main cup regions. This technique creates a shaped band in the front of the bra having a variable dimension from the lower edge of the underband upwards towards the cup regions.

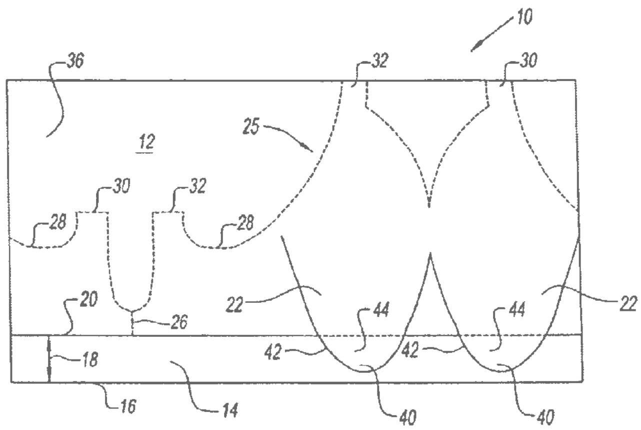

Figure 2.20 Front view of the bra (Mitchell et al., 2005)

After the manufacture of circular knitted bras, fabric tapes are usually sewn on to construct pockets or passages for inserting wires to improve the support of the bras. To reduce the production costs and improve wearing comfort, Lonati et al. (2000) invented a knitted structure that created tunnel-shaped passages for the insertion of wires, as the bra is knitted (see Figure 2.21a). As shown in Figure 2.21b, the passages were created by knitting a series of courses containing knit and miss stitches.

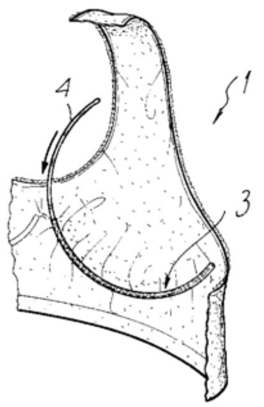

(a) Tunnel-shaped passages for inserting wires

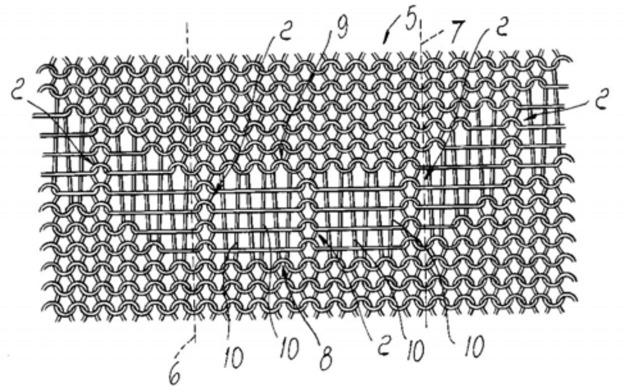

(b) The knitting structure of tunnel-shaped passage

Figure 2.21 Back view of the bra according to the invention (Lonati et al., 2000)

2.5.3.2 The Use of Yarns

The latest seamless circular machine models have the capability to knit using various types of yarns including synthetic, cotton, wool and silk, and combining these yarns with elastomeric fibres, which can be knitted in, floated, or laid in (Bremner, 2005).

According to a report in "Knitting International" ("Global seamless market round-up," 2004a; "Technology spurs seamless growth," 2004b), textured nylon yarn (polyamide) is still the primary yarn used for seamless apparel in Europe and the US, although a few companies, generally active wear companies, are looking at other types of yarn such as polyester that can improve the fabric elasticity, especially in terms of elongation after dyeing. The main demand in seamless underwear is for lighter weight fabrics, and 60-80 denier nylon yarn is largely used for classic ‘microfibre’ garments. On the other hand, stretch elastane yarns have made a significant impact on the seamless knitting sector (Morris, 2003), since 3D surface effects can be created using the stretch elastane yarns and incorporating them with jacquard technologies (Black, 2002). In addition, polypropylene is a new up-and-coming yarn in seamless application, which is mainly used for logos and dyed solutions (Kopell, 2005).

Recent figures from the market reveal that lower power and lower denier Lycra covered yarns remain increasingly popular (“Technology spurs seamless growth,” 2004b; Black, 2002). Furthermore, certain brands in the US and northern Europe focus on producing shaped seamless garments and bras. They generally use a light-weight microfibre in combination with a heavy Lycra for both control and comfort. In addition, in order to capture the more traditional consumer, some producers also knit seamless garments and bras with silky soft fabrics based on flat Tactel (Invista) yarns (“Global seamless market round-up,” 2004a).

2.5.3.3 Seamless Finishing Routes

The production practices of seamless knitted garments are complex and differ depending on the type of final product required. After the garment panels have been knitted, they generally pass through the following finishing processes: (1) cleaning (scouring), (2) garment washing (for garments knitted with dyed yarn), (3) heat setting, (4) making up, (5) dyeing (for garments knitted with undyed yarn), (6) pressing, and (7) packing (“Seamless finishing routes,” 2005).

For garments containing a high elastomeric content, another finishing route is proposed: (1) pre-shrinkage, (2) pre-boarding (heat setting), (3) cleaning (scouring), (4) making up, (5) dyeing (for garments knitted with ecru yarn), (6) pressing, and (7) packing (Liang, 2001).

2.5.4 Advantages and Disadvantages of Seamless Knitted Bras

By eliminating the sewing processes, seamless technology creates a number of advantages in knitting production, such as savings in cost and time, higher productivity, quick response production and other advantages. Due to advances in machinery, manufacturing processes and yarn development, seamless knitted bras are expanding into a new high potential classification in traditional apparel categories. Compared to traditional bras, seamless knitting technology on circular machines offers a seamless bra with a variety of advantages ("Revolution in seamless underwear and outerwear manufacture," 2000; Morris, 2003; Cajah web, 2005), which include:

1) Offer a higher degree of comfort by eliminating seams of cup and side.
2) Designing in a 3D form that provides individualized fit to the customer.
3) The light and soft fabric gives the figure a smooth, streamlined and sleek image.

Obviously, seamless knitted bras have significantly impacted the traditional bra sector. However, they have several disadvantages such as a tendency to compress the breasts, insufficient support and limited simple styles. Some manufacturers and buyers in intimate apparel generally believe that, while the new seamless knitted bra has become an important product in certain bra categories, it is yet not available for the full-figure of

D cup sizes or larger, since it cannot provide sufficient support for heavy breasts (Monget, 1999; Williamson, 2000). Furthermore, the design possibilities are more restricted when using seamless garment technology (Morris, 2003).

2.6 Summary of Literature Review and Remaining Issues

Through the literature review, it can be found that seamless knitted bras have begun to play an important role in the intimate apparel industry. Meanwhile, the development of seamless knitting technologies, especially on SANTONI circular machines, provides many opportunities for knitters to create new innovative bra products.

A number of research projects have been carried out on breast measurement, shape classification, sizing and seamless knitted bras development. However, many problems still exist. After reviewing the above literature, the remaining issues are summarized as follows:

1) It is evident that the current Imperial and Metric bra sizing systems are unreliable and incomplete, which can lead to confusion and ill fitting bras. Although some work has been carried out to propose new methods of breast measurement and to establish new sizing charts, the sizing processes are still based on linear correlations and do not consider 3D breast shape, angle and profile. The intimate apparel market could benefit from a new bra-sizing system, which can help designers to construct the bra in a three dimensional space.
2) Currently developed commercial seamless knitted bras have focused on displaying the features of knitting properties such as flexibility, softness and smoothness. Very

few attempts have been conducted into developing new forms or wires to support the breasts naturally which are also suitable for knitting performance.

3) Breast shape analysis is important for the design and pattern construction of clothing, especially intimate apparel, yet there have been limited studies on breast shape.

4) Finally, there are no systematic studies on the relationships among circular knitting technologies, breast sizes and shapes, and the fitting performance on the wearer.

CHAPTER 3

ACQUISITION OF 3D BREAST ANTHROPOMETRIC DATA

3.1 Introduction

Appropriate fit of a bra is critical in order to provide the required support and desired body shape whilst ensuring comfort for the wearer. Sufficient data on body measurements is necessary to define the shape and dimensions of the upper torso and, particularly, the breast region to inform the design of appropriate shapes and sizing systems.

The sample used in this study consisted of 456 Chinese female subjects aged between 20 and 39. The subjects were volunteers who were randomly chosen stratified by area and age to provide an appropriate consumer database. Subjects were recruited from most demographic areas of China, including Northeastern & Northern areas of China, the Midwest, and Middle reaches & Lower reaches of China. The scanning process was carried out in Beijing. The body dimensions were collected using both a VOXELAN 3D laser body scanner and a Martin's anthropometer.

There are three purposes for carrying out the study: (1) To compare data distributions of key body measurements to the sample which was used to design the existing sizing system, (2) To decide the major measurement items needed for further breast shape analysis, (3) To describe and categorize the detailed female breast dimensions using statistical methods.

3.2 Body Scanning Process

The current study aims to collect the breast measurements for the design of seamless knitted bra which provides natural support and soft reshaping. The key issue is: (1) how to relate the bra design with the measurements of nude breast, (2) how to define the desired position and shape of the breast after wearing a seamless knitted bra.

In order to obtain accurate measurements for the upper torso and breasts, it is important to define and control the standard sampling techniques, appropriate postures, clothing to be worn during the scanning process, determination of body landmarks, measuring devices and measurement items. The data were collected based on the following standard procedures used by the laboratory in AIMER HEC-BICT.

3.2.1 Posture and Clothing

There were several methods of measuring breast. First is measuring the nude figures, second is to measure customer’s desired breast shapes by asking the model to lift her breasts to where she wants the bra to be fit, and third is based on the softly supported breasts by asking the model to wear a soft bra. The method on nude figure was chosen because the determination of customer’s desired breast position varied from one to another and from time to time. Different soft bra styles create different breast shapes but nude breasts give unique original data that can reflect the true size & natural shape of the breasts.

The following procedures were adopted to ensure that the subject's postures were kept consistent. Subjects wore only a close fitting panty and no bra for both manual and scan measurements. In the manual measuring process, the subject was asked to stand erect with bared heels together and feet open at an angle of about 30 degrees, and to look straight ahead with arms hanging naturally (see Figure 3.1.a). In order to obtain more reliable data for 3D scanning, the posture was changed with the heels separated by about 100-150mm and the upper arms held apart from the sides of the torso at an angle of 15-20 degrees (see Figure 3.1.b). The subjects were required to wear a knitted skin color close fitting knitted cap to ensure the accuracy of the head data since the 3D body scanner can not capture the surface data of the black hair.

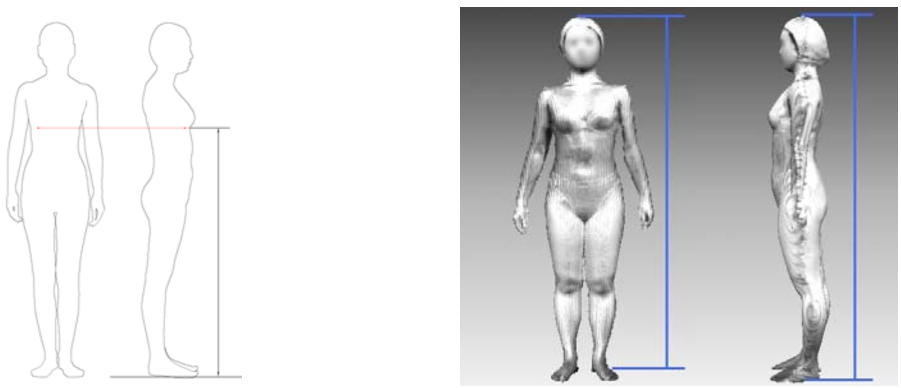

(a) Manual measurements posture (b) 3D scanning posture

Figure 3.1 Standing measurement postures in measuring process (AIMER HEC-BICT, 2004)

3.2.2 Determination of Landmarks

In addition to the traditional methods of determining body landmarks for clothing construction (Miyoshi, 2001), additional measuring points (Zheng, 2002) have been developed and used in this survey, based on the subcutaneous bone framework of the human body related to the breast measurements. The specific upper torso points are shown in Figure 3.2, and all landmarking points are defined in Table 3.1. The common body measuring lines adopted and their definitions (Miyoshi, 2001) are shown in Table 3.2 and Figure 3.3.

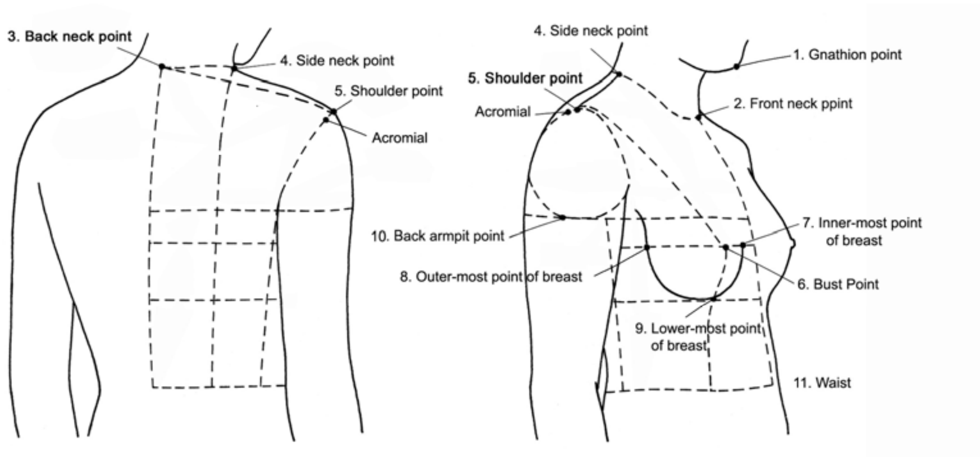

Figure 3.2 Breast anthropometric measuring points (Miyoshi, 2001; Zheng, 2002

Table 3.1 The definitions of breast anthropometric measuring points

Measuring points	Definition
1. Gnathion point	The lowest point of the mandible in the midline.
2. Front neck point	The midpoint between two collarbones, at the centre of the front neck base girth.
3. Back neck point (Cervicale)	The base of the neck portion of the spine, located at the tip of the spinous process of the 7th cervical vertebra, determined by palpation, often found by bending the neck or head forward (McConville, 1979; Jones, 1929; Gordon et al., 1989; O’Brien & Shelton, 1941; ASTM, 1999; Miyoshi, 2001).
4. Side neck point	The intersection point of the neck base line and the anterior border of the trapezius muscle.
5. Shoulder point (Acromion[1])	As viewed from the side, is the intersection point of the arm hole girth passing the acromial and a line running down the middle of the shoulder from the side neck point to the tip of the shoulder.

[1] Acromion: the outer end of the acromial process of the scapula to which the collarbone is attached.

Table 3.1 (continued)

5. Shoulder point (Acromion[2])_continued	It is the most prominent point on the upper edge of the acromial process of the shoulder blade (scapula) as determined by palpation (Jones, 1929; McConville, 1979).
6. Bust point	The centre of the most prominent point on the naked bust, or the most prominent protrusion of the bra cup (Gordon et al., 1989; McConville, 1979; O'Brien & Shelton, 1941).
7. Inner-most point of the breast	The inner intersection point of a horizontal line across the bust point and the under edge of the breast.
8. Outer-most point of the breast	The outer intersection point of a horizontal line across the bust point and the under edge of the breast.
9. Lower-most point of the breast	The lower intersection point of a vertical line across the bust point and the under edge of the breast.
10. Back armpit point	The lowest point of the back axillaries[3] posterior, or the point at the lower (inferior) edge, determined by placing a straight edge horizontally and as high as possible into the armpit without compressing the skin and marking the front and rear points or the hollow part under the arm at the shoulder (McConville, 1979; ASTM, 1999).
11. Waist (natural indentation)	The point of greatest indentation on the silhouette of the right side of the torso as viewed from the front of the subject. The waist position is also defined as half the distance between the 10th rib and iliocristale landmarks (Gordon et al., 1989). Some define it as the location between the lowest rib and the hip identified by bending the body to the side (ASTM, 1999).
12. Crown	Top of the head (ASTM, 1999; O'Brien & Shelton, 1941).
13. Abdominal extrusion	As viewed from the side, is the greatest protuberance point of the abdomen, usually taken at the high hip level (ASTM, 1999), taken approximately 3 inches below the waist, parallel to the floor (ASTM, 1995a; ASTM, 1995b).
14. Hip extrusion	As viewed from the side, is the greatest protuberance point of the hip.

Table 3.2 The definitions of breast anthropometric measuring lines

Measuring lines	Definition
Chest line	Line across the back armpit points.
Bust line	Line across the bust points.
Underbust line	Line across the lowest edge of the breasts. If two breasts vary, the right side breast is used.
Waist line	Line across the inner-most point on the right side of the torso.
Abdomen line	Line across the abdominal extrusive point.
Hip line	Line across the hip extrusive points.

[2] Acromion: the outer end of the acromial process of the scapula to which the collarbone is attached.
[3] Axillary: relating to or located near the axilla.

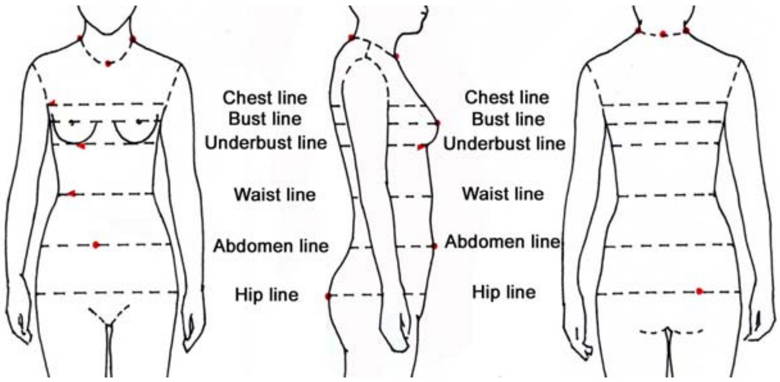

Front view Side view Back view

Figure 3.3 Anthropometric measurement lines

3.2.3 Anthropometric Devices

After identifying the anthropometric measuring points and lines on the surface of the human subjects, the 3D body scanner (VOXELAN LPW-2000FW) was used to record the xyz coordinates from the subjects' surface.

VOXELAN LPW-2000FW (Figure 3.4) is a popular human body measuring system developed by the producer following experience accumulated after over ten years of body measuring. It uses eight CCD cameras and four laser light sources to capture a subject, and has a measurement volume of 200cm (H) × 85cm (W) × 60 cm (D). It can take only 5 seconds to scan one subject by using a vertical laser scanning technique. A 10 seconds measuring routine is also available to obtain more exact data. The structure of this system is designed to be friendly to subjects. The scanner booth is big enough with dimensions of 375cm (W) × 265cm (D) × 162 cm (H) so that the subjects feel easy during scanning. The producer claims that the output data consists of up to 1.1 million points and the accuracy is 1mm (website from Hamano Engineering).

Moreover, in order to obtain more comprehensive information from the breast, Martin's techniques (manual measurements) were used to measure complementary items apart from the 3D body scanned data.

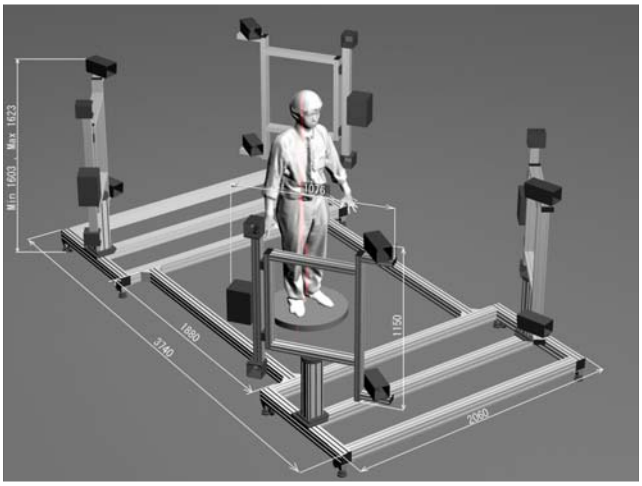

Figure 3.4 3D body scanner -- VOXELAN LPW-2000FW (website from Hamano Engineering)

3.3 Sampling and Conventional Breast Measurements

3.3.1 Sampling

456 female Chinese women subjects aged between 20 and 39 from AIMER HEC-BICT's annual human measuring survey in 2003 were chosen to be part of this study. According to ISO 15535 (2003), the age range of this sample can be divided into four age groups: 20~24 (n=61), 25~29 (n=237), 30~34 (n=119) and 35~39 (n=39). The sample consisted of 78.3% subjects from the Northeastern & Northern of China, 11.2% from the Midwest of China, and 10.5% from of Middle reaches and Lower reaches of the Changjiang River (Zhou et al., 1992). The 456 female subjects were representative

of the general intimate apparel market; 51.1% were married, and about a third had one or two children.

3.3.2 Conventional 3D Body Dimension Data Measurements

The primary objective of the current study is to develop a new sizing chart for bra design. 3D scan data were chosen for further data analysis because an expanded set of body measurement variables can be defined and obtained from the 3D surface based on the x, y, z coordinates; and 3D body scan data are generally regarded as more accurate, numerous and sophisticated than the manual measurement (Loker, Ashdown & Schoenfelder, 2005; Simmons & Istook, 2003; Jones & Rioux, 1997).

First, redundant points were eliminated from the 3D body scan data from VOXELAN LPW-2000FW. Second, missing data was simulated by constructing a polygonal structure to fill the hole. After the 3D body point clouds from the front view and back view were merged, the scan data was transferred into 3D-Rugle (a software package developed by Medic Engineering Corporation) for processing, displaying and measuring. 3D-Rugle software allows a 3D visualization for measuring height, width, thickness, circumference, surface area, slice area and volume.

Twenty-nine variables (see Figure 3.5) that are normally used for identifying the breast shape were selected for measurements from the 3D body scan. They included height, width, thickness, girth, surface distance and detailed breast measurement items.

Vertical measurements	
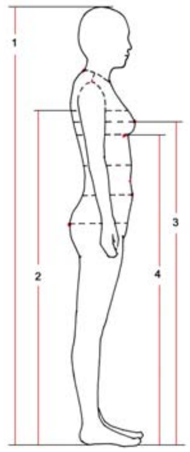	1 D001 Whole body height 2 D010 Chest height 3 D011 Bust height 4 D012 Underbust height

Width and depth measurements	
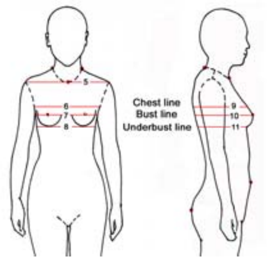 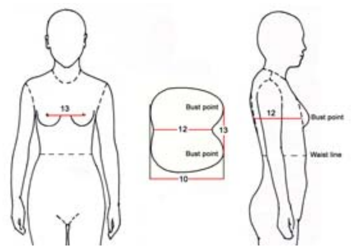	5 D027 Shoulder width 2 6 D038 Chest width 7 D039 Bust width 8 D040 Underbust width 9 D049 Chest depth 10 D050 Bust depth 11 D052 Underbust depth 12 D051 Median chest depth 13 D059 Bust point width

Surface distance measurements	
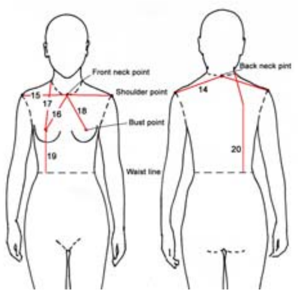	14 D031 Cross shoulder length over back neck point 15 D103 Cross shoulder length over front neck point 16 D068 Length from front neck point to right bust point 17 D069 Length from side neck point to right bust point 18 D104 Length from front neck point to left bust point 19 D066 Front waist length over bust 20 D067 Back waist length over shoulder blade

Girth measurements	
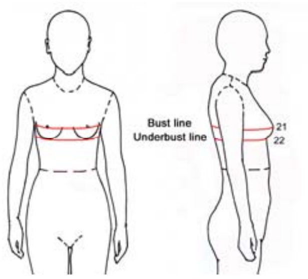	21 D091 Bust girth 22 D092 Underbust girth

Detailed breast measurements and complementary items		
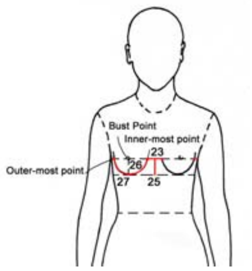	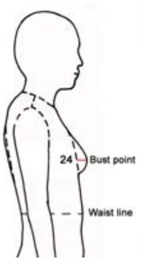 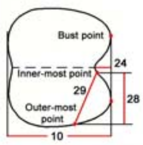	23 D060 Horizontal distance between inner-most point of bust 24 D062 Centre breast depth 25 D083 Centre bridge height 26 D084 Inner arc length of right breast root 27 D085 Total arc length of right breast root 28 D105 Width of the breast_a 29 D110 Width of the breast_b

Figure 3.5 3D measurement variables related to the body and the breast sizing

3.3.3 Complementary Manual Measurements

Camera limitations make the 3D body scanner unable to capture the whole body surface, especially some hidden regions such as armhole and crotch. Therefore, manual measurement data related to “chest girth” were combined into the 3D database for further analysis. Moreover, some variables can only be measured by manual techniques, including “weight”, “fat thickness of the upper arm”, “fat thickness of the back” and “vertical arc length from right bust point to underbust”, which were also added into the 3D database. These five variables were shown in Figure 3.6.

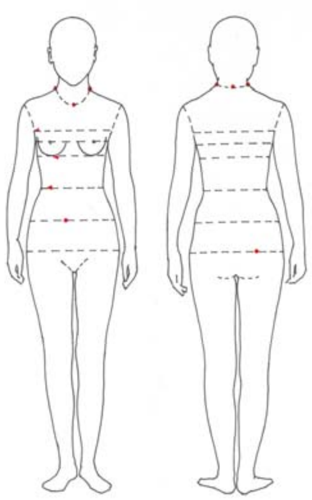	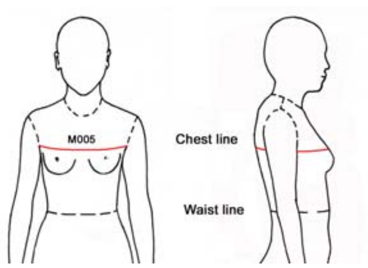	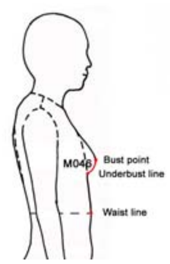
	M005 Chest girth	M046 Vertical arc length from right bust point to underbust (BP~UBL)
	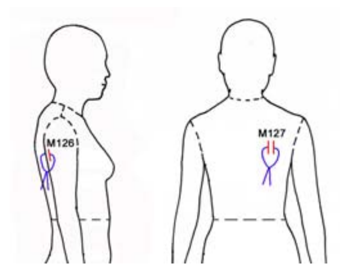	
M130 Weight	M126 Fat thickness of the upper arm	M127 Fat thickness of the back

Figure 3.6 Complementary manual measurement items

3.3.4 Data Preparation

In order to avoid making mistakes in collecting data, statistical and reliability checks were conducted for all the data collected using the Martin method (Martin, 1957; Miyoshi, 2001) and the 3D scanning method before doing further data analysis.

Firstly, according to ISO 15535 (2003), the mean value and the standard deviation of each variable were obtained by using SPSS. Then the measurement data more than ±3 SD (standard deviation) from the mean were reviewed individually for accuracy. Secondly, scatter diagrams such as Box-plots were drawn for each measured dimension to discover the outliers for re-investigating. The data were corrected if the cause of the discrepancy was clear. Alternatively, the data were replaced with "9999" as missing values if the cause was not clear.

The "Empirical Rule[4]" indicates that for normal model data, about 99.7% of the values fall with three standard deviations of the mean. So, in order to avoid incorrect data being included in the database, any data having an absolute value of over 4 standard deviation from the mean were deleted from the original files ("Japanese body size data 1992-1994", 1997).

3.3.5 Descriptive Statistics Results of Conventional Breast Measurements

Descriptive statistics and percentiles for 34 conventional breast measurements were calculated using SPSS. The results, including mean, standard deviation (SD), coefficient of variation (CV) and selected percentiles (5th, 50th, 95th) are presented in Table 3.3. The variability of the different measurements can be observed and compared from indices such as SD and CV. It can be seen that the current sample had particularly large CV values for some measurements, including "M126 Fat thickness of the upper arm", "M127 Fat thickness of the back", "D060 Horizontal distance between inner-most point of bust", and "D062 Centre breast depth".

[4] The rule was first published by Abraham De Moivre in 1733.

Table 3.3 Descriptive statistics summary of new measurement variables

Measurement	N	Mean (cm)	Std. Deviation (cm)	CV (%)	Percentiles 5th	50th	95th
M130 Weight (g)	455	55.46	7.93	14.30	45.25	54.23	69.96
M005 Chest girth	456	84.67	5.44	6.42	77.00	83.70	93.93
M046 Vertical arc length from right bust point to underbust (BP~UBL)	455	6.95	1.17	16.77	5.30	7.00	9.00
M126 Fat thickness of the upper arm	456	29.15	8.17	28.04	16.63	29.00	43.00
M127 Fat thickness of the back	455	24.98	9.20	36.81	12.13	23.50	41.88
D001 Whole body height	456	159.97	5.24	3.27	151.69	159.68	168.83
D010 Chest height	456	117.93	4.50	3.81	111.05	117.92	125.34
D011 Bust height	456	112.84	4.76	4.22	105.32	112.99	120.70
D012 Underbust height	456	107.57	4.51	4.19	100.73	107.66	114.78
D027 Shoulder width 2	456	32.91	1.80	5.45	30.00	33.00	35.59
D031 Cross shoulder length over back neck point (SP2~BNP~SP2)	455	36.59	1.93	5.27	33.50	36.65	39.50
D038 Chest width	456	28.95	1.99	6.86	26.00	28.67	32.66
D039 Bust width	456	27.85	1.90	6.81	25.00	27.66	31.05
D040 Underbust width	456	26.55	1.75	6.59	24.00	26.33	29.66
D049 Chest depth	455	21.58	1.90	8.80	18.75	21.34	24.67
D050 Bust depth	456	22.77	2.36	10.37	19.43	22.50	26.63
D051 Median chest depth	456	19.66	1.92	9.77	17.00	19.45	22.88
D052 Underbust depth	456	20.20	2.25	11.13	17.15	19.72	24.00
D059 Bust point width	456	19.19	1.79	9.33	16.33	19.00	22.33
D060 Horizontal distance between inner-most point of bust	456	1.80	0.72	39.90	0.67	1.70	3.02
D062 Centre breast depth	456	1.80	0.91	50.42	0.61	1.65	3.49
D066 Front waist length over bust	456	40.77	2.29	5.61	37.30	40.60	44.68
D067 Back waist length over shoulder blade	456	39.81	2.05	5.14	36.20	39.80	43.20
D068 Length from front neck point to right bust point (FNP~RBP)	456	21.12	2.18	10.33	18.13	20.80	24.99
D069 Length from side neck point to right bust point (SNP~BP)	455	25.86	2.51	9.71	22.20	25.55	30.28
D083 Centre bridge height	456	5.42	0.99	18.32	3.69	5.46	7.00
D084 Inner arc length of right breast root	456	10.90	1.24	11.36	9.13	10.80	13.20
D085 Total arc length of right breast root	456	22.20	2.33	10.49	19.00	21.90	26.10
D091 Bust girth	456	88.88	7.27	8.18	78.44	87.81	102.14
D092 Underbust girth	456	77.22	6.05	7.83	68.33	76.14	87.71
D103 Cross shoulder length over front neck point (SP2~FNP~SP2)	450	34.57	1.72	4.96	31.70	34.50	37.20

Table 3.3 (continued)

D104 Length from front neck point to left bust point (FNP~LBP)	456	21.45	2.22	10.34	18.40	21.30	25.20
D105 Width of the breast_a	455	12.24	1.25	10.25	10.33	12.16	14.29
D110 Width of the breast_b	455	14.42	1.37	9.50	12.42	14.35	16.69

3.4 Comparison of Sample Distributions

It is clear that the population measures can be used to define the body size range and the body shape differences of people. However, the high cost of obtaining the measurements limits the use of population measures in any sizing system development (Winks, 1997). Therefore, it is very important to identify a representative sample of the population that can reflect the whole population (Ashdown, 2003).

Obviously the sample used in this study cannot cover the whole population of Chinese women aged from 20 to 39. Consequently, it is important to compare the distribution of key dimensions between the current sample and the sample that were used for establishing the existing bra sizing system. The existing bra sizing system, renewed in 2004, was designed based on a sample of size 5,507. The sample was randomly stratified by area and age according to the Chinese population. The dimensions were obtained by manual measurement in 1987 (Zhou et al., 1992). Four key measurements generally relevant for building the bra sizing system were investigated including “bust girth”, “underbust girth”, “weight” and “whole body height”. The two sample histograms for each dimension were put on the same classification scale for easy comparison.

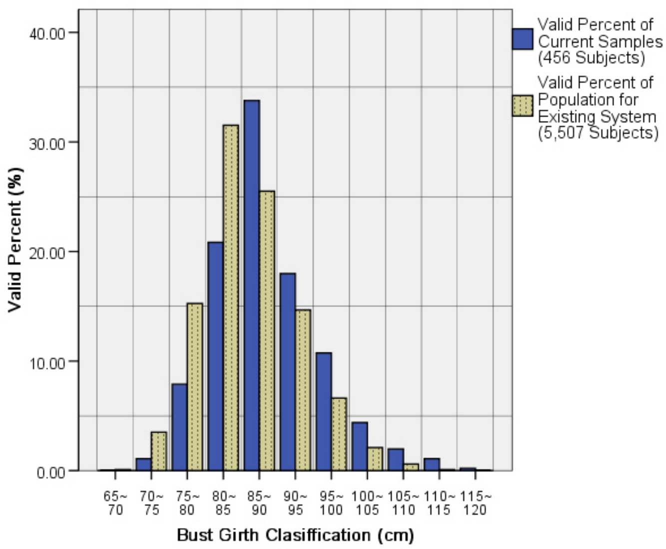

Figure 3.7 The distribution histogram comparison of bust girth for two samples

Table 3.4 Distribution comparisons between the current sample and the sample for building the existing sizing system (bust girth)

Bust girth classification (cm)	Frequency (persons)	Percent of current sample (%)	Valid percent of sampling for existing sizing system (%)
65~70	0	0.00	0.10
70~75	5	1.10	3.51
75~80	36	7.89	15.26
80~85	95	20.83	31.53
85~90	154	33.77	25.50
90~95	82	17.98	14.66
95~100	49	10.75	6.63
100~105	20	4.39	2.11
105~110	9	1.97	0.60
110~115	5	1.10	0.10
115~120	1	0.22	0.00
Total	456	100.00	100.00

Figure 3.7 and Table 3.4 relate to the comparison of bust girth distributions. The histogram shows that the two distributions of samples are approximately symmetric but are slightly skewed to the right. We can see that the two distributions have similar trend curves even though they have different modal groups. The current sample's histogram is

centred on the 85~90cm group. The most of the other histogram is in the 80~85cm group.

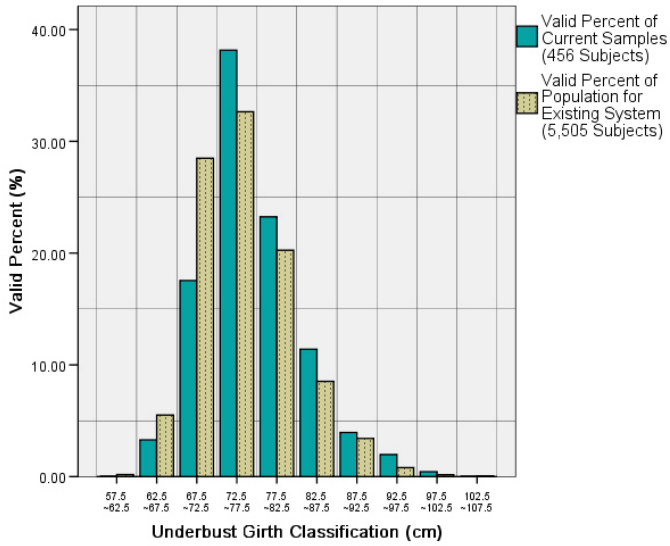

Figure 3.8 The distribution histogram comparison of underbust girth for two samples

Table 3.5 Distribution comparisons between the current sample and the sample for building the existing sizing system (underbust girth)

Underbust girth classification (cm)	Frequency (persons)	Percent of current sample (%)	Valid percent of sampling for existing sizing system (%)
57.5~62.5	0	0.00	0.18
62.5~67.5	15	3.29	5.50
67.5~72.5	80	17.54	28.48
72.5~77.5	174	38.16	32.64
77.5~82.5	106	23.25	20.26
82.5~87.5	52	11.40	8.52
87.5~92.5	18	3.95	3.42
92.5~97.5	9	1.97	0.80
97.5~102.5	2	0.44	0.16
102.5~107.5	0	0.00	0.04
Total	456	100.00	100.00

Figure 3.8 and Table 3.5 show a comparison of the underbust girth distributions. It can be seen that the distributions of the current sample and of the sample for establishing

existing bra sizing system have the same modal group, i.e. the 72.5~77.5cm group. As Table 3.5 reveals, there are about one third of subjects in the centre group in both samples. The two histograms are approximately symmetrical and have a very short tail on the right. According to the descriptive statistic results, the skewness of the current sample and the sample for establishing existing bra sizing system are 0.762 and 0.719, and the kurtosis are 0.690 and 0.632. This means although the two histograms have a very short tail on the right, they still approximately belong to a normal distribution.

Figure 3.9 and Table 3.6 illustrate the comparison of the weight distributions based on the 455 subjects. The histogram shows that the distributions of current sample and the sample for establishing existing bra sizing system have the same centre in the 50~55kg group, which included about one fourth of the subjects in each case.

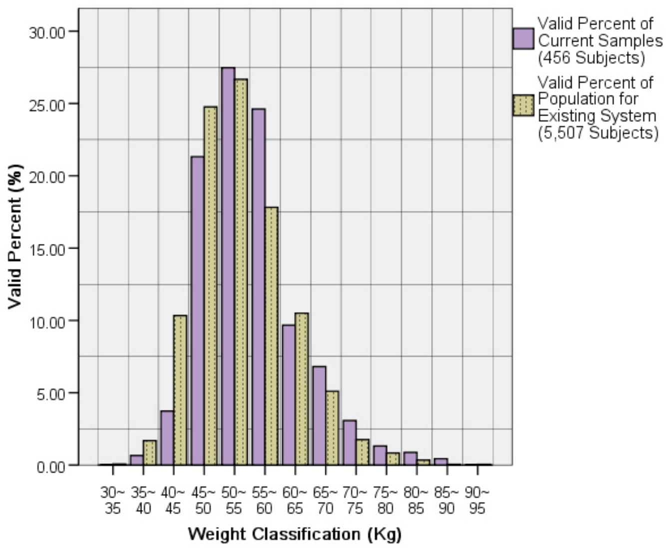

Figure 3.9 The distribution histogram comparison of weight for two samples

Table 3.6 Distribution comparisons between the current sample and the sample for building the existing sizing system (weight)

Weight classification (Kg)	Frequency (persons)	Percent (%)	Valid percent of current sample (%)	Valid percent of sampling for existing sizing system (%)
30~35	0	0.00	0.00	0.07
35~40	3	0.66	0.66	1.69
40~45	17	3.73	3.74	10.34
45~50	97	21.27	21.32	24.76
50~55	125	27.41	27.47	26.67
55~60	112	24.56	24.62	17.82
60~65	44	9.65	9.67	10.50
65~70	31	6.80	6.81	5.10
70~75	14	3.07	3.08	1.76
75~80	6	1.32	1.32	0.84
80~85	4	0.88	0.88	0.35
85~90	2	0.44	0.44	0.05
90~95	0	0.00	0.00	0.05
Missing	1	0.22	100.00	100.00
Total	456	100.00		

As shown in Figure 3.9 and Table 3.6, although the two histograms have a short tail on the right, according to the descriptive statistic results, the skewness of the current sample and the sample for establishing existing bra sizing system are 0.713 and 0.913, they are still nearly symmetrical and approximately belong to a normal distribution.

Figure 3.10 and Table 3.7 reveal the comparison of the whole body height distributions. The two histograms are practically symmetrical. We can also observe that the distributions of the two samples have the same modal group, the 155~160cm group, which included 37.94% and 35.71% of the subjects respectively.

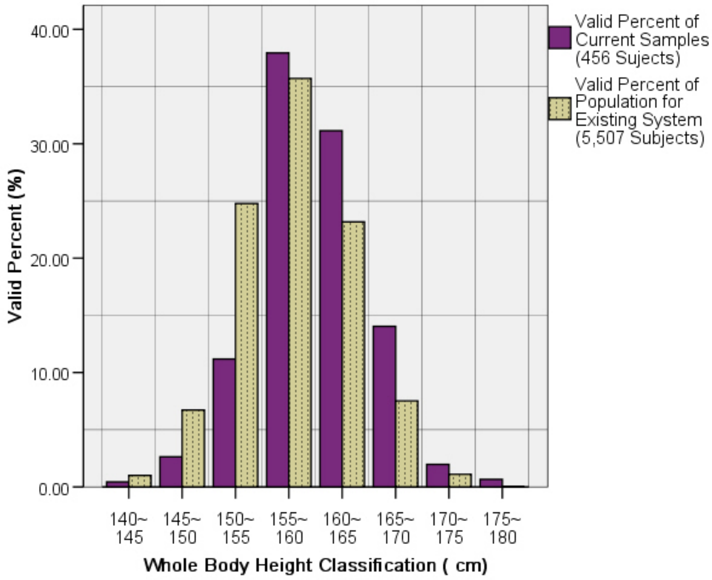

Figure 3.10 The distribution histogram comparison of whole body height for two samples

Table 3.7 Distribution comparisons between the current sample and the sample for building the existing sizing system (whole body height)

Whole body height classification (cm)	Frequency (persons)	Percent of current sample (%)	Valid percent of sampling for existing sizing system (%)
140~145	2	0.44	1.00
145~150	12	2.63	6.72
150~155	51	11.18	24.77
155~160	173	37.94	35.71
160~165	142	31.14	23.17
165~170	64	14.04	7.52
170~175	9	1.97	1.10
175~180	3	0.66	0.00
Total	456	100.00	100.00

The above comparison results indicate that the sample used in this study have similar distributions of key dimensions as one generally used for evaluating the body shape of the population. Furthermore, Chi-square was used to test the homogeneity of the four key measurements between two samples at 5% level of significance. The null hypothesis is that the distribution does not change from current sample to the sample for establishing the existing bra sizing system. As shown in Table 3.8, the test p-values of four key measurements are all over 0.05, namely we can not reject the null hypothesis. Since the sample used for establishing the existing sizing system was representative of the population, the above discussion results mean that we can have a strong confidence that the research findings based on the current subjects can approximately represent the whole related population.

Table 3.8 Chi-square test results of four key measurements

Measurement variable	Chi-square value	P-value
Bust girth	5.647	0.342
Underbust girth	4.580	0.469
Weight	4.944	0.551
Whole body height	2.139	0.710

3.5 One-way ANOVA Analysis for Detailed Breast Measurements Based on Demographic Information

In order to investigate whether there were any significant differences among age groups, One-way ANOVA analysis was conducted for the 3D items relevant to detailed breast measurements. The hypothesis test value was set at the 5% level of significance. Table 3.9 presents the descriptive statistics for the four age groups for each of the nine variables, and their ANOVA test results. Apart from the variables “total arc length of right breast root” and “centre bridge height”, the p-values of the other seven variables are greater than 0.05, namely the overall F-value of other seven variables are not significant. This means that there are no significant differences among different age groups for these seven variables.

Likewise, One-way ANOVA results for the procreation situation are almost similar to the results based on age group factor. From Table 3.10, we can observe that there are significant differences between "has no child" subset and "has one child or more" subset on the variables "total arc length of right breast root", "BP~UBL" and "centre bridge height".

Table 3.9 One-way ANOVA analysis results for 3D measuring items relevant to detailed breast measurements among age groups

Variables	Age group	N	Mean (cm)	Std. Deviation (cm)	95% Confidence Interval for Mean (cm)		Levene test of Homogeneity of Variances (Sig.)	ANOVA test (Sig.)
					Lower Bound	Upper Bound		
D084 Inner arc length of right breast root	20-24	61	10.84	1.24	10.53	11.16	0.086	0.465
	25-29	237	10.83	1.16	10.68	10.98		
	30-34	119	11.00	1.40	10.75	11.25		
	35-39	39	11.09	1.19	10.70	11.47		
D085 Total arc length of right breast root	20-24	61	21.88	2.17	21.32	22.44	0.061	0.004
	25-29	237	21.92	2.19	21.64	22.20		
	30-34	119	22.78	2.60	22.31	23.25		
	35-39	39	22.66	2.18	21.95	23.36		
M046 BP~UBL	20-24	60	7.13	1.15	6.84	7.43	0.386	0.064
	25-29	237	7.03	1.15	6.88	7.17		
	30-34	119	6.80	1.16	6.59	7.01		
	35-39	39	6.64	1.28	6.22	7.05		
D083 Centre bridge height	20-24	61	5.69	1.04	5.43	5.96	0.625	0.001
	25-29	237	5.51	0.94	5.39	5.63		
	30-34	119	5.19	1.05	5.00	5.38		
	35-39	39	5.17	0.85	4.89	5.45		
D060 Horizontal distance between inner-most point of bust	20-24	61	1.82	0.74	1.63	2.01	0.139	0.103
	25-29	237	1.87	0.75	1.77	1.96		
	30-34	119	1.67	0.65	1.56	1.79		
	35-39	39	1.74	0.68	1.52	1.96		
D062 Centre breast depth	20-24	61	1.75	0.84	1.53	1.96	0.856	0.665
	25-29	237	1.79	0.92	1.67	1.90		
	30-34	119	1.87	0.93	1.70	2.04		
	35-39	39	1.69	0.87	1.41	1.97		

Table 3.9 (continued)

D105 Width of the breast_a	20-24	61	12.30	1.09	12.02	12.58	0.244	0.962
	25-29	237	12.21	1.25	12.05	12.37		
	30-34	119	12.20	1.37	11.95	12.45		
	35-39	39	12.26	1.37	11.82	12.71		
D110 Width of the breast_b	20-24	61	14.26	1.22	13.95	14.58	0.319	0.524
	25-29	237	14.38	1.35	14.21	14.55		
	30-34	118	14.51	1.43	14.25	14.77		
	35-39	39	14.61	1.54	14.11	15.11		
D059 Bust point width	20-24	61	18.78	1.61	18.36	19.19	0.556	0.152
	25-29	237	19.26	1.85	19.02	19.50		
	30-34	119	19.16	1.76	18.84	19.47		
	35-39	39	19.55	1.69	19.01	20.10		

Table 3.10 One-way ANOVA analysis results for 3D measuring items relevant to detailed breast measurements depending on procreation situation

Variables	Procreation situation	N	Mean (cm)	Std. Deviation (cm)	95% Confidence Interval for Mean (cm)		Test of Homogeneity of Variances (Sig.)	ANOVA test (Sig.)
					Lower Bound	Upper Bound		
D084 Inner arc length of right breast root	Has no child	284	10.91	1.17	10.77	11.05	0.010	0.672
	One child or above	147	10.96	1.39	10.74	11.19		
D085 Total arc length of right breast root	Has no child	284	21.99	2.17	21.74	22.25	0.005	0.001
	One child or above	147	22.80	2.61	22.37	23.22		
M046 BP~UBL	Has no child	283	7.04	1.14	6.90	7.17	0.260	0.018
	One child or above	147	6.76	1.19	6.56	6.95		
D083 Centre bridge height	Has no child	284	5.60	0.95	5.49	5.72	0.561	0.000
	One child or above	147	5.04	1.00	4.87	5.20		
D060 Horizontal distance between inner-most point of bust	Has no child	284	1.80	0.72	1.72	1.89	0.476	0.280
	One child or above	147	1.73	0.67	1.62	1.84		
D062 Centre breast depth	Has no child	284	1.75	0.95	1.64	1.86	0.258	0.148
	One child or above	147	1.88	0.85	1.74	2.02		
D105 Width of the breast_a	Has no child	284	12.29	1.23	12.15	12.43	0.174	0.156
	One child or above	147	12.10	1.38	11.88	12.33		
D110 Width of the breast_b	Has no child	284	14.41	1.33	14.26	14.57	0.152	0.790
	One child or above	146	14.45	1.50	14.20	14.69		
D059 Bust point width	Has no child	284	19.20	1.83	18.98	19.41	0.668	0.851
	One child or above	147	19.23	1.77	18.94	19.52		

Table 3.11 One-way ANOVA analysis results for 3D measuring items relevant to detailed breast measurements depending on subject location

Variables	Location situation	N	Mean (cm)	Std. Deviation (cm)	95% Confidence Interval for Mean (cm)		Test of Homogeneity of Variances (Sig.)	ANOVA test (Sig.)
					Lower Bound	Upper Bound		
D084 Inner arc length of right breast root	Middle & lower reaches of the Changjiang river	48	11.00	1.11	10.68	11.32	0.212	0.814
	Northeast & North	357	10.89	1.28	10.76	11.02		
	Midwest	51	10.85	1.09	10.54	11.15		
D085 Total arc length of right breast root	Middle & lower reaches of the Changjiang river	48	21.85	1.99	21.27	22.43	0.080	0.035
	Northeast & North	357	22.34	2.41	22.09	22.59		
	Midwest	51	21.53	1.85	21.01	22.05		
M046 BP~UBL	Middle & lower reaches of the Changjiang river	48	6.94	1.32	6.56	7.33	0.626	0.868
	Northeast & North	356	6.94	1.16	6.82	7.06		
	Midwest	51	7.03	1.08	6.72	7.33		
D083 Centre bridge height	Middle & lower reaches of the Changjiang river	48	5.64	0.82	5.40	5.88	0.466	0.250
	Northeast & North	357	5.39	1.01	5.28	5.49		
	Midwest	51	5.45	1.01	5.17	5.74		
D060 Horizontal distance between inner-most point of bust	Middle & lower reaches of the Changjiang river	48	1.64	0.76	1.42	1.86	0.536	0.244
	Northeast & North	357	1.82	0.71	1.75	1.90		
	Midwest	51	1.80	0.75	1.59	2.01		
D062 Centre breast depth	Middle & lower reaches of the Changjiang river	48	1.77	0.99	1.49	2.06	0.632	0.925
	Northeast & North	357	1.79	0.90	1.70	1.89		
	Midwest	51	1.84	0.85	1.60	2.08		
D105 Width of the breast_a	Middle & lower reaches of the Changjiang river	48	12.33	1.18	11.99	12.67	0.722	0.867
	Northeast & North	356	12.23	1.27	12.09	12.36		
	Midwest	51	12.23	1.24	11.88	12.57		
D110 Width of the breast_b	Middle & lower reaches of the Changjiang river	48	14.36	1.11	14.04	14.68	0.114	0.675
	Northeast & North	356	14.44	1.43	14.30	14.59		
	Midwest	51	14.27	1.20	13.94	14.61		
D059 Bust point width	Middle & lower reaches of the Changjiang river	48	18.81	1.47	18.38	19.23	0.353	0.278
	Northeast & North	357	19.25	1.84	19.06	19.44		
	Midwest	51	19.18	1.68	18.71	19.65		

Table 3.11 presents the descriptive statistics and ANOVA test results for the three location groups of the nine variables. It can be seen that, apart from the variable “total arc length of right breast root”, the p-values of the other eight variables are greater than 0.05. This means that there are no significant differences among different location groups for all variables except “total arc length of right breast root”.

It is noticeable that the variable “D085 total arc length of right breast root” gives significant result in the above three cases, and both D085 & “D083 Centre bridge height” give significant results in both cases of age groups and procreation situations. Since the definitions of these two measurements are defined related to the height of the bust point, the above results confirm that the height of the bust point sensitively change depending on several factors, including age, procreation situation and geographic location.

On the whole, it does not seem necessary in future analyses to separate age groups or other factors, since where statistically significant results occur, the differences between the means are not very large.

3.6 New 3D Breast Measurements and Descriptive Statistics Results

Despite the fact that 3D body scanning technologies are developing rapidly, little scientific research has been conducted on the sizing of women’s nude breasts relevant to intimate apparel clothing items such as bras (Lee et al., 2004). In the current study, the research question is how to develop a new bra sizing system based on women’s complex 3D breast shapes. Therefore, the first step was to obtain comprehensive anthropometric data from 3D breast scan data. Apart from the 34 measurements described above, sixty-nine additional 3D measurement items were extracted from the cross-section, side view profile, vertical-section, the breast bottom curve and the whole body.

RapidForm 2004 (a standard software for 3D scanners developed by INST Technology, Inc.) was used to measure variables from the cross-section, the breast bottom curve and the whole body. Shapelin-3D (Zheng et al., 2004) was utilized to obtain vertical information from vertical sections and the side view profile of the upper torso.

3.6.1 New Measurement Variables Relevant to the Breast Cross-section

Before measuring detailed variables, the 3D body scan data were transferred into RapidForm for processing. These data were then re-triangulated, redundant points eliminated, missing data (holes) patched in the scanning process and prepared for measuring. For the breast detail measurements, it was necessary to delete body parts such as head, arms and legs, and to just retain the upper torso for measuring. RapidForm software can visualize 3D body scan data and measure circumference, width, arc length, surface area, volume, and section shape.

Figure 3.11 shows the twenty-two new measurement variables measured on the cross-section through the right side bust point and underbust using RapidForm 2004. Measurements taken on the right breast depended on the four landmarks: the inner-most point of the breast, the outer-most point of the breast, the lower-most point of the breast and bust point (see Table 3.1, no. 6, 7, 8, and 9). The measurements included width, angle, arc length and area of the breast.

D105 Width of the breast_a_inner

D105 Width of the breast_a_outer

D106_1 Thickness of the breast_1

D106_2 Thickness of the breast_2

D107 Outer arc length of right breast (horizontal plane / slanting plane)

D108 Inner arc length of right breast (horizontal / slanting plane)

D109 Outer arc length of left breast (horizontal plane)

D110 Width of the breast_b_inner

D110 Width of the breast_b_outer

D111 Orientation of the breast (angle)

D112 Angle A of right breast cross-section

D113 Angle B of right breast cross-section

Figure 3.11.1 22 additional 3D variables measured from the cross-section of the bust point

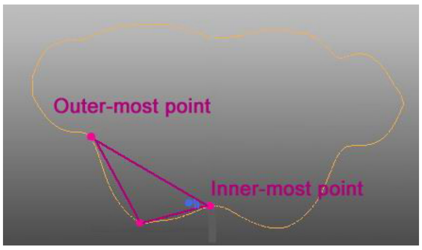

D114 Angle C of right breast cross-section

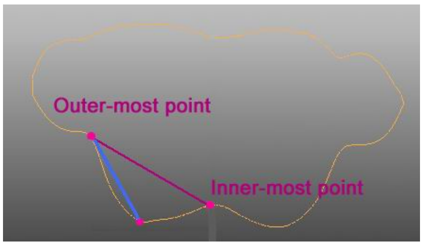

D116 Outer length of right breast cross-section

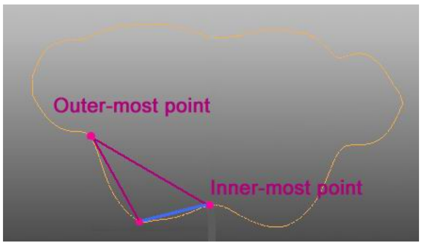

D117 Inner length of right breast cross-section

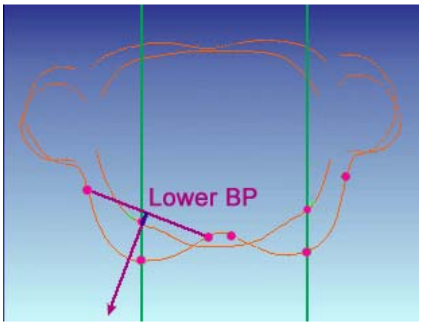

D118 Perpendicular distance from lower-most point of the breast to the base width line of the breast

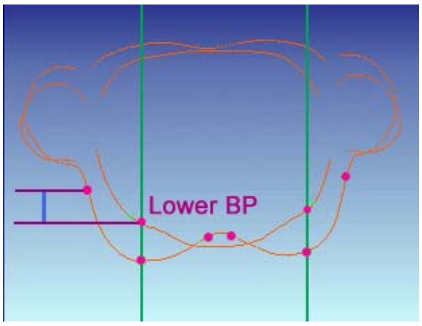

D119 Depth from lower-most point to outer-most point of the breast

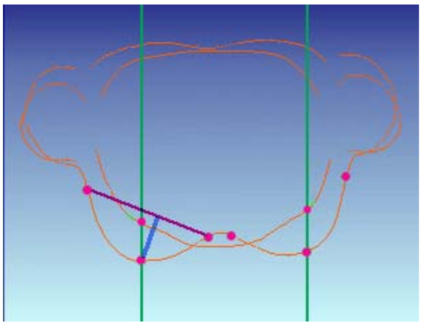

D120 perpendicular distance from bust point to the base width line of the breast (height of the breast)

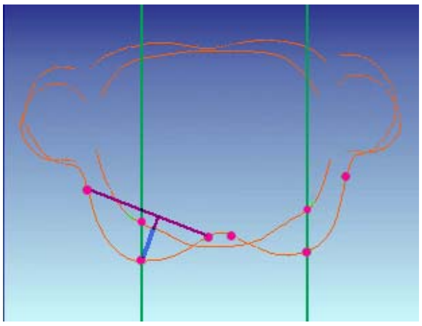

D121 Perpendicular distance from bust point to underbust line

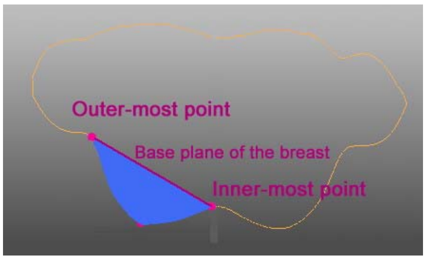

D122 Area of the breast cross-section

Figure 3.11.2 22 additional 3D variables measured from the cross-section of the bust point

3.6.2 New Measurement Variables Relevant to the Breast Root

The global average radius of curvature was used to characterize the breast bottom line. In 2D, the radius of curvature at a point is defined as the radius of the kissing circle that is tangential to the curve at that point. As discussed by Lee et al. (2004), the magnitude of the radius and the direction of circles varied greatly when utilizing the radius of curvature to analyze the breast root curve. “Global average radius of curvature” was therefore suggested as an evaluating parameter and was defined as the radius of the circle passing through three non collinear points.

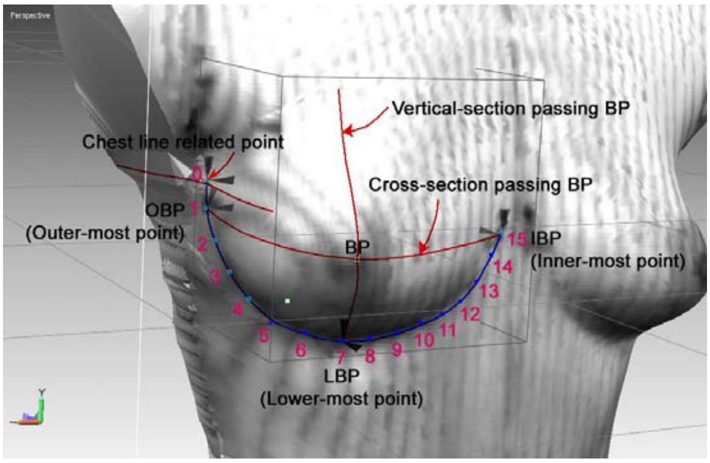

D127 Global average radius of curvature of the under breast curve: the radius of the circle passing through outer-most point (point 1), lower-most point (point 7) and inner-most point (point 15).
D128 Global average radius of curvature of outer breast under curve: the radius of the circle passing through outer-most point (point 1), point 4 and lower-most point (point 7).
D129 Global average radius of curvature of inner breast under curve: the radius of the circle passing through lower-most point (point 7), point 11 and inner-most point (point 15).

Figure 3.12 New added 3D measurement items of the breast under curve

As shown in Figure 3.12, global average radius of curvature was re-defined for “outer breast under curvature”, “inner breast under curvature”, and “under breast curvature” according to the 15 key points around the breast bottom line in the current study. Point 1 is the outer-most point at the intersection of the cross-section through bust point and the breast root curve, whereas point 15 is the inner-most point at the crossing. Point 7 is the lower-most point of the breast bottom line located at the vertical-section through bust point. Then the outer breast under curve was divided into 6 equal portions between point 1 and point 7, whilst the inner breast under curve was segmented into 8 equal fractions from point 7 to point 15. Subsequently, the three global average radii of curvatures were measured based on outer-most point (point 1), point 4, lower-most point (point 7), point 11 and inner-most point (point 15), as shown in Figure 3.12.

3.6.3 New Measurement Variables Relevant to the Volume

Bra cup design is necessarily related to the breast shape. It is very important to measure the volume of whole body, upper torso, chest area and breast for evaluation of the breast shape and the whole body shape. Here, five measurement variables relevant to the volume of different body segments (Figure 3.13) were defined and measured by RapidForm software.

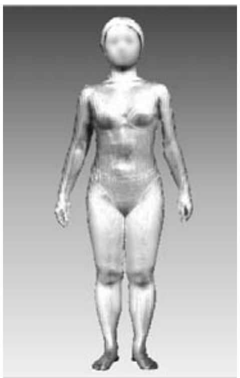

D123 Whole body volume

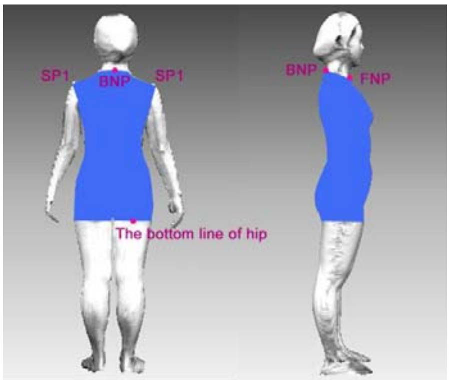

D124 Torso body volume

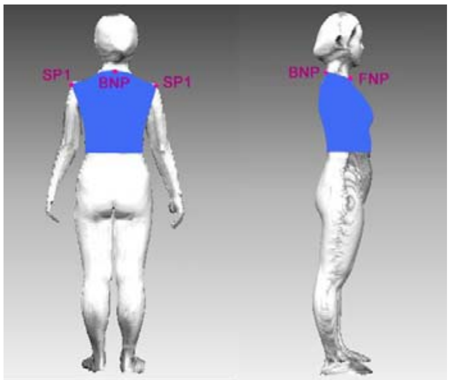

D125 Upper torso body volume

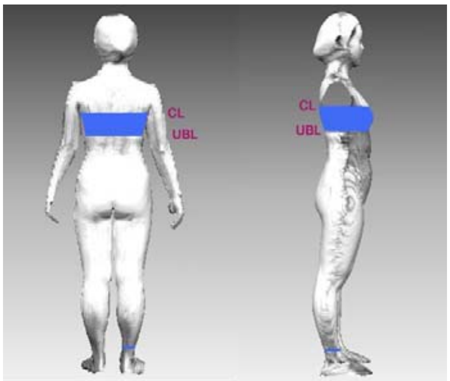

D126 Chest area volume

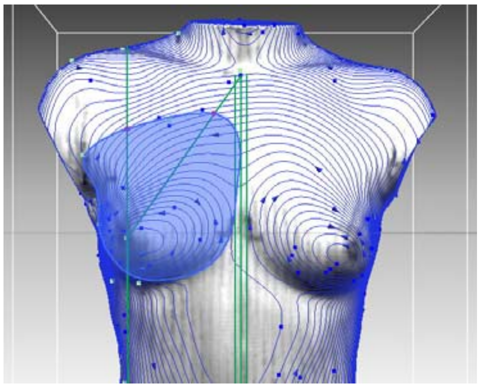

D130 Right breast volume

Figure 3.13 New added 3D measurement items of volume

Before measuring these five variables, any missing data in the scanning process were patched since the volume measures need a closed surface boundary. With the exception of “right breast volume”, the other four measurement items are relatively easy to measure based on the landmarks or measuring lines shown in Figure 3.13.

The breast volume is a very essential dimension related to bra design. Although the volume of a breast can be visualized using the 3D body scan data, it is very difficult to obtain accurate natural breast volumes because the borderline of the breast is not clear enough to be defined separately from the body surface. Medical research studies have investigated breast volume measurements for asymmetry assessment or breast surgery. In contrast, there is limited information relevant to the investigation of the 3D breast shape in the apparel industry. Moreover, many previous studies ignored the curved character of the 3D breast base. Most of the studies assume that the breast base is a circle and the breast bulk is a cone (Lee et al., 2004).

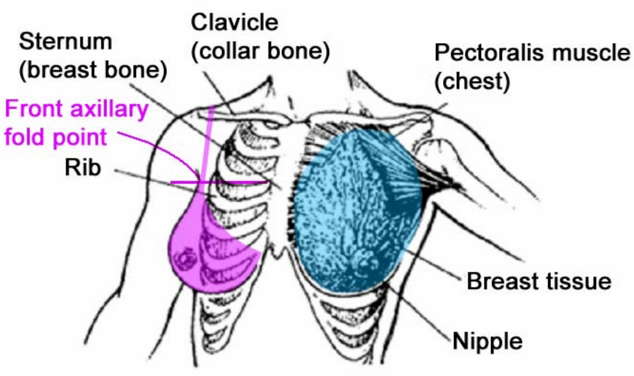

Figure 3.14 The breast anatomy and related bra design area (Yu, 2006)

To achieve a good bra fit, it is important to consider the relationship between the bra dimensions and the breast anatomy (Figure 3.14). Defining the external form of the adult female breast is very difficult since it does not have a clear boundary on the chest wall. Approximately, the breast sits between the second rib to sixth or seventh rib vertically and covers from the costal cartilage to the anterior axillary fold transversely. The upper outer quadrant includes a part of breast tissue extending towards the axilla. The shape of the breast is affected by the fatty tissue, and the lower portion is more rounded than the upper one (Lee et al., 2003/1995; Lamarque, 1981).

As shown in Figure 3.14, the region between two front axillary fold points is the most important area of the body for studying bra design. Normally, the fold point determines the design line for the cup apex, and the underwire curve generally follows the breast root.

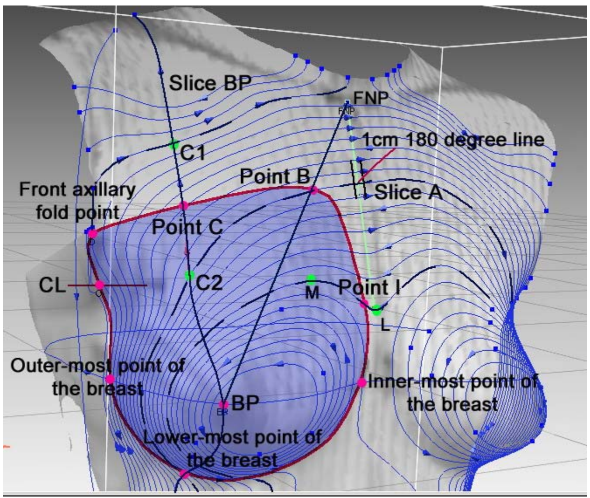

Figure 3.15 The breast boundary defined for volume measure in current study

In this study, a new definition of breast boundary has been established based on vertical slices (Figure 3.15). This 3D breast object contains a total of 20 key points: the 15 points around the breast root mentioned in 3.6.2, a chest line related side point, a front axillary fold point, and 3 newly defined points (denoted by B, C and I). The definitions of these points are given below:

(1) Point B: as shown in Figure 3.15, slice A is the first slice which has a 1cm 180 degree line (horizontal line) at the torso centre from the breast area towards the front neck point. Point B is the intersection point between slice A and the body surface straight line containing the front neck point and the bust point.

(2) Point C: slice BP is the sagittal slice through the right bust point. Point C1 is the intersection point between slice BP and the vertical slice through the right front axillary fold point. C2 is the intersection point between slice BP and vertical slice A. Point C is located on slice BP and is midway between C1 and C2.

(3) Point I: considering the first vertical slice connecting the left breast area and the right breast area, point L is the lowest point at the centre, whereas point M is the highest point on this slice line. Point I is the point between M and L which has the smallest radius of curvature.

3.6.4 New Measurement Variables Relevant to the Breast Vertical-section

Twenty-one measurements were extracted from the vertical side view profile of the upper torso using the Shapeline-3D software. The codes of these measurements, including width length, distance length and angle, are shown in Figure 3.16.

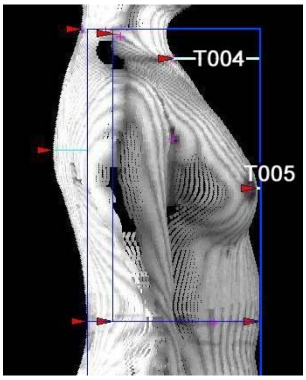

T004/T005

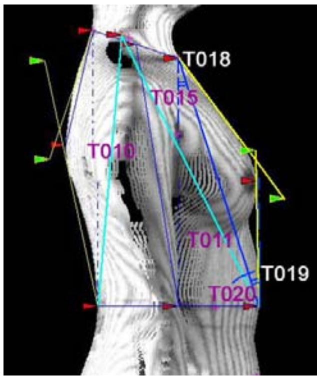

T010, 11, 15, 18, 19, 20

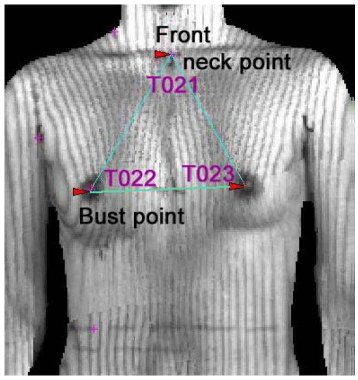

T021, 22, 23

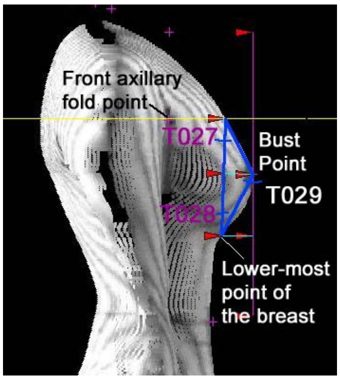

T027, 28, 29

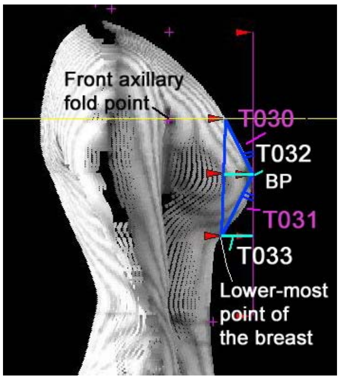

T030, 31, 32, 33

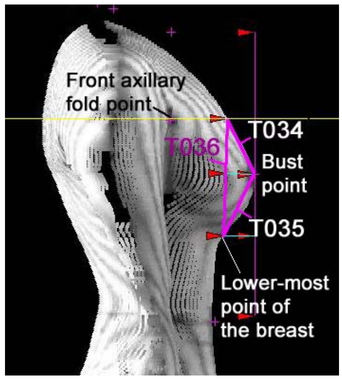

T034, 35, 36

No.	Measurement variables
T004	Horizontal distance from front neck point to front waist centre
T005	Horizontal distance from front waist centre to bust point
T010	Length from side neck point to back waist centre
T011	Length from side neck point to front waist centre
T015	Vertical angle of upper torso from front neck point to front waist centre
T018	Vertical angle of upper breast from front neck point
T019	Vertical angle of lower breast from front waist centre to bust point
T020	Angle rays diverging from the vertex front waist centre to front neck point and bust point
T021	Angle 1 of the breast triangle
T022	Angle 2 of the breast triangle
T023	Angle 3 of the breast triangle
T027	Inner angle of upper breast
T028	Inner angle of lower breast
T029	Inner angle of whole breast
T030	Vertical angle of upper breast
T031	Vertical angle of lower breast
T032	Perpendicular distance from bust point to the slanting line of whole breast
T033	Horizontal distance from lower-most point of the breast to bust point
T034	Length of upper breast leg of breast triangle
T035	Length of lower breast leg of breast triangle
T036	Length of whole breast leg of breast triangle

Figure 3.16 New 3D measurements taken from the vertical shape

3.6.5 New Calculated Measurement Variables

In order to obtain the multi-information about the breast and the whole body, additional calculated measurement variables were defined, based on some of the measurement variables defined in Figures 3.5, 3.6, 3.11.1, 3.11.2 and 3.16. As is shown in Table 3.12, in order to obtain more comprehensive information about the breast, sixteen new calculated variables related to the arc length of the breast, the aspect ratio and chubbiness ratio of the breast were defined. Moreover, the body build indices, Body Mass Index (BMI) (Revicki & Israel, 1986; Gray & Fujioka, 1991) and Volume Height Index (VHI) (Fan et al., 2004a; Fan et al., 2004b), which are regarded as key potential parameters to evaluate the body fat and are highly correlated to body shape classification, were added to the database.

Table 3.12 New calculated measurement variables

No.	Calculated measurement variables
D106	Thickness of the breast = D106 _1 + D106 _2
D134	Total arc length of right breast (horizontal plane) = D107 (horizontal plane) + D108 (horizontal plane)
D135	Total arc length of breast from right to left (horizontal plane) = D107 (horizontal plane) + D108 (horizontal plane) + D059 + D109 (horizontal plane)
D136	Total arc length of right breast (slanting plane) = D107 (slanting plane) + D108 (slanting plane)
C001	Difference between bust girth and underbust girth (3D)
C002	Calculated reverse aspect ratio of bust cross-section = D039 / D050
C003	Calculated reverse aspect ratio of underbust cross-section = D040 / D052
C004	Calculated aspect ratio of the breast 1 = D120 / D110_b (D110_b_inner + D110_b_outer)
C005	Calculated aspect ratio of the breast 2 = D121 / D110_b (D110_b_inner + D110_b_outer)
C006	Calculated chubbiness ratio of the breast 1 = D134 (horizontal plane) / D110 (D110_b_inner + D110_b_outer)
C007	Calculated chubbiness ratio of the breast 2 = D134 (horizontal plane) / D062
C008	Calculated chubbiness ratio of the breast 3 = D136 (slanting plane) / D110_b (D110_b_inner + D110_b_outer)
C009	Calculated chubbiness ratio of the breast 4 = D136 (slanting plane) / D062
C010	Calculated chubbiness ratio of the breast 5 = T032 / T035
C011	Calculated chubbiness ratio of the breast 6 = D134 (horizontal plane) / M046
C012	Calculated chubbiness ratio of the breast 7 = D136 (slanting plane) / M046
C013	Calculated VHI = D123 / $D001^2$ (Volume / $height^2$)
C014	Calculated BMI = M130 / $D001^2$ (Weight / $height^2$)

3.6.6 Descriptive Statistics of the New 3D Breast Measurements

The new measurement data were examined and purified according to the method mentioned in 3.3.4. Descriptive statistics and percentiles for all new measurement variables were calculated using SPSS. The results, including mean, standard deviation (Std. Deviation), coefficient of variation (CV) and selected percentiles (5th, 50th, 95th) are presented in Table 3.13. The variability of the samples in different measurements can be observed from indices such as SD and CV. It can be seen that the current sample had large CVs for some measurements, including angle and ratio items relevant to the gradient of upper torso that have been highlighted in Table 3.13. This means that the gradient of upper torso changed sensitively from person to person.

Table 3.13 Descriptive statistics summary of new measurement variables

		Mean	Std. Deviation	CV	Percentiles		
Measurement	N	(cm)	(cm)	(%)	5th	50th	95th
D105 Width of the breast_a_inner	455	7.75	1.09	14.06	6.11	7.76	9.61
D105 Width of the breast_a_outer	456	4.48	0.92	20.52	3.00	4.43	6.05
D106 Thickness of the breast_1	456	7.52	1.38	18.30	5.32	7.57	9.77
D106 Thickness of the breast_2	456	1.34	0.95	**71.38**	0.09	1.19	3.12
D106 Thickness of the breast	456	8.86	1.38	15.62	6.67	8.81	11.31
D107 Outer arc length of right breast (slanting plane)	456	9.79	1.66	16.90	7.03	9.60	12.50
D107 Outer arc length of right breast (horizontal plane)	456	10.21	1.52	14.89	7.92	10.09	12.88
D108 Inner arc length of right breast (slanting plane)	456	9.04	1.29	14.23	7.10	9.00	11.10
D108 Inner arc length of right breast (horizontal plane)	455	8.08	1.16	14.30	6.32	8.02	10.14
D134 Total arc length of right breast (horizontal plane)	455	18.29	2.16	11.79	14.76	18.08	21.78
D136 Total arc length of right breast (slanting plane)	456	18.83	2.37	12.56	15.30	18.60	23.00
D107 Outer arc length of left breast (horizontal plane)	456	10.40	1.76	16.88	7.77	10.24	13.32
D135 Total arc length of breast from right to left (horizontal plane)	455	47.88	4.77	9.96	40.55	47.53	55.76
D110 Width of the breast_b_inner	455	6.01	1.05	17.50	4.20	6.05	7.64
D110 Width of the breast_b_outer	456	8.41	1.26	14.93	6.60	8.27	10.69
D111 Orientation of the breast (angle)	456	31.53	5.07	16.09	23.09	31.57	39.27
D112 Angle A of right breast cross-section	456	31.07	4.99	16.06	23.14	30.91	39.59

Table 3.13 (continued)

D113 Angle B of right breast cross-section	456	108.67	9.60	8.84	93.31	109.37	124.23
D114 Angle C of right breast cross-section	456	40.26	7.09	17.62	30.45	39.59	52.35
D116 Outer length from right breast cross-section	456	9.86	1.37	13.94	7.82	9.71	12.23
D117 Inner length from right breast cross-section	455	7.92	1.11	14.00	6.17	7.91	9.84
D118 Perpendicular distance from lower-most point of the breast to the base width line of the breast	456	1.98	0.66	**33.33**	0.92	2.03	3.06
D119 Depth from lower-most point to outer-most point of the breast	456	5.08	1.09	21.54	3.39	5.12	6.85
D120 Height of the breast	456	5.07	1.01	19.99	3.47	5.02	6.64
D121 Perpendicular distance from bust point to underbust line	456	2.91	1.03	**35.18**	1.26	2.81	4.64
D122 Area of the breast cross-section (cm^2)	455	41.59	10.90	26.22	24.68	40.22	60.32
D123 Whole body volume (cm^3)	455	56624.33	8244.19	14.56	45961.20	55386.65	71967.63
D124 Torso body volume (cm^3)	455	32045.99	5307.12	16.56	24713.33	31107.27	41083.73
D125 Upper torso body volume (cm^3)	454	15512.15	2818.79	18.17	11487.36	14983.61	20193.12
D126 Chest area volume (cm^3)	455	5671.05	1451.71	25.60	3658.92	5523.04	8393.38
D127 Global average radius of curvature of the breast under curve	456	74.59	7.51	10.06	63.38	73.67	87.61
D128 Global average radius of curvature of outer breast under curve	455	78.30	14.63	18.69	57.86	77.02	105.84
D129 Global average radius of curvature of inner breast under curve	454	70.90	9.29	13.11	57.06	69.95	86.34
D130 Right breast volume (cm^3)	452	381.23	139.53	**36.60**	191.76	367.38	647.04
T004 Horizontal distance from front neck point to front waist centre (°)	455	8.14	1.77	21.74	5.40	8.00	11.28
T005 Horizontal distance from front waist centre to bust point (°)	455	0.09	1.38	**1502.98**	-2.075	0.10	2.48
T010 Length from side neck point to back waist centre (°)	455	36.41	1.67	4.59	33.56	36.43	38.89
T011 Length from side neck point to front waist centre (°)	455	39.06	1.73	4.43	36.22	39.00	41.90
T015 Vertical angle of upper torso from front neck point to front waist centre (°)	455	14.64	3.05	20.82	9.65	14.48	19.95
T018 Vertical angle of upper breast from front neck point (°)	455	27.78	4.58	16.47	20.69	27.59	35.26
T019 Vertical angle of lower breast from front waist centre to bust point (°)	455	0.97	5.84	**603.99**	-7.72	0.39	11.69
T020 Angle rays diverging from the vertex front waist centre to front neck point and bust point (°)	454	15.18	4.99	**32.84**	7.72	14.84	23.64
T021 Angle 1 of the breast triangle (°)	455	53.86	4.62	8.57	45.43	53.95	61.54
T022 Angle 2 of the breast triangle (°)	455	64.05	2.96	4.62	59.48	63.88	69.13
T023 Angle 3 of the breast triangle (°)	455	62.09	2.91	4.68	57.49	62.02	66.38
T027 Inner angle of upper breast (°)	455	27.53	6.58	23.92	17.54	27.14	38.09
T028 Inner angle of lower breast (°)	455	40.99	10.19	24.87	26.01	39.96	59.80

Table 3.13 (continued)

T029 Inner angle of whole breast (°)	454	111.60	12.85	11.52	90.89	111.91	133.48
T030 Vertical angle of upper breast (°)	455	29.09	6.03	20.72	19.22	28.67	39.23
T031 Vertical angle of lower breast (°)	455	35.79	10.87	**30.37**	19.04	35.34	53.47
T032 Perpendicular distance from bust point to the slanting line of whole breast (°)	454	4.46	1.23	27.51	2.62	4.34	6.71
T033 Horizontal distance from lower-most point of the breast to bust point (°)	455	3.69	1.31	**35.61**	1.70	3.60	5.88
T034 Length of upper breast leg of breast triangle (°)	455	9.83	2.20	22.41	6.68	9.42	13.52
T035 Length of lower breast leg of breast triangle (°)	454	6.88	1.14	16.62	5.16	6.81	8.85
T036 Length of whole breast leg of breast triangle (°)	453	13.76	1.62	11.79	11.24	13.62	16.66
C001 Difference between bust girth and underbast girth (3D)	456	11.66	3.30	28.27	6.74	11.37	17.26
C002 Calculated reverse aspect ratio of bust cross-section	456	1.23	0.08	6.77	1.11	1.23	1.38
C003 Calculated reverse aspect ratio of underbust cross-section	456	1.32	0.10	7.20	1.17	1.32	1.48
C004 Calculated aspect ratio of the breast1 (D120/D110-b)	455	0.35	0.06	17.23	0.26	0.35	0.45
C005 Calculated aspect ratio of the breast2 (D121/D110-b)	455	0.20	0.07	**34.47**	0.09	0.19	0.32
C006 Calculated chubbiness ratio of the breast1 (D134 (horizontal plane)/D110-b)	454	1.27	0.09	6.86	1.15	1.26	1.43
C007 Calculated chubbiness ratio of the breast2 (D134 (horizontal plane)/D062)	447	12.78	6.93	**54.22**	5.79	11.21	28.50
C008 Calculated chubbiness ratio of the breast3 (D136 (slanting plane)/D110-b)	455	1.31	0.18	13.37	1.13	1.27	1.58
C009 Calculated chubbiness ratio of the breast4 (D136 (slanting plane)/D062)	456	14.14	10.56	**74.65**	5.90	11.30	29.03
C010 Calculated chubbiness ratio of the breast5 (T032/T035)	453	0.64	0.13	19.81	0.44	0.64	0.86
C011 Calculated chubbiness ratio of the breast6 (D134 (horizontal plane)/M046)	454	2.67	0.34	12.71	2.19	2.65	3.26
C012 Calculated chubbiness ratio of the breast7 (D136 (slanting plane)/M046)	455	2.76	0.43	15.55	2.14	2.71	3.49
C013 Calculated VHI	455	2.21	0.30	13.51	1.81	2.16	2.73
C014 Calculated BMI	455	21.67	2.88	13.27	17.82	21.20	26.59

3.7 Conclusions

456 female subjects aged from 20 to 39, who represent the general intimate apparel market in China, were sampled from the database of AIMER HEC-BICT for the current study according to the sampling techniques of ISO 15535 (2003). In order to obtain more dimensional information, ninety-eight 3D body measurements were selected and measured from 3D body scan data by using the software 3D-Rugle, RapidForm 2004 and Shapeline-3D, while five complementary manual measurements were measured by using Martin's method. After a statistical and reliability check, in order to ensure the reliability of further findings in this study, a comparison of the distributions of the current sample and the sample used for establishing the existing bra sizing system was conducted, based on four key body measurements, namely "bust girth", "underbust girth", "weight" and "whole body height".

The findings of this chapter are summarized as following:

1) The data distribution comparisons indicate that the sample used in this study have similar distributions of key dimensions as those generally used for evaluating the body shape of the population. Therefore, we have confidence in believing that the research findings based on the current sample can approximately represent the whole related population.
2) A set of 103 body and breast measurements, including 3D body scan data and complementary manual measurement data, has been prepared for further breast shape classification and establishing a new sizing chart.

3) ANOVA analysis results indicate that, except for the variables “total arc length of right breast root”, “BP~UBL”, and “the centre bridge height”, there were no significant differences for other detailed breast measurements among demographic variables such as age and procreation. Moreover, for commercial reasons, the 20~39 age group is treated as one, normally named “adult female” in the intimate apparel industry. Therefore, for further study and establishing a new sizing system, the 456 subjects will be regarded as one group.

CHAPTER 4

DEVELOPMENT OF A NEW BRA SIZING SYSTEM

4.1 Introduction

From 1935 till now, bra sizing systems have been based on only 2 measurements - bust girth and underbust girth. Woman's breast shapes are, however, very complex in a 3D space. Conventional linear measurements probably are insufficient to describe the categorization of breast sizes for making well-fit garments, especially bras.

Chapter 3 compared the data distribution of a current sample of 456 subjects and the sample consisting of 5,507 subjects that were used for building the existing sizing system. This chapter focuses on developing a method for classifying the breast size based on the breasts' natural shape, and establishing a new bra sizing system that can provide individuals with a higher accommodation rate and fitting effect than the existing system.

Based on the prepared set of 103 measurement variables mentioned in Chapter 3, two multivariate statistical methods were used to establish a breast sizing system for bra design. Using principal components factor analysis, significant parameters were identified for sizing system development. Then a layered K-means cluster analysis was used to draw up a new bra sizing system. Furthermore, the same evaluating criteria and scale based on mathematical models were used to assess the efficiency of the new bra sizing system and the existing one in three aspects, namely (1) accommodation rate, (2) efficiency of classifying the breast shape, and (3) fit effectiveness for the covered individuals.

4.2 Evaluation and Problem Statement of the Existing Chinese Bra Sizing System

In general, the major goal of any apparel sizing system is to provide a limited number of sizes based on a division of a varied population into different body types. The efficiency of a sizing system should: (1) cover as large a percentage of the population as possible, (2) provide as a good fit as possible for the accommodated (covered) individuals, (3) use as few sizes as possible (Gordon & Friedl, 1994; McCulloch et al., 1998) and (4) show a clear structure containing simple formulas that are easy to understand (Hsu & Wang, 2004). Paal (1997) also mentioned that a sizing system was improved if the performance of any of these criteria had improved without degrading the performance of any other criteria.

The bra sizing system for Chinese women (FZ/T 73012-2004) renewed in 2004 is a metric sizing system, very similar to the other metric or imperial sizing systems used in US, Europe and Japan. As shown in Table 4.1, the Chinese bra sizing system is also structured by the underbust girth (denoted as UB) and the difference between full bust girth and underbust girth (denoted as FB-UB). In the sizing system, the bra size number directly indicates the underbust girth. For example, a bra size 75 corresponds to an underbust measurement of 75 cm. The cup volume is presented by the centimeter difference between the full bust measurement and the underbust. A 12.5cm difference means a cup volume B, while cup C's full bust girth is 15cm larger than the underbust.

Table 4.1 the bra sizing system for Chinese women (FZ/T 73012-2004)

Cup classification	AA	A	B	C	D	E	F	G
The difference between bust girth and underbust girth	7.5	10	12.5	15.0	17.5	20.0	22.5	25.0

Remark: the middle size of underbust girth is 75cm, and the intersize interval is 5cm.

The existing bra sizing system is regarded as one which includes many faults: (a) lack of scientific basis, (b) inaccurate size classification, (c) many different breast shapes in the same cup size (Morris et al., 2002; Pechter, 1998). It has a small fixed number of sizes and clear structure, so it has satisfied two criteria of an efficient sizing system. Therefore, the evaluation of the existing sizing system has been focused on another two criteria. The accommodation rate of the existing bra sizing system of Chinese women was calculated. Distance measures for all the subjects who are classified as the middle size of 75B were compared to investigate whether it provides good fit for all accommodated individuals.

4.2.1 Bra Size Classification Results Based on the Existing Sizing System

Based on the standard FZ/T 73012-2004, the sample of 456 subjects could be divided into different bra size categories using the detailed chart shown in Table 4.2, which is provided in the standard.

The frequency and percentage results of bra classifications for our sample are shown in Figure 4.1 and Table 4.3. The results indicate that there were about 14 subjects (3.07%)

who could not find their own bra size according to the existing bra size criteria. It can be seen from Table 4.3 only a few bra size categories contained 5% or more of the subjects, including 70A, 75A, 75B, 75C and 80A.

Table 4.2 Details of bra size calculation method based on the existing Chinese bra sizing system

	Bra band size (cm)							
	65	70	75	80	85	90	95	100
	Underbust girth (cm)							
	62.5-67.5	67.5-72.5	72.5-77.5	77.5-82.5	82.5-87.5	87.5-92.5	92.5-97.5	97.5-102.5
Bust girth (cm)								
Cup AA	70-75	75-80	80-85	85-90	90-95	95-100	100-105	105-110
Cup A	72.5-77.5	77.5-82.5	82.5-87.5	87.5-92.5	92.5-97.5	97.5-102.5	102.5-107.5	107.5-112.5
Cup B	75-80	80-85	85-90	90-95	95-100	100-105	105-110	110-115
Cup C	77.5-82.5	82.5-87.5	87.5-92.5	92.5-97.5	97.5-102.5	102.5-107.5	107.5-112.5	112.5-117.5
Cup D	80-85	85-90	90-95	95-100	100-105	105-110	110-115	115-120
Cup E	82.5-87.5	87.5-92.5	92.5-97.5	97.5-102.5	102.5-107.5	107.5-112.5	112.5-117.5	117.5-122.5
Cup F	85-90	90-95	95-100	100-105	105-110	110-115	115-120	120-125
Cup G	87.5-92.5	92.5-97.5	97.5-102.5	102.5-107.5	107.5-112.5	112.5-117.5	117.5-122.5	122.5-127.5

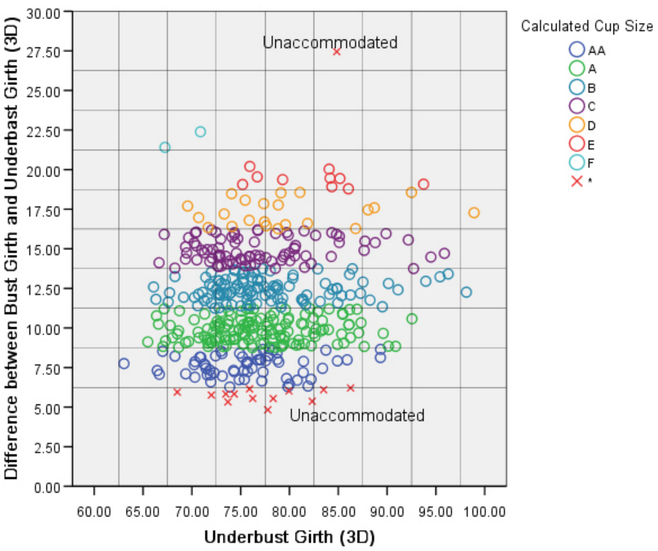

Figure 4.1 The bra size categories based on 456 subjects

Table 4.3 The frequency of bra classification based on existing bra sizing system

	Bra band size (cm)							
	65		70		75		80	
	Frequency	Percent (%)	Frequency	Percent (%)	Frequency	Percent (%)	Frequency	Percent (%)
Cup AA	4	0.88	16	3.51	24	5.26	15	3.29
Cup A	6	1.32	24	5.26	52	11.40	38	8.33
Cup B	2	0.44	16	3.51	49	10.75	22	4.82
Cup C	2	0.44	18	3.95	34	7.46	19	4.17
Cup D			3	0.66	7	1.54	7	1.54
Cup E					3	0.66	1	0.22
Cup F	1	0.22	1	0.22				
Cup G								
	Bra band size (cm)							
	85		90		95		100	
	Frequency	Percent (%)	Frequency	Percent (%)	Frequency	Percent (%)	Frequency	Percent (%)
Cup AA	4	0.88	2	0.44	1	0.22		
Cup A	20	4.39	4	0.88	3	0.66		
Cup B	13	2.85	5	1.10	3	0.66	1	0.22
Cup C	6	1.32	5	1.10	1	0.22		
Cup D	1	0.22	2	0.44	1	0.22	1	0.22
Cup E	5	1.10						
Cup F								
Cup G								
Total								96.93

4.2.2 Investigation of Probability Coverage Rate of the Existing Bra Sizing System

The coverage rate of a sizing system is measured by what percentage of the population a system can accommodate with ready-made garments. According to the descriptive statistic results of current sample, the skewness of UB and FB-UB are 0.762 and 0.605, and the kurtosis of UB and FB-UB are 0.690 and 0.719 respectively. So it can be concluded that the measurements UB and FB-UB approximately belong to a normal distribution (“Japanese body size data 1992-1994”, 1997; Norušis, 2004). The mathematical concept of normal probability density can thus be used to investigate the coverage rate of the existing Chinese bra sizing system on 1-dimension of a key control variable (based on one measurement) and 2-dimensions of key control variables (based on two measurements) respectively (Zhou et al., 1992; Johnson & Wichern, 2002/1982).

4.2.2.1 Investigation of 1-Dimentional Probability Coverage Rate

Suppose a normally distributed (or Gaussian) random variable x has a normal probability density function

$$f(x) = \frac{1}{\sigma\sqrt{2\pi}} \exp\left[-\frac{(x-\mu)^2}{2\sigma^2} \right], \quad \sigma > 0, \tag{4.1}$$

where the parameters of the distribution μ and σ^2 are the mean and variance of x respectively. Then we have

$$\begin{aligned} P\{a \le X \le b\} &= \int_a^b f(x)dx \\ &= \Phi(\frac{b-\mu}{\sigma}) - \Phi(\frac{a-\mu}{\sigma}), \end{aligned} \tag{4.2}$$

where $(b-\mu)/\sigma$ denotes the z score of b, and $(a-\mu)/\sigma$ denotes the z score of a, and

$$\Phi(z) = \int_{-\infty}^{z} f(x)dx, \tag{4.3}$$

From the 3D body scan data, the mean and standard deviation of the underbust and the difference between bust girth and underbust girth were obtained as: 77.22cm, 6.05cm, and 11.66cm and 3.30cm respectively. Using equation (4.2), the probability coverage rate of underband and cup of the existing bra sizing system could be investigated.

Figure 4.2 shows the sample frequency distribution of UB. Table 4.4 reveals the calculated probability coverage rate of the underbands of the existing bra sizing system.

From the Table, it can be seen that the total coverage rate is 99.25%, and the underband size of 75cm and 80cm (referring to underbust size ranges of 72.5~77.5cm and 77.5~82.5cm) have the highest coverage rate with about 30% each. A very low percentage of people are accommodated with the 95cm and 100cm underband sizes. In general, many intimate apparel companies do not produce bras which have an underband of 65cm. In this case, the total probability coverage rate of underband of the existing bra sizing system is decreased to 94.63%.

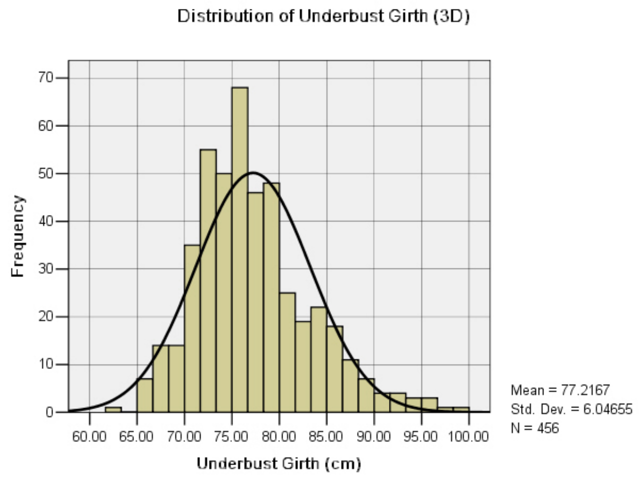

Figure 4.2 The sample frequency distribution of UB (underbust girth)

Table 4.4 Probability coverage rates of underband categories based on the existing bra sizing system

Underband categories (cm)	b (Max. Underbust) (cm)	a (Min. Underbust) (cm)	z score of b	Probability coverage of b	z score of a	Probability coverage of a	Probability coverage rate of Underband (%)
65	67.50	62.50	-1.61	.0537	-2.43	.0075	4.62
70	72.50	67.50	-.78	.2177	-1.61	.0537	16.40
75	77.50	72.50	.05	.5199	-.78	.2177	30.22
80	82.50	77.50	.87	.8078	.05	.5199	28.79
85	87.50	82.50	1.70	.9554	.87	.8078	14.76
90	92.50	87.50	2.53	.9943	1.70	.9554	3.89
95	97.50	92.50	3.35	.9996	2.53	.9943	0.53
100	102.50	97.50	4.18	1.0000	3.35	.9996	0.04
Total							99.25
Without 62.5~67.5cm							94.63

Figure 4.3 shows the sample frequency distribution of FB-UB. Table 4.5 relates to the calculated probability coverage rate of the cups of the existing bra sizing system. Compared with underbust coverage rate, the total percentage of coverage rate of cup sizes is lower, only 94.95%. Among the cup categories, cups A and B contribute a high coverage rate of up to 26% and above. The next highest category is C cup (18.2%). The analysis indicates a very low percentage of people accommodated by both F cup and G cup.

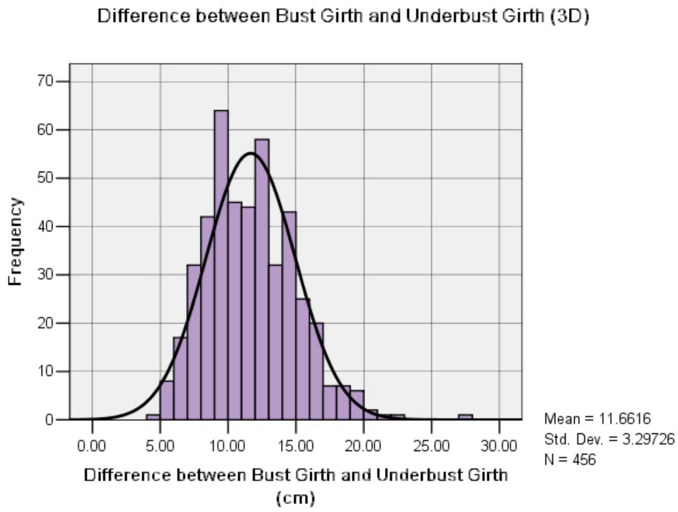

Figure 4.3 The sample frequency distribution of FB-UB (bust girth - underbust girth)

Table 4.5 Probability coverage rates of cup categories of the existing bra sizing system

Cup categories	b (Max. bust) (cm)	a (Min. bust) (cm)	z score of b	Probability coverage of b	z score of a	Probability coverage of a	Probability coverage rate of cup (%)
AA	8.75	6.25	-.88	.1894	-1.64	.0505	13.89
A	11.25	8.75	-.12	.4522	-.88	.1894	26.28
B	13.75	11.25	.63	.7357	-.12	.4522	28.35
C	16.25	13.75	1.39	.9177	.63	.7357	18.20
D	18.75	16.25	2.15	.9842	1.39	.9177	6.65
E	21.25	18.75	2.91	.9982	2.15	.9842	1.40
F	23.75	21.25	3.67	.9999	2.91	.9982	0.17
G	26.25	23.75	4.42	1.0000	3.67	.9999	0.01
Total							94.95

4.2.2.2 Investigation of 2-Dimentional Probability Coverage Rate

The existing bra sizing system was established based on two key dimensions: bust girth and underbust girth. Obviously, it is very important to reveal the 2-dimensional probability coverage rate of sizing system apart from 1-dimentional probability densities. Here the multivariate normal density model was used to investigate the bra size accommodation rate based on our 456 subjects.

Assume two normally distributed random variables with individual parameters $\mu_1 = E(X)$, $\mu_2 = E(Y)$, $\sigma_{11} = \mathrm{Var}(X)$, $\sigma_{22} = \mathrm{Var}(Y)$, and $\rho_{12} = \sigma_{12} \,/\, (\sqrt{\sigma_{11}}\sqrt{\sigma_{22}})$ = Corr(X, Y). We get the expression for bivariate normal density:

$$f(x_1, x_2) = \frac{1}{2\pi\sqrt{\sigma_{11}\sigma_{22}\left(1-\rho_{12}^2\right)}} \times \exp\left\{-\frac{1}{2\left(1-\rho_{12}^2\right)}\left[\left(\frac{x_1-\mu_1}{\sqrt{\sigma_{11}}}\right)^2 + \left(\frac{x_2-\mu_2}{\sqrt{\sigma_{22}}}\right)^2 - 2\rho_{12}\left(\frac{x_1-\mu_1}{\sqrt{\sigma_{11}}}\right)\left(\frac{x_2-\mu_2}{\sqrt{\sigma_{22}}}\right)\right]\right\}. \tag{4.4}$$

Then we have $P\{x_1 \le X \le x_2; y_1 \le Y \le y_2\}$

$$= F(x_2, y_2) - F(x_2, y_1) - F(x_1, y_2) + F(x_1, y_1)\ , \tag{4.5}$$

where
$$F(x_2, y_2) = \int_0^{x_2}\int_0^{y_2} f(x_2, y_2)\, d\,x_2\, d\,y_2\ ,$$
$$F(x_2, y_1) = \int_0^{x_2}\int_0^{y_1} f(x_2, y_1)\, d\,x_2\, d\,y_1\ ,$$
$$F(x_1, y_2) = \int_0^{x_1}\int_0^{y_2} f(x_1, y_1)\, d\,x_1\, d\,y_1\ ,$$

and
$$F(x_1, y_1) = \int_0^{x_1}\int_0^{y_1} f(x_1, y_1)\, d\,x_1\, d\,y_1\ .$$

For the current sample of 456 people, we had $\mu_1 = 77.22$cm, $\mu_2 = 11.66$cm, $\sigma_{11} = 6.05$cm, $\sigma_{22} = 3.30$cm, and $\rho_{12} = 0.137$. By using the equation (4.5), the 2-dimensional probability coverage rates were obtained for each size of the existing bra sizing system. According to Table 4.6, the total probability accommodation rate is about 94%. In light of the fact that many intimate apparel companies do not manufacture all categories of bra sizes, the partial probability coverage rates were calculated. Normally, in actual production, many manufacturers ignore bra sizes when either the underbust size is 65cm or the cup size is AA or G (the shaded sections shown in Figure 4.4). The results indicate that the accommodation rate of the bra sizes without the 65cm underband will decline to 90%, and decrease quite sharply to about 77% when it is calculated without the 65cm underband, AA cup and G cup. As shown in Table 4.6 and Figure 4.5, the relative high coverage rate of bra sizes are concentrated in the range from AA cup to C cup, and underbust sizes only from 70~85cm. It is found that the general manufacturing sizes including underband from 70 to 85cm and cup sizes between AA and C could cover 78.32% of the sample.

Table 4.6 Probability coverage rates of the existing bra sizing system

Underband/cup	AA	A	B	C	D	E	F	G
65	0.8541	1.3484	1.2190	0.6310	0.1868	0.0316	0.0030	0.0002
70	2.6897	4.5953	4.4960	2.5190	0.8074	0.1478	0.0154	0.0009
75	4.3851	8.1060	8.5805	5.2016	1.8044	0.3576	0.0404	0.0026
80	3.7061	7.4121	8.4879	5.5667	2.0895	0.4482	0.0548	0.0038
85	1.6230	3.5125	4.3520	3.0881	1.2543	0.2912	0.0386	0.0029
90	0.3675	0.8610	1.1545	0.8866	0.3898	0.0980	0.0141	0.0011
95	0.0429	0.1088	0.1580	0.1313	0.0625	0.0170	0.0026	0.0003
100	0.0026	0.0071	0.0111	0.0100	0.0052	0.0015	0.0003	0.0000
Total (%)								94.29
Without 65cm underband (%)								90.02
Without 65cm underband, AA cup and G cup (%)								77.19
70~85cm underband & AA~C cup (%)								78.32

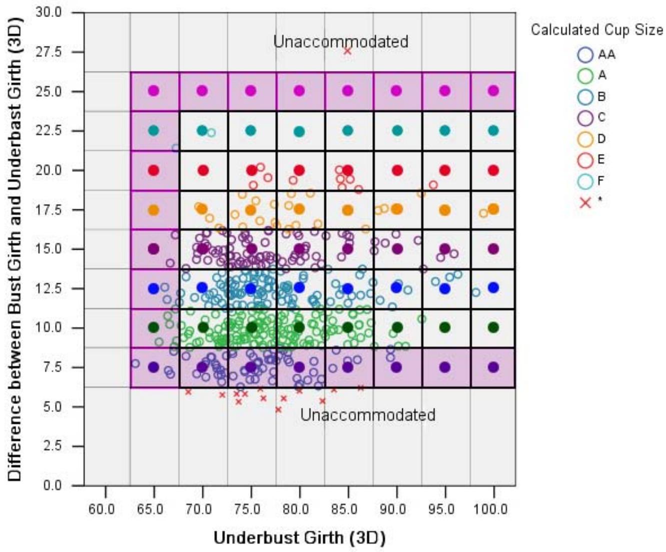

Figure 4.4 The size categories of the existing bra sizing system

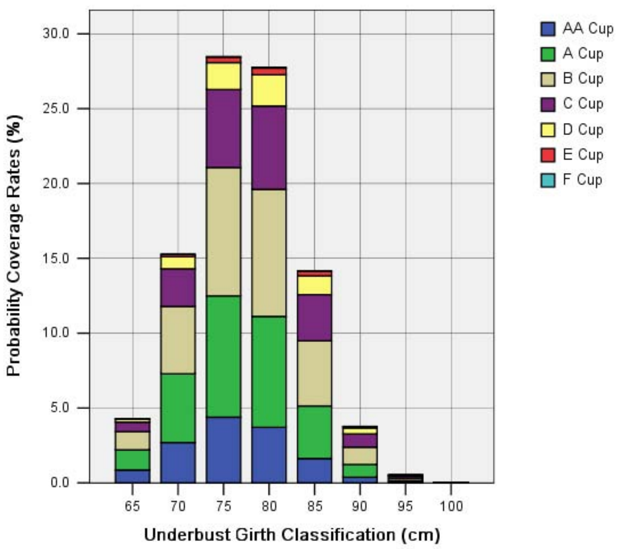

Figure 4.5 The stacked bars of probability coverage rates of the existing bra sizing system based on the 456 subjects

4.2.3 Distance Measure to Explore Similarity of the Breast Cross-section Shape

The general purpose of any sizing system is to accommodate the largest percentage of subjects with the fewest sizes based on clustering the varied population into different homogeneous groups (Gordon & Friedl, 1994; McCulloch et al., 1998; Ashdown, 1998).

In the clustering process, a distance measure is normally applied to identify the subgroups.

One of the methods to measure how far two points are separated is the straight-line distance apart of the two points. This minimum straight-line distance between any two points is referred to as the *Euclidean distance* (Sharma, 1996). In cluster analysis, the Euclidean distance between i and j in p dimensions is given by

$$D_{ij} = \left(\sum_{k=1}^{p} \left(X_{ik} - X_{jk} \right)^2 \right)^{1/2} . \tag{4.6}$$

Bra size 75B is the most representative group and is generally chosen to be a prototype size for bra design. Forty-nine of the subjects in the study group would wear this size. Here using equation (4.6), the individual distances of the 75B subjects from the centre of their bra size were calculated based on two key measurements: UB and FB-UB. The purpose of this task is to explore if there is a considerable difference of breast cross-section shape, and therefore different levels of fit, among individuals in the same bra size category.

In order to ensure the variables were measured on a comparable scale, a proportional distance measure was used. Equation (4.6) can then be rewritten as

$$D_{ij} = \left(\sum_{k=1}^{p} \left(\frac{X_{ik} - X_{jk}}{X_{jk}} \right)^2 \right)^{1/2} , \tag{4.7}$$

where X_{ik} is the body dimensions of the individual, and X_{jk} is the bra dimensions of individual's assigned bra size (75B). Here, D is defined as the individual proportional distance from the assigned size centre. The results of distance measure are shown in Figure 4.6 and Table 4.7 which reveal that there is a very large range between minimum and maximum. Moreover, the Std. Deviation is very large. Three subjects with small, medium and large distance measures were randomly selected in order to compare the similarity of their breast cross-section shapes.

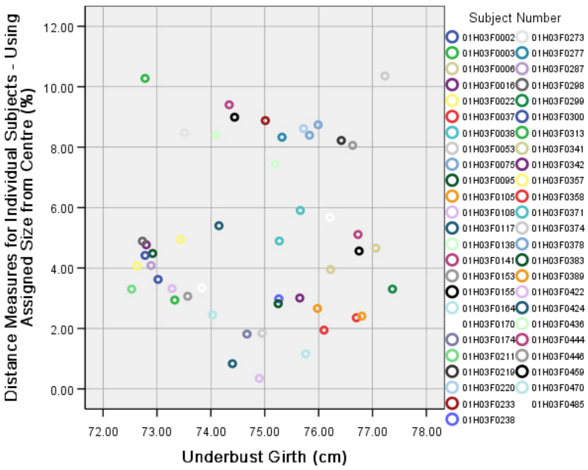

Figure 4.6 Scatter plot of proportional distance measure for 75B bra size subjects

Table 4.7 Summary of proportional distance measure (%)

N	Minimum (%)	Maximum (%)	Range (%)	Mean (%)	Std. Deviation (%)
49	0.35	10.36	10.01	4.98	2.72

The existing bra sizing system was established using only the cross-section shapes of full bust girth and underbust girth. Apart from D (%), the reverse aspect ratio, that is equal to the width of the cross-section divided by the depth of the cross-section, was used to evaluate the shape of bust and underbust. The descriptive statistic reveals that the mean of the reverse aspect ratio of bust cross-section and underbust cross-section of 75B are 1.22 and 1.33 respectively (see Table 4.8). Figure 4.7 shows the individual figure that has the average reverse aspect ratio of UB and FB. This figure can be used as a reference figure to compare with the other individuals' overlapping cross-section figures.

Table 4.8 Descriptive statistic summary of the reverse aspect ratio of bust & underbust cross-sections

Measurement	N	Minimum	Maximum	Range	Mean	Std. Deviation
Reverse aspect ratio of bust cross-section	49	1.12	1.39	0.27	1.22	0.06
Reverse aspect ratio of underbust cross-section	49	1.17	1.54	0.37	1.33	0.08

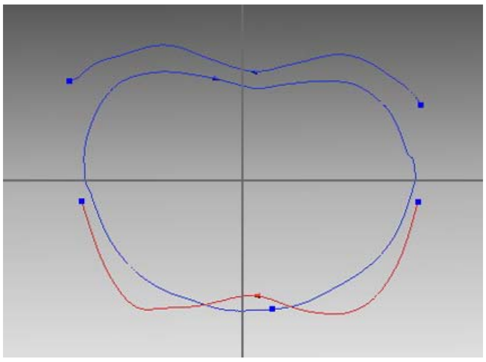

Figure 4.7 Individual figure that has average reverse aspect ratio of UB and FB of 75B

Table 4.9 shows the three cases with different distance measure results. The attached cross-section figures of bust and underbust illustrate the differences among individual body shapes of those who are the same bra size, 75B. As shown in Table 4.9, Case 1 has an approximately average reverse aspect ratio of underbust cross-section (1.31) and a small breast. Case 2 has an average reverse aspect ratio of bust cross-section (1.22) and a slightly smaller than average reverse aspect ratio of underbust cross-section (1.29) and a full breast. Case 3 has a larger than average reverse aspect ratio of bust cross-section (1.28) , a larger underbust cross-section (1.46) than average and a full breast.

It can also be seen from Table 4.9 that, although the three subjects have exactly the same bra size, 75B, the curve shapes of the breasts, the root widths of the breasts and the depths of the breasts are not the same. Based on the above discussion, we see that the current criteria for identifying the breast size based on the difference between the bust girth and underbust girth cannot exactly represent the shape of the breast. Furthermore, this limitation can also affect the bra fit.

Table 4.9 Comparisons of the breast shape similarity between individual subjects of 75B based on distance measurement result

Case 1: small distance measure (small breast, small back, round-shape rib cage)		
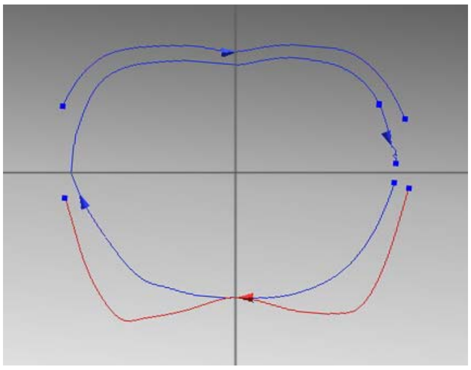	Bust girth (cm)	87.36
	Underbust girth (cm)	74.90
	Bust width (cm)	27.33
	Bust depth (cm)	23.50
	Reverse aspect ratio of bust cross-section	1.16
	Underbust width (cm)	26.00
	Underbust depth (cm)	19.84
	Reverse aspect ratio of underbust cross-section	1.31
	D (%)	0.3467
Case 2: medium distance measure (full breast, average back, round-shape rib cage)		
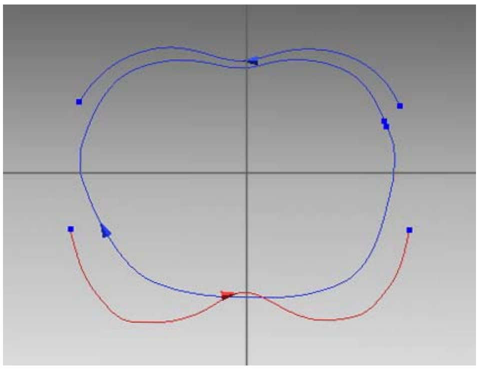	Bust girth (cm)	89.39
	Underbust girth (cm)	76.21
	Bust width (cm)	27.85
	Bust depth (cm)	22.84
	Reverse aspect ratio of bust cross-section	1.22
	Underbust width (cm)	25.35
	Underbust depth (cm)	19.67
	Reverse aspect ratio of underbust cross-section	1.29
	D (%)	5.6742
Case 3: large distance measure (large breast, muscular back, wide rib cage & oval-shape)		
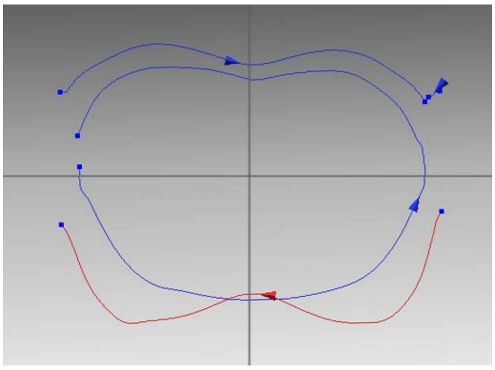	Bust girth (cm)	90.97
	Underbust girth (cm)	77.23
	Bust width (cm)	28.71
	Bust depth (cm)	22.5
	Reverse aspect ratio of bust cross-section	1.28
	Underbust width (cm)	27.74
	Underbust depth (cm)	19.00
	Reverse aspect ratio of underbust cross-section	1.46
	D (%)	10.3560

4.3 Drawing up a New Bra Sizing System

In Section 4.2 we have evaluated the accommodation rate and fitting success of the existing bra sizing system and revealed its limitations. One major problem of the existing sizing system is that it cannot distinguish the subjects according to the 3D shape and dimensions of the breast, as is demonstrated in Table 4.9. This section proposes a new method used to develop a bra sizing system with quantitative descriptions of individual breast shapes.

4.3.1 Review of Sizing System Structure Design

A successful sizing system should be designed by using appropriate anthropometric data to represent the quality of garment fit (Winks, 1997; Paal, 1997). These appropriate anthropometric data are generally defined as control dimensions such as UB and FB-UB.

A number of research studies have revealed that the sizing systems resulting from either the percentile or the regression analysis methods, based on one or two dimensions, could not adequately represent the variability of complex body dimensions (McCulloch et al., 1998; Ashdown, 1998; Pechoux & Ghosh, 2002). They all commented that existing sizing systems do not fully satisfy either consumers or manufacturers.

The multivariate method is another technique used for establishing sizing systems, based on principal components analysis, which combines a large number of measurement variables into a small set depending on their correlation or covariance.

Some surveys utilized this method to cover 90% of the population using a bivariate distribution (Pechoux & Ghosh, 2002; Salusso et al., 1985-86). However, the shortcoming of this method is that the resulting size range cannot cover the subjects outside the elliptical area that encompasses 90% of the observations.

Paal (1997) and McCulloch et al. (1998) proposed an optimization approach to construct an apparel sizing system based on a mathematical model of garment fit. Their findings revealed that the proposed method enabled the development of a sizing system that could satisfy three aspects of a good sizing system: (1) increase the accommodation of the population, (2) reduce the number of sizes in the system, and (3) improve overall fit in the accommodated individuals. However, the sizing system built by this method did not possess a clear structure containing a relative simple formula that is easy to understand, resulting in difficulties in size selection by the customer.

In the current study, the research question is how to develop a new bra sizing system that can put the individuals into different subgroups based on their complex 3D breast shape. Are there any key measurements of the breast that can be extracted from all of the breast dimensions to adequately represent and categorize very complicated breast shapes? Are there any approaches that can be used to establish a new sizing system that can include complex information on the breast shape and also has a clear structure? How to control the number of sizes? In summary, the question is focused on developing a new bra sizing system which can accommodate as large a percentage of the population as possible, provide the best fit possible for covered individuals, use as few sizes as possible, and show a clear structure to both manufacturers and customers.

4.3.2 Principal Components Factor Analysis and Results

A set of 103 measurements, including 98 3D body scanned measurements and 5 one-dimensional measurements (manual measurements), discussed in the last chapter was used for current study. In order to identify the key parameters to describe the breast shape, principal components factor analysis was conducted.

Sharma (1996) advised that one of the objectives of factor analysis is to identify the smallest number of common factors that could best explain or account for the correlations among the indicators. Johnson (1998) also mentioned that for “people-type” data, five or six principal components might be required to account for more than 70% to 75% of the total variance.

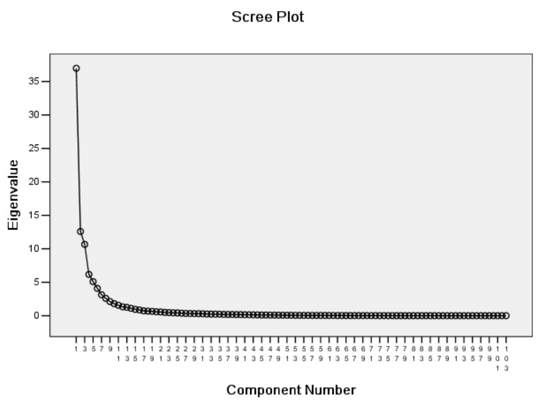

Figure 4.8 The scree plot of initial eigenvalues

Using the sample correlation matrix, 103 measurement variables were used to carry out principal components factor analysis using varimax rotation. The result of the scree plot (Figure 4.8) of initial eigenvalues indicated that seven to fourteen factors might be optimal. The analysis results revealed that eight factors seemed to be the most ideal (Table 4.10). These eight factors could explain approximately 80% of total sample variance. The complete factor loading results are shown in a Table in the Appendix Ⅰ. According to the analysis results, thirty-three measurements were loaded in factor 1, twenty-nine measurements in factor 2, twelve measurements in factor 3, ten variables in factor 4, eight measurements in factor 5, three measurements in both factor 6 and factor 7, and five variables loaded in factor 8. It can be seen (Table 4.10) that the first factor accounts for 23.51% of the total variance, while the second factor accounts for nearly 20% of the total variance. The first two factors together account for 43.26% of the total variance, much larger than the combined effect of the other six factors. The rotated factor loadings shown in Appendix Ⅰ reveal the correlations between the original variables and the factors.

Table 4.10 Summary of principal components factor analysis based on eight factors

	Factor 1	Factor 2	Factor 3	Factor 4	Factor 5	Factor 6	Factor 7	Factor 8
Loaded measurements	33	29	12	10	8	3	3	5
Initial eigenvalues	36.98	12.58	10.66	6.17	5.09	4.09	3.14	2.59
Rotation sums of squared loadings	24.22	20.34	9.77	7.63	6.37	4.64	4.40	3.94
% of variance explained	23.51	19.75	9.48	7.41	6.18	4.51	4.27	3.82
Cumulative proportion of total sample variance explained (%)	23.51	43.26	52.74	60.15	66.33	70.84	75.11	78.93

(a) Factor 1: overall body build

(+) Fat (-) Thin

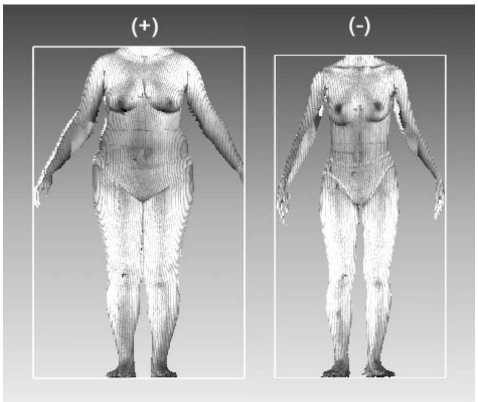

(b) Factor 2: volume of the breast

(+) Large (-) Small

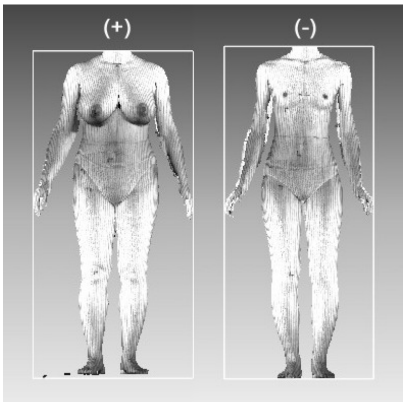

Figure 4.9.1 Extreme figures of factors

(c) Factor 3: inner breast shape

(+) Wide and firm (-) Narrow and low

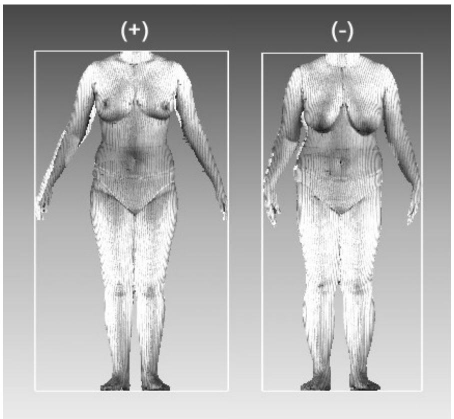

(d) Factor 4: outer breast shape

(+) Wide and firm (-) Narrow and low

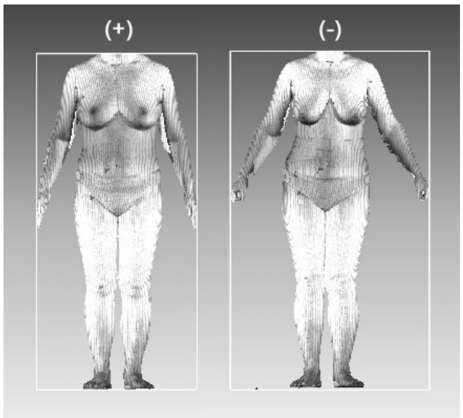

(e) Factor 5: overall height proportion

(+) Tall (-) Short

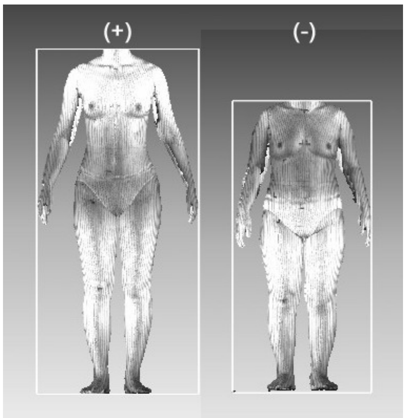

(f) Factor 6: orientation of the breast

(+) Spreading (-) Close

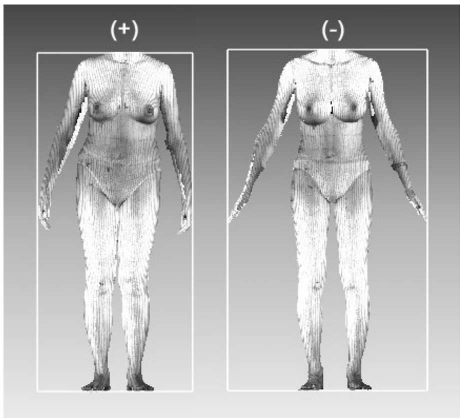

(g) Factor 7: gradient of the breast

(+) Slant (-) Straight

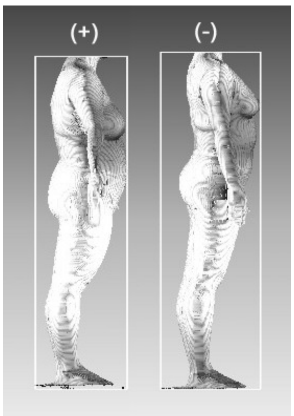

(h) Factor 8: lower breast shape

(+) Round (-) Flat

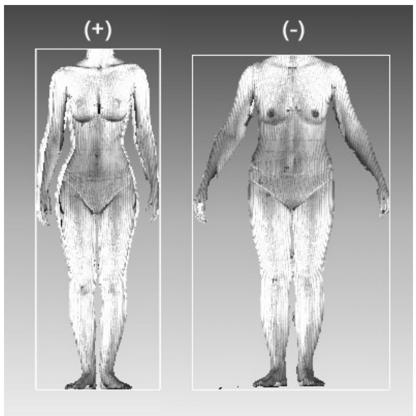

Figure 4.9.2 Extreme figures of factors

Each factor could be defined according to the estimated factor loadings and communality results. For example, as shown in Appendix Ⅰ, most of variables with relatively high loading in factor 1 were relevant to circumference variables, body build indices variables, depth and width variables. Therefore, the first factor was labeled as “overall body build”. In the same way, the other factors were defined as follows: factor 2 as “volume of the breast”, factor 3 as “inner breast shape”, factor 4 as “outer breast shape”, factor 5 as “overall height proportion”, factor 6 as “orientation of the breast”, factor 7 as “gradient of upper breast” and factor 8 as “lower breast shape”. The extreme two representative figures of the subjects measured of each factor are presented in Figure 4.9.

4.3.3 Breast Shape Classification Based on K-means Cluster Analysis

Eight factors have been identified to evaluate the breast shape. This section aims to classify the breast shape into different categories based on the results of principal components factor analysis.

The purpose of a sizing system is to act as an important communication tool or rule among manufactures, retailers and consumers. The sizing system should be based on a clear structure to provide manufacturers with body size specifications for product development (Hsu & Wang, 2004). The existing bra sizing system does not lack structure, and also can cover total 94% population when all sizes are provided. However, it fails to take account of the shape of the breast. The control variable of difference between the bust girth and underbust girth do not help either manufacturers or consumers to categorize breast shapes.

In principal components factor analysis, factor loadings are indicators that reveal which of the original variables are influential in forming new variables (factors). The higher the loading is, the more important the variable is in forming the factor score and vice versa (Sharma, 1996; Johnson & Wichern, 2002). According to the factor loadings shown in the Appendix Ⅰ, "underbust girth" was most closely correlated with factor 1 of "overall body build", the high loading of 0.940 indicated that underbust girth (UB) was very influential in forming factor 1. The high correlations of –0.947 and 0.9396 between factor 2 ("volume of the breast") and the variables "angle B of right breast cross-section" and "calculated aspect ratio of the breast 1 (D120/D110_b)" respectively revealed that these two items are the most closely correlated to form factor 2. Conversely, the variable "difference between the bust girth and underbust girth" (FB-UB) presented a relative lower correlation of 0.625. Similarly, the variable "right breast volume", normally considered an important indicator of breast shape, also showed a lower correlation of 0.642.

In addition, the first two factors together accounted for nearly 45% of the total variance, much larger than the contribution of the other six factors. Considering that a sizing system should possess a clear structure and should be easy to operate, the two most important key parameters in forming factor 1 and factor 2 separately were identified to classify the breast shapes in drawing up the new bra sizing system. They were "underbust girth" and "calculated aspect ratio of the breast 1 (D120/D110_b)" named as "depth width ratio" or DWR (see Figure 4.10). "Angle B of right breast cross-section" is also a significant parameter but it is difficult for the end users to accurately measure by themselves, and that can be presented by DWR too.

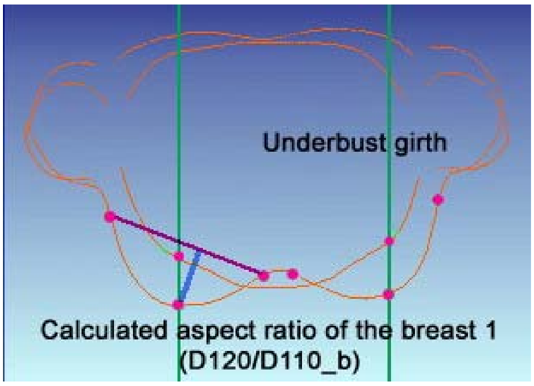

Figure 4.10 The two key measurements for establishing a new bra sizing system

Since modern bras generally use extensible fabrics in the underband area, along with an adjustable hooks and eyes for fastening, the size interval of five centimeters of underbust girth (UB) specified in the existing bra sizing system were chosen to remain unchanged for the new bra sizing system. Furthermore, a layered clustering method based on dividing the subjects into different underbust subgroups was carried out to classify the breast shape.

Cluster analysis (or clustering) is a data mining technique used for combining observations into subgroups or clusters. The observations in each group or cluster are similar to each other, in certain characteristics. The observations in one group should be different from the observations in other groups (Sharma, 1996; Abdali et al., 2004). In particular, the definition of similarity or homogeneity varies from analysis to analysis depending on the objectives of the study, e.g. subgroup individuals with similar body types.

Results of previous studies have shown that the K-means algorithm and other nonhierarchical clustering algorithms perform poorly when random initial partitions are used. However, their performance is generally much better than other methods when a priori initial partition or cluster solution is used (Sharma, 1996; Milligan, 1980).

In the current study, as the first step, 456 subjects were classified into different underband categories from 65cm to 100cm with 5cm intervals according to their underbust girth dimensions (see the first column in Table 4.11). Secondly, a hierarchical clustering was firstly conducted, and then a layered K-means cluster analysis was carried out using the variable "calculated aspect ratio of the breast 1 (D120/D110_b)", referring to the preliminary hierarchical results in SPSS.

Five separate cluster analyses were run with six, seven, eight, nine and ten clusters to test the ideal number of breast shape categories. Each K-means cluster result was evaluated according to the practical commercial considerations of minimizing the number of sizes, accommodating the maximum number of subjects and acknowledging probable garment tolerances between the largest and the smallest base values (Laing et al., 1999). Reviewing the objectives of an efficient sizing system mentioned in 4.2, it is clear that a good sizing system should provide high accommodation rate and use as few sizes as possible (Tryfos, 1986; McCulloch et al., 1998). Although nine or ten clusters can accommodate more people, this would increase the sizes from the existing bra sizing system by 8 to 16 size combinations. On the other hand, six or seven clusters will decrease the sizes in the system by 8 to 16 sizes and cannot provide similar intervals from one group centre to the next. Eight clusters (Table 4.11) appeared to be the best choice since it showed similar intervals among subgroups, and had the same number of sizes as the existing bra sizing system. Size intervals were adjusted to be evenly spaced, based on the mode or mean of the centres of the breast shape categories from the K-means analysis. New bra sizes referring to the breast shapes were re-defined as presented in Table 4.11.

Table 4.11 The centre points of the breast shape categories and new sizing system centre points based on eight clusters

Underband size classification (cm)	The centre points of the breast shape categories based on "calculated aspect ratio of the breast 1 (D120/D110_b)"							
	Cluster 1	Cluster 2	Cluster 3	Cluster 4	Cluster 5	Cluster 6	Cluster 7	Cluster 8
65	0.26	0.30	0.33	0.37	0.41	0.46		
70	0.25	0.30	0.35	0.39	0.42	0.44	0.48	
75	0.27	0.31	0.34	0.38	0.42	0.46	0.50	0.55
80	0.25	0.29	0.33	0.38	0.41	0.45		
85	0.25	0.31	0.34	0.37	0.41	0.44		
90	0.29	0.31	0.34	0.38	0.43	0.46	0.50	
95		0.32		0.38	0.41		0.51	
100				0.38				
	New bra sizing system centre points							
Adjusted centre point	**0.25**	**0.30**	**0.34**	**0.38**	**0.42**	**0.46**	**0.50**	**0.55**

4.4 Evaluation of the Accommodation Rate of the New Bra Sizing System

4.4.1 Bra Size Classification Results Based on the New Sizing System

Table 4.12 shows the new bra sizing system based on the two key variables of "underbust girth" (UB) and "calculated aspect ratio of the breast 1 (D120/D110_b)". In order to be distinguished from the cup sizes AA~G in the existing bra sizing system, the cup sizes in the new bra sizing system are labeled as AA* to G**. Except for one missing subject, the bra sizes of the 455 subjects were re-classified according to the new system and the results are shown in Figure 4.11. They reveal that there were 5 subjects (1.1%) who could not find a suitable bra size in the new bra sizing system. The frequency distribution of the new bra size categories are shown in Table 4.13. It can be seen that the bra sizes with higher covered percentages are focused in the sizes 70A*, 75A*, 75B*, 75C*, 75D*, 80A*, 80B* and 80C*.

Compared with the existing bra sizing system, the new system has the same number of sizes, and also has a clear structure, and the accommodation rate is almost 2% better (Table 4.3 and 4.13). Therefore, the new bra sizing system has met those of the objectives of an efficient sizing system, namely limited sizes, an easy to understand structure, and a good coverage (accommodation) rate.

Table 4.12 The new bra sizing system for Chinese women

Cup classification	AA*	A*	B*	C*	D*	E*	F*	G*
Calculated aspect ratio of the breast 1 (D120/D110_b)	0.25	0.30	0.34	0.38	0.42	0.46	0.50	0.55

Remark: the middle size of underbust girth is 75cm, and the intersize interval is 5cm.

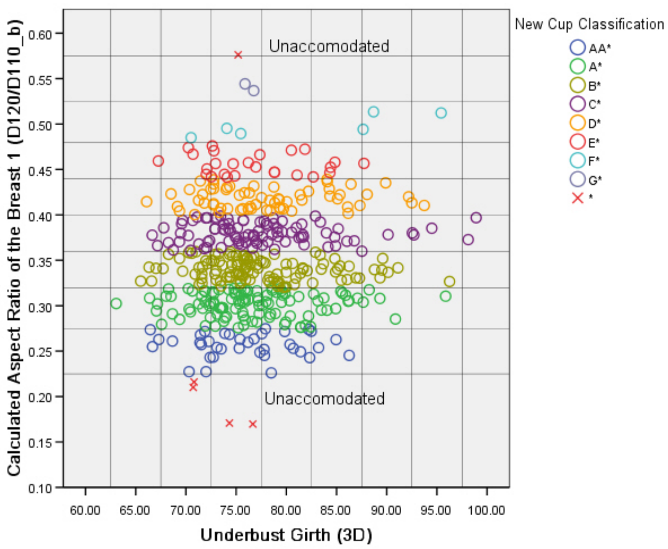

Figure 4.11 The new bra size categories for 455 subjects

Table 4.13 The frequency of bra size categories based on the new bra sizing system

	Bra band size (cm)							
	65		70		75		80	
Cup categories	Frequency	Percent (%)	Frequency	Percent (%)	Frequency	Percent (%)	Frequency	Percent (%)
AA*	3	0.66	9	1.97	10	2.19	12	2.63
A*	4	0.88	20	4.39	43	9.43	26	5.70
B*	4	0.88	16	3.51	49	10.75	23	5.04
C*	2	0.44	18	3.95	33	7.24	24	5.26
D*	1	0.22	10	2.19	21	4.61	16	3.51
E*	1	0.22	4	0.88	11	2.41	5	1.10
F*			1	0.22	2	0.44		
G*					2	0.44		
	Bra band size (cm)							
	85		90		95		100	
	Frequency	Percent (%)	Frequency	Percent (%)	Frequency	Percent (%)	Frequency	Percent (%)
AA*	3	0.66						
A*	12	2.63	4	0.88	1	0.22		
B*	14	3.07	6	1.32	1	0.22		
C*	9	1.97	2	0.44	3	0.66	2	0.44
D*	10	2.19	3	0.66	2	0.44		
E*	4	0.88	1	0.22				
F*			2	0.44	1	0.22		
G*								
Total								98.68

4.4.2 Investigation of the Coverage Rate of the New Bra Sizing System

As mentioned in 4.2.2, the accommodation rate of a sizing system means the coverage percentage that the sizes can provide to subjects. Here, the accommodation rate of the new bra sizing system was evaluated using the same method of 1-dimentional and 2-dimentional probability coverage rate which was defined in 4.2.2.

4.4.2.1 Investigation of 1-Dimentional Probability Coverage Rate

Since the new bra sizing system uses the same control criteria to define the underband size as the existing sizing system, equation (4.2) was used to investigate 1-dimensional probability coverage rate of the new cup categories.

Figure 4.12 shows the sample frequency distribution of “calculated aspect ratio of the breast 1 (D120/D110_b)”. From the descriptive statistics of the 3D body scan data, the mean and standard deviation of variable “calculated aspect ratio of the breast 1 (D120/D110_b)” are 0.3516 and 0.06059. Table 4.14 reveals the calculated results of the new probability coverage rate of cup categories. Compared with the existing sizing system, the total coverage rate has increased to 98.16%. As shown in the Table, B* cup and C* cup hold the two highest coverage rates with 25.42% and 23.24% respectively. The next two highest categories are A* cup (19.77%) and D* cup (13.98%). G* only provides 0.2% coverage.

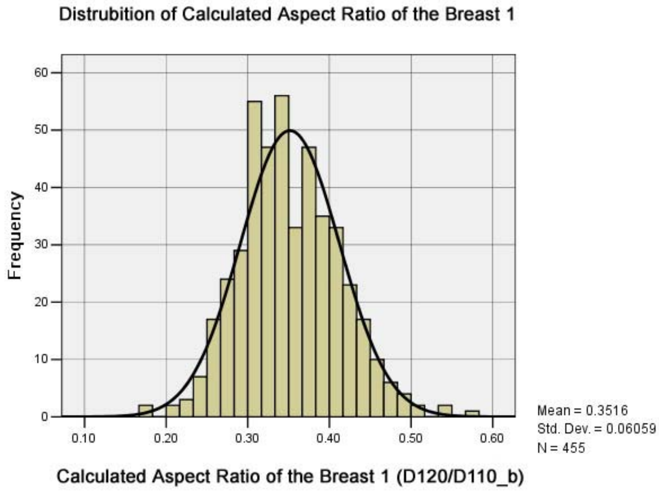

Figure 4.12 The sample frequency distribution of calculated aspect ratio of the breast 1 (D120/D110_b)

Table 4.14 Probability coverage rates of cup categories of the new bra sizing system

Cup	b (Cup biggest size)	a (Cup smallest size)	z score of b	Probability coverage of b	z score of a	Probability coverage of a	Probability coverage rate of cup (%)
AA*	0.275	0.225	-1.26	0.1038	-2.09	0.0183	8.55
A*	0.32	0.275	-0.52	0.3015	-1.26	0.1038	19.77
B*	0.36	0.32	0.14	0.5557	-0.52	0.3015	25.42
C*	0.4	0.36	0.80	0.7881	0.14	0.5557	23.24
D*	0.44	0.4	1.46	0.9279	0.80	0.7881	13.98
E*	0.48	0.44	2.12	0.983	1.46	0.9279	5.51
F*	0.525	0.48	2.86	0.9979	2.12	0.983	1.49
G*	0.575	0.525	3.69	0.9999	2.86	0.9979	0.20
Total							98.16

4.4.2.2 Investigation of 2-Dimentional Probability Coverage Rate

2-dimensional probability density was also used to investigate the accommodation rate of the new bra sizing system (Figure 4.13). From the 3D body scan data, we had μ_1 = 77.22cm, μ_2 = 0.3516, σ_{11} = 6.047cm, σ_{22} = 0.06059, and ρ_{12} = 0.099. Also using equation (4.5), the 2-dimensional probability coverage rates were calculated for each size. The results are shown in Table 4.15.

Table 4.15 Probability coverage rates of the new bra sizing system

Underband/cup	AA*	A*	B*	C*	D*	E*	F*	G*
65	0.5213	1.0672	1.2098	0.9800	0.5194	0.1800	0.0424	0.0048
70	1.6362	3.5480	4.2389	3.6094	2.0109	0.7328	0.1816	0.0219
75	2.6734	6.1389	7.7276	6.9153	4.0493	1.5510	0.4047	0.0517
80	2.2766	5.5356	7.3411	6.9038	4.2486	1.7103	0.4697	0.0635
85	1.0100	2.6007	3.6336	3.5914	2.3228	0.9828	0.2841	0.0406
90	0.2330	0.6354	0.9354	0.9719	0.6608	0.2939	0.0894	0.0136
95	0.0278	0.0805	0.1248	0.1364	0.0975	0.0456	0.0147	0.0023
100	0.0017	0.0053	0.0086	0.0099	0.0074	0.0037	0.0012	0.0002
Total (%)								97.43
Without 65cm underband (%)								92.91
Without 65cm underband, AA* cup and G* cup (%)								84.86

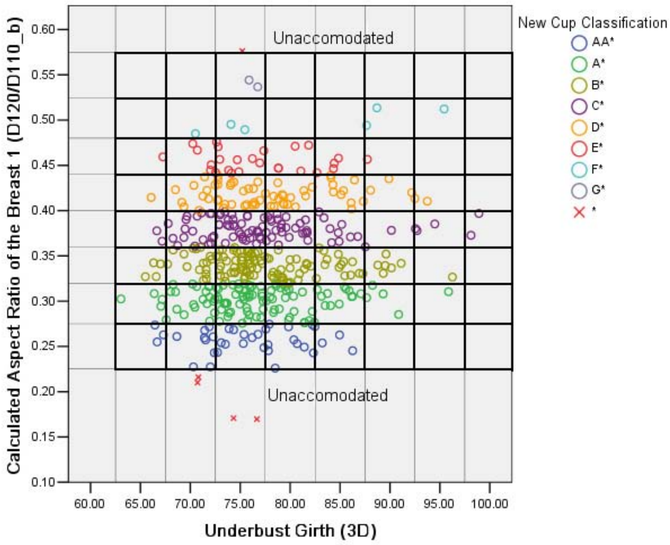

Figure 4.13 The size categories of the new bra sizing system

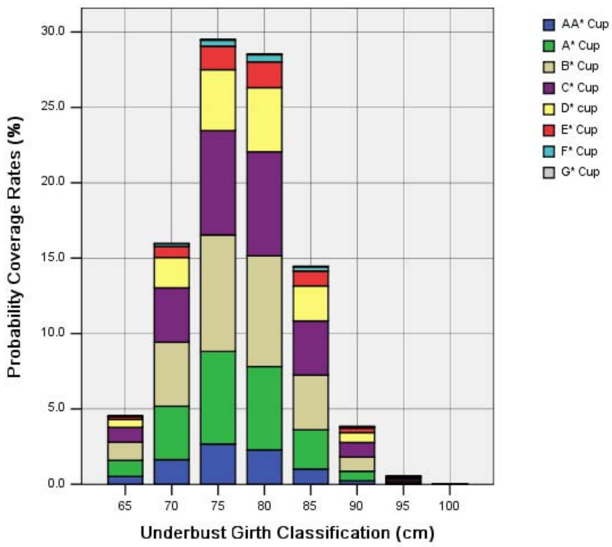

Figure 4.14 The stacked bars of probability coverage rates of the new bra sizing system

As shown in Table 4.15, compared with the existing bra sizing system, the total probability accommodation rate increased to nearly 98%. It also can be seen that the partial probability coverage rate of “without 65cm underband” showed a higher percentage of 92.9% than the previous one of 90%. Particularly, the partial probability coverage rate of “without 65cm underband, AA* cup and G* cup (%)” keeps a much higher coverage, around 85%. As is shown in Table 4.15, Figure 4.13 and Figure 4.14, relative high coverage rate of bra sizes are mostly focused on B* cup, C* cup, A* cup, D* cup and AA* cup, while the underbust sizes vary from 70cm to 85cm.

4.5 Efficiency Comparison of the Two Sizing Systems

According to the above investigation results and discussion, it is found that the new bra sizing system provides a higher accommodation of the population, with a clear structure, by using the same numbers of size categories as the existing one. In view of objective (2) of an efficient sizing system, the aim of this section is to evaluate the performance of the two bra sizing systems in fitting the population. In the apparel industry, distance measure was proposed to measure the fit goodness of a sizing system (Paal, 1997; McCulloch et al., 1998; Ashdown, 1998). The same criteria and scales were used to compare the effectiveness of the two bra sizing system, namely:

1) Dissimilarity measures based on factor scores
2) Aggregate fit loss assessment based on key measurements.

4.5.1 Dissimilarity Distance Measures Based on Factor Scores

The results of principal components factor analysis revealed that the breast shape could be evaluated using eight factors, including “overall body build”, “volume of the breast”, “inner breast shape”, “outer breast shape”, “overall height proportion”, “orientation of the breast”, “gradient of upper breast” and “lower breast shape”. Figure 4.15 shows scatter plot comparisons between the two sizing systems, based on the individual scores of pairs of factors related to the eight factors from factor 1 & 2 to factor 7 & 8 respectively. Figure 4.15.1 shows the comparison of two sizing system by using individual factor scores of factor 1 (overall body build) & 2 (volume of the breast). For factor 2, compared with the existing bra sizing system (the left figure), the distribution of scatter plots labeled by the new sizing system (see the right figure) present better transitions of breast volumes from AA* cup to G* cup orderly according to the scores of factor 2 changed from negative values to positive values. Figure 4.15.2 shows the individual factor scores of two sizing systems related to factor 3 (inner breast shape) & 4 (outer breast shape). Figure 4.15.3 is a diagraph revealing the individual factor scores of factor 5 & 6 related to “overall height proportion” and “orientation of the breast”. Figure 4.15.4 reveals the comparison of the two systems by using individual factor scores of factor 7 (gradient of upper breast) & 8 (lower breast shape). In these three cases, different from Figure 4.15.1, the scatter plots depending on the new sizing system cannot show better or clearer patterns than the scatter plots marked by the existing sizing system.

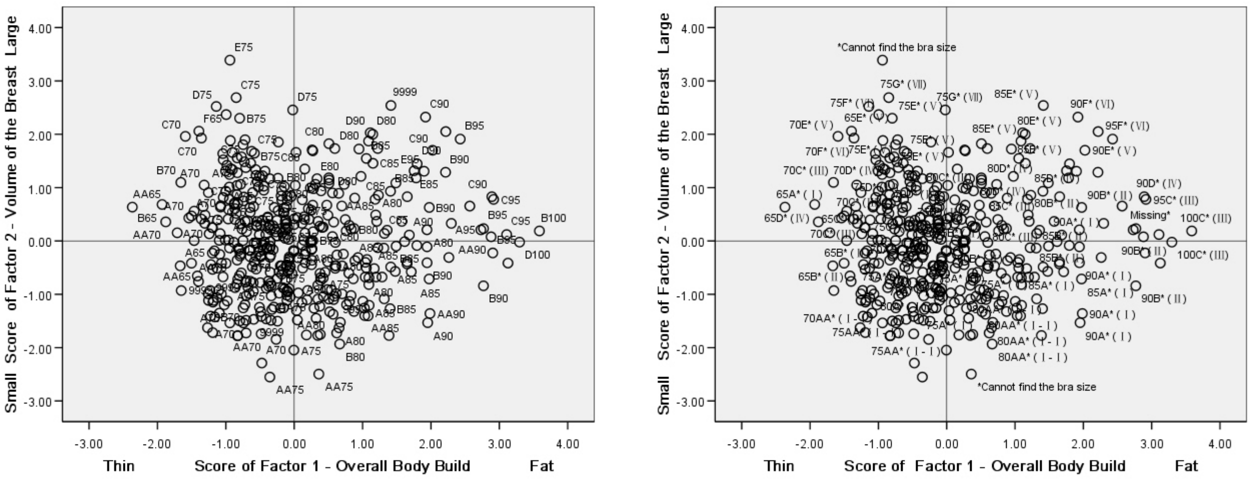

Figure 4.15.1 Scatter plots comparison between two sizing systems based on scores of factor 1 & factor 2

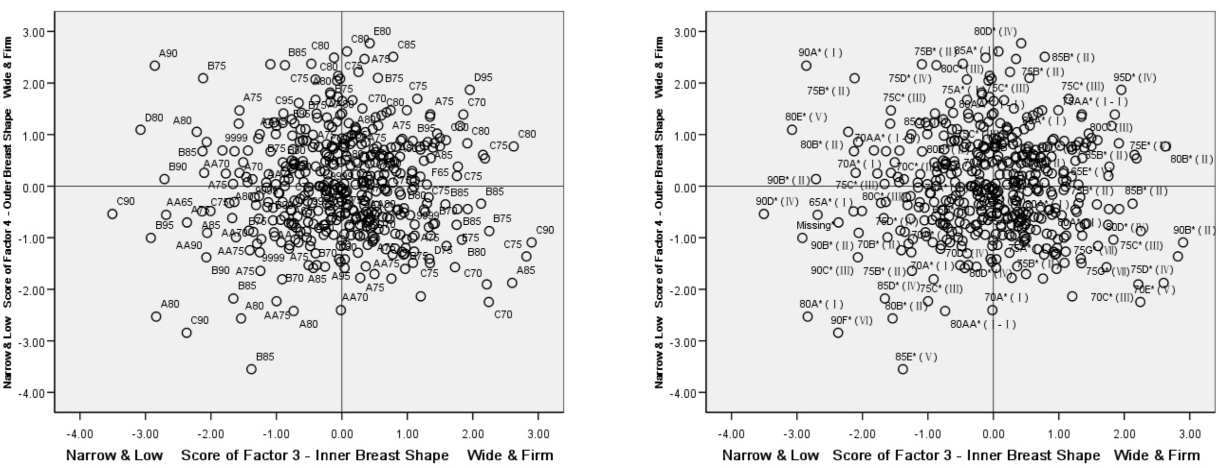

Figure 4.15.2 Scatter plots comparison between two sizing systems based on scores of factor 3 & factor 4

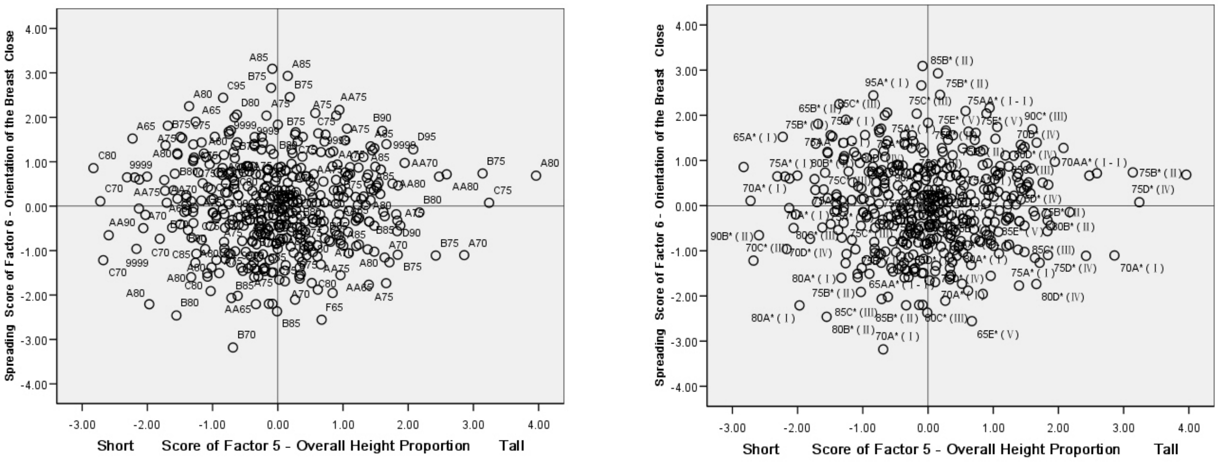

Figure 4.15.3 Scatter plots comparison between two sizing systems based on scores of factor 5 & factor 6

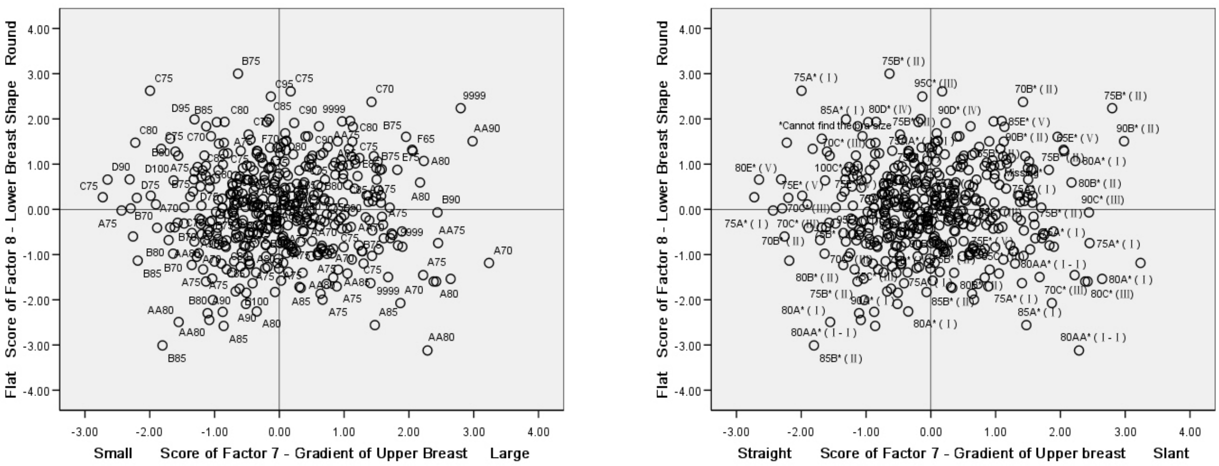

Figure 4.15.4 Scatter plots comparison between two sizing systems based on scores of factor 7 & factor 8

Furthermore, to measure the fitting performance of the two bra sizing systems, the notion of a distance function defined as a dissimilarity measure was used to assess the straight-line distance between individuals and the centre points of their assigned sizes, depending on the eight-dimensional factor scores. The more efficient sizing system is defined as one that has a smaller value of aggregate dissimilarity. Figures 4.16 and 4.17 show the measurements of individuals and the centre points of their assigned size categories, based on the different key control variables of the two bra sizing systems.

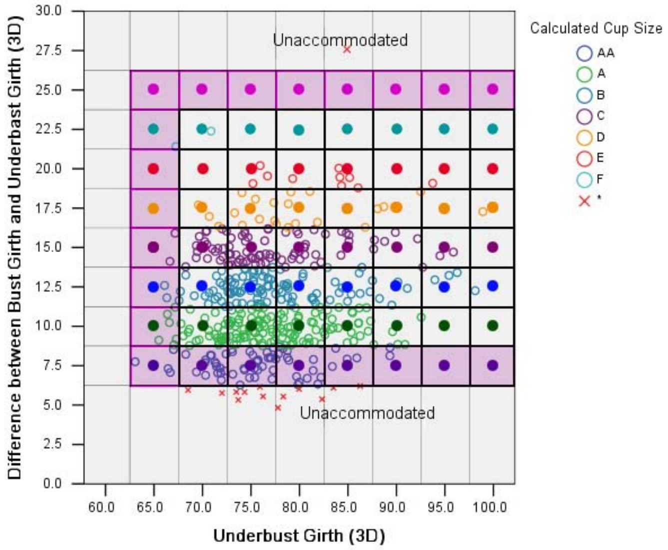

Figure 4.16 The bra size categories based on the existing sizing system

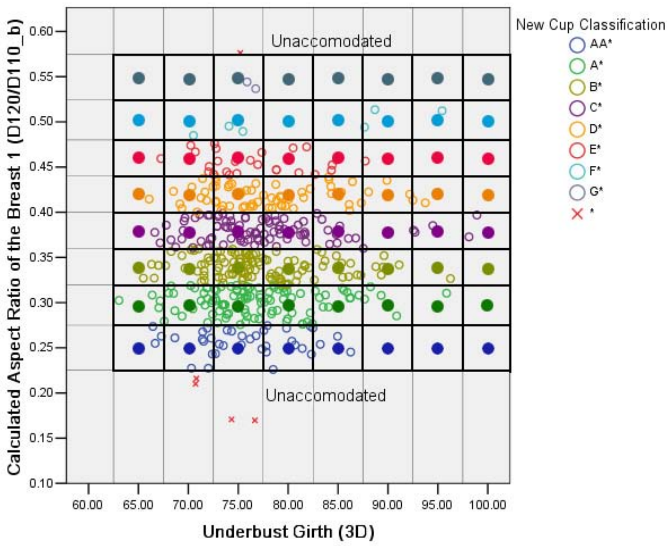

Figure 4.17 Bra size categories based on the new sizing system

Squared Euclidean distance was used to assess the factor score aggregate dissimilarity. Suppose that $d(x_n, y_s)$ presents the straight-line distance between an individual *n* and her assigned bra size *s*, which can be calculated by a sum of squared dissimilarities over each of the *f* factors:

$$d(x_{ni}, y_{si}) = \sum_{i=1}^{f} [d_i(x_{ni} - y_{si})]^2, \tag{4.8}$$

where x_{ni} is the factor score of ith factor of nth individual, and y_{si} is the mean factor score of the ith factor of the sth size category assigned to the nth individual.

The absolute dissimilarity magnitudes were calculated using equation (4.8) to assess the size clustering effect of the two sizing systems. It was noted that if there was only one subject in the sub-sizing groups, this individual's dissimilarity value was changed using the mean of the dissimilarity value of the total sample so that the outliers would not affect the overall score disproportionately. In addition, for unaccommodated individuals, their dissimilarity value was re-defined as the largest dissimilarity value of the accommodated individuals. The result reveals that the total aggregate factor score dissimilarity of the new sizing system based on 456 subjects is 2681.404, a decrease of 278.718 from that of the existing sizing system. Clearly, the new bra sizing system is superior to the existing system in the aspect of classifying the breast shape since it reduces the value of aggregate dissimilarity by approximately 10%.

In order to compare the dissimilarity results more clearly, the average value of d_i depending on the scores of eight factors for the subjects was calculated. The result (Table 4.16) shows that the mean of eight factor score dissimilarity of the new bra sizing system is 5.880, i.e. 0.611 smaller than the existing one. It can be seen that the standard deviation of factor score dissimilarity of the new bra sizing system is 4.534, less than the comparable factor score dissimilarity of 5.160 of the existing sizing system; the CV of the new sizing system is also smaller than the existing sizing system.

Table 4.16 Comparison of dissimilarity measures of factor scores for the two bra sizing systems (average value based on 456 subjects)

		Factor score dissimilarity of the new sizing system	Factor score dissimilarity of the existing sizing system
Mean		5.880	6.491
Std. Deviation		4.534	5.160
CV (%)		77.1	79.5
Minimum		0.697	0.663
Maximum		28.605	27.150
Range		27.908	26.487
Percentiles	25th	3.082	3.393
	50th	4.855	5.156
	75th	7.230	7.763

4.5.2 Key Measurements Aggregate Fit Loss Assessment

The first part of this section evaluated the efficiency of the two bra sizing systems using absolute dissimilarity measures. This section compares the aggregate fit loss of the two systems based on the key measurements related to bra pattern design.

The aggregate loss function has been proposed as an approach to finding an efficient sizing system which has a minimum observation’s distance from the closest prototype (Paal, 1997; McCulloch et al., 1998; Ashdown, 1998). This function was also defined according to a mathematical model of dissimilarity measure. As this distance function describes how far a garment made in the appropriate size would be from the key measurements of the individual, two additional terms were added: (1) an appropriate penalty on poor fit for an individual, depending on the different types of clothing to be worn, and (2) logarithmic transformation of measurements was used to predict the fit proportion since fit is better assessed by a proportional rather than a absolute difference (Mellian et al., 1990).

In the current study, this aggregate loss function was used to evaluate and compare the efficiency of the two bra sizing systems in fitting the population depending on the key measurements related to bra cup fitting. Based on bra pattern design criteria discussed in previous research studies (Haggar, 2004/1990; Morris et al., 2002; Chan et al., 2001; Thomas, 1995), five key measurements were selected from the 103 measurement items as the assessment variables to meet assessment criteria. They were: (1) D130 Right breast volume, (2) D134 Total arc length of right breast (horizontal plane), (3) M046 Vertical arc length from right bust point to underbust (BP~UBL), (3) D110 Width of the breast_b, and (5) D120 Height of the breast. The choice of these five measurements were confirmed in discussions with the experienced pattern designers who have had ten or more years experience of making bra patterns.

The following criteria were used to assess the re-adjusted aggregate fit loss function based on the specification proposed by Paal (1997) and McCulloch et al. (1998).

(1) The fit performance of a sizing system is related to how the individual's measurements differ from the assigned bra size.
(2) Research findings have suggested using proportional differences instead of absolute distance differences to predict the fit efficiency (Sharma, 1996). The aggregate of percentage differences between an individual and the assigned bra size over the five body dimensions are therefore used for assessment in the current study.
(3) The distance losses of individuals are evaluated and given different weighted penalties according to the percentage differences between an individual and the assigned bra size. A range around the centre point of the sizes that shows small

percentage differences between an individual and the assigned bra size is regarded as having perfect fit. If the individual distance loss value is out of this perfect range, a weighted penalty would be given to the distance loss value.

(4) Different measurements might have different perfect fit range according to the design features of the bra.

According to the above specification of the distance loss function, suppose that $d(x_n, y_s)$ can be written by a sum of squared dissimilarities over each of the *m* key measurements:

$$d(x_{nj}, y_{sj}) = \sum_{j=1}^{m}[d_j(x_{nj} - y_{sj})]^2, \qquad (4.9)$$

where x_{nj} is the datum of the *j*th measurement of the *n*th individual, and y_{sj} is the sample mean of the *j*th measurement of *s*th size category assigned to the *n*th individual.

The fit loss function for each measurement is redefined as follows

$$d_j(x_{nj}\ ,\ y_{sj}) = \begin{cases} w_j^l\left(\dfrac{y_{sj}(1-p_j^l)-x_{nj}}{y_{sj}(1-p_j^l)}\right) & \text{if } x_{nj} < y_{sj}(1-p_j^l) \\ 0, & \text{if } y_{sj}(1-p_j^l) \leqslant x_{nj} \leqslant y_{sj}(1+p_j^h) \\ w_j^h\left(\dfrac{x_{nj}-y_{sj}(1+p_j^h)}{y_{sj}(1+p_j^h)}\right) & \text{if } x_{nj} > y_{sj}(1+p_j^h) \end{cases}. \qquad (4.10)$$

Figure 4.18 illustrates how to measure the fit loss between individual and her assigned bra size for the *j*th measurement formulated in (4.10). As shown in Figure 4.18, p_j^l and p_j^h represent the negative or positive fractional differences that the individual's *j*th measurement could differ from the centre of her assigned size to be defined as a perfect fit range. The weighted coefficients w_j^l and w_j^h represent the penalties imposed on the individuals whose measurements are outside the perfect fit range.

Based on experienced practitioners' opinions and the pattern design features of the bra, the constants specification used for equation (4.10) are defined in Table 4.16. The discrepancies, p_j^l and p_j^h from the size centre were chosen based on generally accepted bra size misfit tolerances in the perfect fit range according to fabric features and flexibility. In this study, p_j^l is selected as twice p_j^h, and the weighted coefficient w_j^h is defined as twice w_j^l in consideration of the fact that if the bra is too small it may be more uncomfortable for the wearer than if it is too large.

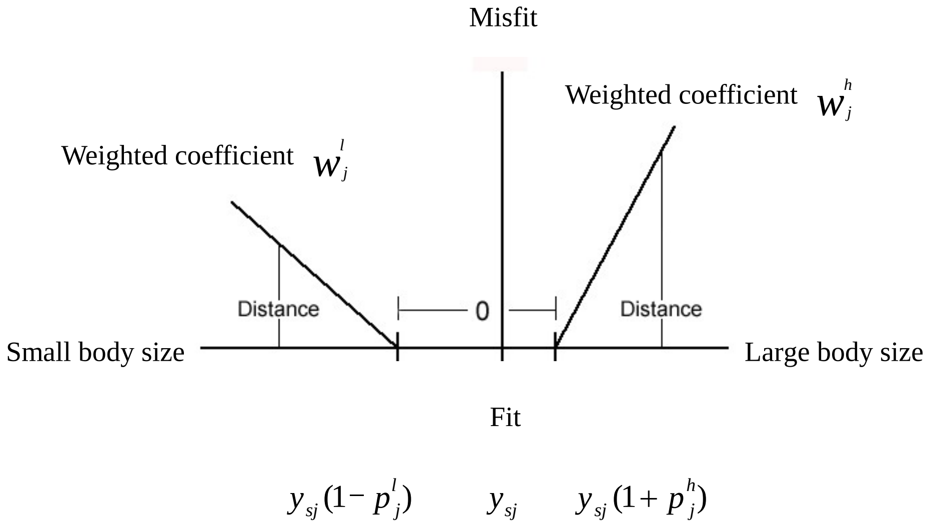

Figure 4.18 The fit loss function $d_j(x_{nj}, y_{sj})$ that measures the misfit between individual and her assigned bra size for the *j*th measurement

The overall performances of the two bra sizing systems were assessed using the loss function formulated in equation (4.9) and the selected constants shown in Table 4.17. The comparison result of total aggregate loss based on the 456 subjects reveals that, based on the five key dimensions, the aggregate loss of the new bra sizing system is 89.5342, i.e. 31% less than the existing system value of 129.9705.

Table 4.17 Estimated constants for the fit loss function given by equation (4.10)

	Constant			
	w_j^l	w_j^h	p_j^l	p_j^h
D130 Right breast volume	1	2	0.1(10%)	0.05(5%)
M046 BP~UBL	1	2	0.04(4%)	0.02(2%)
D134 Total arc length of right breast (Horizontal plane)	1	2	0.04(4%)	0.02(2%)
D110 Width of the breast_b	1	2	0.04(4%)	0.02(2%)
D120 Height of the breast	1	2	0.04(4%)	0.02(2%)

The results of average value of d_j depending on five key measurements are shown in Table 4.18. The results show that the mean of loss measure of the new bra sizing system is 0.1963, 0.0887 smaller than the existing one of 0.2850. It can be seen that the standard deviation of loss measure of the new bra sizing system is 0.4684, less than the comparable one of 0.6976 related to the existing sizing system.

Table 4.18 Comparison of loss measure of 5 key measurements between two bra sizing systems (average value based on 456 subjects)

		Loss measure (Squared Euclidean distance)	
		New sizing system	Existing sizing system
Mean		0.1963	0.2850
Std. Deviation		0.4684	0.6976
Minimum		0.0000	0.0000
Maximum		3.6185	3.8417
Range		3.6185	3.8417
Percentiles	25th	0.0154	0.0224
	50th	0.0557	0.0725
	75th	0.1618	0.2003

Table 4.19 Comparison of loss measure of each measurement between two bra sizing systems (Squared Euclidean distance, 456 subjects)

		Mean	Std. Deviation	Minimum	Maximum	Percentiles		
						25th	50th	75th
D130 Right breast volume	New	0.1227	0.3357	0.0000	2.3593	0.0000	0.0125	0.0883
	Existing	0.1739	0.4446	0.0000	2.3062	0.0000	0.0187	0.1063
M046 BP~UBL	New	0.0408	0.1093	0.0000	0.7172	0.0000	0.0052	0.0267
	Existing	0.0360	0.0956	0.0000	0.4884	0.0001	0.0039	0.0227
D134 Total arc length of right breast (horizontal plane)	New	0.0116	0.0320	0.0000	0.2361	0.0000	0.0008	0.0084
	Existing	0.0129	0.0364	0.0000	0.1861	0.0000	0.0008	0.0069
D110 Width of the breast_b	New	0.0093	0.0217	0.0000	0.1406	0.0000	0.0009	0.0078
	Existing	0.0124	0.0353	0.0000	0.1898	0.0000	0.0005	0.0078
D120 Height of the breast	New	0.0120	0.0273	0.0000	0.1653	0.0000	0.0015	0.0102
	Existing	0.0498	0.1300	0.0000	0.6712	0.0005	0.0065	0.0315

Apart from comparing the overall aggregate fit loss of the two bra sizing systems, the loss value assessment and the average value for each dimension were conducted. According to Table 4.19, the results indicate that compared to the existing bra sizing system, the new system is much better for the two measurements “D130 right breast volume” and “D120 height of the breast”, slightly better for the variables “D134 total arc length of right breast (horizontal plane)” and “D110 Width of the breast_b”, but worse for the item “M046 BP~UBL” (vertical arc length from bust point to underbust).

Furthermore, in order to evaluate the efficiency of the two bra sizing systems more extensively, the higher frequency size category groups were assessed. The frequency of bra classification results from the two bra sizing systems are reported in sections 4.2.1 and 4.4.1 respectively; it was found that most of subjects are classified in the size categories with cup sizes from AA (or AA*) to D (or D*) and for underband sizes from 70cm to 85cm. According to these results, 378 subjects who are in the sizes ranging from 70AA* to 85D* were assessed for aggregate fit loss assessment. The comparison results reveal that the aggregate fit loss of the new bra sizing system covering the 378 subjects was 63.4849, about 42.5% reduced from the 110.2961 achieved by the existing one. It is clear that the new bra sizing system is much superior to the existing system so far as performance of fitting the population is concerned.

Table 4.20 shows the results of average value of d_j based on 378 subjects. The mean of loss measure of the new bra sizing system is 0.1679, much smaller than the mean from existing system of 0.2918. It also can be seen that the standard deviation of the new bra sizing system is 0.3156, much less than the standard deviation of the existing sizing of 0.7285.

Table 4.20 Comparison of loss measure of 5 key measurements between two bra sizing systems based on primary bra classifications (Squared Euclidean distance, 378 subjects)

		Aggregate loss measure (Squared Euclidean distance)	
		New sizing system	Existing sizing system
Mean		0.1679	0.2918
Std. Deviation		0.3156	0.7285
Minimum		0.0000	0.0000
Maximum		2.6280	3.8417
Range		2.6280	3.8417
Percentiles	25th	0.0166	0.0245
	50th	0.0574	0.0689
	75th	0.1628	0.1955

The loss value assessment and the average value for each dimension across the 378 subjects were also conducted for both the existing and the new sizing system. The results shown in Table 4.21 indicate the loss value for all dimensions is better for the new system than the results achieved by the existing sizing system, especially on the two measurements “D130 right breast volume” and “D120 height of the breast”.

Table 4.21 Comparison of loss measure of each measurement between two bra sizing systems (Squared Euclidean distance, 378 subjects)

		Mean	Std. Deviation	Minimum	Maximum	Percentiles		
						25th	50th	75th
D130 Right breast volume	New	0.1058	0.2535	0.0000	2.3593	0.0001	0.0147	0.0959
	Existing	0.1794	0.4626	0.0000	2.3062	0.0000	0.0200	0.1063
M046 BP~UBL	New	0.0350	0.0879	0.0000	0.7172	0.0001	0.0052	0.0263
	Existing	0.0387	0.1001	0.0000	0.4884	0.0001	0.0040	0.0241
D134 Total arc length of right breast (Horizontal plane)	New	0.0092	0.0225	0.0000	0.2361	0.0000	0.0008	0.0080
	Existing	0.0131	0.0376	0.0000	0.1861	0.0000	0.0008	0.0074
D110 Width of the breast_b	New	0.0076	0.0167	0.0000	0.1406	0.0000	0.0007	0.0063
	Existing	0.0127	0.0361	0.0000	0.1898	0.0000	0.0005	0.0080
D120 Height of the breast	New	0.0103	0.0222	0.0000	0.1653	0.0000	0.0014	0.0093
	Existing	0.0478	0.1316	0.0000	0.6712	0.0005	0.0055	0.0303

4.6 Conclusions

In order to develop a new bra sizing system, two multivariate statistical methods, including principal components factor analysis and K-means cluster analysis, were used to determine sizing criteria and to establish a new sizing system based on a set of 103 static anthropometric variables.

A summary of the findings follows:

1) A new bra sizing system has been developed based on 456 subjects by using two control variables, namely underbust girth (UB) and "calculated aspect ratio of the breast 1 (D120/D110_b)" (for easy understanding purpose, will be denoted as "breast depth width ratio" in the later chapters), which had the highest factor loading on factor 1 and factor 2 in the principal components factor analysis.
2) Probability densities were used to investigate the population accommodation rate of the new sizing system and the existing one. The results indicated that the 2-dimensional probability coverage rate of the new system was nearly 98%, better than the 95% achieved by the existing system. Many intimate apparel companies do not produce bras with 65cm underbands, AA cups or G cups. In this case, the partial probability coverage rate "without 65cm underband, AA* cup and G* cup (%)" showed a much higher percentage coverage rate, around 85% for the new system, superior to the 77% calculated for the existing sizing system.
3) As one of the approaches, dissimilarity distance measures based on factor scores were conducted to evaluate the efficiency of the two bra sizing systems in

classifying the breast shapes. It was found that the aggregate factor score dissimilarities of the new bra sizing system was 2681.404, less than the 2960.122 of the existing one − reduced by approximately 10%. It is clear that the new bra sizing system is better than the existing one on classifying the breast shape.

4) Aggregate fit loss assessments based on five key measurements were also measured to assess the two sizing system performances for fitting the population. The results across 456 subjects revealed that the aggregate loss of the new bra sizing system was 89.5342, much less than the aggregate loss of 129.9705 of the existing one. Furthermore, the same loss function was re-measured for only the subjects in the high frequency coverage bra sizes. The result for these 378 subjects indicates a better fit performance for these subjects than for the subjects as a whole. The aggregate fit loss of the new system for the 378 subjects was 63.4849, about 42.5% reduced from the 110.2961 achieved by the existing one. Clearly, the new bra sizing system is much superior to the existing system for fitting the population.

In summary, compared to the existing sizing system, the new bra sizing system is a more efficient sizing system that satisfies several requirements, including covering a larger percentage of the population, providing a better fit to the accommodated individuals, having a clear structure and keeping the same size number of sizes in the system.

CHAPTER 5

FUNDAMENTAL EXPERIMENT FOR SEAMLESS BRA DESIGN

5.1 Introduction

In general, seamless knitted bras can be designed to provide better comfort and gentler breast-support than the normal “cut and sewn” bras, because of the fabric’s flexibility. In conventional bra design, a good fit bra should provide support from the strap, underband, bust circumference and two intersecting arcs of cups (Starr et al., 2005). Moreover, a bra should be designed in an accurate 3D structure and should use proper fabric stretch to fit the body measurements with careful pattern making (Li et al. 2003; Lim et al. 2006).

In chapter 4, two key measurements, underbust girth and “breast depth width ratio” were used to establish a new bra sizing system. This emphasizes that underband and cup are very important for bra design. In the seamless knitting experiments, these two regions (underband and cup) were investigated. The relationships between fabric strength, loop density and yarn tension will help to identify the key parameters for further seamless bra development. A circular knitting machine of the SANTONI SM8-Top2 model of 14" 28G 1248 Ndl, which is a common machine for producing medium size bodywear in commercial market was used to conduct the experiments.

A full 2^4 factorial design experiment was conducted to investigate underband tension using three types of common yarns including 78-68-1 Nylon 66, 20-20/10/1 cover yarn and 210D bare elastic. For the cup strain measurement, a 2^3 factorial design experiment was used based on the same yarns of 78-68-1 Nylon 66 and 20-20/10/1 cover yarn. Minitab 14 was used to analyze the experimental data and to establish prediction models for seamless bra underband tension (N) and cup strain (%).

5.2 Knitting Machine Used

The SANTONI SM8-TOP2 (Figure 5.1) is an 8-feed single jersey electronic circular knitting machine with two selection points per feed. It is suitable for producing underwear, outwear, swimwear, sportswear and sanitary knitted garments with single garment separation (SANTONI's website, 2006).

Figure 5.1 SANTONI SM8-TOP2 circular knitting machine (SANTONI's website, 2006)

5.3 Pilot Test of Seamless Knitted Bra Prototype

The aim of the pilot test is to identify the finishing process that can be used to control the shrinking size of seamless bras for further experiment design. Since the seamless knitted bra can be designed with either a single or a double-layer by using the SANTONI SM8–TOP2 machine, the research question here is: are there any differences between these two patterns depending on the same experimental conditions? Which finishing process can be used to control the shrinking size of the seamless knitted bras?

In the pilot test, four prototypes were knitted using 78-68-1 Nylon 66, 17-20/15/1 cover yarn and 240D bare elastic. Using the same style (see Figure 5.2), two bra prototypes were knitted with a single layer, and the other two prototypes with a double-layer. The different regions of the knitted bra tube were measured after pre-shrinking and after dyeing. Pre-shrinking was done using steam for 25 minutes using the "LAB WINCH" machine. The bras were dyed in an "Overhead Paddle Dyeing M/C" machine for 100 minutes, as in the normal method for dyeing Nylon with acid dyes.

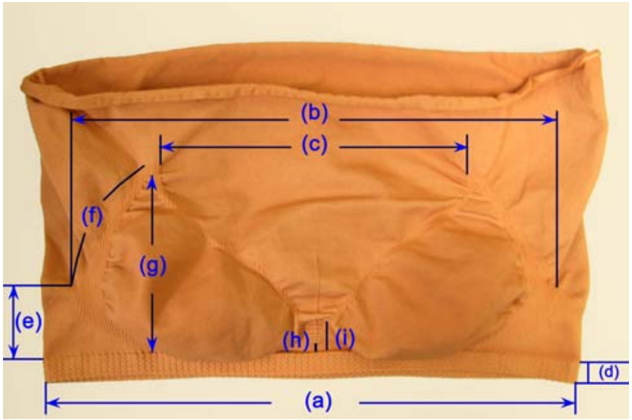

Figure 5.2 Definitions of different regions of seamless bra prototype

As shown in Figure 5.2, the sizes of different regions were measured for the seamless knitted bra tube prototypes. These included underband length (a), horizontal length from left outer-point of the cup to right outer-point of the cup (b), horizontal length between left inner-point of the cup apex and right inner-point of the cup apex (c), underband height (d), vertical length from the upper underband to the right outer-point of the cup (e), right arc length from outer-point of the cup to outer-point of the cup apex (f), cup height (g), height of the gore centre (h) and height of the side gore (i).

Table 5.1 reveals the measurement results. Figure 5.3 shows the means for the different measurements after pre-shrinking and after dyeing. It can be seen that the shrinkage rate was nearly the same regardless of the knitting structure of each part in different manufacturing procedures. It can also be seen that the size of the different regions of the bra prototypes were reduced by less than 5% additional shrinkage after the dyeing procedure in comparison to the size after preshrinking.

Table 5.1 The measurements in different regions

No.	Items	Measuring items								
		a	b	c	d	e	f	g	h	i
Style 1 (single layer)	① After pre-shrinking (cm)	30.90	28.00	17.70	1.40	4.00	9.20	11.50	0.73	3.10
	② After dyeing (cm)	30.40	27.40	17.40	1.40	3.80	8.80	10.75	0.70	2.95
	Pre-shrinkage percentage (②/①) (%)	98.4	97.9	98.3	100.0	95.0	95.7	93.5	95.9	95.1
Style 1 (single layer)	① After pre-shrinking (cm)	30.90	28.00	17.70	1.40	4.00	9.20	10.95	0.70	3.00
	② After dyeing (cm)	30.60	27.50	17.70	1.40	3.82	8.90	10.60	0.67	2.90
	Pre-shrinkage percentage (②/①) (%)	99.0	98.2	100.0	100.0	95.5	96.7	96.8	95.7	96.7
Style 1 (double-layer)	① After pre-shrinking (cm)	31.20	29.60	18.20	2.00	4.10	9.60	11.10	0.70	3.12
	② After dyeing (cm)	30.80	29.20	18.05	2.00	4.10	9.20	10.60	0.70	3.08
	Pre-shrinkage percentage (②/①) (%)	98.7	98.6	99.2	100.0	100.0	95.8	95.5	100.0	98.7
Style 1 (double-layer)	① After pre-shrinking (cm)	32.40	30.70	18.50	1.48	4.20	9.40	11.10	0.75	3.15
	② After dyeing (cm)	31.40	29.50	18.10	1.45	4.10	9.10	10.50	0.70	3.00
	Pre-shrinkage percentage (②/①) (%)	96.9	96.1	97.8	98.0	97.6	96.8	94.6	93.3	95.2
Mean of Pre shrinkage percentage (②/①) (%)		98.25	97.70	98.83	99.50	97.03	96.25	95.10	96.23	96.43

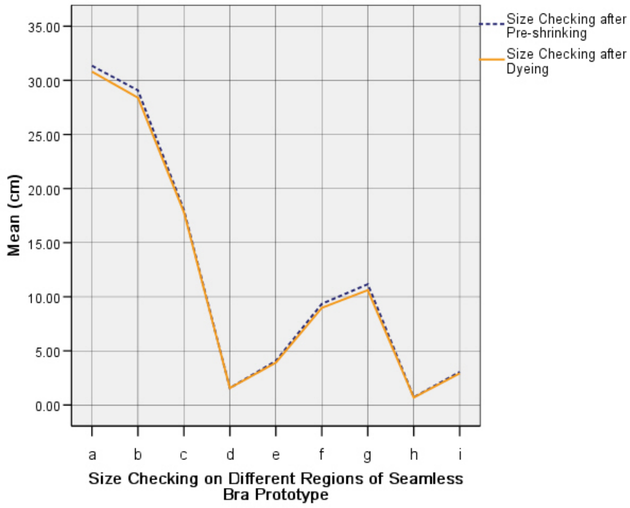

Figure 5.3 Measurement of different regions after pre-shrinking and after dyeing

In order to investigate whether there were significant differences between one layer and double-layer prototype bras, one-way ANOVA analysis was conducted at the 5% level. The results show that the p-values of “after pre-shrinking” and “after dyeing” are 0.898 and 0.905. This means that there are no significant differences between two patterns (one layer and double-layer) on both processes of “after pre-shrinking” and “after dyeing”.

Based on the above results, considering it is difficult to control the dyeing effects in different processes in lab experiments, the pre-shrinking state was chosen as the processing procedure to be used in further experimental design.

5.4 Factorial Experiment on Seamless Knitted Bra’s Underband Tension

Previous work has indicated a relationship between the wearers’ comfort and the bra pressure exerted on the body (Costantakos & Watkins, 1982; Makabe et al., 1991; Li et al. 2003). It has been reported that fabric tension and the body dimensions (curvature) were the key parameters influencing the clothing pressure (Yoshimura & Ishikawa, 1983; Ito et al., 1986).

As shown in Figure 5.4, when the bra is worn, the underband stretches to fit the wearer's body and holds the bra cups in position. Therefore, the elastic band is usually made shorter than the wearer's underbust girth. For seamless knitted bras, information on how to make a "knit-in" bra band with proper tension is very important.

Front view Side view Back view

Figure 5.4 Seamless knitted bra prototype

The underband tension of a bra is one of the key measures for bra fitting. The current experiment had two purposes, (1) to define the key knitting parameters for underband design for further seamless bra development, and (2) to establish regression models for predicting the underband tensions of seamless knitted bras from its original size to fit different medium underbust sizes.

5.4.1 Design of the Experiment

Previous pilot tests for product development have shown that many factors influence the seamless bra's design. They include the type of yarns used, loop density, yarn tension (controlled by the machine), knitting structure, production environment (temperature & humidity) and finishing processes. After discussion with experienced knitters, several major knitting parameters have been selected for the current experiment as described in the following section. The whole experiment was conducted in a controlled condition similar to the practical manufacturing environment in a knitting factory.

5.4.1.1 2^4 Factorial Experiment

The experiment was conducted using a 2^4 full factorial design (Montgomery, 2001; Montgomery, 2005). There were four factors included in this experiment: loop density, elastic yarn tension, cover yarn tension and Nylon yarn tension. As shown in Table 5.2, each factor has a low level and a high level production value, which are normally the maximum and minimum in practice. In order to test whether a linear model was adequate and to investigate the underband tension at the middle level between the low and high levels, four centre points were added to this experiment in runs 17 to 20 (Table 5.3). The centre point level for each factor is presented in Table 5.2.

Table 5.2 2^4 factorial experiment of 4 factors at 2 levels with additional centre point levels

Factor	Low level	High level	Centre point level
A: loop density	−40	+40	0
B: elastic (bare Lycra) yarn tension (g)	20	12	16
C: cover yarn tension (g)	3.5	1.5	2.5
D: Nylon yarn tension (g)	5	3	4

Table 5.3 shows the test matrix of current experiment. Runs from 2 to 16 are represented by a series of lowercase letters in the column of "treatment combination". If a letter is present, then the corresponding factor is set at the high level at that run; if a letter is absent, the factor is run at its low level. For example, an entry "abd" (run 12) indicate that factors A, B, D are at the high level and factor C is at the low level. Runs 17 to 20 are added centre points, which the four factors are set at "centre point level" shown in Table 5.2.

Table 5.3 The full 2^4 experiment design for the current experiment

Run	Treatment combination	Basic design			
		A	B	C	D
1	(1)	−	−	−	−
2	a	+	−	−	−
3	b	−	+	−	−
4	ab	+	+	−	−
5	c	−	−	+	−
6	ac	+	−	+	−
7	bc	−	+	+	−
8	abc	+	+	+	−
9	d	−	−	−	+
10	ad	+	−	−	+
11	bd	−	+	−	+
12	abd	+	+	−	+
13	cd	−	−	+	+
14	acd	+	−	+	+
15	bcd	−	+	+	+
16	abcd	+	+	+	+
17	Center point	0	0	0	0
18	Center point	0	0	0	0
19	Center point	0	0	0	0
20	Center point	0	0	0	0

The bra size classification results in section 4.2.1 shows that the female with underbust girth between 70cm to 80cm occupy a high percentage of 77%. Since the bra size 75B (or 75B* in the new sizing system) is generally used as a medium size for bra design and sample making, the current study on the Chinese women's market focused on the response of underband tension for fitting underbust girths from 70cm to 80cm. It was tested at the following 3 levels.

Response 1: underband tension when fitting 70cm underbust girth (UB)

Response 2: underband tension when fitting 75cm underbust girth (UB)

Response 3: underband tension when fitting 80cm underbust girth (UB)

5.4.1.2 Conditions of the Experiment

1) Yarn Selection

According to "Knitting International" ("Global seamless market round-up," 2004a; "Technology spurs seamless growth," 2004b), textured Nylon yarn (polymide) is the primary yarn used for seamless apparel in Europe, US and China. Since seamless underwear is all light weight, 60-80 denier Nylon yarn is largely used. Stretch elastane yarns have made a significant impact on the seamless knitting sector (Morris, 2003), because it can create 3D surface effects when incorporated with jacquard technologies (Black, 2002). Based on the above consideration, the yarns used in this experiments included 78/68/1 Nylon 66 from NYLSTAR, 20-20/10/1 cover yarn from ITOCHU, 210D bare elastic from INVISTA.

2) Knitting Environment of Temperature and Humidity

The knitting experiment was conducted in ITC's air-conditioned workshop with constant temperature and humidity environment same as the factory environment at 20℃ and 65% relative humidity.

3) Finishing Process Selection

Based on the previous pilot test, pre-shrinking was conducted to control the shrinkage of seamless knitted fabric samples and seamless "underband ring" specimens in this experiment by using the same control conditions.

4) Knitting Structure

1 × 1 and 1 × 3 are two major types of knitting structures can be designed in underband region. In our experiment, 1 × 3 knitting structure that is normally used in commercial knitted bras was chosen (Figure 5.5).

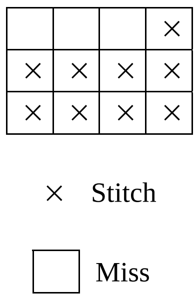

Figure 5.5 Notation for a 1 × 3 knitting structure

5.4.2 Tensile Test

The tensile data were collected according to ASTM D4964-96 (1996/2004) procedures, using an INSTRON 4411 (CRE type tensile testing machine).

5.4.2.1 Specimens of Underband Ring

Nine specimens of underband ring samples were knitted for each run shown in Table 5.3. After finishing the pre-shrinking process, 9 specimens were divided into 3 subgroups randomly. Each group of specimens was stretched to the lengths of 70cm, 75cm, and 80cm respectively at a speed of 500 mm/min for 3 cycles (Figure 5.6). The stress-strain data was recorded at the third cycle and the tension test was repeated three times.

5.4.2.2 1 × 3 Underband Fabric Specimens

1 × 3 underband fabric samples were also knitted by SANTONI electronic circular machine for each run shown in Table 5.3. After the pre-shrinking process, a total of twelve 350 × 100 mm specimens were cut and sewn into a loop of 250 mm circumference for each run. Of these, six specimens were along the wale direction, six specimens were along the course direction. For each direction, three sets of double-layer specimens were extended to a maximum tension of 50N at a speed of 500 mm/min for 3 cycles. The strain (%) data were recorded at the third cycle at the loading tensions of 5N and 10N, which were the extreme values of tension at the centre points when the underband ring was extended to 70cm ~ 80cm.

Figure 5.6 Underband specimen in place on pins

5.4.3 Analysis of Underband Ring Specimens

5.4.3.1 Screening Design

The objective of a screening design is to select important factors that have large effects on the response variable. A multiple regression model is used to determine which factors are significantly related to the responses at the 5% level. The normal probability plots of the standardized effects of the three response variables are shown in Figures 5.7 to 5.9.

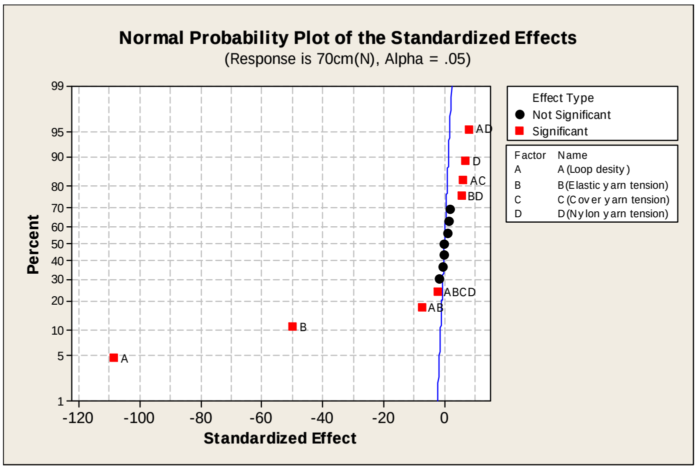

Figure 5.7 Normal probability plots of the standardized effects of response 1

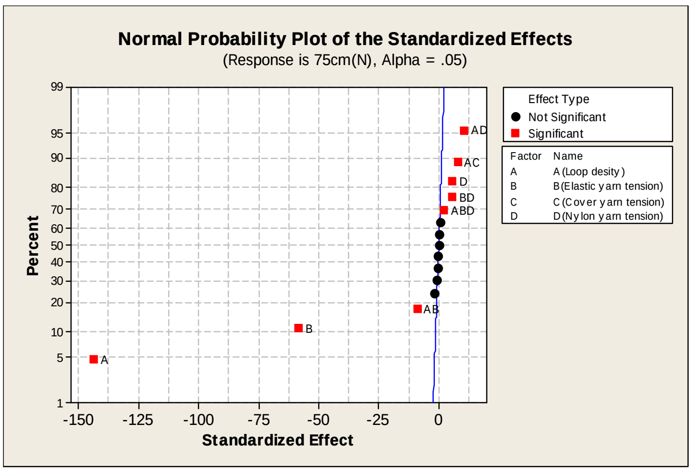

Figure 5.8 Normal probability plots of the standardized effects of response 2

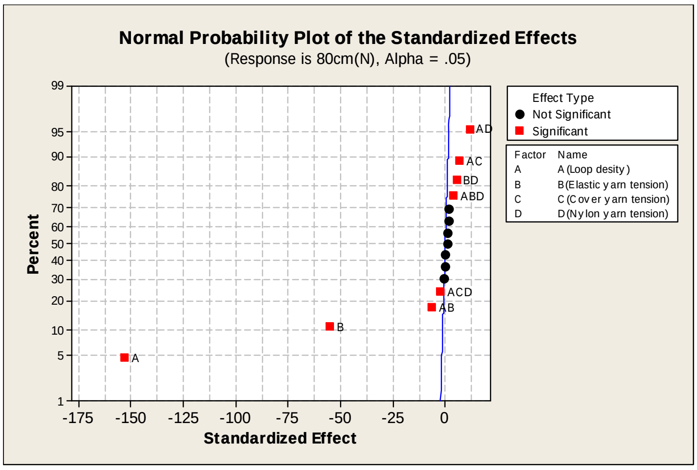

Figure 5.9 Normal probability plots of the standardized effects of response 3

It can be seen that in all three figures, factor A and factor B fall well away from the line and have much larger effects than the other factors and their interactions (Minitab Inc., 2003; Montgomery, 2005). This reveals that factor A and factor B are the major factors that influence the three responses.

5.4.3.2 Data Means Observation

The observation means for the three response variables (stretch tension) at each run are shown in Table 5.4. From the results, it will be observed that each response has its maximum in the 1st run (i.e. all factors at low level), and its minimum in the 4th run (i.e. factors A & B at the high level and factors C & D at the low level). The underband tension of the centre point for each response is approximately midway between the minimum and the maximum.

Table 5.4 Data means of different response variables at different treatment combination situation (N)

Run	Treatment combination	Levels of A B C D	Tension for fitting 70cm	Tension for fitting 75cm	Tension for fitting 80cm
1	(1)	－－－－	10.51	13.02	15.70
2	a	＋－－－	4.92	6.53	8.00
3	b	－＋－－	8.23	10.69	13.33
4	ab	＋＋－－	1.52	3.22	4.51
5	c	－－＋－	10.42	12.70	15.34
6	ac	＋－＋－	5.23	6.80	8.36
7	bc	－＋＋－	8.05	10.46	12.97
8	abc	＋＋＋－	2.19	3.62	5.14
9	d	－－－＋	10.42	12.66	15.03
10	ad	＋－－＋	5.27	6.84	8.27
11	bd	－＋－＋	8.36	10.78	12.84
12	abd	＋＋－＋	2.86	4.33	5.72
13	cd	－－＋＋	9.97	12.34	14.89
14	acd	＋－＋＋	5.68	7.24	8.45
15	bcd	－＋＋＋	8.18	10.24	12.61
16	abcd	＋＋＋＋	3.04	4.60	6.04
17~20	Center point	0 0 0 0	6.49	8.12	9.53

5.4.3.3 Fit Reduced Models

According to the results of the standardized effects of each factor in the full factorial model, a regression model was fitted for each response variable using only the significant factors. The new factorial fit results (see Tables 5.5 ~ 5.7) indicate that all terms have p-value less than 0.05. The adjusted coefficient of multiple determination (adjusted R^2) for three response variables are all greater than 98%.

In order to check the adequacy of the models, the residuals[1] of the models were examined for three basic assumptions: independence, constant variance and normality (Montgomery, 2005). The residual plots are shown in Figures 5.10 to 5.12. The

[1] The residuals are defined as the n differences $e_i = Y_i - \hat{Y}_i$, i = 1, 2, …, n where Y_i is an observation and $\hat{Y}_i$ is the corresponding fitted value obtained by use of fitted regression equation.

normality test of residuals for each fitted model indicated that the p-value for response 1 was 0.169, response 2 was 0.409, and response 3 was 0.323, all of them were greater than 0.10, so the normality assumptions for all three responses can be accepted. As shown in the three figures, the plots of residuals against the fitted values form an approximate horizontal band evenly distributed around the horizontal axis respectively. Therefore, constant variance assumptions for all three responses are also acceptable. Since the plots of residuals versus the order of the data are scattered evenly around the horizontal order-axis randomly in all the three figures, the independence assumptions are also reasonable.

For response variables, according to the factorial fit Tables (5.5 to 5.7), the regression equations for underband stretch tensions can be written with coded variables as follows:

$$y_1 = 6.552 - 2.715x_1 - 1.250x_2 - 0.188x_1x_2 \qquad (5.1)$$

$$y_2 = 8.504 - 3.108x_1 - 1.262x_2 - 0.192x_1x_2 \qquad (5.2)$$

$$y_3 = 10.451 - 3.638x_1 - 1.306x_2 - 0.154x_1x_2 \qquad (5.3)$$

where y_1, y_2, y_3 are the underband stretch tensions (N) of seamless knitted bra when fitting 70cm, 75cm and 80cm underbust girths, x_1 is the coded loop density, x_2 is the coded elastic yarn tension, and $x_1 x_2$ is the interaction of x_1 and x_2. The variables x_1 and x_2 are defined on a coded scale from -1 to $+1$ (the low and high levels of factor A & B). For each factor, the relationship between the natural variable and the coded variable can be given as (Montgomery, 2001):

$$\text{Coded variable} = \frac{\text{Natural variable} - {\left(\text{High level} + \text{Lower level}\right)}\big/{2}}{{\left(\text{High level} - \text{Lower level}\right)}\big/{2}}$$

Table 5.5 Factorial fit: the stretch tension (N) for fitting 70cm underbust girth versus A (loop density), B (elastic yarn tension)

Estimated effects and coefficients for the stretch force (N) of 70cm underbust girth (coded units)					
Term	Effect	Coef	SE Coef	t	P
Constant		6.552	0.05208	125.82	0.000
A (loop density)	-5.430	-2.715	0.05208	-52.13	0.000
B (elastic yarn tension)	-2.499	-1.250	0.05208	-23.99	0.000
A (loop density)*B (elastic yarn tension)	-0.375	-0.188	0.05208	-3.60	0.001
Ct Pt		-0.060	0.11645	-0.51	0.611
S = 0.360800 R-Sq = 98.36% R-Sq (adj) = 98.25%					

Analysis of variance for the stretch tension (N) of 70cm underbust girth (coded units)						
Source	DF	Seq SS	Adj SS	Adj MS	F	P
Main effects	2	428.769	428.769	214.384	1646.87	0.000
2-Way interactions	1	1.688	1.688	1.688	12.96	0.001
Curvature	1	0.034	0.034	0.034	0.26	0.611
Residual error	55	7.160	7.160	0.130		
Pure error	55	7.160	7.160	0.130		
Total	59	437.650				

(* Where "Coef" is coefficients, "SE Coef" is standard error of coefficients, "t" is t-value, "P" is p-value, "S" is standard deviation, "R-Sq" is R^2, "R-Sq (adj)" is adjusted R^2, "DF" is the degree of freedom, "Seq SS" is sequential sum of squares, "Adj SS" is adjusted sum of squares, "Adj MS" is adjusted mean squares and "F" is F-value.)

Table 5.6 Factorial fit: the stretch tension (N) for fitting 75cm underbust girth versus A (loop density), B (elastic yarn tension)

Estimated effects and coefficients for the stretch force (N) of 75cm underbust girth (coded units)					
Term	Effect	Coef	SE Coef	t	P
Constant		8.504	0.05006	169.89	0.000
A (loop density)	-6.215	-3.108	0.05006	-62.08	0.000
B (elastic yarn tension)	-2.524	-1.262	0.05006	-25.21	0.000
A (loop density)*B(elastic yarn tension)	-0.385	-0.192	0.05006	-3.84	0.000
Ct Pt		-0.389	0.11193	-3.47	0.001
S = 0.346809 R-Sq = 98.80% R-Sq (adj) = 98.71%					

Analysis of variance for the stretch tension (N) of 75cm underbust girth (coded units)						
Source	DF	Seq SS	Adj SS	Adj MS	F	P
Main effects	2	540.009	540.009	270.004	2244.87	0.000

Table 5.6 (continued)

2-Way interactions	1	1.775	1.775	1.775	14.76	0.000
Curvature	1	1.449	1.449	1.449	12.05	0.001
Residual error	55	6.615	6.615	0.120		
Pure error	55	6.615	6.615	0.120		
Total	59	549.848				

Table 5.7 Factorial fit: the stretch tension (N) for fitting 80cm underbust girth (N) versus A (loop density), B (elastic yarn tension)

Estimated effects and coefficients for the stretch force (N) of 80cm underbust girth (coded units)

Term	Effect	Coef	SE Coef	t	P
Constant		10.451	0.05347	195.45	0.000
A (loop density)	-7.276	-3.638	0.05347	-68.04	0.000
B (elastic yarn tension)	-2.611	-1.306	0.05347	-24.42	0.000
A (loop density)*B (elastic yarn tension)	-0.308	-0.154	0.05347	-2.88	0.006
Ct Pt		-0.925	0.11957	-7.74	0.000

S = 0.370462 R-Sq = 98.97% R-Sq (adj) = 98.90%

Analysis of variance for the stretch tension (N) of 80cm underbust girth (coded units)

Source	DF	Seq SS	Adj SS	Adj MS	F	P
Main effects	2	717.149	717.149	358.575	2612.72	0.000
2-Way interactions	1	1.138	1.138	1.138	8.29	0.006
Curvature	1	8.218	8.218	8.218	59.88	0.000
Residual error	55	7.548	7.548	0.137		
Pure error	55	7.548	7.548	0.137		
Total	59	734.053				

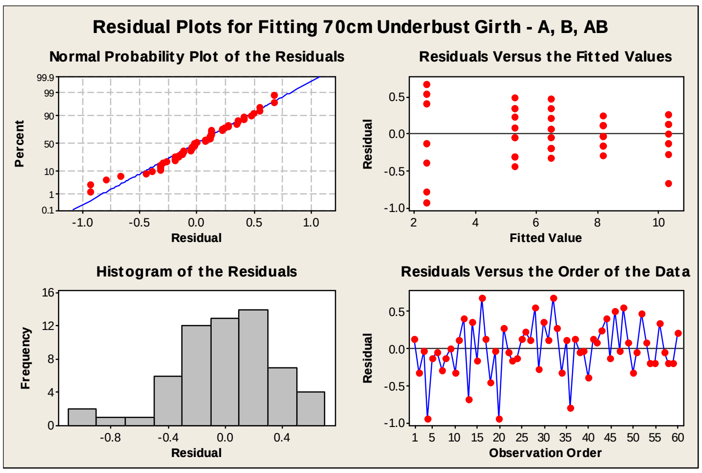

Figure 5.10 The residual plots check for response 1

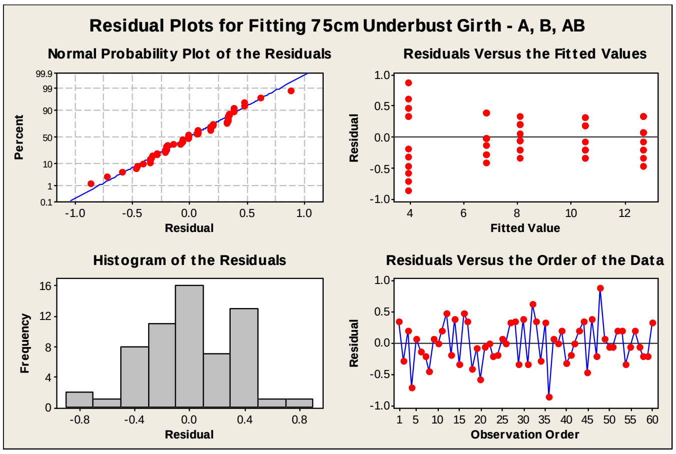

Figure 5.11 The residual plots check for response 2

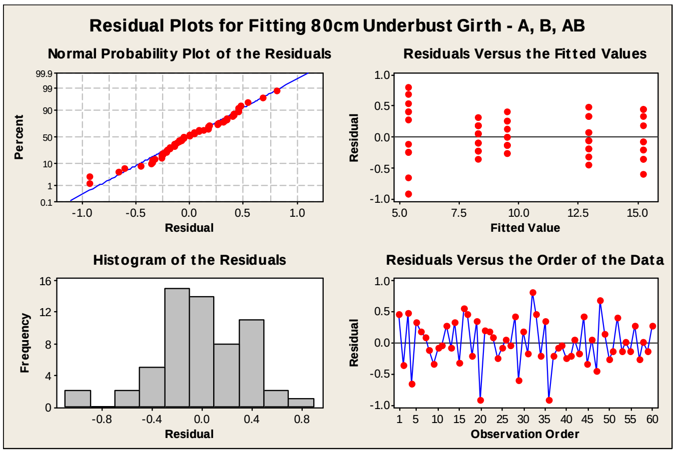

Figure 5.12 The residual plots check for response 3

Moreover, according to the analysis of variance Tables (5.5 to 5.7), the p-values of curvature for response 2 and response 3 are less than 0.05, but the p-value of curvature for response 1 is 0.611. The results indicate strong evidence of quadratic curvature for both response 2 and response 3. But there is no evidence of quadratic curvature for response 1. Is it necessary to incorporate second-order effects to obtain an adequate quadratic model? Montgomery (2001) suggested that if the interaction term was added to a main-effect model, curvature was introduced to the response surface model. Considering that the purpose of this experiment was to investigate a fitting range for underband tension and to identify the key knitting parameters, not improving the fitting tension for the seamless bra's underband, it was decided not to do further experiments to develop quadratic models.

5.4.4 Data Analysis of Underband Fabric Specimens

From the tensile tests of underband ring, we knew that the tension at the centre points for fitting 70cm to 80cm were from 5N to 10N. The average value is shown in Table 5.4. Therefore, the strain data were recorded and analyzed at the loading tensions of 5N and 10N. Table 5.8 presents the data means of each run with different treatment combination at 5N and 10N loading tensions along the wale and course directions. For the 5N loading tension, the results indicate that along the fabric course direction, there was a minimum strain of 9.82% at the first run and a maximum strain of 29.38% at 16th run. The data mean at the centre point is 17.53%. But for the fabric wale direction, it can be seen that the minimum strain of 21.27% is at the 5th run, and the maximum strain of 65.48% course at the 4th run. And the data mean at the centre point is 40.29%. This means that the knitting factors have different effects on wale and course directions.

For the 10N loading tension, the results are very similar to the results for the 5N loading tension. In the course direction, there is a minimum strain of 14.11% at the first run and a maximum strain of 29.92% at the 16th run. For the wale direction, it can be seen that the minimum strain of 26.64% is at the 5th run, and the maximum strain of 95.44% is at 4th run. As shown in Table, for centre points, the data mean for the course direction is 17.53%, exactly equal to the result for the 5N loading tension; and the data mean for the wale direction is 41.26%, also close to the value of 40.29% for the 5N loading tension. This reveals that the four knitting factors have the same effects at 5N and 10N loading tension if the factor values are set at centre point levels.

Table 5.8 Data means of different response strain at different treatment combination situation (%)

Run	Treatment combination	Basic design	Strain (%) of 5N loading tension		Strain (%) of 10N loading tension	
			Course direction	Wale direction	Course direction	Wale direction
1	(1)	－－－－	9.82	21.80	14.11	27.42
2	a	＋－－－	19.59	49.12	20.53	73.13
3	b	－＋－－	11.67	28.13	15.91	22.22
4	ab	＋＋－－	25.50	65.48	25.73	95.44
5	c	－－＋－	9.95	21.27	14.40	26.64
6	ac	＋－＋－	20.62	48.18	21.57	71.32
7	bc	－＋＋－	12.19	27.91	14.89	21.97
8	abc	＋＋＋－	24.47	61.01	27.17	89.32
9	d	－－－＋	10.42	21.36	14.79	27.07
10	ad	＋－－＋	20.02	49.90	21.02	73.25
11	bd	－＋－＋	11.71	27.56	16.56	25.86
12	abd	＋＋－＋	26.66	59.08	27.07	86.59
13	cd	－－＋＋	10.93	21.87	15.78	27.86
14	acd	＋－＋＋	21.47	47.01	22.50	68.95
15	bcd	－＋＋＋	11.81	26.87	16.73	25.29
16	abcd	＋＋＋＋	29.38	53.52	29.92	78.29
17~20	Center point	0 0 0 0	17.53	40.29	17.53	41.26

5.5 Fundamental Experiment on a Seamless Bra's Cup Strain

The stretch ratios of knitted fabric and elastic materials can significantly affect the garment fit (Lim et al., 2006). The cup strain of a bra is another key measure for bra fitting. The current experiment had two objectives: (1) to define the key knitting parameters on cup design, and (2) to establish regression models for predicting the cup strain of seamless knitted bras on the special loading tension defined according to the maximum optimal pressure value around the ribcage.

5.5.1 Design of the Experiment

5.5.1.1 Response Variables

It is emphasized that underwear should provide good extensibility at low force to ensure comfort for body expansion during breathing or after meals (Jiao et al., 2001). In general, a breast can weight from 200gms to 800gms or above. To provide support to the breast with comfort pressure, seamless bra cup needs to give sufficient volume with the appropriate fabric tension. Previous studies on clothing pressure developed prediction models by using non-uniform biaxial stress in both the wale and course directions, as well as body curvature radius (Yoshimura & Ishikawa, 1983; Ito et al., 1986).

In our experiment, the cup strain was tested in both the wale and course directions. To determine the loading force, we considered several factors including the comfort pressure range, the bust geometry and curvature. Roedel et al. (2002) reported that, the optimal blood circulation occurred at a pressure range of 15-25mmHg for the lower arm tube. Assuming the ridcage region is like a cylinder bounded by a bra, the comfort range of tensile force can be calculated using Ng and Hui's (2001) equation as follows:

$$T = PR \tag{5.4}$$

where P is the garment pressure, T is the force applied to the fabric, and R is the curvature radius of the body part defined by the width and thickness using equation 5.5,

$$R = \frac{(a/2)^2 + b^2}{2b} \qquad (5.5)$$

where *a* is width and *b* is the thickness of the body at certain level e.g. bust level.

Based on 49 female subjects whose breast size are 75B*, the mean of the bust width is 27.2cm and the bust thickness is 23.0cm, then we have R as 15.5cm by equation 5.5. According to the optimal pressure range of 15-25 mmHg, where 1mmHg is equal to 0.0133231N/cm^2, the desirable tension range on the medium size bust can be calculated as, T = PR = (15 ~ 25) × 0.0133231N/cm^2 × 15.5cm = 3.1 ~ 5.1N/cm.

The major purpose of current experiment is to define the key knitting parameters influencing the fabric tension in the cup area that provide optimal pressure to the breast. Integer 5N loading tension (force) was the maximum theoretic value being used to perform the elongation tests along the wale and course directions. Furthermore, the bias direction was also tested for investigation. There were three response variables:

Response 1: cup strain along bias direction at 5N loading tension

Response 2: cup strain along course direction at 5N loading tension

Response 3: cup strain along wale direction at 5N loading tension

5.5.1.2 2^3 Factorial Experiment

As shown in Table 5.9, three factors were included in this experiment: loop density, cover yarn tension and Nylon yarn tension. The design of the current 2^3 factorial experiment (Montgomery, 2001) is shown in Table 5.10. Each factor has a low level and a high level. In addition, in order to test whether a first–order model is adequate and to explore the cup strain at the middle level between the low and high levels, three central points were added to this experiment (runs 9 to 11).

Table 5.9 2^3 factorial experiment design of 3 factors at 2 levels with additional centre point levels

Factor	Low level	High level	Centre point level
A: loop density	−40	+40	0
B: cover yarn tension (g)	3.5	1.5	2.5
C: Nylon yarn tension (g)	5	3	4

Table 5.10 The full 2^3 experiment design with added centre points for the current experiment

Run	Treatment combination	Basic design		
		A	**B**	**C**
1	(1)	−	−	−
2	a	+	−	−
3	b	−	+	−
4	ab	+	+	−
5	c	−	−	+
6	ac	+	−	+
7	bc	−	+	+
8	abc	+	+	+
9	Centre point	0	0	0
10	Centre point	0	0	0
11	Centre point	0	0	0

5.5.1.3 Conditions of the Experiment

The conditions differed from 5.4.1.2 are described in the following:

1) Yarn Selection

The yarns used in current experiment were 78/68/1 Nylon 66 from NYLSTAR, and 20-20/10/1 cover Lycra from ITOCHU.

2) Knitting Structure

Plain jersey is a common knitting structure used in the cup region of commercial seamless bras. Considering the cup region requires a natural smooth look, plain jersey (Figure 5.13) was also chosen in the current experiment.

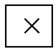

× Full stitch

Figure 5.13 The notation for a plain jersey knitting structure

5.5.2 Tensile Test

The tensile data were collected according to ASTM D4964-96 using an INSTRON 4411 (CRE type tensile testing machine). After knitting the bra tube and pre-shrinking, three 350 × 100 mm specimens were cut along the bias, course and wale directions. In all, 9 specimens were sewn into loops of 250 mm circumference for each run. For each fabric direction, each specimen was extended to a maximum tension of 50N at a speed of 500 mm/min for 3 cycles. The strain (%) data were recorded at the third cycle at loading tensions of 5N. For each dimension, the strain test was repeated three times.

5.5.3 Analysis of Cup Specimens

5.5.3.1 Screening Design

A multiple regression model was also used to screen significant factors using a 5% level of significance. The normal probability plots of standardized effects of the three response variables are shown in Figure 5.14. It can be seen that factor **A** falls well away from the line in all these figures. This reveals that for each response variable, factor **A** (loop density) has the strongest effect among all factors (Minitab Inc., 2003; Montgomery, 2005). Factor **C** (Nylon yarn tension) had the next definite effect in both the bias and course directions. Factor **B** and the interaction of factor **A** and factor **B** had the negative effects in the wale direction.

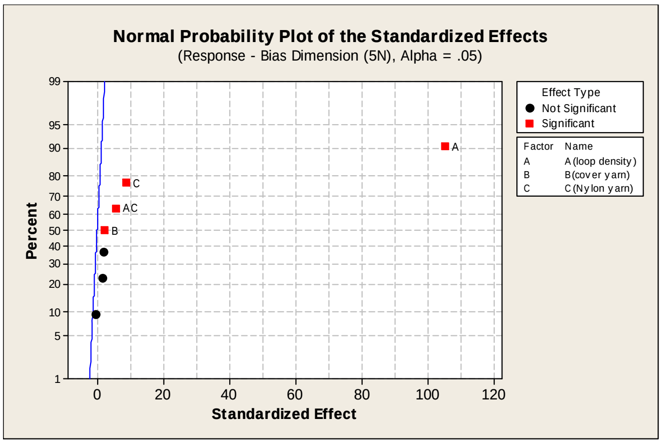

(a) Response 1 (bias direction)

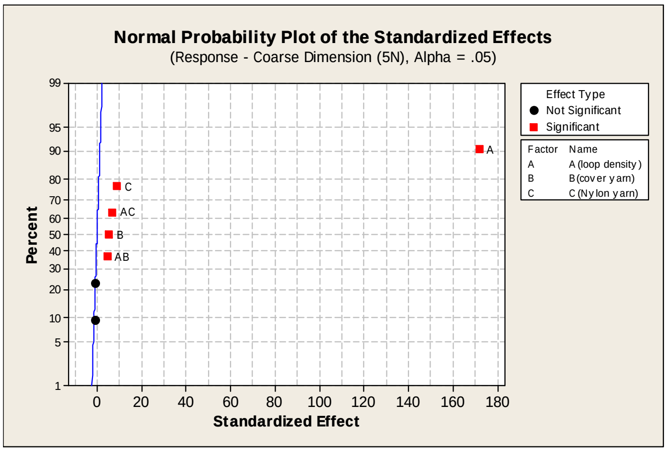

(b) Response 2 (course direction)

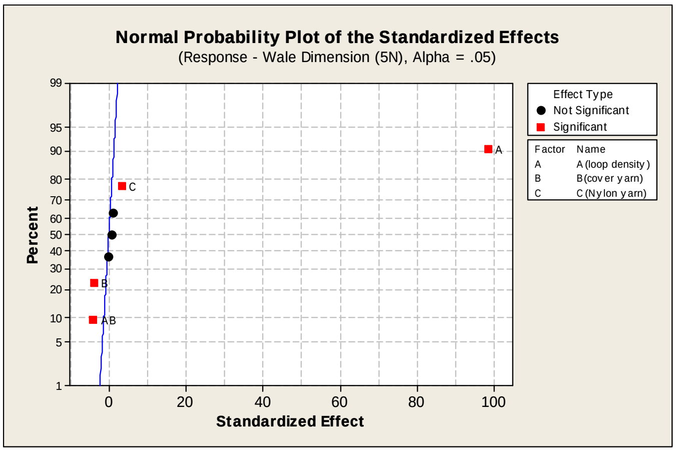

(c) Response 3 (wale direction)

Figure 5.14 Normal probability plots of the standardized effects of responses 1, 2 & 3

5.5.3.2 Data Means Observation

The means of the three response variables (cup strain) at each run are shown in Table 5.11. It can be seen that each response variable has a maximum strain at the 8th run, in which the all factors are set at their high level. In addition, the first two response variables have a minimum at the 1st run, in which the all factors are set at the low level. The last response variable (wale direction) has a minimum strain at the 3rd run, in which factors **A** (loop density) & **C** (Nylon yarn tension) are set at the low level and factor **B** (cover yarn tension) is at its high level. It also can be found from the Table that, for the centre point, the strains in the wale direction (79.80) are larger than in the course direction (68.39) and the bias direction (65.55). The results also reveal that the strain in the course direction has a relative larger range from the minimum strain to the maximum strain than the other two directions.

Table 5.11 Data means of different response variables at different treatments combination situation (%)

Run	Treatment combination	Levels of **A B C**	Bias (5N)	Course (5N)	Wale (5N)
1	(1)	−−−	29.59	27.45	34.20
2	a	+−−	88.85	128.81	111.00
3	b	−+−	30.80	28.10	33.27
4	ab	++−	87.91	136.57	104.37
5	c	−−+	31.13	28.86	35.24
6	ac	+−+	95.40	140.41	113.54
7	bc	−++	32.84	29.33	36.39
8	abc	+++	98.38	145.52	108.29
9-11	Centre point	0, 0, 0	65.55	68.39	79.80
	Std.D.		0.8275	0.8992	1.0699

5.5.3.3 Fit Reduced Models

A new model using only the terms significant at the 5% level was fitted for each response. The new factorial fit results (see Tables 5.12 to 5.14) indicate that all terms of different response variables have p-value less than 0.05. The adjusted coefficient of multiple determination (adjusted R^2) of three response variables are all greater than 99%.

In order to check the adequacy of the models, the residuals of the models were also examined for the three basic assumptions described in 5.4.3.3. The computer results by Minitab (Montgomery, 2005; Minitab Inc., 2003) reveal that for the normal probability test of residuals, the p-values were 0.231 at response 1, 0.656 at response 2, 0.573 at response 3; all are greater than 0.10. So the normality of residuals is considered good for each response. The residual plots (omitted here) of all three responses also indicate that the results are definitely acceptable for the assumptions of constant variance and response independence.

According to coefficients included in the factorial fit Tables (Tables 5.12 to 5.14), the first-order regression equations with interactions for cup strain at loading tensions of 5N are as shown below:

$$y_1 = 61.862 + 30.774x_1 + 2.575x_3 + 1.681x_1x_3 \qquad (5.6)$$

$$y_2 = 83.13 + 54.69x_1 + 1.75x_2 + 2.9x_3 + 1.47x_1x_2 + 2.24x_1x_3 \qquad (5.7)$$

$$y_3 = 72.039 + 37.261x_1 - 1.458x_2 + 1.327x_3 - 1.512x_1x_2 \qquad (5.8)$$

where y_1 is the cup strain along the bias direction at 5N loading, y_2 is the cup strain along the course direction at 5N loading tension, y_3 is cup strain along the wale direction at 5N loading tension. x_1 is the coded loop density, x_2 the coded cover yarn tension, and x_3 the coded Nylon yarn tension. In addition, the results indicate evidence of quadratic curvature for all the response variables. However, the aim of the current experiment is not to improve the cup strain value, but to screen the key factors influencing the cup strain. The interaction terms in the above three equations have introduced curvature into the response surface. So it was determined not to conduct further response surface experiments here.

Table 5.12 Factorial fit: bias dimension **--** 5N force versus **A** (loop density), **C** (Nylon yarn tension)

Estimated effects and Coefficients for Bias dimension: 5N force (coded units)

Term	Effect	Coef	SE Coef	t	P
Constant		61.862	0.3239	191.00	0.000
A (loop density)	61.547	30.774	0.3239	95.01	0.000
C (Nylon yarn tension)	5.149	2.575	0.3239	7.95	0.000
A (loop density)***C** (Nylon yarn tension)	3.362	1.681	0.3239	5.19	0.000
Ct Pt		3.692	0.6202	5.95	0.000

S = 1.58670 R-Sq = 99.70% R-Sq(adj) = 99.65%

Analysis of variance for bias dimension: 5N force (coded units)

Source	DF	Seq SS	Adj SS	Adj MS	F	P
Main effects	2	22887.5	22887.5	11443.7	4545.45	0.000
2-Way interactions	1	67.8	67.8	67.8	26.94	0.000
Curvature	1	89.2	89.2	89.2	35.44	0.000
Residual error	28	70.5	70.5	2.5		
Pure error	28	70.5	70.5	2.5		
Total	32	23115.0				

Table 5.13 Factorial fit: course direction -- 5N force versus **A** (loop density), **B** (cover yarn) and **C** (Nylon yarn tension)

Estimated effects and coefficients for course direction: 5N force (coded units)

Term	Effect	Coef	SE Coef	t	P
Constant		83.13	0.3190	260.63	0.000
A (Loop density)	109.39	54.69	0.3190	171.48	0.000
B (elastic yarn tension)	3.50	1.75	0.3190	5.48	0.000
C (Nylon yarn tension)	5.79	2.90	0.3190	9.08	0.000
A (loop density)*__B__ (elastic yarn tension)	2.94	1.47	0.3190	4.60	0.000
A (loop density)*__C__ (Nylon yarn tension)	4.48	2.24	0.3190	7.02	0.000
Ct Pt		-14.74	0.6108	-24.13	0.000

S = 1.56259 R-Sq = 99.91% R-Sq(adj) = 99.89%

Analysis of variance for course direction: 5N force (coded units)

Source	DF	Seq SS	Adj SS	Adj MS	F	P
Main effects	3	72071.3	72071.3	24023.8	9838.94	0.000
2-Way interactions	2	172.1	172.1	86.1	35.25	0.000
Curvature	1	1421.5	1421.5	1421.5	582.17	0.000
Residual error	26	63.5	63.5	2.4		
Lack of fit	2	5.3	5.3	2.6	1.08	0.354
Pure error	24	58.2	58.2	2.4		
Total	32	73728.4				

Table 5.14 Factorial fit: wale direction -- 5N force versus **A** (loop density), **B** (cover yarn) and **C** (Nylon yarn tension)

Estimated effects and coefficients for wale direction: 5N force (coded units)

Term	Effect	Coef	SE Coef	t	P
Constant		72.039	0.3707	194.32	0.000
A (loop density)	74.523	37.261	0.3707	100.51	0.000
B (elastic yarn tension)	-2.916	-1.458	0.3707	-3.93	0.001
C (Nylon yarn tension)	2.654	1.327	0.3707	3.58	0.001
A (loop density)*__B__ (elastic yarn tension)	-3.025	-1.512	0.3707	-4.08	0.000
Ct Pt		7.765	0.7099	10.94	0.000

S = 1.81617 R-Sq = 99.74% R-Sq(adj) = 99.69%

Analysis of variance for wale direction: 5N force (coded units)

Source	DF	Seq SS	Adj SS	Adj MS	F	P
Main effects	3	33415.3	33415.3	11138.4	3376.85	0.000
2-Way interactions	1	54.9	54.9	54.9	16.64	0.000
Curvature	1	394.6	394.6	394.6	119.64	0.000
Residual error	27	89.1	89.1	3.3		
Lack of fit	3	6.6	6.6	2.2	0.64	0.594
Pure error	24	82.4	82.4	3.4		
Total	32	33953.8				

5.6 Conclusions

Based on the two key measurements (underbust girth and “breast depth width ratio”), the underband and cup of a bra were selected to be studied in seamless knitting experiments using factorial experimental designs. Several key conclusions can be given, as follows:

1) Loop density and elastic yarn tension are the major factors affecting the underband tension of a seamless knitted bra. The underband tension has larger data when all factors are set at low level, and has smaller data when loop density and elastic yarn tension are at the high level and cover yarn tension and Nylon yarn tension at the low level. The underband tension for fitting underbust girth from 70cm to 80cm can be predicted using equations derived from the experimental results.
2) Loop density is the strongest factor affecting the cup strain of seamless knitted bras. The cup strain has a maximum tension when all knitting factors are set at their high levels, and has a minimum strain when the loop density and Nylon yarn tension are set at the low levels. With the use of specified commercial yarns, the cup strain can be predicted according to the level of loop density, cover yarn tension and Nylon yarn tension.

CHAPTER 6

DEVELOPMENT OF A 3D SOFT SUPPORTING WIRE

6.1 Introduction

Underwires are used to provide the desirable shape and support to bras and close-fitting undergarments. A bra wire is often regarded as a key element for bra fitting, especially to the breast root. It is also one of the major sources that may cause uncomfortable sensation (Kim et al., 2000; Lee et al., 2001). Although wireless bra is sometimes preferred for its comfort and soft touch, underwires are still necessary and generally used in bras due to their supporting and shaping functions. To make the bras more comfortable to wear, new types of 2D bra wires such as modified cross-sectional elliptical wires and shape memory wires have been continually developed (Lee & Hong, 2007). For seamless knitted bras, how to design a soft 3D supporting wire to hold the breast shape in a natural manner is a challenging question.

6.2 Determination of Breast Root

6.2.1 Conventional Bra Underwire and Its Fitting Test for Seamless Knitted Bra

A pair of underwires made of metallic or plastic materials, are generally inserted into the wire casing under the two cups of a bra, so as to provide a framework and to impart a desired shape to the breasts. The conventional underwires are rigid, flat and bended into a specified degree of curvature (Thakur & Horta, 2002).

However, the conventional underwires were not able to conform to the wearer's body in many aspects (Werner, 2000). They have a number of disadvantages (Powell & Seymour, 2002) described as follows:

1) The underwire can cause discomfort by pressing against the ribs under the breasts (It needs to use softer material to make it acceptable to the wearer).
2) Further discomfort may be caused by digging into the flesh in the underarm region. The key reason is that the wire is essentially two-dimensional, rather than being formed to fit a 3D breast root.

The underwire is normally maintained in a channel or casing that is formed from a soft bias-cut fabric binding along the bottom curve of bra cup. However, when we put a set of 75B underwire into the tunnel of our developed seamless knitted bra (see Figure 6.1), it could not fit the breast root of the hard dummy very well. It was digging at the centre front and the underarm positions.

The conventional bra underwire does not fit the breast root of the wearer effectively because it is too rigid to fit into the knitting structure of seamless bras. Therefore, a 3D soft underwire is necessary.

Front view (without underwire)

Front view (with underwire)

Figure 6.1 Demonstration of the conventional underwire fitting test

6.2.2 3D Coordinates of Breast Root

As reviewed in 2.4.3, many researchers and manufacturers have developed new materials for underwires to enhance the bra fitting sensation. However, geometrical consideration of the 3D breast shape has not been completely investigated for designing optimal bra underwires, probably because the nude breast root is difficult to identify even using the 3D body scanner. To design an ergonomic bra wire, Lee and Hong (2007) explored the curvature of breast root based on the 3D anthropometric measurements of 21 middle-aged women volunteers. They reported that the 3D shape of women's breast root would be a desirable design guideline of the bras that fit to the bony thorax. Lee et al. (2001) found that for comfort bras, women preferred a wide distance between two bust points as its natural width in nude. The ergonomic underwire with 0.0015N/mm^{2}mm torsional rigidity was then developed by considering the global average radius of breast root. However, the new underwire was still in a two-dimensional structure.

Figure 6.2 shows a topographic view presenting the relationships between a 3D soft supporting wire and the breast. A new 3D underwire is hoped to contact the breast root curve closely from OBP (outer- most point), passing LBP (lower-most point), to IBP (inner-most point).

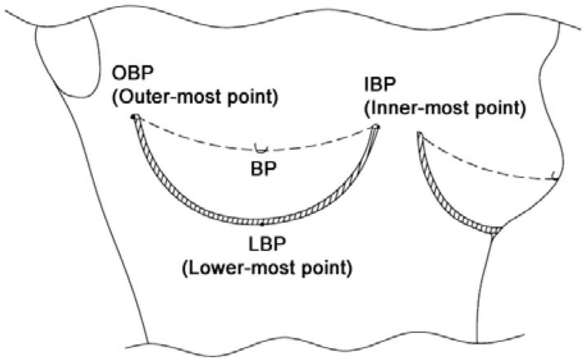

Figure 6.2 A topographic view illustrating the design concept of a new 3D supporting wire

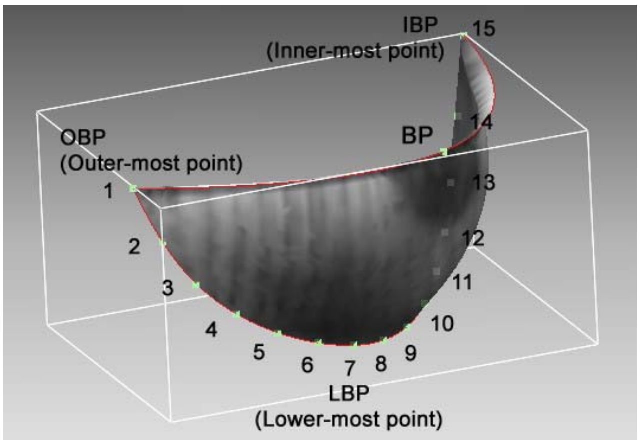

Figure 6.3 The definitions of 15 key points along the right breast root

First, the coordinates of 15 key points were defined along the breast root of size 75B* in the new bra sizing system. As shown in Figure 6.3, point 1 and point 15 are the outer-most point and inner-most point of the breast shape at the horizontal cross-section through the bust point, whereas point 7 is the lower-most (base) point of the breast mass measured from a vertical cross-section through the bust point. Then we divided the outer breast under curve into 6 equal portions between point 1 and point 7, and the inner breast under curve into 8 equal fractions from point 8 to point 15.

From 49 female subjects whose breast size are 75B*, the X, Y, Z coordinates of the bust point and 15 key points of the right breast have been measured by using the software RapidForm. The coordinates of bust point of each subject were set as 0, 0, 0. The X, Y, Z coordinates of 15 key points were calculated based on their distances from the bust point. Considering that the seamless bras are generally designed for invisibility, the point 15 (inner-most point) is not included. After examining and purifying the data using the same method mentioned in 3.3.4, descriptive statistics were calculated. Table 6.1 presents the mean of new X, Y, Z coordinates of key determination points of breast root.

Table 6.1 The mean X, Y, Z coordinates of key determination points of 75B* breast root

Point items/ Coordinates	X	Y	Z
Bust point	0.0000	0.0000	0.0000
Point 1	-44.3477	0.0000	-86.259
Point 2	-40.6545	-16.6723	-80.786
Point 3	-35.9457	-29.713	-73.4162
Point 4	-29.7879	-39.8496	-64.5247
Point 5	-21.6039	-47.9981	-54.6885
Point 6	-11.4607	-53.9509	-44.572
Point 7	-0.0179	-57.0607	-34.7363
Point 8	11.2003	-57.4842	-26.1896
Point 9	22.9969	-55.5946	-19.0747
Point 10	34.8349	-51.5654	-13.6426
Point 11	46.3386	-45.5051	-10.0674
Point 12	57.0303	-37.4605	-8.2472
Point 13	66.2818	-27.5301	-7.7298
Point 14	73.632	-15.2814	-8.241

6.3 3D Soft Supporting Wire Prototype

6.3.1 3D Soft Supporting Wire Models

Fourteen key points that describe the breast root profile of 75B* women have been used for the 3D underwire development. As shown in Figure 6.4, by connecting the key points to the bust point, a shell of a half cone shape can be created geometrically to present the average middle-size breast shape. By using UniGraphics (UG), a 3D CAD bra underwire model was created (see Figure 6.5) based on connecting the key points from point 1 to point 14 together smoothly.

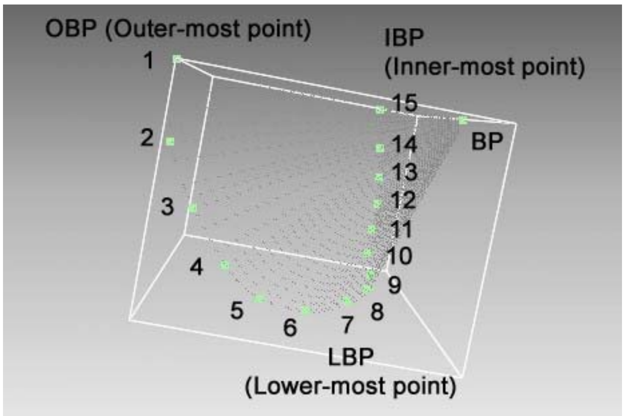

Figure 6.4 A demonstration figure of the breast shell model

In order to enlarge the contacting area between the underwire and the breast bottom mass to support the breast well, the cross-section of the new 3D underwire was designed as a three-fifth segment of a circle with 2.5mm diameter, which has 1.5mm thickness. As illustrated in Figure 6.6, the new structure of 3D underwire can provide a wider contact region with 2.5mm width. For convenient insertion, the center front end has a conic shape with 4.5mm length.

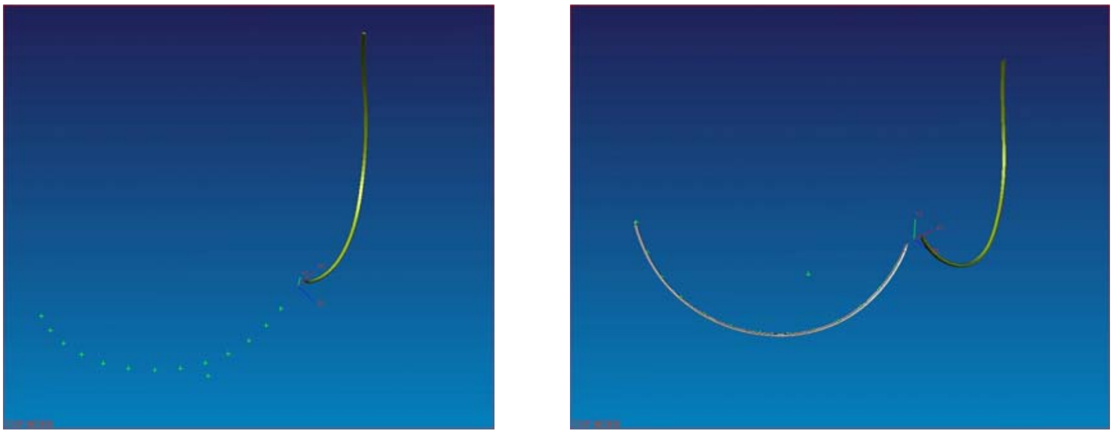

(a) A 3D CAD bra underwire model of right breast (b)A set of 3D CAD bra underwire model

Figure 6.5 A set of 3D CAD bra underwire model designed by UniGraphics (UG)

(a) The structure of cross-section (b) The structure of centre part

Figure 6.6 The detailed structure design of the new 3D CAD bra underwire model

6.3.2 Stereolithography (SLA) Prototype

Stereolithography (SLA) can be used to build complex product models that require a high degree of dimensional precision. A file of the 3D CAD bra underwire model was sent to a SLA rapid prototyping machine for high-precision physical prototype fabrication. The key features are described below (HKPC, 2006):

1) A laser beam draws the shape of the bottom slice of the new designed 3D bra underwire models on the surface of a tank of resin.
2) The laser-struck part of the top resin layer turns into a solid plastic film (about 0.05mm-0.15mm thick), to become the bottom slice of the 3D underwire prototype, which is located on a movable platform known as “elevator”.
3) With the moving of the “elevator”, the bottom model slice is transported into the resin bath to allow new liquid resin to cover the surface.
4) The process is then repeated with the laser beam drawing and forming the second slice of the models over the bottom slice.
5) The process is again repeated until the entire 3D underwire prototype has been built.
6) Fabricated SLA prototypes were polished and cured for surface quality enhancements (see Figure 6.7).

Figure 6.7 SLA sample with polishing

6.4 Polyurethane (PU) Duplication of 3D Supporting Wire

In order to enhance surface quality and material performance of the 3D supporting wire model, functional polyurethane (PU) soft underwire models were duplicated from the high-precision Stereolithography (SLA) prototypes. The specific properties of PU used in current study are presented in Table 6.2.

Table 6.2 The specific properties of PU used in current study

Model	Vantico K.K. Industrial Model #100
Color	White, color additives allowed
Grade	Low viscosity grades suitable to the atmospheric condition, casting liquid resin
Tensile Strength	26 Mpa
Elongation	8 %
Flexural Strength	39 Mpa
Flexural Modulus	885 MPa
Compressive Strength	450
Impact Strength	3.0 kg·cm/cm
Shrinkage	1.3 %
Heat Distortion Temp.	73 °C

A vacuum machine was used to eliminate bubbles in the mould and the duplicate model using a vacuum forming process. Figure 6.8 shows a finished set of 3D soft PU supporting wires. The process of producing a PU duplicate of the SLA prototypes with individualized features is described as follows:

1) Two silicone mould halves were made from the SLA prototypes master.
2) SLA prototypes were removed after the silicone moulds formed.
3) Internal chamber of silicone moulds were sprayed with mould release agent.
4) PU liquid was fed and set in the silicone moulds.

5) Moulds were split apart and PU model duplicates were removed.

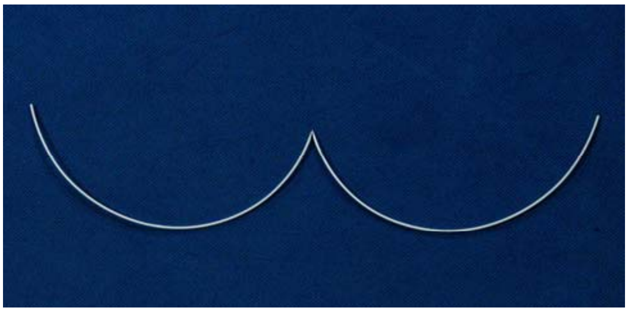

Figure 6.8 A finished set of 3D soft PU supporting wire of bra size 75B*

The new 3D soft wire was inserted into a seamless knitted bra to test its fitting performance on the dummy again. As shown in Figure 6.9, it fits the breast root well, without digging into the torso at both the inner and the outer of the breast probably because of its 3D shape and the stretchability of the PU material.

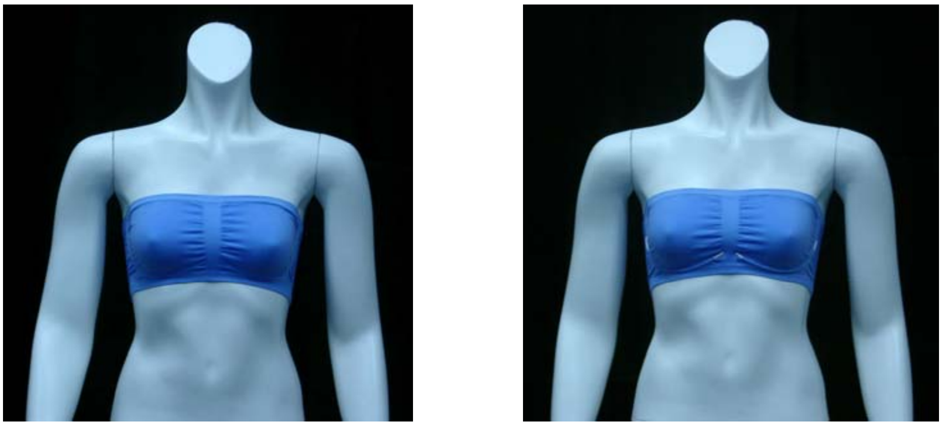

Front view (without underwire) Front view (with underwire)

Figure 6.9 Demonstration for the new 3D soft PU supporting wire

6.5 Conclusions

A new 3D soft supporting wire has been developed using 3D coordinates of 14 key points around the breast bottom curve based on 49 subjects whose breast sizes are 75B*. In order to enhance the supporting performance of the 3D underwire prototype, the cross-section of the new 3D underwire was constructed as a three-fifth segment of a circle. With the aim of providing natural shape and comfortable support, a soft polyurethane material was used to duplicate the SLA prototype of the 3D underwire.

The pilot testing results have shown that compared with conventional 2D underwire, the new 3D soft PU supporting wire can provide good fitting performance to the breast bottom profile without digging into the flesh at either the inner and outer breast.

CHAPTER 7

SEAMLESS KNITTED BRA DEVELOPMENT AND FITTING EVALUATION

7.1 Introduction

As mentioned in section 1.1, the existing seamless knitted bras exhibit problems, such as improper sizing, compression of the breasts, cup volume restriction and insufficient support.

For the improvement of bra sizing, a new system has been established and reported in Chapter 4. The relationships between body parameters and knitting parameters were investigated (see Chapter 5). A 3D soft supporting wire for seamless knitted bras was designed (see Chapter 6). This chapter presents the development of the 3D seamless knitted bras supported with 3D soft underwires in size 75B* of the new sizing system, and the evaluation of their fitting performance.

In an attempt to improve current seamless knitted bras, 15 test bra samples were developed based on 3 new styles in 5 experimental runs by changing 2 key knitting parameters - loop density and elastic yarn tension.

The bra samples to be evaluated include 15 new bras and 4 commercial bras. Two of the commercial bras are 75B cut & sewn conventional bras (Figure 7.5) and two are seamless bras in the same size (Figure 7.6). We invited 6 women subjects whose bra size is 75B* in the new bra sizing system to participate in an objective bra pressure assessment, a subjective rating on comfort & pressure sensations, and a breast shape evaluation using 3D body scanning.

7.2 Seamless Knitted Bra Development

7.2.1 Features of New Prototype Seamless Knitted Bras

Limited studies were available to show the relationships among circular knitting methods, the wearer's breast shape, and fitting performance. The existing commercial bras failed to provide adequate cup pressure and support.

For these experiments, the goal was to provide comfortable underband pressure, to increase cup volume by low-density knitting and to keep the wing of the bra fitted to the body by special knitting structure. As 75B & 75B* are the most representative groups in the existing and the new bra sizing systems respectively, 75B is generally selected as a prototype size for the conventional bra design, while 75B* of the new bra sizing system was chosen as the prototype size for the new seamless bra development & fitting evaluation.

Three new design styles of seamless knitted bras were developed using 78/68/1 Nylon 66, 20-20/10/1 cover yarn and 210D bare elastic. The design details of each prototype bra are delineated in figure 7.1. The common design features are described as follows:

1) In order to increase the cup volumes, different stitch densities were used in the cup regions. In the SANTONI SM8-TOP2 knitting machine, there are 8 independent step motors. Each step motor connects one single stitch cam, which can change the stitch density of specific bra regions (Instruction manual of SM8-TOP2, 2001). As shown in Figure 7.2, the bra cup regions have three distinct areas with increasing stitch density of the parts indicated by color shifts from yellow, to ochre and to azure. This means that the step motor moves to loosen the stitch (loop density) from "0" (yellow areas) to "+15" (ochre areas), then to "+25" (azure areas) when knitting the bra cup regions.
2) Each bra has two underwire tunnels along the bottom curve of the cups, for inserting a set of 3D soft supporting wire. The notation of knitting structure of the tunnel is presented in Figure 7.3.
3) The underband of each prototype bra uses a 1×3 knitting structure.
4) For each bra, special knitting structures were designed to provide adequate fit performance at the gore, the side wing and the back wing.

Style	Front view	Back view	Design features
1	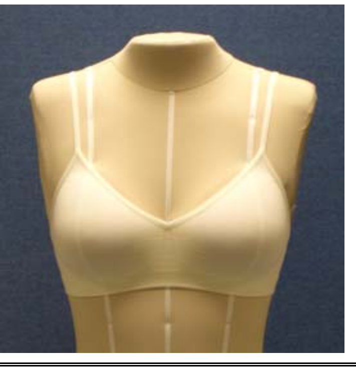		• Relatively larger coverage of cup area provides a secure feeling and support. • Two slim shoulder straps and special knitting structure results in a versatile design.

Figure 7.1.1 Three new design styles of prototype seamless knitted bras

2			• A strapless seamless bra top designed for bare shoulder fashions. • Mesh application at the side offers better air ventilation.
3			• This style is a backless bra designed with transparent neck strap and lower wing. It is suitable for evening dress or fashionable garment with deep neckline and V-back. • Centre pleats provides more cup volume to the breasts.

Figure 7.1.2 Three new design styles of prototype seamless knitted bras

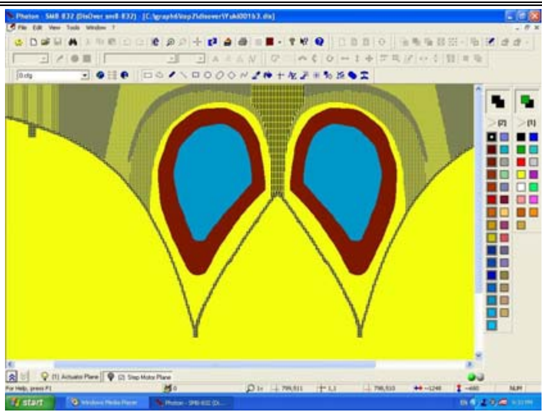

(a) Style 1

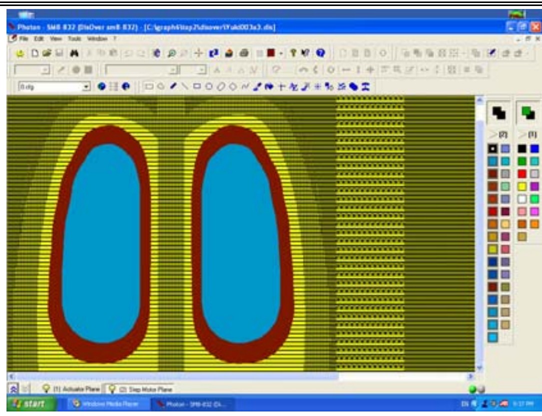

(b) Style 2

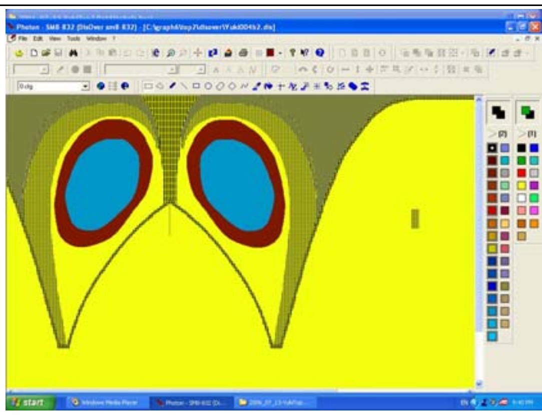

(c) Style 3

Figure 7.2 Knitting patterns of three new prototype seamless knitted bras

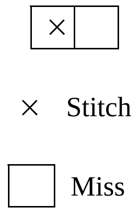

Figure 7.3 The notation of the knitting structure of the bra underwire tunnel

7.2.2 Preparation of Bra Samples for Fitting Experiment

In order to explore the effects of knitting parameters on the bra fitting performance, several samples with varying degrees of sizes and fitting were produced for each of three styles of newly developed seamless knitted bras.

Chapter 5 indicated that loop density and elastic yarn tension were two major factors affecting the underband tension, and loop density was the strongest factor affecting the cup strain of a seamless knitted bra. Therefore, three factors were considered in producing the 3D seamless knitted bra samples for the current fitting evaluation experiments. The factors are style, loop density and elastic yarn tension. For each style, a 2^2 full factorial design of experiment (see Table 7.1) was conducted. In this experiment, ±25 was used as high and low level of loop density, instead of ±40 as mentioned in Chapter 5. These levels are to ensure the cup rigidity and volume.

Table 7.1 2^2 factorial experiment of 2 factors at 2 levels with additional centre point levels for each style

Factor	Low level	High level	Centre point level
A: loop density	−25	+25	0
B: elastic (bare Lycra) yarn tension (g)	20	12	16

Table 7.2 shows the test matrix for producing the experimental prototype bra samples for each style. In order to investigate the pressure values at the middle level, a centre point was added to the experiment in run 5. The centre point level for each factor is presented in Table 7.1. According to the above experiment design, three styles in all resulting in 15 seamless knitted bra samples were developed by using the same SANTONI SM8-TOP2 machine. The production conditions were controlled using the protocol described in section 5.4.1.

Table 7.2 The full 2^2 experiment design for each of three prototype seamless knitted bra styles

Run	Treatment combination	Basic design	
		A	B
1	(1)	−	−
2	a	+	−
3	b	−	+
4	ab	+	+
5	Center point	0	0

7.3 Bra Fitting Evaluation

7.3.1 Understanding of Bra Fitting

Fit is an important factor that contributes to the confidence and comfort of the wearers (Alexander et al., 2005). According to the NPD (New Product Development) report (1998), 42% of respondents singled out fit and comfort as the most important factors for purchasing bras. Physicians and nurses were more interested in the healthiness of proper breast support for the bras than in their fashionability (Chan et al., 2001).

Bra fit is difficult to identify accurately and objectively. Starr et al. (2005) reported that bra fit was very subjective and varied from person to person.

Chan et al. (2001) found that cup, underwire and straps were major areas that commonly cause discomfort in bras.

Previous' studies (Yu, 2006; Hardaker & Fozzard, 1997; Costantakos & Watkins, 1982; Barron et al., 1970) report that a well-designed and fit bra should have the following features:

1) The bra is shaped to fit the 3D complex body contours, support the soft breast tissues and to satisfy consumers' needs.
2) The bra should provide appropriate support by a well-fitted underband, properly designed straps, and fitted cups.
3) The bra should prevent concentration of pressure on sensitive areas, including certain veins, arteries, and portions of the skeletal structure, particularly those which appear near skin surface.
4) The bra needs to furnish a comfort sensation to wearers, which are linked primarily to soft materials and shielding the fasteners from the skin surface.

For conventional bras, Yu (2006) defined a greatly detailed checklist and set of procedures for a fitting assessment. As shown in Figure 7.4, 10 bra assessment areas from A to J are: gore, cup, neckline, underarm, wire, cradle, wing, strap, underband and fasteners. Yu emphasized that for the propose of fitting the body, a good bra should give the breasts necessary coverage, hold the breasts with reduced movement in action, be compatible to the breast root, and support the weight of the breasts.

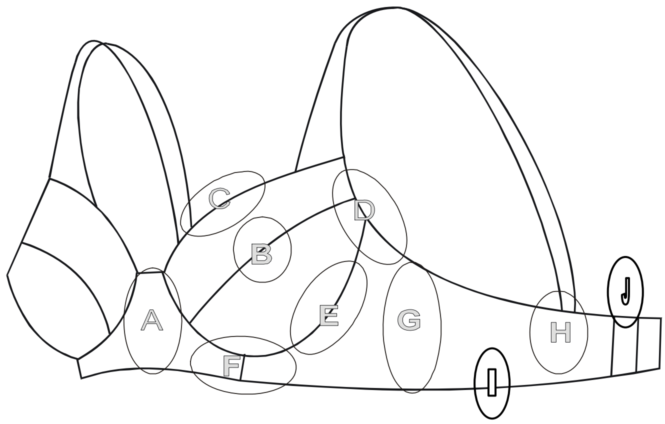

Figure 7.4 Fitting checklist for a conventional bra (Yu, 2006)

7.3.2 Selection of Commercial Experimental Bras

To contrast the fitting performance of the new seamless knitted bras, we also tested 4 commercial bras that were the best selling items of the major intimate apparel brands in China.

As shown in Figure 7.5, two conventional bras chosen from brands “Aimer” and “Wacoal” were 75B traditionally cut and sewn bras which were designed using typical materials and have two three-quarter cups with underwires. Figure 7.6 presents two commercial seamless bras without underwires selected from brands of “Jockey” and “Benetton”. “Jockey” is a sport bra knitted by 75% Nylon and 25% Lycra. “Benetton” is a daily use bra using 92% Polyamide and 8% Spandex with softening finishing. Each of the two commercial seamless bras is produced in only one size.

(a) “Aimer” bra (b) “Wacoal” bra

Figure 7.5 Two conventional cut & sewn bras selected for fitting assessment comparison

(a) “Jockey” bra (b) “Benetton” bra

Figure 7.6 Two commercial seamless knitted bras selected for fitting assessment comparison

To identify the test bra samples, the referred abbreviate names and descriptions of all 19 samples are described in Table 7.3.

Table 7.3 The referred abbreviative names and details of test bra samples

Bra category	Abbreviate name	Description
Commercial bra	Aimer	A three-quarter cup conventional bra with underwire from Aimer brand
	Wacoal	A three-quarter cup conventional bra with underwire from Wacoal brand
	Jockey	A seamless knitted bra without underwire selected from Jockey brand
	Benetton	A seamless knitted bra without underwire selected from Benetton brand

Table 7.3 (continued)

New developed seamless knitted bra (each has a set of knitted tunnels for inserting a set of 3D soft supporting wires)	ST1L-25Y20	Style 1 / loop density -25 / elastic yarn tension 20
	ST1L-25Y12	Style 1 / loop density -25 / elastic yarn tension 12
	ST1L0Y16	Style 1 / loop density 0 / elastic yarn tension 16
	ST1L+25Y12	Style 1 / loop density +25 / elastic yarn tension 12
	ST1L+25Y20	Style 1 / loop density +25 / elastic yarn tension 20
	ST2L-25Y20	Style 2 / loop density -25 / elastic yarn tension 20
	ST2L-25Y12	Style 2 / loop density -25 / elastic yarn tension 12
	ST2L0Y16	Style 2 / loop density 0 / elastic yarn tension 16
	ST2L+25Y12	Style 2 / loop density +25 / elastic yarn tension 12
	ST2L+25Y20	Style 2 / loop density +25 / elastic yarn tension 20
	ST3L-25Y20	Style 3 / loop density -25 / elastic yarn tension 20
	ST3L-25Y12	Style 3 / loop density -25 / elastic yarn tension 12
	ST3L0Y16	Style 3 / loop density 0 / elastic yarn tension 16
	ST3L+25Y12	Style 3 / loop density +25 / elastic yarn tension 12
	ST3L+25Y20	Style 3 / loop density +25 / elastic yarn tension 20

7.3.3 Human Subjects

Six female subjects aged between 23 and 30 were recruited as the bra fitting test live models. These six subjects have the same breast size of 75B* according to the new bra sizing system. In order to assure the accuracy of the fitting evaluation results, the subjects were screened based on two key measurements: underbust girth and breast depth width ratio. The 3D body scanner VOXELAN LPW-2000FW was used to record each volunteer’s surface data. The major body measurements results of six subjects, including mean, standard deviation (SD) and coefficient of variation (CV) are shown in Table 7.4.

After passing the breast size screening, each participant was asked to sign an informed consent form (see Appendix II).

Table 7.4 Descriptive statistics summary of key body measurements of six human subjects

Body measurements	Mean	Std. Deviation	CV (%)
Age	26.50	2.17	8.18
Weight (Kg)	52.40	2.69	5.14
Whole body height (cm)	163.90	6.37	3.89
Bust height (cm)	117.79	4.99	4.24
Underbust height (cm)	111.53	5.19	4.65
Bust point width (cm)	20.09	0.94	4.69
Length from front neck point to right bust point (FNP~RBP) (cm)	20.14	1.07	5.34
Length from front neck point to left bust point (FNP~LBP) (cm)	20.30	1.30	6.41
Bust girth (cm)	88.01	4.58	5.21
Underbust girth (cm)	75.47	4.57	6.06
Waist girth (cm)	68.45	4.36	6.36
Hip girth (cm)	89.28	2.52	2.82
Vertical arc length from right bust point to underbust (BP~UBL) (cm)	7.23	0.76	10.47
Outer arc length of right breast (cm)	9.47	2.02	21.35
Inner arc length of right breast (cm)	9.14	0.47	5.13
Width of the breast_b (cm)	14.79	0.82	5.54
Height of the breast (cm)	5.17	0.27	5.29
The breast width depth ratio	0.35	0.01	2.86
Right breast volume (cm^3)	430.74	53.49	12.42

7.3.4 Process of Bra Fitting Evaluation

The fitting assessments included objective pressure evaluation, subjective questionnaire of comfort & pressure sensation and 3D breast shape evaluation. Each subject wore 19 different bra samples at the Human Body Measuring Laboratory of AIMER HEC-BICT. During the process, the subjects were asked to select the bra samples randomly. The fitting assessment procedure is shown in Figure 7.7. Each subject first stands still with arms down at her sides and then raise her arms up over her head. The complete fitting process took 1 to 1.5 hours for wearing each bra sample. The pressure evaluation test was conducted twice on the seamless knitted bras, first with 3D soft supporting wire and second without the wire. A pressure evaluation test was conducted only once on the four commercial bras.

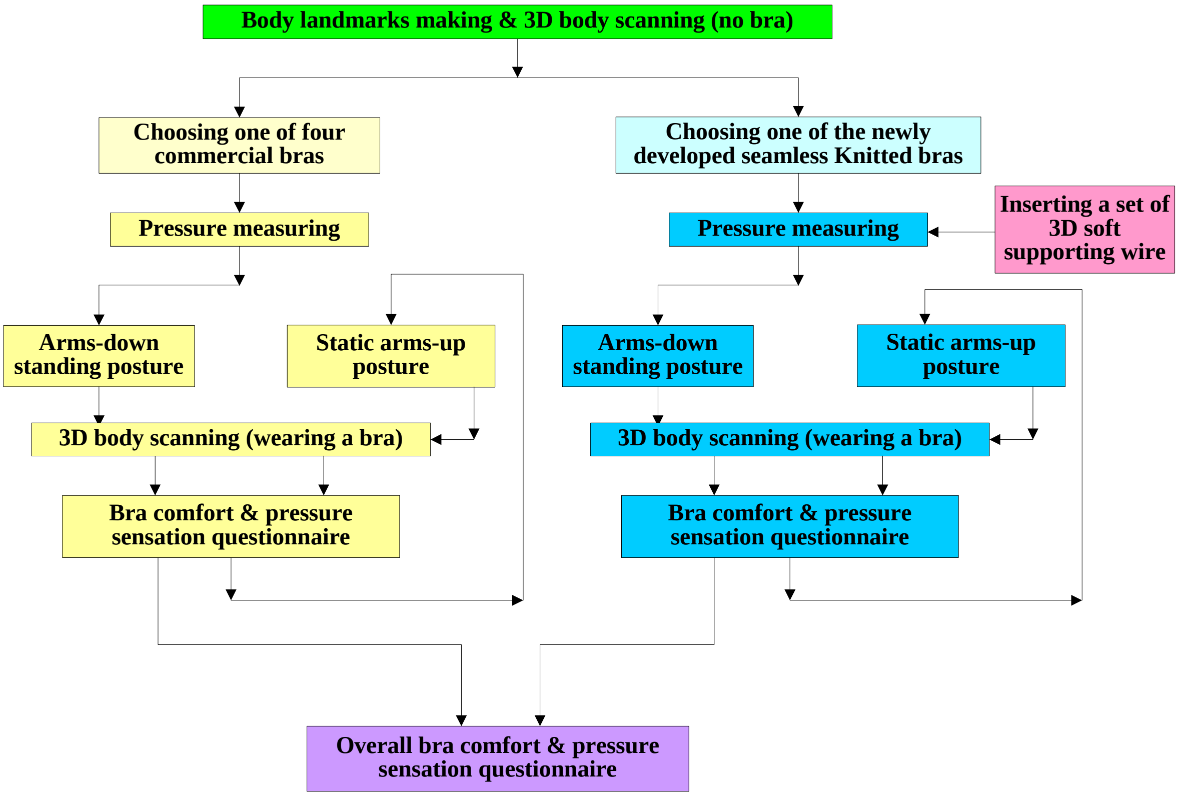

Figure 7.7 Process of bra fitting assessment

7.3.5 Objective Evaluation

Different bra styles, materials and components give specific functional support, pressure and comfort sensations to the wearers. Researchers had proposed various methods to test the bra pressure. Makabe et al. (1991) measured bra pressure at six points, including:

Point 1, where underbust line and undercup cross;

Point 2, where the underbust line and anterior axillary line cross (seam);

Point 3, where underbust line and scapular line cross;

Point 4, where lateral area of cup and ribcage band cross;

Point 5, where ribcage band and anterior axillary line cross (seam);

Point 6, where the bras straps cross over the shoulder.

Costantakos & Watkins (1982) used five body points to assess bra pressure. They were:

Point 1, at the top of the shoulder on the trapezius muscle under the bra strap;

Point 2, directly inferior to the center of armpit, in the middle of each side panel;

Point 3, under the top elastic of each panel, directly inferior to the center of the armpit;

Point 4, under the elastic band at the base of the bra, directly inferior to the nipple;

Point 5, 4 to 5 cm from each side of the center back clasp, directly inferior to the crest of each shoulder blade.

Morooka et al. (2005) measured seven points when studying the pressure in a static posture and in dynamic postures. They included:

Point 1, underwire directly inferior to the nipple,

Point 2, front side panel,

Point 3, underband inferior to the front side panel,

Point 4, intersection point of underband and side seam,

Point 5, underbust line and scapular line cross point,

Point 6, back wing,

Point 7, strap on the shoulder.

The measuring points for the current study were selected with reference to Morooka et al. (2005) and considering the design features of seamless knitted bras. The points to be measured are specified in Figure 7.8 to 7.10 with detailed definitions in Table 7.5 to 7.7.

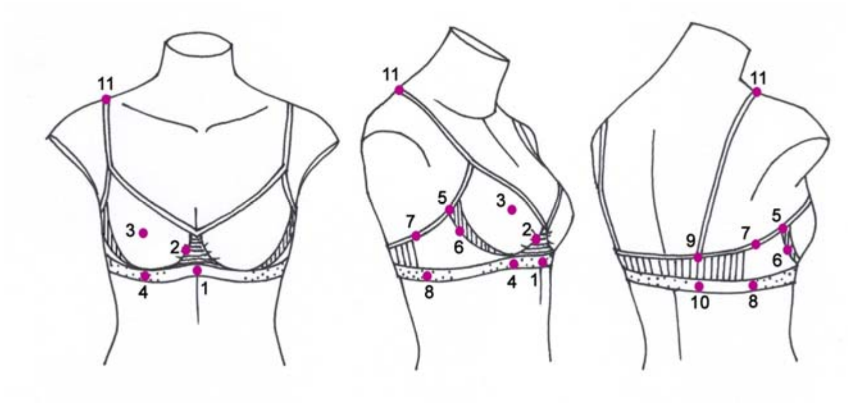

Figure 7.8 Pressure measuring points for new seamless bra style 1

and the 4 commercial bras

Table 7.5 Definitions of pressure measuring points for new seamless bra style 1

and the 4 commercial bras

Pressure measuring points	Name
1	Centre front
2	Inner wire
3	Apex
4	Cup base point
5	Underarm
6	Outer wire
7	Side upperband
8	Side bottomband
9	Back strap
10	Back strap end
11	Shoulder point

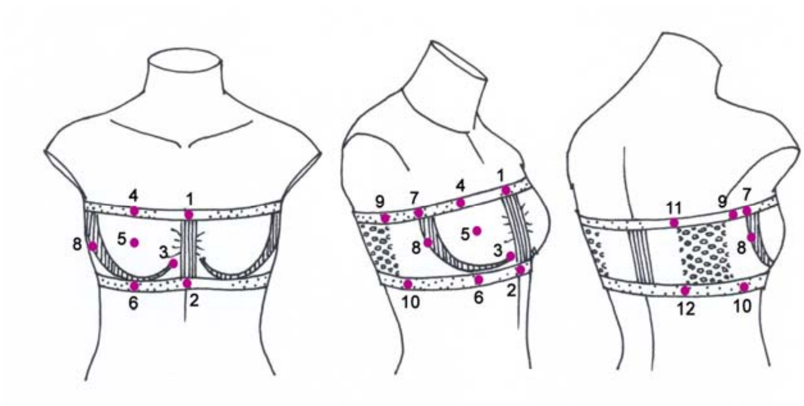

Figure 7.9 Pressure measuring points for new seamless bra style 2

Table 7.6 Definitions of pressure measuring points for new seamless bra style 2

Pressure measuring points	Name
1	Upper centre front
2	Centre front
3	Inner wire
4	Bust upperband
5	Apex
6	Cup base point
7	Underarm upperband
8	Outer wire
9	Side upperband
10	Side bottomband
11	Back strap upperband
12	Back strap bottomband

Bra objective evaluation was conducted by means of the Novel pressure measure system (see Figure 7.11). The single sensor was used to measure the pressure of relative measuring points on the right side of the body. To ensure accuracy, pressure values were measured three times for each posture. Each time pressure data was collected for 20 seconds. Ten pressure measurements per second were recorded.

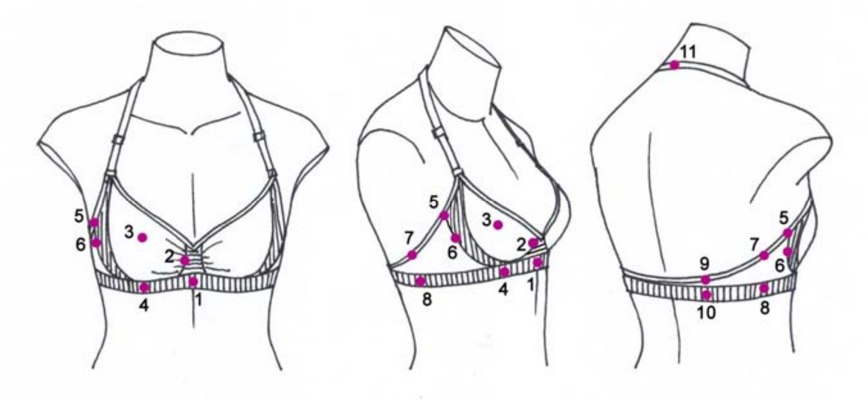

Figure 7.10 Pressure measuring points for new seamless bra style 3

Table 7.7 Definitions of pressure measuring points for new seamless bra style 3

Pressure measuring points	Name
1	Centre front
2	Inner wire
3	Apex
4	Cup base point
5	Underarm
6	Outer wire
7	Side upperband
8	Side bottomband
9	Back strap
10	Back strap end
11	Back shoulder strap point

Figure 7.11 The Novel pressure measure system

7.3.6 Subjective Evaluation

To investigate the effect of bra pressure on comfort & pressure sensations during wearing, a seven-point scale questionnaire (see Figure 7.12) was used for subjective evaluation. With reference to Yu's bra fitting checklist (2006), subjects were asked to assess wearing sensations in specific regions. Figure 7.13 shows the areas that were evaluated, including A. gore, B. cup, C. underwire, D. side wing, E. back wing and F. shoulder strap. The full versions of the questionnaires are presented in Appendix III.

Comfort sensation	Very bad			Neutral			Very good
Score	1	2	3	4	5	6	7
Pressure sensation	Very weak			Neutral			Very strong
Score	1	2	3	4	5	6	7

Figure 7.12 The seven-point scale for comfort & pressure sensation evaluation

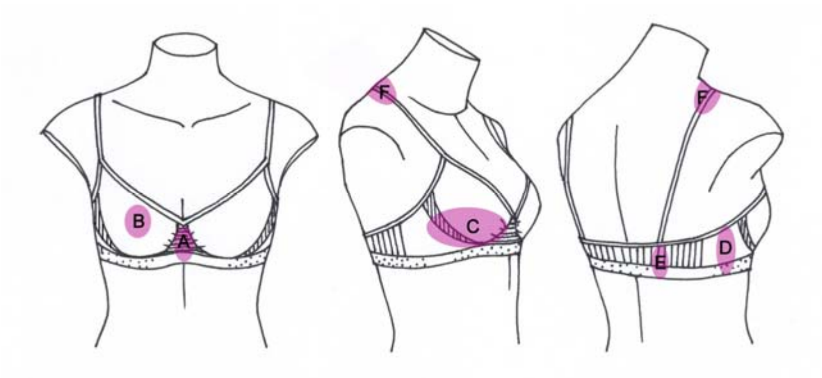

(a) For developed seamless bra style 1 and other 4 commercial bras

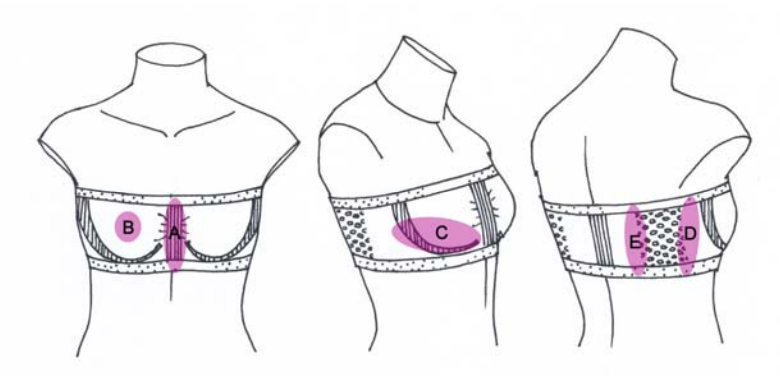

(b) For developed seamless bra style 2

Figure 7.13.1 The bra regions for comfort & pressure sensation evaluations

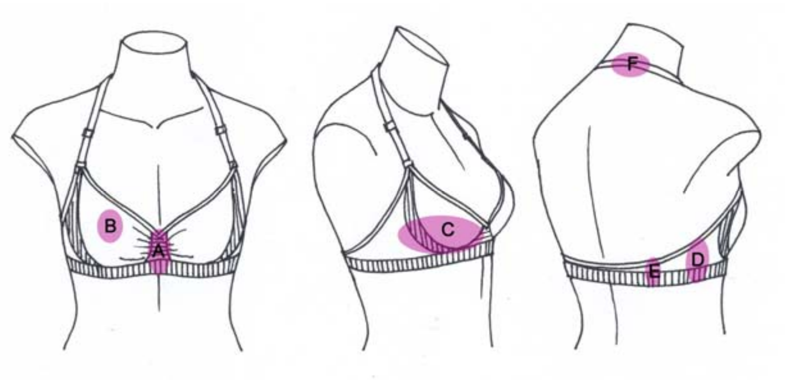

(c) For developed seamless bra style 3

Figure 7.13.2 The bra regions for comfort & pressure sensation evaluations

In addition, an overall bra comfort & pressure sensation evaluation was conducted using a seven-point scale questionnaire, and three questions.

1. When you wear developed seamless knitted bras, do you think the fabric handle and comfort sensation are overall better than the conventional bras?
2. When you wear developed seamless knitted bras, do you think your breast shape appears to be natural?
3. When you wear developed seamless knitted bras adding 3D underwires, do you feel they provide better support than before?

The details are shown in Appendix IV.

7.3.7 Breast Shape Evaluation

To investigate the subjects' breast shape changes with bras, the 3D body scanner VOXELAN LPW-2000FW was used to scan each subject's breast surface with the nineteen different bra samples.

RapidForm 2004 and 3D Measure Workshop were used to draw the cross-sections and vertical-sections of the body for assessing the breast shape changes.

7.4 Data Analysis and Discussion

7.4.1 Objective Evaluation

Bra localized pressure values are the key factors influencing bra fit and comfort sensations. In this section, we will compare the pressure values measured on different bra styles and measuring postures.

First, the pressure data of each measuring point of each bra were box-plotted in the scattered diagrams to discover the outliers. In order to avoid incorrect data being included, any data having a value over 4 standard deviations from the mean was deleted from the spreadsheet. After examined and purified, the pressure values for each measuring point of each bra were evaluated based on the 3 sets of data collected for 20 seconds on 6 subjects.

7.4.1.1 Pressure Value Comparisons of Commercial Bras

Figure 7.14 and Table 7.8 show a comparison of the average pressure values at each measuring point in the arms-down standing posture for each commercial bra in this investigation. It can be seen that the two conventional cut & sewn bras appear to have higher pressure values at most of the measuring points than the two commercial seamless knitted bras, especially at the locations of points 2 (inner wire), 6 (outer wire), 8 (side bottomband) and 11 (shoulder point). The two seamless bras had almost zero pressure values at points 2, 5 (underarm) and 6. It can be observed that each of four commercial bras has a relatively low pressure value at point 1 (centre front). This means the gore of each bra just barely sits against the sternum.

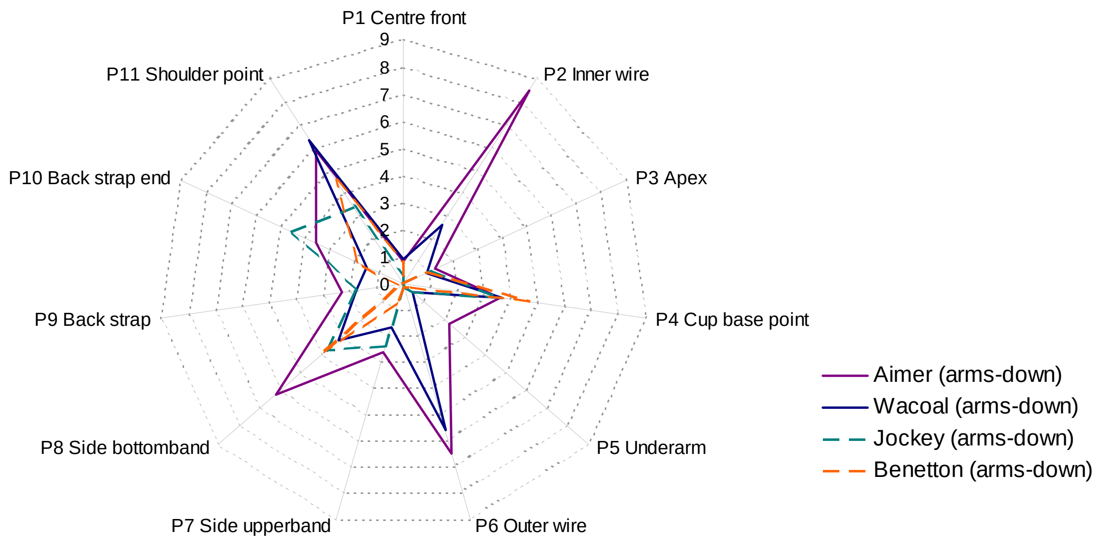

Figure 7.14 Average pressure (n = 6) at different measuring points of 2 conventional bras and 2 commercial seamless bras in arms-down standing posture (unit in Kpa)

Remark: the definitions of 11 pressure measuring points are defined in Figure 7.8 & Table 7.5

Table 7.8 Average pressure values (n = 6) at different measuring points of 2 conventional bras and 2 commercial seamless bras in arms-down posture (unit in Kpa)

Brand	Statistic items (n = 6)	Point 01	Point 02	Point 03	Point 04	Point 05	Point 06	Point 07	Point 08	Point 09	Point 10	Point 11
Aimer	Mean (Kpa)	0.81	8.47	1.28	3.57	2.26	6.48	2.60	6.19	2.29	3.56	5.85
	Std. D (Kpa)	0.80	2.43	1.21	1.50	1.26	1.36	0.76	4.41	0.80	4.02	1.39
Wacoal	Mean (Kpa)	0.90	2.59	0.97	3.68	0.44	5.57	1.65	3.17	1.74	1.45	6.30
	Std. D (Kpa)	0.88	1.72	0.71	2.54	0.42	1.24	1.04	1.91	0.71	1.28	1.74
Jockey	Mean (Kpa)	0.35	0.00	1.15	3.65	0.45	0.08	2.38	3.71	1.67	4.48	3.32
	Std. D (Kpa)	0.24	0.00	0.53	1.20	0.31	0.15	0.87	1.22	1.66	6.26	0.97
Benetton	Mean (Kpa)	0.84	0.00	0.98	4.69	0.23	0.11	0.75	3.78	0.16	1.87	4.51
	Std. D (Kpa)	0.63	0.00	0.33	1.95	0.28	0.17	0.74	1.86	0.23	2.41	1.19

Figure 7.15 and Table 7.9 present a comparison of the average pressure values in arms-up standing posture. It can be seen that the Aimer bra has the highest pressure values at all measuring points except 3 (apex) and 4 (cup base point). The Wacoal bra showed the second highest pressure values at most measuring points. Compared with the two conventional bras, the two commercial seamless knitted bras displayed lower pressure values at most of the measuring points, except points 4 (cup base), 11 (shoulder point), 8 (side bottomband) and 10 (back strap end). Compared with the arms-down posture, the pressure value of point 2 (inner wire) considerably decreased when the arms were raised.

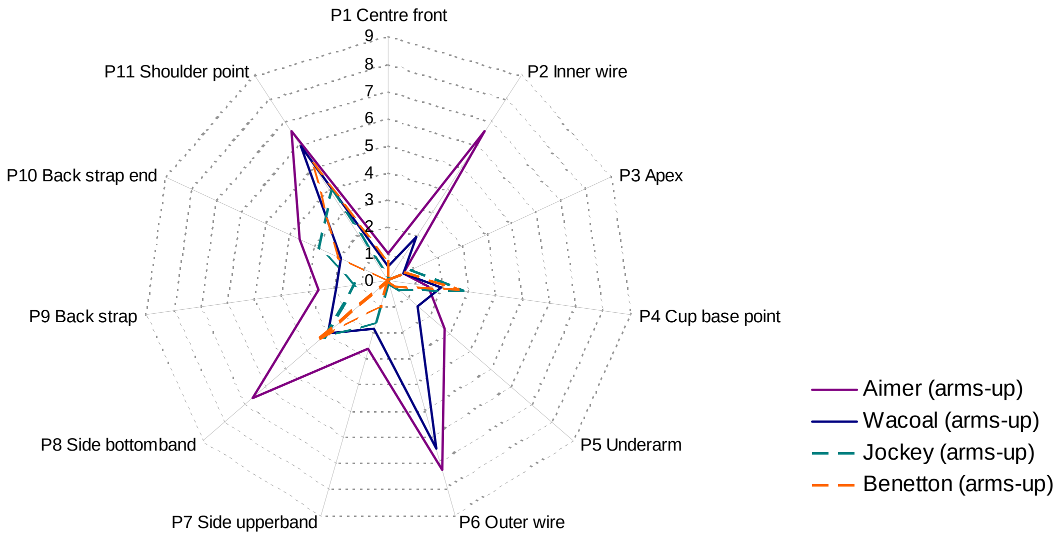

Figure 7.15 Average pressure (n = 6) of 2 conventional bras and 2 commercial seamless bras in arms-up posture (unit in Kpa)

At point 4 (cup base) in both postures, the two commercial seamless knitted bras show higher pressure values than the two conventional bras, due to the limited cup volume and stretchability of the knitted underband. From the results, we can find that the seamless knitted bras have superior properties to make wearers more comfortable at all bra regions except the regions of “cup base point”, “side bottomband”, “back strap end”, “shoulder point” and “apex”.

Table 7.9 Average pressure (n = 6) of 2 conventional bras and 2 commercial seamless bras in arms-up posture (unit in Kpa)

Brand	Statistic items (n = 6)	Point 01	Point 02	Point 03	Point 04	Point 05	Point 06	Point 07	Point 08	Point 09	Point 10	Point 11
Aimer	Mean (Kpa)	0.98	6.53	0.60	1.48	2.74	7.22	2.60	6.58	2.61	3.59	6.52
	Std. D (Kpa)	1.01	3.37	0.48	0.85	1.50	4.07	0.49	2.62	0.97	3.32	3.76
Wacoal	Mean (Kpa)	0.53	1.92	0.60	1.95	1.41	6.46	1.88	2.95	1.90	1.89	5.87
	Std. D (Kpa)	0.64	1.20	0.68	0.88	0.97	2.93	1.22	1.91	0.77	1.65	2.21
Jockey	Mean (Kpa)	0.19	0.00	0.94	2.82	0.51	0.07	1.60	3.16	1.19	2.83	3.87
	Std. D (Kpa)	0.16	0.00	0.45	1.14	0.38	0.16	0.68	1.44	1.16	2.51	1.68
Benetton	Mean (Kpa)	0.70	0.00	0.72	2.64	0.35	0.00	0.98	3.24	0.03	1.98	5.07
	Std. D (Kpa)	0.59	0.00	0.40	1.22	0.41	0.00	0.47	1.33	0.07	1.96	1.84

Paired-sample T test was used to compare the overall pressure values of each commercial test bra taken in the two standing postures at 5% level of significance. As shown in Table 7.10, the all paired testing p-values are over 0.05. The results revealed that there is no significant difference of overall pressure values between arms-down standing posture and arms-up posture for each commercial bra.

Table 7.10 Paired-sample T test results for each of the 4 commercial bras (arms-down vs arms-up posture)

		Mean (n = 6)	Std. D	Std. Error Mean	95% Confidence Interval of the Difference		t	df	Sig. (2-tailed)
					Lower	Upper			
Pair 1	Aimer: standing vs arms-up	0.175	0.990	0.298	-0.490	0.840	0.586	10	0.571
Pair 2	Wacoal: standing vs arms-up	0.100	0.765	0.231	-0.414	0.614	0.434	10	0.674
Pair 3	Jockey: standing vs arms-up	0.370	0.585	0.176	-0.023	0.762	2.096	10	0.062
Pair 4	Benetton: standing vs arms-up	0.200	0.674	0.203	-0.253	0.653	0.985	10	0.348

7.4.1.2 Comparisons among Seamless Commercial Bras & Newly Developed Bras

- **Style 1**

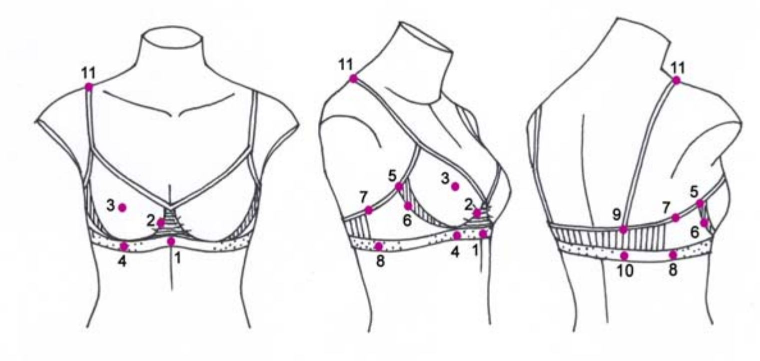

a) No wire, arms-down

As the new seamless bra style 1 has a design similar to the two commercial seamless bras, it was chosen for pressure comparisons with the commercial bras. Figure 7.16 and Table 7.11 show the average pressure value comparisons among the two commercial seamless bras and the newly developed bra style 1 “ST1L0Y16” without 3D wires in standing posture with arms down. The results show that all three seamless bras have low pressure values at points 1(centre front), 2 (inner wire), 5 (underarm) and 6 (outer wire), but have high pressure values at points 4 (cup base point), 8 (side bottomband) and 11 (shoulder point).

When compared with the two commercial seamless bras, the newly developed bra shows lower pressure values at points 5, 8 and 10 (back strap end), and higher values at point 4 and 7 (side upperband) and 11. This is probably because of the design features, including the extrusive underwire tunnel for inserting the 3D wire and the elastic upperband and shoulder strap.

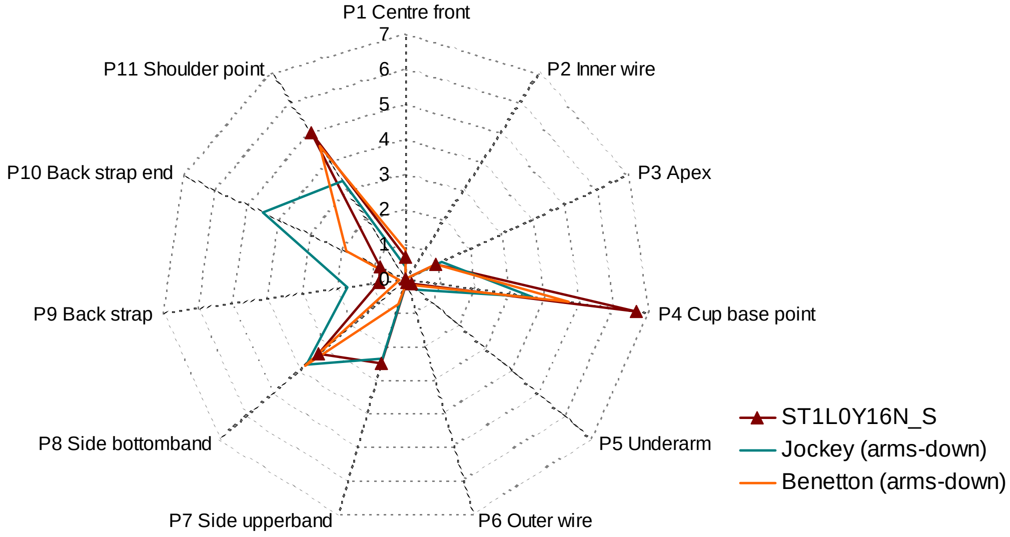

Figure 7.16 Average pressure (n =6)of style 1 and two commercial seamless bras without 3D soft wires in arms-down standing posture, denoted as "N_S", unit in Kpa)

Remark: the definitions of 11 pressure measuring points are defined in Figure 7.8 & Table 7.5

Table 7.11 Average pressure (n = 6) of style 1 and two commercial seamless bras without 3D soft wires in arms-down standing posture (denoted as "N_S")

Brand	Statistic items (n = 6)	Point 01	Point 02	Point 03	Point 04	Point 05	Point 06	Point 07	Point 08	Point 09	Point 10	Point 11
ST1L0Y16N_S	Mean (Kpa)	0.61	0.01	0.96	6.66	0.22	0.10	2.51	3.28	0.76	0.79	4.97
	Std. D (Kpa)	0.55	0.02	0.47	3.09	0.20	0.23	1.02	0.91	0.43	0.77	0.99
Jockey	Mean (Kpa)	0.35	0.00	1.15	3.65	0.45	0.08	2.38	3.71	1.67	4.48	3.32
	Std. D (Kpa)	0.24	0.00	0.53	1.20	0.31	0.15	0.87	1.22	1.66	6.26	0.97
Benetton	Mean (Kpa)	0.84	0.00	0.98	4.69	0.23	0.11	0.75	3.78	0.16	1.87	4.51
	Std. D (Kpa)	0.63	0.00	0.33	1.95	0.28	0.17	0.74	1.86	0.23	2.41	1.19

The results also indicate that two commercial seamless bras have significantly higher values at point 10 (back strap end), show higher or similar values at point 3 (apex). This means that the two commercial bras have relatively higher cup volume restriction and tighter back underband than style 1.

b) No wire, arms-up

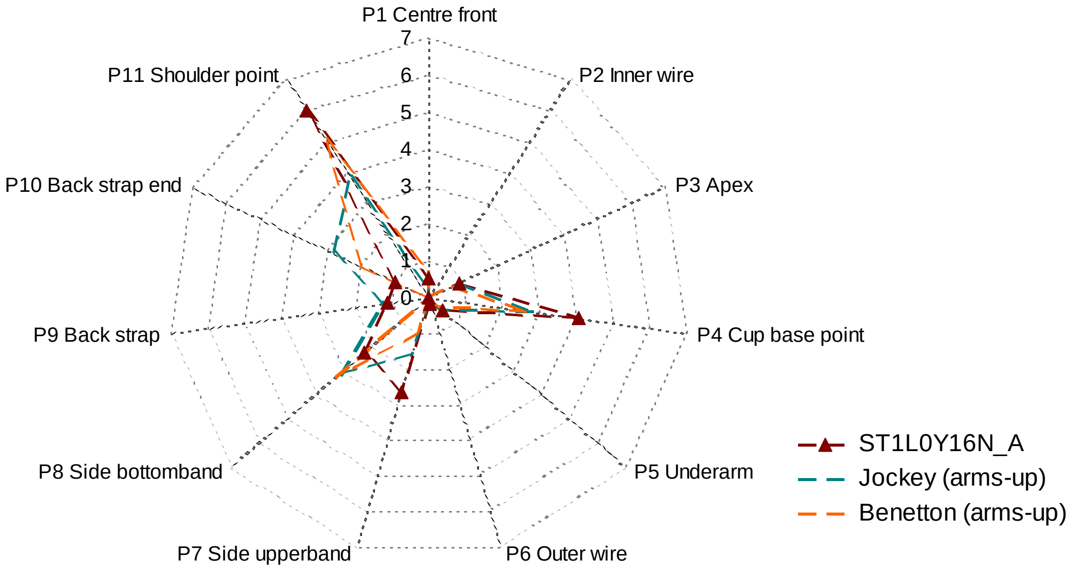

Figure 7.17 Average pressure (n =6) of style 1 and two commercial seamless bras without 3D soft wires in arms-up standing posture, denoted as "N_A" (unit in kPa)

Table 7.12 Average pressure value comparisons (n =6) among style 1 and two commercial seamless bras (Jockey & Benetton) (without 3D soft wires / arms-up posture, denoted as "N_A")

Brand	Statistic items (n = 6)	Point 01	Point 02	Point 03	Point 04	Point 05	Point 06	Point 07	Point 08	Point 09	Point 10	Point 11
ST1L0Y16N_A	Mean (Kpa)	0.50	0.00	0.88	4.06	0.52	0.17	2.66	2.27	1.10	1.00	5.99
	Std. D (Kpa)	0.52	0.00	0.46	1.39	0.47	0.24	1.11	0.49	0.64	0.86	1.84
Jockey	Mean (Kpa)	0.19	0.00	0.94	2.82	0.51	0.07	1.60	3.16	1.19	2.83	3.87
	Std. D (Kpa)	0.16	0.00	0.45	1.14	0.38	0.16	0.68	1.44	1.16	2.51	1.68
Benetton	Mean (Kpa)	0.70	0.00	0.72	2.64	0.35	0.00	0.98	3.24	0.03	1.98	5.07
	Std. D (Kpa)	0.59	0.00	0.40	1.22	0.41	0.00	0.47	1.33	0.07	1.96	1.84

Figure 7.17 and Table 7.12 present the average pressure value comparisons among two commercial seamless bras and the newly developed bra "ST1L0Y16" without 3D wires at each measuring point in arms-up posture. Compared with the results of arms-down posture, the pressure values of the 3 test samples significantly decreased at points 4 (cup base point) and 8 (side bottomband), whereas increased at point 11 (shoulder point). This is probably because arms-up posture causes the breasts and shoulders to move up,

and therefore to decrease the pressure value at the bra underband resulting from the weight of the breasts, but to increase the shoulder pressure of the stretching shoulder strap.

c) Wired, arms-down

Figure 7.18 and Table 7.13 show the average pressure value comparisons among two seamless commercial bras and newly developed bra “ST1L0Y16” with a 3D soft wire in posture with arms down. The results reveal that compared with the situation of no wire (see Figure 7.16), “ST1L0Y16” has considerably lower pressure at points 4 (cup base point) and 8 (side bottomband), and shows similar pressure values as the unwired bras at the other nine measuring points. This means that the set of the 3D supporting wire can help to hold the breasts and decrease the pressure values resulting from the weight of the breasts.

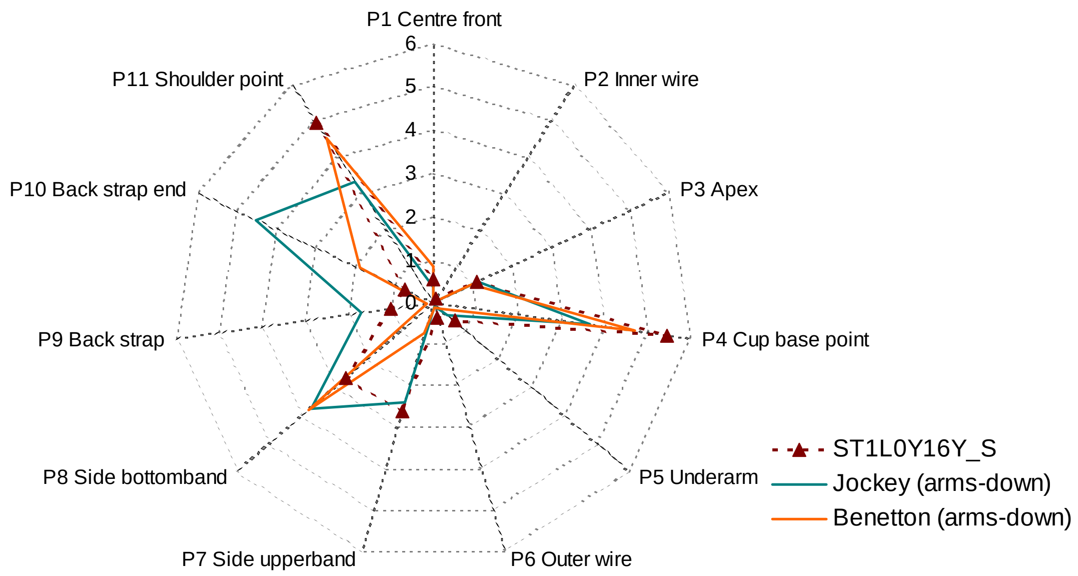

Figure 7.18 Average pressure value comparisons (n = 6) among style 1 and two commercial seamless bras (Jockey & Benetton) (with 3D soft wires / arms-down posture, denoted as “Y_S”, unit in Kpa)

Table 7.13 Average pressure (n = 6) of style 1 and two commercial seamless braswith 3D soft wires in arms-down posture, denoted as "Y_S"

Brand	Statistic items (n = 6)	Point 01	Point 02	Point 03	Point 04	Point 05	Point 06	Point 07	Point 08	Point 09	Point 10	Point 11
ST1L0Y	Mean (Kpa)	0.54	0.10	1.08	5.45	0.66	0.36	2.61	2.66	0.97	0.71	4.94
16Y_S	Std. D (Kpa)	0.56	0.17	0.38	2.40	0.32	0.50	1.35	0.31	0.66	0.74	1.27
Jockey	Mean (Kpa)	0.35	0.00	1.15	3.65	0.45	0.08	2.38	3.71	1.67	4.48	3.32
	Std. D (Kpa)	0.24	0.00	0.53	1.20	0.31	0.15	0.87	1.22	1.66	6.26	0.97
Benetton	Mean (Kpa)	0.84	0.00	0.98	4.69	0.23	0.11	0.75	3.78	0.16	1.87	4.51
	Std. D (Kpa)	0.63	0.00	0.33	1.95	0.28	0.17	0.74	1.86	0.23	2.41	1.19

d) Wired, arms-up

Figure 7.19 and Table 7.14 present the average pressure value comparisons among two commercial seamless bras and the newly developed bra "ST1L0Y16" with 3D soft wires in arms-up posture. The results are similar to the above three situations.

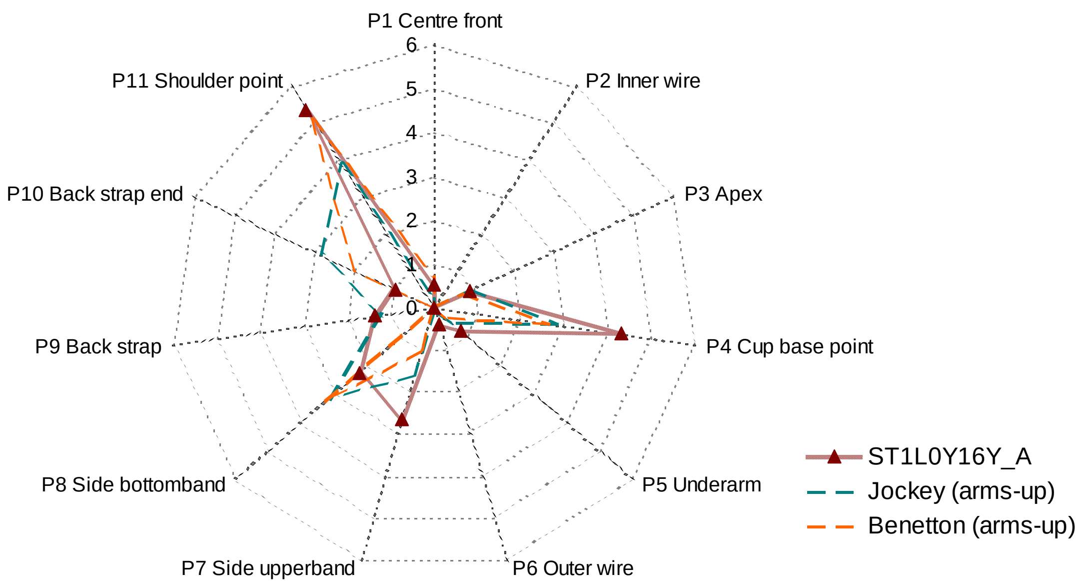

Figure 7.19 Average pressure (n = 6) of style 1 and two commercial seamless bras with 3D soft wires in arms-up posture, denoted as "Y_A" (unit in Kpa)

Table 7.14 Average pressure (n = 6) of style 1 and two commercial seamless bras with 3D soft wires in arms-up posture, denoted as “Y_A”

Brand	Statistic items (n = 6)	Point 01	Point 02	Point 03	Point 04	Point 05	Point 06	Point 07	Point 08	Point 09	Point 10	Point 11
ST1L0Y1 6Y_A	Mean (Kpa)	0.51	0.00	0.90	4.28	0.81	0.41	2.61	2.24	1.34	0.97	5.35
	Std. D (Kpa)	0.54	0.00	0.46	1.11	0.39	0.32	0.89	0.34	0.89	0.79	2.10
Jockey	Mean (Kpa)	0.19	0.00	0.94	2.82	0.51	0.07	1.60	3.16	1.19	2.83	3.87
	Std. D (Kpa)	0.16	0.00	0.45	1.14	0.38	0.16	0.68	1.44	1.16	2.51	1.68
Benetton	Mean (Kpa)	0.70	0.00	0.72	2.64	0.35	0.00	0.98	3.24	0.03	1.98	5.07
	Std. D (Kpa)	0.59	0.00	0.40	1.22	0.41	0.00	0.47	1.33	0.07	1.96	1.84

7.4.1.3 Comparisons among Seamless Bras of Different Loop Density & Elastic Yarn Tension

Table 7.15 and 7.16 show the average pressure values of 5 cases of new seamless bra style 1 without 3D soft wires at each measuring point in standing with arms-down and with arms-up postures. Table 7.17 and 7.18 show the average pressure values of 5 cases of style 1 with 3D soft wires in the two postures respectively.

Table 7.15 Average pressure of 5 knitting conditions of the new seamless bra style 1, loop density from -25 low (ST1L-25Y20N_S) to 25 high (ST1L+25Y20N_S) without 3D soft wires and in arms-down posture, denoted as “N_S”)

Style	Statistic items (n = 6)	Point 01	Point 02	Point 03	Point 04	Point 05	Point 06	Point 07	Point 08	Point 09	Point 10	Point 11
ST1L-25 Y20N_S	Mean (Kpa)	$\boxed{0.91}$	$\boxed{0.99}$	$\boxed{1.05}$	7.83	$\boxed{0.52}$	$\boxed{0.31}$	2.81	$\boxed{4.02}$	1.49	$\boxed{2.64}$	$\boxed{5.60}$
	Std. D (Kpa)	0.77	2.27	0.53	4.85	0.39	0.35	1.57	1.42	0.57	3.54	2.23
ST1L-25 Y12N_S	Mean (Kpa)	0.66	0.00	0.97	$\boxed{10.29}$	0.44	0.28	$\boxed{2.97}$	3.08	$\boxed{2.25}$	1.81	5.37
	Std. D (Kpa)	0.63	0.00	0.45	4.00	0.35	0.30	0.99	1.39	1.47	1.64	2.63
ST1L0Y 16N_S	Mean (Kpa)	0.61	0.01	0.96	6.66	0.22	0.10	2.51	3.28	0.76	0.79	4.97
	Std. D (Kpa)	0.55	0.02	0.47	3.09	0.20	0.23	1.02	0.91	0.43	0.77	0.99
ST1L+25 Y12N_S	Mean (Kpa)	0.27	0.00	0.79	6.35	0.20	0.01	1.81	2.22	0.57	0.99	3.88
	Std. D (Kpa)	0.35	0.00	0.41	3.43	0.16	0.03	1.11	1.13	0.23	1.80	2.23
ST1L+25 Y20N_S	Mean (Kpa)	0.43	0.00	0.88	6.42	0.31	0.05	2.46	2.81	0.78	1.09	4.22
	Std. D (Kpa)	0.44	0.00	0.61	4.94	0.33	0.15	1.12	1.57	0.86	1.19	1.81

$\boxed{}$ means the highest pressure value at each measuring point

Table 7.16 Average pressure values of 5 knitting conditions of the new seamless bra style 1, loop density from -25 low (ST1L-25Y20N_A) to 25 high (ST1L+25Y20N_A) without 3D soft wires and in arms-up posture, denoted as "N_A"

Style	Statistic items (n = 6)	Point 01	Point 02	Point 03	Point 04	Point 05	Point 06	Point 07	Point 08	Point 09	Point 10	Point 11
ST1L-25	Mean (Kpa)	0.74	$\boxed{0.64}$	0.86	4.56	0.83	$\boxed{0.46}$	2.71	$\boxed{3.41}$	2.33	$\boxed{2.91}$	$\boxed{7.20}$
Y20N_A	Std. D (Kpa)	0.69	1.48	0.51	2.58	0.66	0.38	1.55	1.83	0.98	3.32	2.77
ST1L-25	Mean (Kpa)	$\boxed{0.78}$	0.00	$\boxed{0.99}$	$\boxed{5.68}$	$\boxed{1.01}$	0.38	$\boxed{3.73}$	2.70	$\boxed{3.12}$	2.23	5.64
Y12N_A	Std. D (Kpa)	0.66	0.00	0.79	2.09	0.69	0.41	1.06	1.06	1.67	1.97	5.34
ST1L0Y	Mean (Kpa)	0.50	0.00	0.88	4.06	0.52	0.17	2.66	2.27	1.10	1.00	5.99
16N_A	Std. D (Kpa)	0.52	0.00	0.46	1.39	0.47	0.24	1.11	0.49	0.64	0.86	1.84
ST1L+25	Mean (Kpa)	0.30	0.00	0.53	3.72	0.26	0.06	2.26	1.58	0.92	1.22	4.44
Y12N_A	Std. D (Kpa)	0.37	0.00	0.45	1.65	0.15	0.12	1.57	1.37	0.61	1.77	1.64
ST1L+25	Mean (Kpa)	0.30	0.00	0.61	3.38	0.80	0.00	2.45	2.22	1.01	1.32	5.86
Y20N_A	Std. D (Kpa)	0.41	0.00	0.45	1.79	0.50	0.00	1.51	1.13	0.95	1.19	2.15

$\boxed{}$ means the highest pressure value at each measuring point

Table 7.17 Average pressure of 5 knitting conditions of the new seamless bra style 1, loop density from -25 Low (ST1L-25Y20Y_S) to 25 high (ST1L+25Y20Y_S) with 3D soft wires and in arms-down posture, denoted as "Y_S"

Style	Statistic items (n = 6)	Point 01	Point 02	Point 03	Point 04	Point 05	Point 06	Point 07	Point 08	Point 09	Point 10	Point 11
ST1L-25	Mean (Kpa)	$\boxed{0.89}$	$\boxed{1.01}$	$\boxed{1.13}$	4.57	$\boxed{0.94}$	0.69	2.61	$\boxed{3.76}$	1.96	$\boxed{2.29}$	$\boxed{6.33}$
Y20Y_S	Std. D (Kpa)	0.74	2.33	0.57	0.96	0.73	0.54	1.89	1.89	1.66	2.70	2.06
ST1L-25	Mean (Kpa)	0.65	0.25	0.96	$\boxed{6.62}$	0.78	$\boxed{0.71}$	$\boxed{2.72}$	2.84	$\boxed{3.01}$	1.57	5.52
Y12Y_S	Std. D (Kpa)	0.64	0.56	0.45	1.19	0.45	0.36	1.84	1.27	1.60	1.58	1.64
ST1L0Y	Mean (Kpa)	0.54	0.10	1.08	5.45	0.66	0.36	2.61	2.66	0.97	0.71	4.94
16Y_S	Std. D (Kpa)	0.56	0.17	0.38	2.40	0.32	0.50	1.35	0.31	0.66	0.74	1.27
ST1L+25	Mean (Kpa)	0.34	0.00	0.85	4.56	0.48	0.32	2.07	1.99	0.80	0.83	3.87
Y12Y_S	Std. D (Kpa)	0.37	0.00	0.39	1.47	0.27	0.30	0.95	1.26	0.51	1.58	1.57
ST1L+25	Mean (Kpa)	0.45	0.02	0.98	3.89	0.72	0.21	2.15	3.24	0.86	0.98	4.20
Y20Y_S	Std. D (Kpa)	0.40	0.05	0.66	0.91	0.39	0.40	1.11	2.38	0.51	1.08	2.21

$\boxed{}$ means the highest pressure value at each measuring point

Table 7.18 Average pressure of 5 knitting conditions of the new seamless bra style 1, loop density from -25 low (ST1L-25Y20Y_A) to 25 high (ST1L+25Y20Y_A) with 3D soft wires and in arms-up posture, denoted as "Y_A"

Style	Statistic items (n = 6)	Point 01	Point 02	Point 03	Point 04	Point 05	Point 06	Point 07	Point 08	Point 09	Point 10	Point 11
ST1L-25 Y20Y_A	Mean (Kpa)	$\boxed{0.77}$	$\boxed{0.54}$	$\boxed{0.88}$	4.44	0.87	0.61	2.60	$\boxed{3.52}$	2.02	$\boxed{2.88}$	$\boxed{6.49}$
	Std. D (Kpa)	0.69	1.24	0.48	2.47	0.46	0.60	1.58	2.00	0.71	3.11	3.85
ST1L-25 Y12Y_A	Mean (Kpa)	0.62	0.13	0.83	$\boxed{5.10}$	$\boxed{0.90}$	$\boxed{0.94}$	$\boxed{2.80}$	2.55	$\boxed{3.51}$	2.16	5.26
	Std. D (Kpa)	0.61	0.31	0.50	1.18	0.74	0.55	1.09	0.97	1.84	1.97	3.30
ST1L0Y 16Y_A	Mean (Kpa)	0.51	$\underline{0.00}$	0.81	4.28	0.81	0.41	2.61	2.59	1.34	0.97	5.35
	Std. D (Kpa)	0.54	0.00	0.39	1.11	0.39	0.32	0.89	2.58	0.89	0.79	2.10
ST1L+25 Y12Y_A	Mean (Kpa)	$\underline{0.33}$	$\underline{0.00}$	0.63	$\underline{2.55}$	$\underline{0.73}$	$\underline{0.09}$	2.50	$\underline{2.24}$	$\underline{1.11}$	$\underline{1.09}$	$\underline{4.66}$
	Std. D (Kpa)	0.39	0.00	0.42	1.10	0.55	0.15	1.44	0.34	0.53	1.82	1.66
ST1L+25 Y20Y_A	Mean (Kpa)	0.39	$\underline{0.00}$	$\underline{0.62}$	3.64	1.00	0.42	$\underline{2.33}$	3.02	1.29	1.23	5.00
	Std. D (Kpa)	0.39	0.00	0.45	1.89	0.64	0.52	1.26	2.22	0.84	1.16	1.48

$\boxed{\quad}$ means the highest pressure value at each measuring point

The four tables show consistent results for different levels of loop density & elastic yarn tension. The bras which have a relatively larger loop density (factor A at the high level), present lower pressure values, whereas the bras which have a smaller loop density (factor A at the lower level) have the highest pressure values.

7.4.1.4 Comparisons between Bras with & without 3D Soft Wires

To investigate the differences of the newly developed seamless bras between the bras with & without 3D soft wires in detail, for each style, the average pressure values of 5 test bras and the percentage difference between bras with & without 3D soft wires at each measuring point were calculated in the two postures respectively. The results are shown in Tables 7.19, 7.20 to 7.21.

For style 1 (see Table 7.19), the pressure is greater with 3D wires at point 6 (cup base point), 5 (apex), 2 (centre point) and 9 (side upperband) in both arms-down and arms-up postures.

Style 2 (see Table 7.20) shows relatively higher pressure at point 8 (outer wire) and 5 (apex) in both postures when using 3D wires.

Table 7.19 Comparisons of average pressure values of style 1 between with & without 3D soft wires (arms-down & arms-up postures)

Situation	Point 01	Point 02	Point 03	Point 04	Point 05	Point 06	Point 07	Point 08	Point 09	Point 10	Point 11
N_S (Kpa)	0.58	0.20	0.93	7.51	0.34	0.15	2.51	3.29	1.17	1.46	4.81
Y_S (Kpa)	0.57	0.28	1.00	5.02	0.72	0.46	2.43	2.90	1.52	1.28	4.97
S: (Y-N)/N	0%	38%	8%	-33%	112%	205%	-3%	-12%	30%	-13%	3%
N_A (Kpa)	0.52	0.13	0.77	4.28	0.68	0.21	2.76	2.60	1.70	1.74	5.83
Y_A (Kpa)	0.52	0.13	0.77	4.00	0.86	0.49	2.57	2.78	1.85	1.67	5.35
A: (Y-N)/N	0%	5%	0%	-6%	26%	131%	-7%	7%	9%	-4%	-8%

(* S: (Y-N)/N = Increased % of pressure by wired bra in arms-down posture

$= \frac{(Y\_S)-(N\_S)}{(N\_S)} \times 100\%$;

A: (Y-N)/N = Increased % of pressure by wired bra in arms-up posture)

Table 7.20 Comparisons of average pressure values of style 2 between with & without 3D soft wires (arms-down & arms-up postures)

Situation	Point 01	Point 02	Point 03	Point 04	Point 05	Point 06	Point 07	Point 08	Point 09	Point 10	Point 11	Point 12
N_S (Kpa)	0.04	0.16	0.38	1.83	0.97	2.98	1.35	0.12	2.79	3.54	1.54	2.29
Y_S (Kpa)	0.03	0.16	0.26	1.57	1.08	3.02	1.40	0.22	2.77	3.65	1.63	2.33
S: (Y-N)/N	-6%	0%	-31%	-14%	12%	1%	3%	79%	-1%	3%	6%	2%
N_A (Kpa)	0.02	0.09	0.33	1.08	0.63	2.26	1.08	0.19	3.59	3.64	1.85	2.45
Y_A (Kpa)	0.02	0.09	0.26	1.06	0.75	2.00	1.12	0.31	3.39	3.44	1.96	2.40
A: (Y-N)/N	-25%	0%	-22%	-2%	18%	-12%	4%	67%	-5%	-6%	6%	-2%

Style 3 (Table 7.21) presents two higher pressure points at 6 (outer wire) and 5

(underarm) in both postures. All of these points of higher pressure at the cup, underband and underwire regions are caused by the 3D soft wires. But we can see that all of these points present very small pressure values no matter whether 3D wires are used or not. This means even though the pressure values increased, it may not increase the uncomfortable sensations for the wearers. Most of the other measuring points show equal or smaller pressure values after using 3D wires.

Table 7.21 Comparisons of average pressure values of style 3 between with & without 3D soft wires (arms-down & arms-up postures)

Situation	Point 01	Point 02	Point 03	Point 04	Point 05	Point 06	Point 07	Point 08	Point 09	Point 10	Point 11
N_S (Kpa)	0.53	0.00	0.96	5.36	0.28	0.14	2.42	3.49	2.00	1.65	2.23
Y_S (Kpa)	0.48	0.00	1.02	4.71	0.42	0.27	2.32	3.39	2.02	1.74	2.35
S: (Y-N)/N	-9%	0%	7%	-12%	53%	99%	-4%	-3%	1%	5%	5%
N_A (Kpa)	0.49	0.00	0.83	3.41	0.63	0.28	2.44	3.04	2.78	1.93	0.94
Y_A (Kpa)	0.45	0.00	0.86	3.31	0.71	0.36	2.48	3.01	2.66	2.02	0.93
A: (Y-N)/N	-9%	0%	4%	-3%	13%	27%	1%	-1%	-4%	5%	0%

To investigate whether there is any difference between the wired and non-wired newly developed seamless bra in two postures at each measuring point, Paired-sample T tests were conducted. The results (see Appendix V.1 & Appendix V.6) reveal that styles 2 and 3 show no significant difference between wired and non-wired seamless bras at most of the measuring points.

7.4.1.5 Comparisons between Two Postures for Newly Developed Seamless Bras

To investigate the detailed difference between standing with arms-down and with arms-up postures, the average pressure values of the 5 test bras in two postures and their variance were calculated. Since the Paired-sample T test results show there is no significant difference between the bras with & without 3D wires at most of the measuring points, the tests on pressure were focused on comparing the pressure values on the bras without wires. As shown in Table 7.22, style 1 presents considerably higher pressure values at points 5 (underarm), 6 (outer wire) and 9 (back strap), but shows lower values at points 2 (inner wire) and 4 (cup base point).

Table 7.22 Comparisons of average pressure values of style 1 between arms-down and arms-up postures (without 3D soft wires)

Situation	Point 01	Point 02	Point 03	Point 04	Point 05	Point 06	Point 07	Point 08	Point 09	Point 10	Point 11
N_S (Kpa)	0.58	0.20	0.93	7.51	0.34	0.15	2.51	3.29	1.17	1.46	4.81
N_A (Kpa)	0.52	0.13	0.77	4.28	0.68	0.21	2.76	2.60	1.70	1.74	5.83
N: (A-S)/S	-9%	-36%	-17%	-43%	102%	43%	10%	-21%	45%	19%	21%

(# N: (A-S)/S = Increased % of non-wired pressure by arms-up posture = $\frac{(N\_A)-(N\_S)}{(N\_S)}\times 100\%$)

Table 7.23 shows the pressure comparisons for style 2. The results indicate that without 3D wires, the difference percentage between two postures show higher values at points 8 (outer wire) & 9 (side upperband), looser values at points 2 (centre front), 4 (bust upperband), 5 (apex) & 1 (upper center front).

Table 7.23 Comparisons of average pressure values of style 2 between arms-down and arms-up postures (without 3D soft wires)

Situation	Point 01	Point 02	Point 03	Point 04	Point 05	Point 06	Point 07	Point 08	Point 09	Point 10	Point 11	Point 12
N_S (Kpa)	0.04	0.16	0.38	1.83	0.97	2.98	1.35	0.12	2.79	3.54	1.54	2.29
N_A (Kpa)	0.02	0.09	0.33	1.08	0.63	2.26	1.08	0.19	3.59	3.64	1.85	2.45
N: (A-S)/S	-33%	-42%	-13%	-41%	-35%	-24%	-20%	52%	29%	3%	20%	7%

Table 7.24 Comparisons of average pressure values of style 3 between arms-down and arms-up postures (without 3D soft wires)

Situation	Point 01	Point 02	Point 03	Point 04	Point 05	Point 06	Point 07	Point 08	Point 09	Point 10	Point 11
N_S (Kpa)	0.53	0.00	0.96	5.36	0.28	0.14	2.42	3.49	2.00	1.65	2.23
N_A (Kpa)	0.49	0.00	0.83	3.41	0.63	0.28	2.44	3.04	2.78	1.93	0.94
N: (A-S)/S	-8%	0%	-13%	-36%	126%	103%	1%	-13%	39%	17%	-58%

Table 7.24 relates to the comparisons of style 3. The difference percentage between two postures show relatively higher pressure values at points 5 (underarm), 6 (outer wire) & 9 (back strap), and lower values at points 11 (back shoulder strap point) & 4 (cup base point).

To investigate whether there is any difference between two postures at each measuring point of each seamless bra style, Paired-sample T tests were conducted. The tests (see Appendix VI.1 & Appendix VI.3) show similar results to Table 7.22 to 7.24, the pressure value differences are significant at most of the measuring points, especially in the cup, underwire and upperband regions.

7.4.1.6 Comparisons among 3 Styles of Seamless Bras

To investigate whether there are any differences among the newly developed seamless bras, One-way ANOVA analysis was conducted on the same measuring points for the three styles including pressure values with & without 3D wires in two postures respectively at 5% level of significance. For the arms-down posture, the results (see Table 7.25) indicate that apart from the measuring points “centre point” (0.013), “cup base point” (0.001) and “underarm” (0.00), the p-values of other 7 points are greater than 0.05, indicating that there are no significant differences among the three seamless styles for these 7 measuring points. The reason for the three points which rejected the null hypothesis is probably related to the different design features among the three styles.

Table 7.25 One-way ANOVA analysis results of 3 newly developed seamless bras in arms-down posture

		Sum of Squares	df	Mean Square	F	Sig.
Centre front	Between Groups	0.536	2	0.268	6.394	0.013
	Within Groups	0.503	12	0.042		
	Total	1.039	14			
Inner wire	Between Groups	0.361	2	0.180	2.149	0.159
	Within Groups	1.007	12	0.084		
	Total	1.368	14			
Apex	Between Groups	0.028	2	0.014	0.350	0.712
	Within Groups	0.479	12	0.040		
	Total	0.506	14			
Cup base point	Between Groups	51.210	2	25.605	14.849	0.001
	Within Groups	20.693	12	1.724		
	Total	71.903	14			
Underarm	Between Groups	3.640	2	1.820	19.381	0.000
	Within Groups	1.127	12	0.094		
	Total	4.767	14			
Outer wire	Between Groups	0.002	2	0.001	0.033	0.967
	Within Groups	0.334	12	0.028		
	Total	0.336	14			
Side upperband	Between Groups	0.369	2	0.184	0.295	0.750
	Within Groups	7.496	12	0.625		
	Total	7.864	14			
Side bottomband	Between Groups	1.083	2	0.541	0.773	0.483
	Within Groups	8.406	12	0.701		
	Total	9.489	14			
Back strap	Between Groups	1.739	2	0.870	2.635	0.113
	Within Groups	3.960	12	0.330		
	Total	5.700	14			
Back strap end	Between Groups	1.859	2	0.930	2.593	0.116
	Within Groups	4.303	12	0.359		
	Total	6.162	14			

Table 7.26 presents the One-way ANOVA analysis results from the arms-up posture. The results show fewer measuring points which have significant differences among the three styles, with significance found only at “centre front” (0.004) and “cup base point” (0.006).

Table 7.26 One-way ANOVA analysis results of 3 newly developed seamless bras in arms-up posture

		Sum of Squares	df	Mean Square	F	Sig.
Centre front	Between Groups	0.581	2	0.291	9.061	0.004
	Within Groups	0.385	12	0.032		
	Total	0.966	14			
Inner wire	Between Groups	0.282	2	0.141	3.546	0.062
	Within Groups	0.476	12	0.040		
	Total	0.758	14			
Apex	Between Groups	0.108	2	0.054	1.677	0.228
	Within Groups	0.387	12	0.032		
	Total	0.495	14			
Cup base point	Between Groups	10.236	2	5.118	8.112	0.006
	Within Groups	7.571	12	0.631		
	Total	17.808	14			
Underarm	Between Groups	0.596	2	0.298	3.014	0.087
	Within Groups	1.186	12	0.099		
	Total	1.782	14			
Outer wire	Between Groups	0.023	2	0.012	0.282	0.759
	Within Groups	0.493	12	0.041		
	Total	0.516	14			
Side upperband	Between Groups	3.520	2	1.760	2.832	0.098
	Within Groups	7.457	12	0.621		
	Total	10.977	14			
Side bottomband	Between Groups	2.697	2	1.348	2.601	0.115
	Within Groups	6.221	12	0.518		
	Total	8.918	14			
Back strap	Between Groups	3.439	2	1.720	2.553	0.119
	Within Groups	8.082	12	0.673		
	Total	11.521	14			
Back strap end	Between Groups	1.383	2	0.692	1.327	0.301
	Within Groups	6.254	12	0.521		
	Total	7.637	14			

7.4.1.7 Summary of Pressure Testing Values

Based on the above discussions, we can summarize the key findings of pressure measuring results as follows:

1) Compared with the two conventional cut & sewn bras, the fifteen newly developed seamless knitted bra and two commercial seamless bras showed significantly lower pressure values at most of the measuring points, especially at the points of “inner wire” and “outer wire”.
2) Newly developed seamless knitted bra samples presented considerably higher pressure values at the point of “cup base point” during the bra testing processes without the 3D wires, but this significantly decreased after using the set of 3D soft wires.
3) The pressure values of the “centre front” and “apex” presented marginal differences among each of the testing samples.
4) Compared with the two commercial seamless bras, the testing samples of the newly developed seamless knitted bras, which were produced using a larger loop density +25 (factor A at the higher level), resulted in the lowest pressure values at most of the measuring points in both the arms-up and arms-down postures, especially at the “apex” and “side bottomband”; whereas the seamless knitted bra that was produced using a loop density of -25 (factor A at the lower level) had the highest pressure values.
5) The pressure values show no significant differences between the bras with and without 3D wires for styles 2 and 3 at most of the measuring points, but do present

significant differences between the two postures, especially in the cup, underwire and upperband regions at 5% level of significance.

6) There is no significant difference among three different styles at most of the pressure measuring points at 5% level of significance.

7.4.2 Subjective Comfort Evaluation

A seven-point scale questionnaire was used to evaluate subjects' comfort & pressure sensations while wearing the test bras. Each subject wore the test bra each time for approximately one hour before rating. A higher pressure sensation score means a stronger pressure sensation and vice versa. On the other hand, a higher comfort sensation score means a higher comfort sensation.

7.4.2.1 Comparisons of Commercial Bras

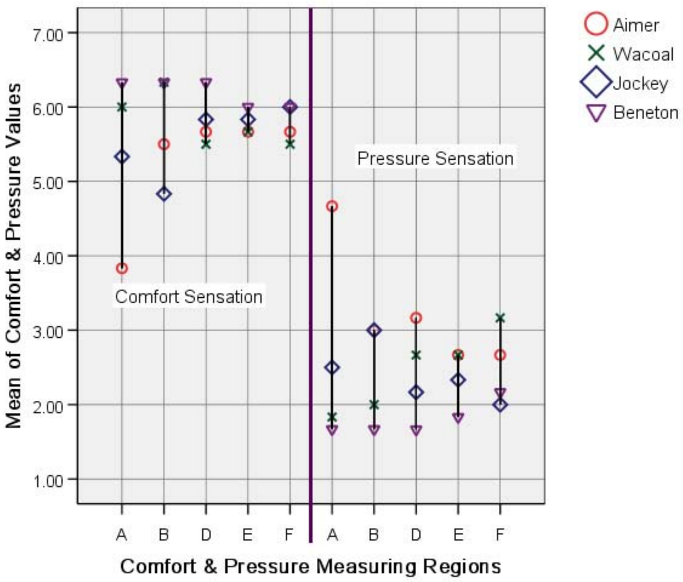

Figure 7.20 Comfort & pressure value comparisons among two conventional bras and two commercial seamless bras

Remark: The definitions of evaluation regions are defined in Figure 7.13

Figure 7.20 shows the comfort & pressure values of two conventional bras and two commercial seamless bras. The results indicate that the seamless bra “Benetton” provides the best comfort sensations at all measuring points and the weakest pressure sensations at almost all points. In contrast, the two conventional cut and sewn bras show the worst comfort sensations and the strongest pressure sensations. The four commercial samples tested show relatively smaller differences in the regions of the back wing and shoulder strap.

7.4.2.2 Comparisons among Newly Developed Seamless Bras of Different Loop Density & Elastic Yarn Tension

- **Style 1**

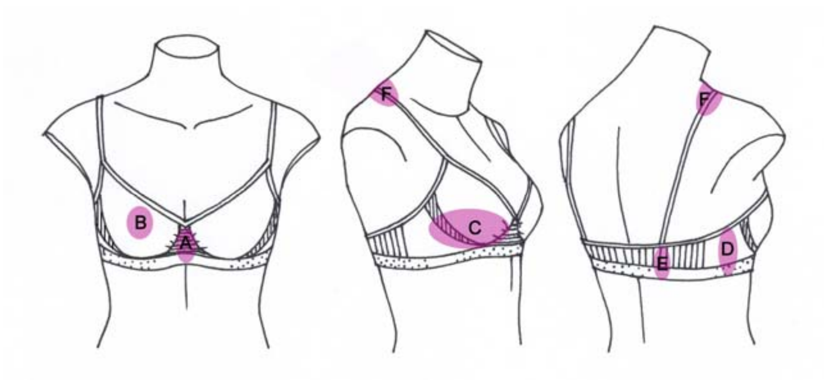

Table 7.27 and Table 7.28 show the comfort & pressure values of five seamless test bras of style 1 without and with 3D soft wire respectively. It can be seen that the bras ST1L+25Y12 and ST1L+25Y20, which have relatively higher loop density tend to have higher comfort scores and lower pressure scores at all measuring regions. The comparisons of style 2 & 3 also present similar results (the Tables are shown in Appendix VII).

Table 7.27 Average comfort & pressure ratings of five seamless bras of style 1, loop densities range from a low value of -25 (ST1L-25Y20N) to a high value of 25 (ST1L+25Y20N) without 3D soft wires

Style	Statistic items	Comfort sensation					Pressure sensation				
		Gore	Cup	Side wing	Back wing	Strap	Gore	Cup	Side wing	Back wing	Strap
ST1L-25Y20N	Mean	4.67	2.83	3.00	3.33	4.33	3.17	5.67	5.00	4.83	3.67
	Std. D	2.16	1.83	1.55	1.97	2.07	1.83	1.86	1.55	1.83	2.07
ST1L-25Y12N	Mean	4.67	3.17	3.83	3.83	4.17	3.17	4.67	4.33	4.17	3.67
	Std. D	2.16	1.60	2.48	1.83	1.33	1.83	1.63	2.42	1.83	1.63
ST1L0Y16N	Mean	5.50	5.00	5.00	4.67	5.00	2.67	3.50	3.00	3.33	3.00
	Std. D	1.64	1.90	1.90	1.63	1.55	1.51	1.64	1.90	1.63	1.55
ST1L+25Y12N	Mean	**6.33**	5.33	**6.00**	**5.83**	**5.33**	***1.67***	2.67	***2.00***	***2.17***	***2.67***
	Std. D	1.03	1.51	1.55	1.47	1.51	1.03	1.51	1.55	1.47	1.51
ST1L+25Y20N	Mean	5.83	**5.50**	5.83	**5.83**	**5.33**	2.00	***2.50***	***2.00***	***2.17***	***2.67***
	Std. D	1.47	1.97	1.47	1.47	1.51	1.55	1.97	1.55	1.47	1.51
Average	Mean	5.40	4.37	4.73	4.70	4.83	2.54	3.80	3.27	3.33	3.14
	Std. D	1.69	1.76	1.79	1.67	1.59	1.55	1.72	1.79	1.65	1.65

□ means the lowest comfort & highest pressure sensation. Comfort ratings from 1 (very bad) to 7 (very good). Pressure ratings from 1 (very weak) to 7 (very strong).

Table 7.28 Average comfort & pressure ratings of five seamless bras of style 1, loop densities range from a low value of -25 (ST1L-25Y20Y) to a high value of 25 (ST1L+25Y20Y) with 3D soft wires

Style	Statistic items	Comfort sensation						Pressure sensation					
		Gore	Cup	Wire	Side wing	Back wing	Strap	Gore	Cup	Wire	Side wing	Back wing	Strap
ST1L-25 Y20Y	Mean	4.67	2.67	4.67	3.67	3.33	3.83	3.33	5.67	3.00	4.50	4.67	4.17
	Std. D	2.25	1.75	2.25	2.42	1.97	0.98	2.25	1.86	2.00	2.17	1.97	0.98
ST1L-25 Y12Y	Mean	4.50	3.33	5.17	3.67	3.00	4.17	3.33	5.00	2.83	4.33	4.83	3.67
	Std. D	2.07	1.63	1.33	2.42	2.00	1.33	1.75	1.67	1.33	2.42	1.72	1.63
ST1L0Y 16Y	Mean	5.50	4.83	5.50	5.17	5.17	5.50	2.67	3.83	2.67	3.17	3.00	2.50
	Std. D	1.64	1.72	1.64	2.04	1.33	1.64	1.51	2.04	1.21	2.04	1.26	1.64
ST1L+25 Y12Y	Mean	**6.17**	5.50	**6.00**	5.50	**6.00**	**5.83**	***1.83***	2.83	***2.00***	2.50	***2.00***	2.50
	Std. D	1.17	1.38	1.55	1.64	1.55	1.47	1.17	1.72	1.55	1.64	1.55	1.64
ST1L+25 Y20Y	Mean	5.83	**5.83**	5.83	**5.83**	5.83	5.67	2.17	***2.50***	2.17	***2.00***	2.17	***2.33***
	Std. D	1.47	1.47	1.47	1.47	1.47	1.37	1.47	1.38	1.47	1.55	1.47	1.37
Average	Mean	5.33	4.43	5.43	4.77	4.67	5.00	2.67	3.97	2.53	3.30	3.33	3.03
	Std. D	1.72	1.59	1.65	2.00	1.66	1.36	1.63	1.73	1.51	1.96	1.59	1.45

□ means the lowest comfort & highest pressure sensation. Comfort ratings from 1 (very bad) to 7 (very good). Pressure ratings from 1 (very weak) to 7 (very strong).

7.4.2.3 Comparisons between Wired and Non-wired Seamless Bras

The Paired-sample T test results for style 1 (Table 7.29) reveal that only the gore region shows significant difference of pressure sensation scores in the presence and absence of 3D soft wires, at 5% significant level. Although the previous pressure tests showed that wire gave higher pressure at the "cup base", "apex" and "centre point", subjects cannot sensitively feel the differences probably because of the pressure values of these regions are relatively low.

Table 7.29 Paired-sample T test results of comfort & pressure sensation for style 1 with & without 3D wires

	With 3D soft wires vs without 3D soft wires	Mean	Std. D	Std. Error Mean	95% Confidence Interval of the Difference		t	df	Sig. (2-tailed)
					Lower	Upper			
Pair 1	Pressure sensation-Gore	0.133	0.075	0.033	0.041	0.226	4.000	4	0.016
Pair 2	Pressure sensation-Cup	0.167	0.167	0.075	-0.040	0.374	2.236	4	0.089
Pair 3	Pressure sensation-Side Wing	0.033	0.361	0.162	-0.415	0.482	0.206	4	0.847
Pair 4	Pressure sensation-Back Wing	0.000	0.391	0.175	-0.485	0.485	0.000	4	1.000
Pair 5	Pressure sensation-Strap	-0.100	0.384	0.172	-0.576	0.376	-0.583	4	0.591
Pair 6	Comfort sensation-Gore	-0.067	0.091	0.041	-0.180	0.047	-1.633	4	0.178
Pair 7	Comfort sensation-Cup	0.067	0.224	0.100	-0.211	0.344	0.667	4	0.541
Pair 8	Comfort sensation-Side Wing	0.033	0.431	0.193	-0.502	0.569	0.173	4	0.871
Pair 9	Comfort sensation-Back Wing	-0.033	0.492	0.220	-0.644	0.577	-0.152	4	0.887
Pair 10	Comfort sensation-Strap	0.167	0.425	0.190	-0.361	0.694	0.877	4	0.430

Table 7.30 Paired-sample T test results of comfort & pressure sensation for style 2 with & without 3D wires

	With 3D soft wires vs without 3D soft wires	Mean	Std. D	Std. Error Mean	95% Confidence Interval of the Difference		t	df	Sig. (2-tailed)
					Lower	Upper			
Pair 1	Pressure sensation-Gore	0.067	0.190	0.085	-0.169	0.303	0.784	4	0.477
Pair 2	Pressure sensation-Cup	-0.267	0.091	0.041	-0.380	-0.153	-6.532	4	0.003
Pair 3	Pressure sensation-Side Wing	0.300	0.247	0.111	-0.007	0.607	2.714	4	0.053
Pair 4	Pressure sensation-Back Wing	-0.200	0.139	0.062	-0.373	-0.027	-3.207	4	0.033
Pair 5	Comfort sensation-Gore	0.167	0.204	0.091	-0.087	0.420	1.826	4	0.142
Pair 6	Comfort sensation-Cup	-0.233	0.149	0.067	-0.418	-0.048	-3.500	4	0.025
Pair 7	Comfort sensation-Side Wing	0.533	0.740	0.331	-0.385	1.452	1.612	4	0.182
Pair 8	Comfort sensation-Back Wing	-0.300	0.447	0.200	-0.855	0.255	-1.500	4	0.208

The Paired-sample T test for style 2, the strapless version (see Table 7.30), shows significant pressure differences in the areas of the cup and back wing, and significant comfort difference in the cup region when using 3D soft wires.

The Paired-sample T test results for style 3 (see Table 7.31) show that all of p-values are greater than 0.05, so there is no significant difference of comfort & pressure sensation scores between wired and non-wired bras at 5% significant level.

Table 7.31 Paired-sample T test results of comfort & pressure sensation for style 3 with & without 3D wires

	With 3D soft wires vs without 3D soft wires	Mean	Std. D	Std. Error Mean	95% Confidence Interval of the Difference		t	df	Sig. (2-tailed)
					Lower	Upper			
Pair 1	Pressure sensation-Gore	-0.233	0.450	0.201	-0.792	0.326	-1.159	4	0.311
Pair 2	Pressure sensation-Cup	0.100	0.279	0.125	-0.246	0.446	0.802	4	0.468
Pair 3	Pressure sensation-Side Wing	0.000	0.118	0.053	-0.146	0.146	0.000	4	1.000
Pair 4	Pressure sensation-Back Wing	-0.100	0.303	0.135	-0.476	0.276	-0.739	4	0.501
Pair 5	Pressure sensation-Strap	-0.133	0.183	0.082	-0.360	0.093	-1.633	4	0.178
Pair 6	Comfort sensation-Gore	0.200	0.274	0.122	-0.140	0.540	1.633	4	0.178
Pair 7	Comfort sensation-Cup	-0.200	0.380	0.170	-0.672	0.272	-1.177	4	0.305
Pair 8	Comfort sensation-Side Wing	0.067	0.190	0.085	-0.169	0.303	0.784	4	0.477
Pair 9	Comfort sensation-Back Wing	-0.033	0.139	0.062	-0.206	0.140	-0.535	4	0.621
Pair 10	Comfort sensation-Strap	0.033	0.139	0.062	-0.140	0.206	0.535	4	0.621

7.4.2.4 Comparisons among 3 New Seamless Styles

To investigate whether there are any differences among 3 newly developed seamless bra styles for comfort & pressure sensation assessment, One-way ANOVA was conducted with & without 3D wires respectively at 5% level of significance. The results (see Table 7.32 & 7.33) reveal that both with and without the underwire, all of p-values are greater than 0.05. There is no significant difference among three styles.

Table 7.32 One-way ANOVA of comfort & pressure values among 3 new seamless styles (with 3D wires)

		Sum of Squares	df	Mean Square	F	Sig.
Pressure sensation-Gore	Between Groups	1.081	2	0.541	1.574	0.247
	Within Groups	4.122	12	0.344		
	Total	5.204	14			
Comfort Sensation-Gore	Between Groups	0.737	2	0.369	0.750	0.493
	Within Groups	5.900	12	0.492		
	Total	6.637	14			
Pressure sensation-Cup	Between Groups	0.633	2	0.317	0.164	0.851
	Within Groups	23.189	12	1.932		
	Total	23.822	14			
Comfort Sensation-Cup	Between Groups	0.281	2	0.141	0.079	0.925
	Within Groups	21.489	12	1.791		
	Total	21.770	14			
Pressure sensation-Side Wing	Between Groups	0.059	2	0.030	0.024	0.976
	Within Groups	14.822	12	1.235		
	Total	14.881	14			
Comfort Sensation-Side Wing	Between Groups	0.133	2	0.067	0.060	0.942
	Within Groups	13.311	12	1.109		
	Total	13.444	14			
Pressure sensation-Back Wing	Between Groups	0.026	2	0.013	0.010	0.990
	Within Groups	14.833	12	1.236		
	Total	14.859	14			
Comfort Sensation-Back Wing	Between Groups	0.226	2	0.113	0.081	0.923
	Within Groups	16.744	12	1.395		
	Total	16.970	14			

Table 7.33 One-way ANOVA of comfort & pressure values among 3 new seamless styles (without 3D wires)

		Sum of Squares	df	Mean Square	F	Sig.
Pressure sensation-Gore	Between Groups	0.181	2	0.091	0.196	0.825
	Within Groups	5.567	12	0.464		
	Total	5.748	14			
Comfort Sensation-Gore	Between Groups	0.178	2	0.089	0.183	0.835
	Within Groups	5.833	12	0.486		
	Total	6.011	14			
Pressure sensation-Cup	Between Groups	1.270	2	0.635	0.346	0.714
	Within Groups	22.000	12	1.833		
	Total	23.270	14			
Comfort Sensation-Cup	Between Groups	0.900	2	0.450	0.297	0.748
	Within Groups	18.156	12	1.513		
	Total	19.056	14			

Table 7.33 (continued)

Pressure sensation-Side Wing	Between Groups	0.478	2	0.239	0.183	0.835
	Within Groups	15.678	12	1.306		
	Total	16.156	14			
Comfort Sensation-Side Wing	Between Groups	1.078	2	0.539	0.427	0.662
	Within Groups	15.144	12	1.262		
	Total	16.222	14			
Pressure sensation-Back Wing	Between Groups	1.115	2	0.557	0.516	0.610
	Within Groups	12.967	12	1.081		
	Total	14.081	14			
Comfort Sensation-Back Wing	Between Groups	0.959	2	0.480	0.478	0.631
	Within Groups	12.033	12	1.003		
	Total	12.993	14			

7.4.2.5 Overall Comfort Sensation

For the overall comfort & pressure sensation (refer to Appendix IV), subjects reported (see Table 7.34) that the fabric handle and comfort sensation of the new seamless knitted bras were overall better than the conventional bras. The average score of Q1 (refer to Appendix IV) is 6.50, closely to the highest scale of 7. They also thought their breast shape appeared to be natural when wearing the new seamless knitted bras. The average score of Q2 is 6.85. Moreover, the subjects felt that they obtained better support from the bras using the 3D soft supporting wires; the average score of Q3 is 5.55.

Table 7.34 Descriptive statistics results of overall comfort & pressure sensation

	Mean	Std. Deviation
Q1	6.50	0.84
Q2	6.83	0.41
Q3	5.33	1.03

7.4.2.6 Summary of Subjective Comfort Testing

Based on the above discussion, the findings related to comfort & pressure sensation evaluation results can be summarized as bellow:

1) The commercial cut & sewn bras have lower comfort sensation scores and higher pressure sensation scores, compared with the seamless bras.
2) Among the 15 newly developed seamless knitted bras, the testing samples which have a relatively larger value of loop density of +25, show better comfort sensation scores and lower pressure sensation scores.
3) After adding 3D soft wires to the newly developed seamless bras, the comfort & pressure sensation scores show significant differences at the gore for style 1 and at the cup and back wing for style 2.
4) There is no significant difference among three styles with & without 3D soft wires respectively.

7.4.3 Breast Shape Evaluation

7.4.3.1 Breast Cross-sectional Shape

Using the software RapidForm 2004 and 3D Measure Workshop, the cross-sectional and vertical-sectional shapes of each subject's nude breasts and the breasts wearing the test bra were drawn for comparison. The typical examples are shown in sections 7.4.3.1 to 7.4.3.3. The comparisons of bra wearing effects of all test samples and all subjects will be discussed in the sections 7.4.3.4, 7.4.3.5 and 7.4.3.6.

Figure 7.21 shows the breast cross-sectional shapes of subject 6 in nude, and in wearing the three commercial bras. Since the seamless knitted bra "Jockey" is a black bra which could not be captured, so it is not included in the shape analysis. As shown in the figures, "Benetton" tends to show a natural and smooth curve, but a slightly compressed shape, while the two conventional bras, especially "Aimer" bra, creates a closer, rounder and fuller breast shape than the other bras.

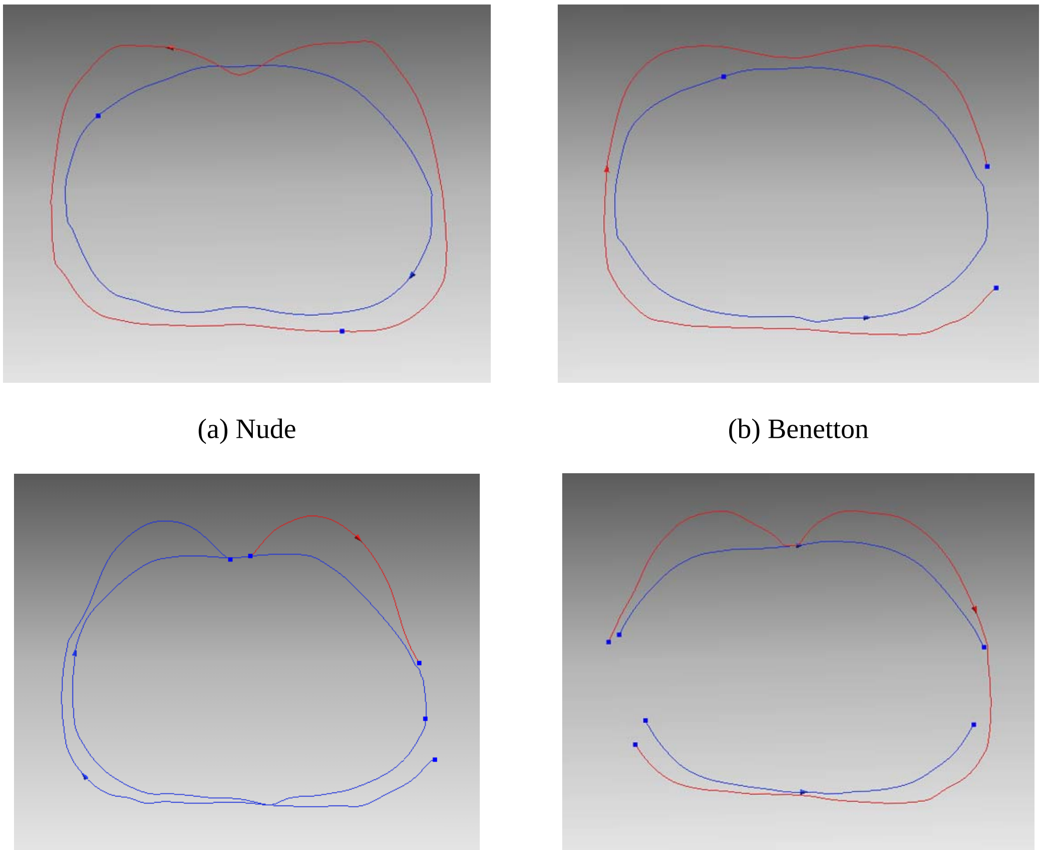

(a) Nude (b) Benetton

(c) Aimer (d) Wacoal

Figure 7.21 Comparisons of the breast cross-sectional shapes of subject 6 in naked and wearing three commercial bras

Figure 7.22 presents the breast cross-sectional shapes of subject 4 in nude, and in wearing the five samples of style 1 seamless knitted test bras with 3D wires inserted. It can be seen that the two test samples (b) and (c) which have a low level of loop density -25, show relatively compressed breast shapes when compared with the nude shape.

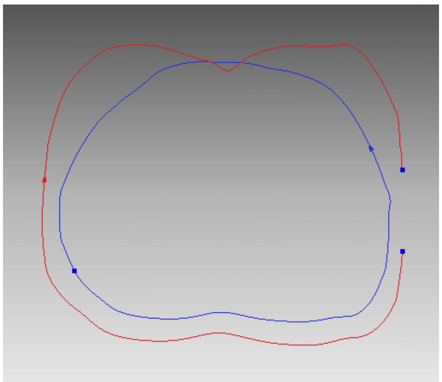

(a) Nude

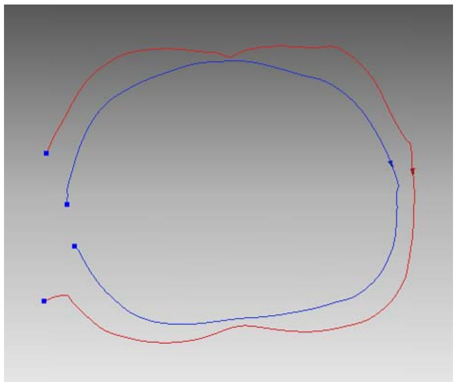

(b) S1L-25Y20Y

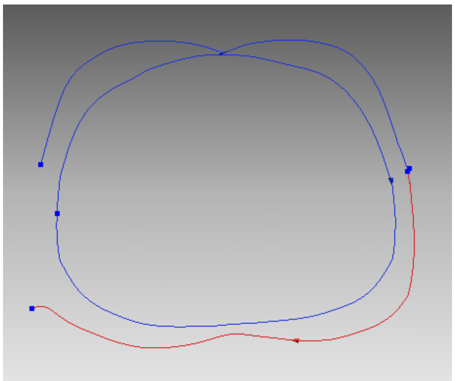

(c) S1L-25Y12Y

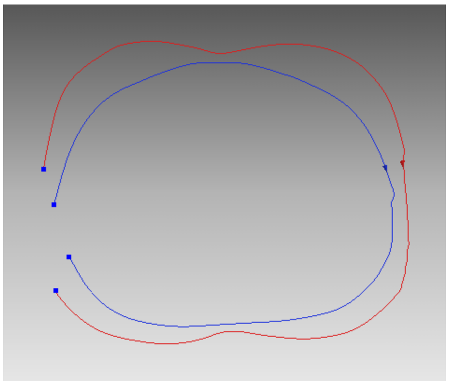

(d) S1L0Y16Y

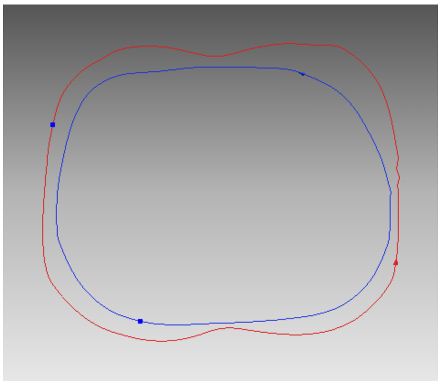

(e) S1L+25Y12Y

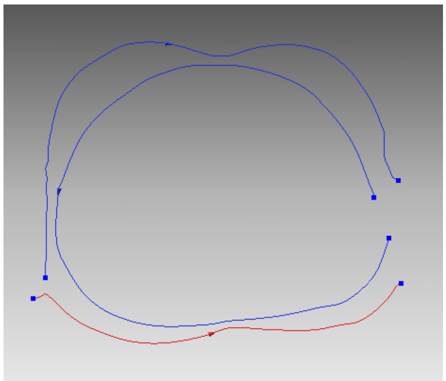

(f) S1L+25Y20Y

Figure 7.22 Comparisons of the breast cross-sectional shapes of subject 4 in naked and wearing five testing seamless knitted bras of style 1 with 3D wires

7.4.3.2 Breast Front View

To explore whether the 3D soft supporting wire provides better support to the breasts for the newly developed seamless knitted bras, vertical-section images were extracted from the 3D body scanning data. Figure 7.23 shows the front views of subject 1 wearing the bra “S2L+25Y12” with and without 3D wires. It can be seen that the breasts have been brought upward and closer by using 3D wires (Figure 7.23b).

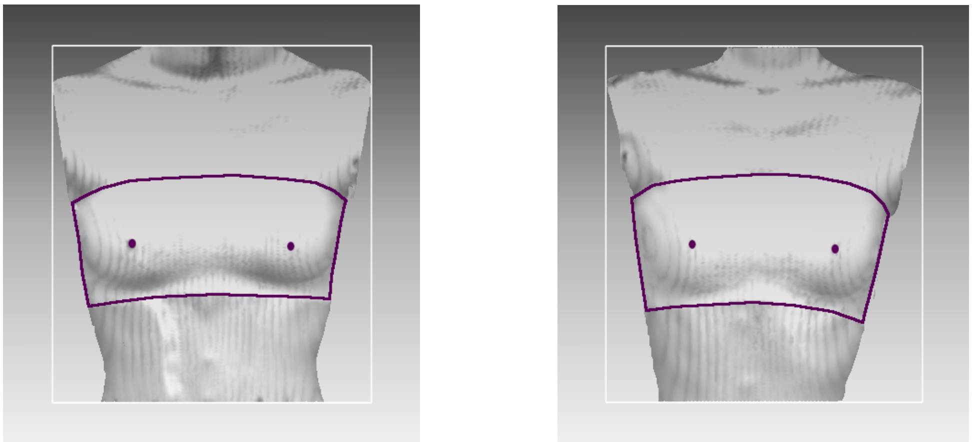

(a) Without wires (b) With wires

Figure 7.23 Body shapes of subject 1 during wearing bra S2L+25Y12

7.4.3.3 Breast Side Profile

The comparison results of breast side profile can also help to confirm the function of the 3D wire. Figure 7.24 shows overlapping images of vertical profiles of subject 1 in the nude compared to seamless bra “S2L+25Y12” (with & without 3D soft underwires) (Figure 7.24a) and the seamless bra with underwires compared to the commercial seamless knitted bra “Benetton” (Figure 7.24b). From Figure 7.24a, it can be seen that the side profile of the subject wearing bra “S2L+25Y12” with 3D wires has a higher bust point than the profile of the subject wearing the bra "S2L+25Y12" without 3D wires and in the nude. As shown in (b), for the subject wearing the bra "S2L+25Y12" with 3D wires, the vertical profile of the breast has a fuller shape than the profile of the "Benetton".

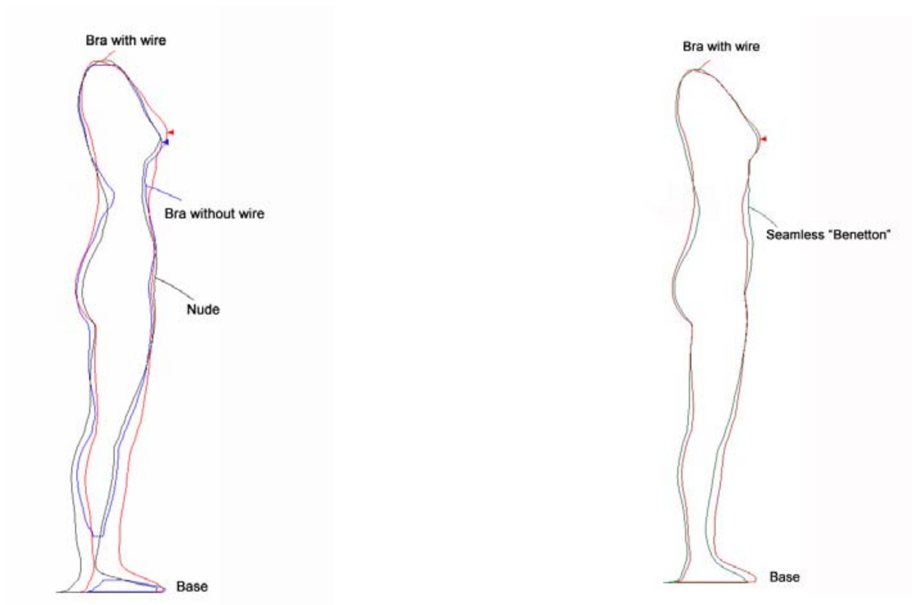

(a) Nude vs wired & non-wired seamless bra (b) Wired seamless bra vs "Benetton"

Figure 7.24 Comparisons of vertical profiles of subject 1 in nude, new seamless bras (with & without 3D soft underwires of "S2L+25Y12") and seamless knitted bra "Benetton"

7.4.3.4 Bra Push-up & Push-in Effect

To further investigate the breast shape changes exhibited by the nineteen test bra samples, five breast measurements including "bust height", "bust point width", "length from front neck point to right bust point (FNP~RBP)", "length from front neck point to left bust point (FNP~LBP)" and "bust girth" were measured from the 3D body scanning data. From these data, it is possible to determine if a bra lifts up the breasts well and gives a fuller breast shape i.e. "bust height" and "bust girth" are greater than the nude measurements, and if the bra brings the breasts closer together i.e. the “bust point width”, length from “FNP~RBP” and length from “FNP~LBP” become shorter.

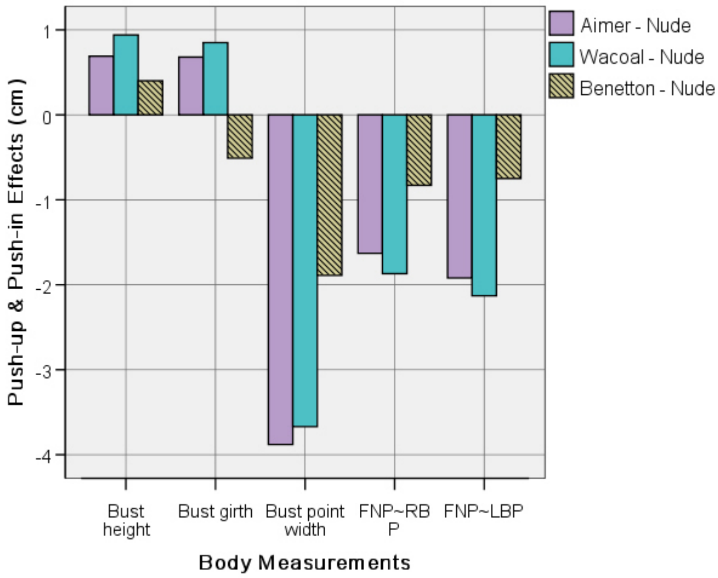

Figure 7.25 Comparisons of the push-up & push-in effects of 3 commercial bras

Table 7.35 Comparison results of the push-up & push-in effects (n = 6) of 3 commercial bras

Body measurements	Statistic items	Mean of nude Size (n =6)	Aimer-Nude	Wacoal-Nude	Benetton-Nude
Bust height	Mean	117.79	0.69	0.94	0.40
	Std. Deviation	4.99	1.30	0.90	1.40
Bust girth	Mean	88.01	0.68	0.85	-0.51
	Std. Deviation	4.58	3.12	1.52	2.26
Bust point width	Mean	20.09	-3.88	-3.67	-1.89
	Std. Deviation	0.94	1.64	1.32	1.24
FNP~RBP	Mean	20.14	-1.63	-1.87	-0.83
	Std. Deviation	1.07	0.87	0.42	0.73
FNP~LBP	Mean	20.30	-1.92	-2.13	-0.75
	Std. Deviation	1.30	1.30	1.04	0.79

Figure 7.25 and Table 7.35 show the comparison results of both the push-up & push-in effects of the 3 commercial bras “Aimer”, “Wacoal” and “Benetton”. Compared with the nude body, the two conventional cut & sewn bras have larger mean measurements

of “bust height” and “bust girth”, and smaller mean measurements of “bust point width”, length from “FNP~RBP” and length from “FNP~LBP”, that demonstrate significant push-up & push-in effects. The commercial seamless bra “Benetton” shows a reduced bust girth that indicates the bra compresses the breasts.

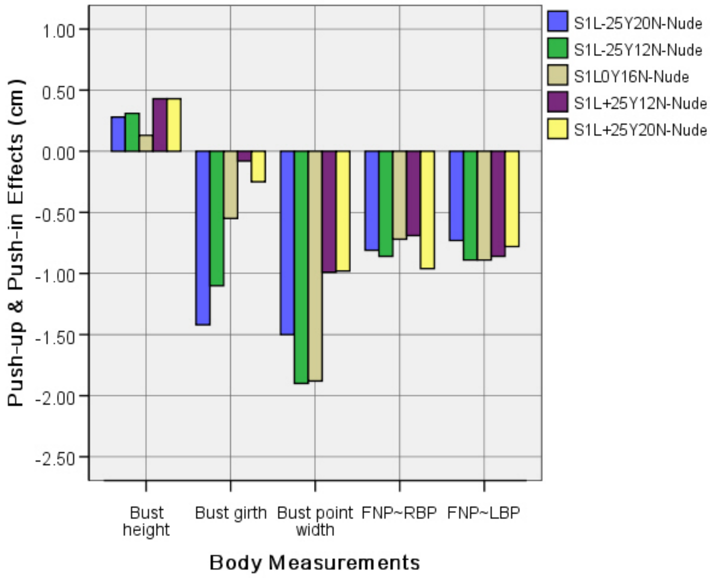

Figure 7.26 Comparisons of the push-up & push-in effects of five style 1 bras (without 3D wires)

Table 7.36 Comparison results of the push-up & push-in effects (n = 6) of five style 1 bras (without 3D wires)

Body measurements	Statistic items	Mean of nude size (n = 6)	S1L-25Y20N - Nude	S1L-25Y12N - Nude	S1L0Y16N - Nude	S1L+25Y12N - Nude	S1L+25Y20N - Nude
Bust height	Mean	117.79	0.28	0.31	0.13	0.43	0.43
	Std. D	4.99	1.29	1.82	1.42	1.22	0.83
Bust girth	Mean	88.01	-1.42	-1.11	-0.55	-0.08	-0.25
	Std. D	4.58	1.78	2.15	1.81	2.57	1.57
Bust point width	Mean	20.09	-1.50	-1.90	-1.88	-0.99	-0.98
	Std. D	0.94	1.22	1.45	0.93	2.19	0.79
FNP~RBP	Mean	20.14	-0.81	-0.86	-0.72	-0.69	-0.96
	Std. D	1.07	0.61	1.11	1.00	0.73	0.68
FNP~LBP	Mean	20.30	-0.73	-0.89	-0.89	-0.86	-0.78
	Std. D	1.30	0.20	0.65	0.70	1.09	0.53

Figure 7.26 and Table 7.36 show the push-up & push-in results of the newly developed style 1 bras without 3D soft wires. Figure 7.27 and Table 7.37 show the results with 3D

wires. When using 3D wires, the 5 test bras show relatively larger push-up & push-in results. However, all the newly developed bras reduced the bust girth, except the bra “S1L+25Y20” with wire. This clearly indicates that the 3D wire can definitely improve the breast shape by bringing the breasts closer and that the seamless knit bras can avoid compressing the breasts if higher level of loop density (+25) is used to knit the bra cups.

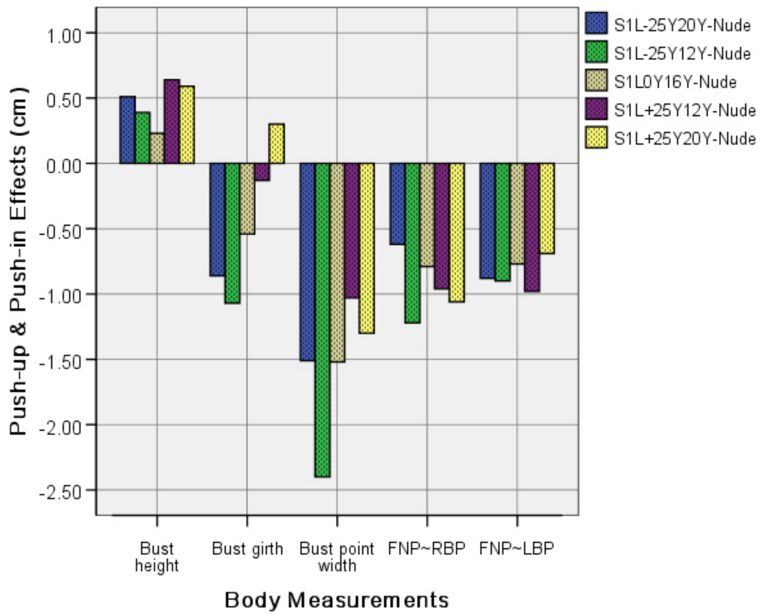

Figure 7.27 Comparisons of the push-up & push-in effects of five style 1 bras (with 3D wires)

Table 7.37 Comparison results of the push-up & push-in effects (n = 6) of five style 1 bras (with 3D wires)

Body measurements	Statistic items	Mean of nude size (n = 6)	S1L-25Y20Y - Nude	S1L-25Y12Y - Nude	S1L0Y16Y - Nude	S1L+25Y12Y - Nude	S1L+25Y20N - Nude
Bust height	Mean	117.79	0.51	0.39	0.23	0.64	0.59
	Std. D	4.99	1.06	2.07	1.38	1.42	1.00
Bust girth	Mean	88.01	-0.86	-1.07	-0.54	-0.13	0.30
	Std. D	4.58	1.40	1.83	1.36	2.08	1.86
Bust point width	Mean	20.09	-1.51	-2.40	-1.52	-1.03	-1.30
	Std. D	0.94	0.97	1.44	0.87	1.24	1.38
FNP~RBP	Mean	20.14	-0.62	-1.22	-0.79	-0.96	-1.06
	Std. D	1.07	0.52	1.05	0.99	0.70	1.08
FNP~LBP	Mean	20.30	-0.88	-0.90	-0.77	-0.98	-0.69
	Std. D	1.30	0.47	1.21	0.49	1.07	0.44

7.4.3.5 Comparisons among 3 Styles of Seamless Bras

To compare the difference of push-up & push-in effects among 3 new seamless bras, the average value of each style was calculated in both wired and non-wired situations as shown in Figure 7.28 to 7.29 and Table 7.38. It can be found that the bra push-up & push-in effects with 3D wires show better effects i.e. larger "bust height" and "bust girth", smaller "bust point width", length from "FNP~RBP" and length from "FNP~LBP" than those without 3D wires. Among three styles, style 1 shows the best push-up & push-in effects. The results of One-way ANOVA at 5% level of significance (see Appendix VIII) indicate that after using 3D wires, 3 styles show better push-up and push-in effects in five breast measurements.

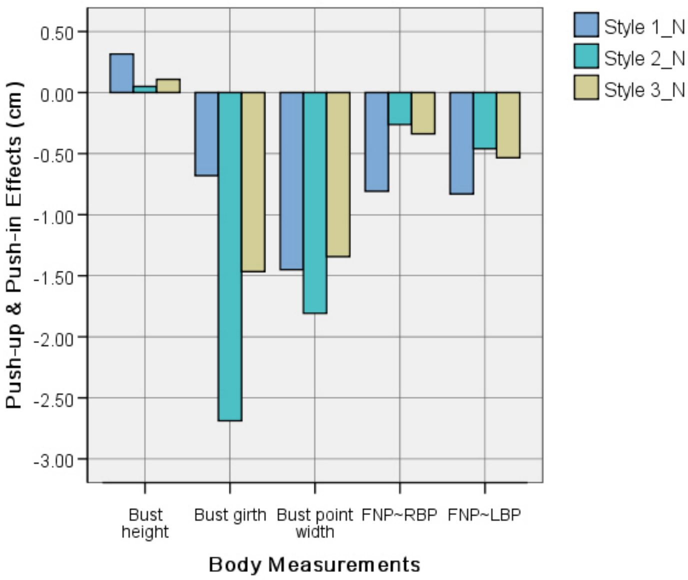

Figure 7.28 Comparisons of the average push-up & push-in effects (n = 30) of 3 newly developed seamless bras (without 3D wires)

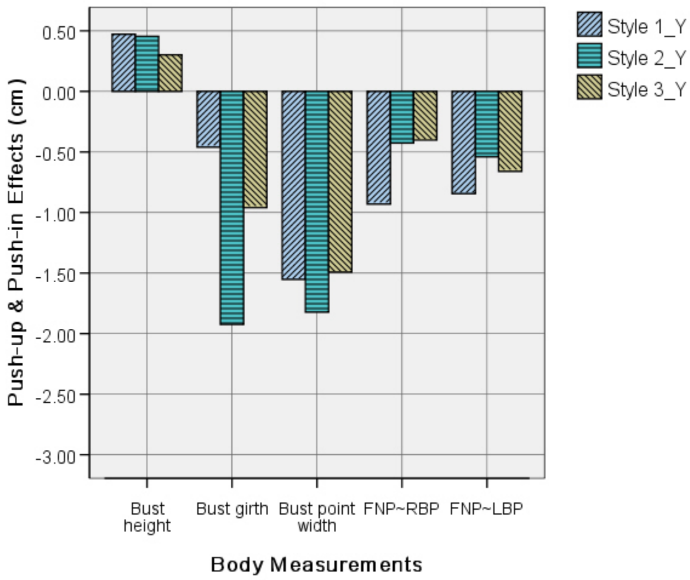

Figure 7.29 Comparisons of the average push-up & push-in effects (n = 30) of 3 newly developed seamless bras (with 3D wires)

Table 7.38 Average comparison results of the push-up & push-in effects (n = 30) of 3 newly developed seamless bras (with & without 3D wires)

Body measurements	Statistic items (n = 30)	Without 3D soft wires			With 3D soft wires		
		Style 1	Style 2	Style 3	Style 1	Style 2	Style 3
Bust height	Mean	0.32	0.05	0.11	0.47	0.45	0.30
	Std. Deviation	0.12	0.15	0.06	0.16	0.18	0.11
Bust girth	Mean	-0.68	-2.69	-1.47	-0.46	-1.92	-0.96
	Std. Deviation	0.57	1.16	0.21	0.55	1.45	0.75
Bust point width	Mean	-1.45	-1.81	-1.34	-1.55	-1.82	-1.49
	Std. Deviation	0.45	0.29	0.36	0.51	0.33	0.62
FNP~RBP	Mean	-0.81	-0.26	-0.34	-0.93	-0.43	-0.40
	Std. Deviation	0.11	0.11	0.63	0.23	0.17	0.29
FNP~LBP	Mean	-0.83	-0.46	-0.53	-0.84	-0.54	-0.66
	Std. Deviation	0.07	0.18	0.11	0.11	0.20	0.27

7.4.3.6 Comparisons Based on Key Knitting Parameters

Further to compare the push-up & push-in effects influenced by various knitting parameter combinations, the corresponding data of three design styles were averaged in both wired and non-wired situations. As shown in Figure 7.30 to 7.31 and Table 7.39, the bras knitted with higher level values of loop density and elastic yarn tension show better push-up & push-in effects.

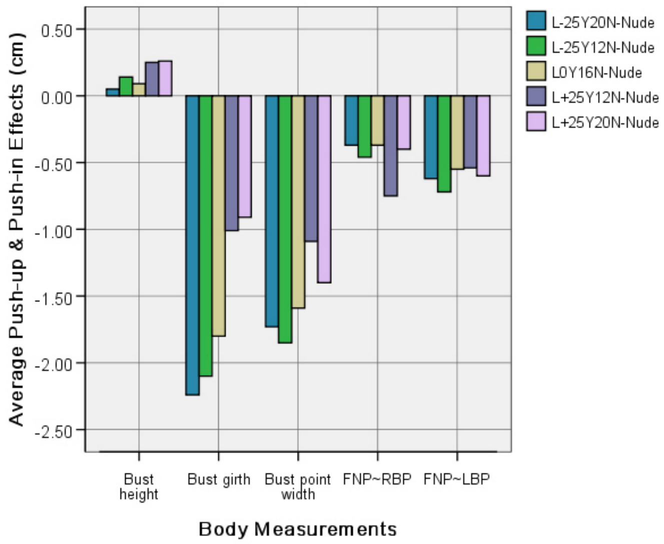

Figure 7.30 Comparison of the average push-up & push-in effects (n = 18) of 5 knitting parameter combinations (without 3D wires)

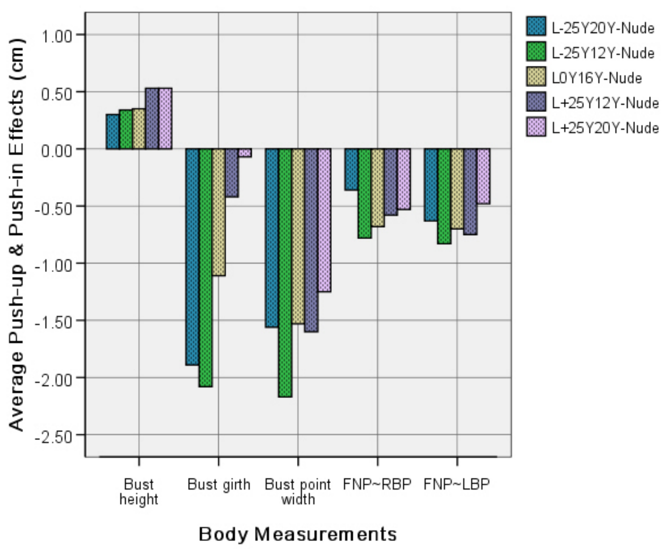

Figure 7.31 Comparison of the average push-up & push-in effects (n = 18) of 5 knitting parameter combinations (with 3D wires)

Table 7.39 Average comparison results of the push-up & push-in effects (n = 18) of 5 knitting parameter combinations (with & without 3D wires)

Body measurements	Statistic items (n = 18)	Knitting parameter combinations (without 3D soft wires)					Knitting parameter combinations (with 3D soft wires)				
		1	2	3	4	5	1	2	3	4	5
Bust height	Mean	0.05	0.14	0.09	0.25	0.26	0.30	0.34	0.35	0.53	0.53
	Std. Deviation	0.25	0.15	0.03	0.15	0.15	0.19	0.12	0.18	0.16	0.06
Bust girth	Mean	-2.24	-2.10	-1.80	-1.01	-0.91	-1.89	-2.08	-1.11	-0.42	-0.07
	Std. Deviation	1.15	1.29	1.50	0.81	0.58	1.25	1.11	1.02	0.34	0.38
Bust point width	Mean	-1.73	-1.85	-1.59	-1.09	-1.40	-1.56	-2.17	-1.53	-1.60	-1.25
	Std. Deviation	0.23	0.15	0.29	0.29	0.61	0.12	0.22	0.23	0.49	0.80
FNP~RBP	Mean	-0.37	-0.46	-0.37	-0.75	-0.40	-0.36	-0.78	-0.68	-0.58	-0.53
	Std. Deviation	0.40	0.35	0.31	0.66	0.57	0.30	0.41	0.13	0.36	0.47
FNP~LBP	Mean	-0.62	-0.72	-0.55	-0.54	-0.60	-0.63	-0.83	-0.70	-0.75	-0.48
	Std. Deviation	0.12	0.16	0.34	0.28	0.16	0.32	0.10	0.14	0.29	0.22

Knitting parameter combination: 1 means L-25Y20; 2 means L-25Y12; 3 means L0Y16; 4 means L+25Y12; 5 means L+25Y20.

Based on above discussion, it can be found that for each style, the test bra which has larger values of loop density +25 & elastic yarn tension 20 and using 3D soft wires, show a larger size or nearly same size of “bust girth” as the breast nude size. The design with 3D soft wire, higher level of loop density & elastic yarn tension is the best choice of the seamless knitted bras to lift up the breasts and give a natural shape while not compressing the breasts.

7.4.4 Prediction of Seamless Knitted Bra Pressure Values

There is very limited information in the literature on the relationships between bra pressure values and comfort sensations for any bra styles, and particularly for seamless knitted bras. Hatakeyama and Aoki (1990) explored the bra pressure and comfort sensations using five conventional underwired bras and eight subjects. They found that the pressure range of the most comfortable bra was 80 ~ 160 g/cm^2 (about 3.9 ~ 7.8

Kpa). Makabe et al. (1991) reported in a study of the pressure values of two three-quarter cup bras and two full cup bras on eight subjects, the pressure of the most comfortable bra in their experiment was 24mmHg (3.2 Kpa) at the point where the strap and the shoulder line cross, and 11~16mmHg (1.5~2.1Kpa) at the point of the underbust line & lateral top area of the cup.

As discussed in the section of 7.4.1, the pressure at all measuring points for the seamless bras developed for this study were relatively low values under 4Kpa except the points "cup base point" (in all three styles), "side bottomband" (in all three styles) and "shoulder point" (in style 1), and most of them were under 1.5Kpa. The results of comfort & pressure sensation evaluation also revealed that the test bra samples which have relatively larger value of loop density +25, show relative better comfort sensation scores 6 or above (the highest score is 7). The experimental results indicate that the seamless knitted bras are more comfortable due to the low pressure values.

It would be interesting to predict the pressure value in various positions of seamless knitted bras based on the key knitting parameters. As underbust girth and the breast "depth width ratio" have been proposed to establish our new bra sizing system, the two corresponding measuring points "apex" (response 1) and "side bottomband" (response 2) were selected as the pressure points to be investigated first using MANOVA (multiple analysis-of-variance).

The mean of these two pressure measuring points are the two responses influenced by "knitting factors". Although the p-value of three-way interactions of "Style * Knitting factors * Subjects" in the Tables 7.40 & 7.41 were smaller than 0.05, the main effects of "Style" and "Subjects" did not reject the null hypothesis of no difference between means. Hence, the three-way interactions can be ignored. According to the MANOVA results, "knitting factors" is a significant factor that influences the two responses. The experiment results in Chapter 5 has determined that loop density and elastic yarn tension are the major factors affecting the underband tension of a seamless knitted bra, and loop density is the strongest factor affecting the cup strain of seamless knitted bras. The new seamless knitted bra samples of each style were developed using a 2^2 full factorial design by varying the key knitting parameters (loop density & elastic yarn tension). Therefore, a regression model was developed for each response.

Table 7.40 Tests of effects for "pressure at the apex"

Source		Sum of squares	df	Mean square	F	Sig.
Intercept	Hypothesis	245.14	1	245.14	34.04	0.00
	Error	36.01	5	7.20		
Style	Hypothesis	0.56	2	0.28	0.50	0.62
	Error	5.56	10	0.56		
Knitting factors	Hypothesis	6.65	4	1.66	4.62	0.01
	Error	7.21	20	0.36		
Subjects	Hypothesis	36.03	5	7.21	10.85	0.05
	Error	7.62	11	0.66		
Style * Knitting factors	Hypothesis	2.85	8	0.36	1.43	0.21
	Error	9.95	40	0.25		
Style * Subjects	Hypothesis	5.56	10	0.56	2.31	0.06
	Error	9.67	40	0.24		
Knitting factors * Subjects	Hypothesis	7.24	20	0.36	1.45	0.16
	Error	9.99	40	0.25		
Style * Knitting factors * Subjects	Hypothesis	10.00	40	0.25	14.61	0.00
	Error	3.90	228	0.02		

Table 7.41 Tests of effects for “pressure at the side bottomband”

Source		Sum of squares	df	Mean square	F	Sig.
Intercept	Hypothesis	3769.72	1	3769.72	68.55	0.00
	Error	274.96	5	54.99		
Style	Hypothesis	30.31	2	15.15	2.90	0.10
	Error	52.31	10	5.23		
Knitting factors	Hypothesis	119.34	4	29.84	3.03	0.04
	Error	197.25	20	9.86		
Subjects	Hypothesis	275.11	5	55.02	11.19	0.06
	Error	12.26	2	4.92		
Style * Knitting factors	Hypothesis	41.13	8	5.14	0.50	0.85
	Error	407.87	40	10.19		
Style * Subjects	Hypothesis	52.35	10	5.23	0.53	0.86
	Error	394.36	40	9.84		
Knitting factors * Subjects	Hypothesis	198.26	20	9.91	0.97	0.52
	Error	409.82	40	10.25		
Style * Knitting factors * Subjects	Hypothesis	410.20	40	10.25	52.27	0.00
	Error	44.73	228	0.20		

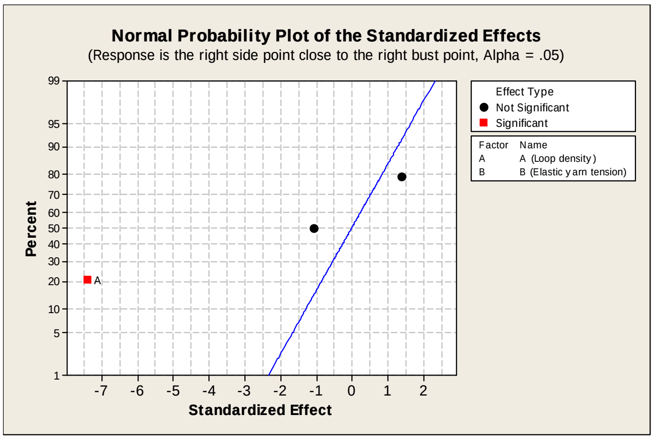

(a) Pressure at the apex

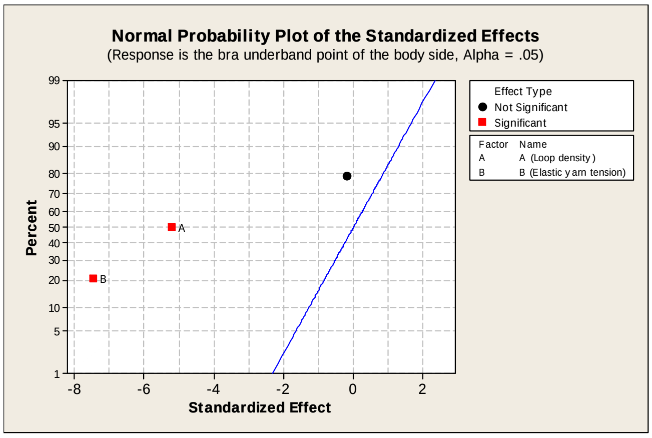

(b) Pressure at the side bottomband

Figure 7.32 Normal probability plots of the standardized effects of two pressure measuring responses

The screening designs of the two responses (see Figure 7.32) revealed that factor A (loop density) was the strongest factor affecting response 1 “pressure at the apex”, and factors A & B (elastic yarn tension) were the major factors affecting the response 2 "pressure at the side bottomband". Then a regression model was fitted for each response using only these 2 significant factors.

The factorial fit results of response 1 (see Table 7.42) reveal that all terms have p-value less than 0.05, and the adjusted coefficient of multiple determination (adjusted R^2) is 78.42%. The p-value of "curvature" (0.114) indicates that there is no evidence of quadratic curvature for response 1.

The factorial fit results of response 2 (see Table 7.43) also show that all terms have p-value less than 0.05, and the adjusted coefficient of multiple determination (adjusted R^2) is 86.2%. The p-value of curvature (0.907) also reveals that there is no evidence of quadratic curvature for response 2.

According to the factorial fit (Tables 7.42 to 7.43), the regression equations for two pressure value responses can be written with coded variables as follows:

$$y_1 = 0.94 - 0.105x_1 \qquad (7.1)$$

$$y_2 = 3.443 - 0.391x_1 - 0.559x_2 \qquad (7.2)$$

where y_1 is "pressure at the apex", y_2 is "pressure at the side bottomband", x_1 is the coded loop density, x_2 is the coded elastic yarn tension. The variables x_1 and x_2 are defined on a coded scale from -1 to $+1$ (the low and high levels of factor A & B described in 7.2.2). For each factor, the relationship between the natural variable and the coded variable can be given in equation 7.3 (Montgomery, 2001):

$$\text{Coded variable} = \frac{\text{Natural variable} - {(\text{High level} + \text{Lower level})}/{2}}{{(\text{High level} - \text{Lower level})}/{2}} \tag{7.3}$$

Table 7.42 Factorial fit: pressure at the apex versus A (loop density)

Estimated effects and coefficients for the pressure at the apex (coded units)					
Term	Effect	Coef	SE Coef	t	P
Constant		0.9400	0.01485	63.29	0.000
A (loop density)	-0.2100	-0.1050	0.01485	-7.07	0.000
Ct Pt		0.0567	0.03321	1.71	0.114
S = 0.0514512 R-Sq = 81.51% R-Sq (adj) = 78.42%					

Analysis of variance for the pressure at the apex (coded units)						
Source	DF	Seq SS	Adj SS	Adj MS	F	P
Main effects	1	0.132300	0.132300	0.132300	49.98	0.000
Curvature	1	0.007707	0.007707	0.007707	2.91	0.114
Residual error	12	0.031767	0.031767	0.002647		
Pure error	12	0.031767	0.031767	0.002647		
Total	14	0.171773				

(* Where "Coef" is coefficients, "SE Coef" is standard error of coefficients, "t" is t-value, "P" is p-value, "S" is standard deviation, "R-Sq" is R^2, "R-Sq (adj)" is adjusted R^2, "DF" is the degree of freedom, "Seq SS" is sequential sum of squares, "Adj SS" is adjusted sum of squares, "Adj MS" is adjusted mean squares and "F" is F-value.)

Table 7.43 Factorial fit: pressure at the side bottomband versus A (loop density), B (elastic yarn tension)

Estimated effects and coefficients for the pressure at the side bottomband (coded units)					
Term	Effect	Coef	SE Coef	t	P
Constant		3.4425	0.07173	48.00	0.000
A (loop density)	-0.7817	-0.3908	0.07173	-5.45	0.000
B (elastic yarn tension)	-1.1183	-0.5592	0.07173	-7.80	0.000
Ct Pt		-0.0192	0.16038	-0.12	0.907
S = 0.248463 R-Sq = 89.16% R-Sq (adj) = 86.20%					

Analysis of variance for the pressure at the side bottomband (coded units)						
Source	DF	Seq SS	Adj SS	Adj MS	F	P
Main effects	2	5.58502	5.58502	2.79251	45.23	0.000
Curvature	1	0.00088	0.00088	0.00088	0.01	0.907
Residual error	11	0.67908	0.67908	0.06173	11	0.67908
Lack of Fit	1	0.00301	0.00301	0.00301	0.04	0.837
Pure error	10	0.67607	0.67607	0.06761		
Total	14	6.26497				

To check the adequacy of the models, the residuals of the two models were also examined for three basic assumptions: independence, constant variance and normality. Figure 7.33 to 7.34 show the normal probability plot of residuals of the two responses. The normality tests of residuals indicate that the p-value for response 1 is 0.326, response 2 is 0.095, all of them are close to or greater than 0.10, so the normality assumptions for two responses can be accepted. The residual plots (omitted here) also reveal the results of two responses are definitely acceptable for the two other assumptions.

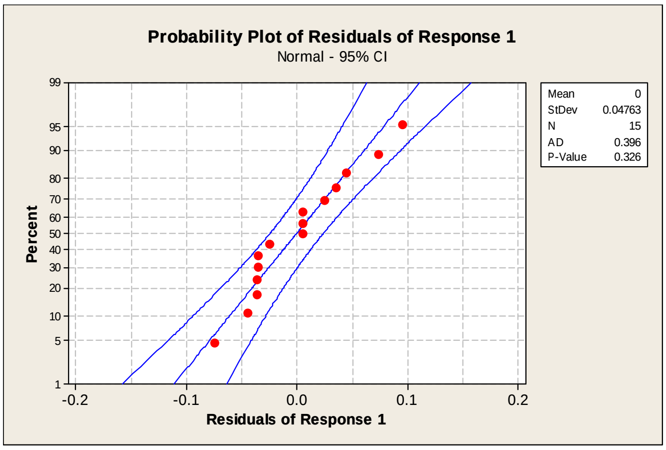

Figure 7.33 The normal probability plot of residuals of response 1 (pressure at the apex)

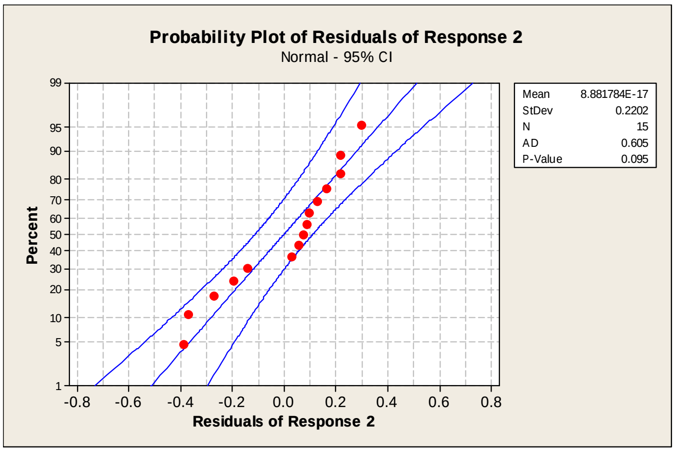

Figure 7.34 The normal probability plot of residuals of response 2 (pressure at the side bottomband)

7.5 Conclusions

How to make a seamless knitted bra with optimal fit and comfort is a very interesting research problem, as seamless knitting is a new technology, and bra fitting has not been studied academically. In this chapter, based on the fitting evaluation results of the newly developed seamless knitted bras and the four commercial bras, the following key conclusions and recommendations are drawn:

1) Compared with conventional cut & sewn bras, the seamless knitted bras showed significantly lower pressure values and higher comfort sensation scores at most of the measuring points, especially at the underwire region.
2) The seamless knitted bras with higher level of loop density, presented considerably lower pressure values, better comfort and less pressure sensation scores.
3) The 3D supporting wires can provide definite support to the breast, especially for the seamless knitted bras with higher level of loop density. There is no significant difference of pressure values between with or without 3D wire at most of the measuring points in both arms-up and arms-down standing postures respectively (at the 5% level of significance). The same conclusion can be drawn for the comfort & pressure sensation evaluations between with or without 3D wire.
4) For objective pressure evaluation, the pressure values present a significant difference at most of the measuring points between the arms-up and arms-down postures, especially in the cup, underwire and upperband regions.

5) For objective pressure evaluation and comfort & pressure sensation evaluation, there is no significant difference at most of the measuring points among three styles at 5% level of significance.

6) For the key pressure evaluations, loop density was the strongest factor affecting the “pressure at the apex”, and loop density & elastic yarn tension were the major factors affecting “pressure at the side bottomband”. In the current study, empirical prediction equations were also established for these two pressure points.

CHAPTER 8

CONCLUSIONS AND RECOMMENDATIONS

8.1 General Summary

The bra is one of the most close fitting garments for females, which is designed to support and mould the breast soft tissues, provide comfort to the wearer and provide a aesthetically pleasing appearance. In addition, the commercial bra should be produced in a wide range of sizes to cover the variations existing, in terms of breast shape and size, in the female population (Hardaker & Fozzard, 1997). However, it has often been reported (Young, 1995; Lipton, 1996; Boyes, 1996; Pechter, 1998) that 70% or more of women wear the wrong size bra due to the problems with the existing bra sizing system. The seamless knitted commercial bra has demonstrated several disadvantages such as compressed breasts, insufficient support, unaffective styles as well as sizing problems. In this study, the relationships among breast sizing, seamless knitting parameters and bra fitting performances were investigated.

8.1.1 Anthropometric Study

To accurately describe very complex 3D breasts, 98 measurements obtained from 3D body scanning and 5 supplementary manual measurements were defined and collected from 456 women subjects aged between 20 and 39. The measuring items included all relevant breast parameters of angle, surface distance, width, thickness, volume and curvature. To identify whether the current sample reflects the whole population or not, the distributions of four key measurements including bust girth, underbust girth, weight and body height that are generally relevant for building the bra sizing system were compared with the sample that was used for establishing the existing bra sizing system. The existing system, renewed in 2004, was designed based on manual measurements collected in 1987 from 5,507 women randomly sampled and stratified by area and age according to the Chinese population (Zhou et al., 1992). The results indicate that the sample used in this study is able to represent the Chinese population.

8.1.2 Development of a New Bra Sizing System

Two multivariate statistical methods, including principal components factor analysis and K-means cluster analysis, were used to determine the sizing criteria and to establish a new bra sizing system for Chinese women based on a set of 103 static anthropometric variables. Principal components factor analysis was used with varimax rotation to determine the optimal groups of factors. Eight factors have been identified to evaluate the breast shape, including overall body build, volume of the breast, inner breast shape, outer breast shape, overall height proportion, orientation of the breast, gradient of the upper breast and lower breast shape. These eight factors could explain 78.93% of the total sample variance. The results show that the first factor accounts for 23.51% of the total variance, while the second factor covers nearly 20% of the total variance. The first two factors together tell 43.26% of the total variance, much larger than the combined effect of the other six factors.

Two key measurements, “underbust girth” and “breast depth width ratio DWR ”, which had the highest factor loading on factor 1 and factor 2 in the principal components factor analysis, were identified as significant parameters to draw up a new bra sizing system.

The newly discovered parameter DWR can be measured by a light & small sliding caliper by the woman herself. The breast depth width ratio is easily calculated by dividing the bust depth by the bust width. The customer can find her bra cup category from the breast sizing table as proposed.

Retaining the same size interval of 5cm at the underbust girth for the new system, layered K-means cluster analysis was carried out using the variable “breast depth width ratio”. Eight clusters were proposed to show similar intervals among subgroups, resulting in the same number of sizes as the existing bra sizing system. The cup sizes in the new bra sizing system are denoted by AA* to G* to be distinguished from the cup sizes AA ~ G in the existing one.

8.1.3 Efficiency Test of Sizing Systems

To evaluate its efficiency, the new bra sizing system was compared with the existing bra sizing system in terms of (1) accommodation (coverage) rate, (2) efficiency of classifying the breast shape, and (3) fit performance for the covered individuals.

Probability densities were used to explore the population accommodation rate of the two sizing systems. The results indicated that the two-dimensional probability coverage rate of the new system was 97.43%, which was better than 94.29% as achieved by the existing system. If the bra categories of 65cm underbands, AA (AA*) cups or G (G*) cups were excluded that are generally not included in manufacturing, the partial probability coverage rate showed a much higher percentage (84.86%) for the new system, much superior than 77.19% in the existing sizing system.

Dissimilarity distance measures based on factor scores were conducted to evaluate the efficiency of the two systems on classifying the breast shape. The results revealed that the aggregate factor score dissimilarities of the new bra sizing system was 2681.4, which was less than 2960.1 in the existing one – an approximately 10% reduction.

Aggregate fit loss assessments (Paal, 1997; McCulloch et al., 1998; Ashdown, 1998) based on five key measurements were also measured to evaluate the two system performances in fitting the population. The results across 456 subjects showed that the aggregate loss of the new bra sizing system was 89.5, that was much less than 130.0 in the existing one. Furthermore, for the high frequency coverage bra sizes, the results relevant to 378 subjects showed that the aggregate fit loss of the new system was 63.5, about 42.5% reduction from 110.3 as achieved by the existing one.

The assessment results revealed that the new bra sizing system is more efficient than the existing sizing system. It covers a larger percentage of the population, provides better fit to the accommodated individuals, while maintaining a clear structure and keeping the same number of size categories.

8.1.4 Fundamental Seamless Knitting Experiments

As an application study, circular knitting performances of seamless knitted bras were investigated based on the understanding of the breast dimensions and shapes. Considering the medium breast size 75B which is generally chosen to be a prototype size for bra design in manufacturing, the new seamless knitted bra prototypes were developed to fit the breast size of 75B* in the new bra sizing system with comfort and natural support.

To achieve proper underband tension and sufficient cup strain of seamless knitted bras, the key knitting parameters were investigated in a 2^4 and a 2^3 factorial experimental design respectively. The factors include: loop density, elastic yarn tension, cover yarn tension and Nylon yarn tension. Based on common practice, the yarns used in the fundamental experiments included 78/68/1 Nylon 66, 20-20/10/1 cover yarn and 210D bare elastic. It was shown that the underband tension is mainly affected by loop density and elastic yarn tension. The underband has greater tension when all factors are set near the low level, and has less tension when the loop density and elastic yarn tension are at a high level and the cover yarn tension and Nylon yarn tension are at a low level. Moreover, the most important factor affecting the cup strain is loop density only.

Providing the current experimental conditions, empirical prediction equations are also established to estimate the underband tension and cup strain. The adjusted coefficients of multiple determinations (adjusted R^2) for the response variables are all greater than 98%.

8.1.5 Development of a 3D Supporting Wire

To create a seamless knitted bra that holds the breast shape in a natural manner, a soft 3D supporting wire was designed based on the determination of breast root of size 75B*. From 49 female subjects, the X, Y, Z coordinates of 15 key points were extracted along the breast bottom curve from the outer-most point of the breast, passing the lower-most point, to the inner-most point of the breast. Except the inner-most point, the average coordinates of the other 14 points were used to design a 3D CAD underwire model. After confirming the underwire shape, soft material of polyurethane was used to duplicate the Stereolithography (SLA) prototype of 3D underwire.

8.1.6 Development of Advanced Seamless Knitted Bras

Three new styles of seamless knitted bras were developed focusing on improving the performance of existing seamless knitted bras. It included: creating the select values of comfort and support of the underband, utilizing different levels of loop density in the cup regions for increasing cup volume, using a different knitting structure to provide good fit of the wing to the body. Then fifteen testing bra samples were produced in three new styles using two key knitting parameters identified in the fundamental knitting experiments – loop density and elastic yarn tension. The same yarns used for the knitting fundamental experiments were used to create the bra prototypes.

8.1.7 Fitting Evaluation

To compare the fitting performance between the new developed seamless knitted bras and four commercial bras (two cut & sewn conventional bras, and two commercial seamless bras), fitting assessments including objective evaluation (bra pressure value assessment), subjective evaluation (comfort & pressure sensation assessment) and breast shape evaluation (image comparisons from 3D body scanning) were conducted using six human subjects whose bra size is 75B*.

Compared with conventional cut & sewn bras, the seamless knitted bras showed significantly lower pressure values and higher comfort feeling scores at most of the measuring points, especially in the underwire region. The seamless knitted bras with relatively larger loop density values, were compared to the seamless knitted bras with relatively smaller loop density values, and exhibited considerably lower pressure values, better comfort feeling scores and weaker compressive feeling scores.

From the fit tests on the 6 subjects, it was confirmed that the 3D supporting wires can provide definite support to the breasts and improve the breast vertical-sectional profiles through the bust point, especially for the seamless knitted bras which have a relatively larger value of loop density. The objective evaluation results also revealed that whether using 3D soft supporting wires or not, there is no significant difference at most of the pressure measurement points in either the arms-down & arms-up standing posture at the 5% level of significance.

For pressure value evaluations of key bra design regions, it was confirmed that loop density was the strongest factor affecting the pressure of apex, and loop density & elastic yarn tension were the major factors affecting the pressure of the side bottomband. Given the current experimental conditions, empirical equations were also built to predict the pressure at these two measuring points. The adjusted coefficients of multiple determinations (adjusted R^2) for these two equations are 78.42% and 86.2% respectively.

Based on the above, a series of prediction equations were developed that are useful to predict the underband tension and cup strain of the seamless knitted bra based on the knitting parameters. The key pressure values related to cup and underband regions may also be predicted. This could improve the efficiency and effectiveness of developing new seamless knitted bra products.

The present study is significant as:

1) This is the first time that a bra sizing system protocol has been proposed based on 3D nude breast characteristics.
2) It improves our knowledge of the relationships among the breast shapes, knitting parameters and seamless knitted bra fitting evaluations.
3) It demonstrates a novel approach to design a 3D soft supporting wire by characterizing the breast root curve.
4) It provides empirical prediction equations for assessing the pressure values of key regions of seamless knitted bras, estimating the underband tension and cup strain based on the current experimental conditions.

8.2 Limitations

Some limitations have been found in this study. Firstly, female body data used for extracting measurements and developing the new bra sizing system was obtained from a convenience sample in the AIMER HEC-BICT's size survey in Beijing. Although it was a randomized sample that covers the intimate apparel consumer markets, it could not cover all geographic regions of China.

For fundamental knitting experiments and seamless knitted bra development, due to limited resources, only three types of common practical yarns were included that are mainly used in the markets of Europe, US and Mainland China. It would be better to use different types of yarns in future studies.

Owing to limited resources, the seamless knitted bra fitting assessments were only conducted using six human subjects. Comparisons were made to only two conventional bras and two commercial seamless bras. It would be ideal to have more subjects and more experimental bra samples in further studies.

8.3 Recommendations for Future Research

There are many possibilities for future research. As mentioned, the new bra sizing system was established based on 456 female subjects aged from 20 to 39 in this study. For further study, a much larger sample which can cover a wide geographic region and greater age groups would be better to improve the effectiveness in statistical validity for the whole female population of China.

In the present study, a 3D soft supporting wire was designed using the medium breast size of 75B* only in the new sizing system. For future study, other sizes of 3D underwire could be made because different breast sizes would have different breast root samples. Moreover, the material for the underwire was limited to one kind of polyurethane; other varieties of materials could be explored.

The development of seamless knitted bra prototypes and fitting evaluations were conducted on the medium size 75B*. To effectively investigate the relationships among the breast sizes, knitting performances and fitting tests, it would be necessary to carry out further research on other groups of bra sizes.

In addition, the prediction equations developed in present study are built based on using three types of common yarns. Further research on a series of yarns is needed to improve the effects of the prediction equations. Furthermore, the different breast sizes may affect the results, and should be investigated and manipulated into the prediction equations.

APPENDIX I

Principal Components Factor Analysis Based on Eight Factors

	Factor loadings							
Measurement	Factor 1	Factor 2	Factor 3	Factor 4	Factor 5	Factor 6	Factor 7	Factor 8
D092 Underbust girth	0.940	0.086	0.030	0.051	0.109	0.021	-0.016	-0.101
D052 Underbust depth	0.935	0.063	0.002	0.065	0.066	0.185	-0.005	0.017
C014 Calculated BMI	0.909	0.181	-0.031	0.094	-0.126	0.007	0.107	-0.038
M005 Chest girth	0.907	0.198	0.047	0.089	0.171	-0.014	0.055	-0.055
C013 Calculated VHI	0.885	0.178	0.008	0.075	-0.106	-0.005	0.080	-0.035
M130 Weight	0.883	0.152	0.003	0.093	0.302	0.031	0.105	-0.022
D051 Median chest depth	0.876	0.099	0.042	0.086	0.088	0.241	0.039	0.071
D124 Torso body volume	0.869	0.168	0.000	0.094	0.290	0.021	0.117	-0.001
D091 Bust girth	0.867	0.355	0.161	0.138	0.081	0.012	-0.061	0.089
D049 Chest depth	0.866	0.175	0.053	0.062	0.063	0.194	-0.117	0.061
D040 Underbust width	0.859	0.080	0.054	0.056	0.061	-0.146	0.098	-0.195
D123 Whole body volume	0.857	0.152	0.036	0.073	0.316	0.017	0.078	-0.020
D050 Bust depth	0.853	0.358	0.033	0.084	0.054	0.136	-0.028	0.111
D039 Bust width	0.822	0.129	0.206	0.211	0.076	-0.150	0.132	-0.051
D125 Upper torso body volume	0.820	0.218	-0.002	0.075	0.309	0.012	0.114	0.044
M127 Fat thickness of back	0.777	0.035	0.041	0.137	-0.080	-0.028	0.063	0.001
T004 Horizontal distance from front neck point to front waist centre	0.744	-0.071	0.041	0.139	-0.026	0.045	-0.316	0.206
D038 Chest width	0.728	0.153	0.144	0.268	0.195	-0.098	0.109	-0.129
T015 Vertical angle of upper torso from front neck point to front waist centre	0.703	-0.078	0.037	0.124	-0.188	0.052	-0.354	0.171
D126 Chest area volume	0.669	0.442	0.038	0.119	0.135	0.033	0.358	0.183
D136 Total arc length of right breast (slanting plane)	0.612	0.498	-0.029	0.301	-0.092	0.030	0.268	0.023
M126 Fat thickness of the upper arm	0.612	0.085	0.046	0.149	-0.172	0.070	0.083	-0.098
C003 Calculated reverse aspect ratio of underbust cross-section	-0.610	-0.012	0.035	-0.056	-0.045	-0.427	0.103	-0.191
D135 Total arc length of breast from right to left (horizontal plane)	0.557	0.498	0.446	0.344	0.120	0.113	0.061	0.146
D085 Total arc length of right breast root	0.556	0.160	0.178	0.340	-0.069	0.030	0.340	0.343
D027 Shoulder width 2	0.510	0.171	0.090	0.099	0.382	-0.242	0.015	-0.154
D103 Cross shoulder length over front neck point (SP2~FNP~SP2)	0.509	0.061	0.156	0.148	0.412	-0.108	0.037	-0.181
T018 Vertical angle of upper breast from front neck point	0.497	0.177	0.144	0.134	-0.145	-0.044	-0.483	0.187
D107 Outer arc length of left breast (horizontal plane)	0.494	0.347	0.082	0.372	0.153	0.030	-0.041	0.252
D084 Inner arc length of right breast root	0.490	0.137	0.327	0.126	-0.025	0.045	0.301	0.402
D107 Outer arc length of right breast (slanting plane)	0.480	0.278	-0.309	0.452	-0.083	-0.015	0.148	-0.040
D031 Cross shoulder length over back neck point (SP2~BNP~SP2)	0.454	0.067	0.061	0.010	0.369	-0.250	-0.102	-0.061
C002 Calculated reverse aspect ratio of bust cross-section	-0.441	-0.415	0.126	0.071	0.000	-0.367	0.186	-0.208

Appendix I (continued)

D113 Angle B of right breast cross-section	-0.098	-0.947	-0.013	-0.083	-0.008	-0.053	0.064	0.002
C004 Calculated aspect ratio of the breast1 (D120/D110-b)	0.016	$\boxed{0.940}$	0.162	0.002	0.034	0.023	-0.084	0.014
C006 Calculated chubbiness ratio of the breast1 (D134 (horizontal plane)/D110-b)	0.078	0.923	0.019	0.061	0.039	0.034	-0.057	0.068
C005 Calculated aspect ratio of the breast2 (D121/D110-b)	0.219	0.886	-0.082	-0.127	-0.044	0.076	0.146	0.054
D121 Perpendicular distance from bust point to underbust line	0.326	0.844	0.087	0.061	-0.025	0.078	0.155	0.086
D062 Centre breast depth	0.256	0.841	0.017	0.059	-0.006	-0.227	-0.013	0.133
D114 Angle C of right breast cross-section	0.253	0.792	-0.362	0.300	-0.035	0.109	-0.034	-0.026
D120 Height of the breast	0.204	0.790	0.424	0.315	0.055	0.028	-0.042	0.056
T020 Angle rays diverging from the vertex front waist centre to front neck point and bust point	0.138	0.790	-0.011	0.152	-0.120	-0.073	0.003	0.126
D106 Thinkness of the breast_2	0.155	0.767	-0.033	0.113	0.042	-0.386	-0.078	0.084
T033 Horizontal distance from lower-most point of the breast to bust point	0.318	0.748	0.254	-0.048	-0.024	0.309	0.171	0.149
T031 Vertical angle of lower breast	0.295	0.744	-0.066	-0.201	-0.076	0.360	0.262	-0.167
T019 Vertical angle of lower breast from front waist centre to bust point	-0.238	0.737	-0.027	0.074	-0.003	-0.086	0.230	0.058
T005 Horizontal distance from front waist centre to bust point	-0.249	0.732	-0.003	0.079	0.006	-0.110	0.184	0.011
C010 Calculated chubbiness ratio of the breast5 (T032/T035)	0.359	0.714	-0.062	-0.095	-0.091	0.387	0.237	-0.170
C007 Calculated chubbiness ratio of the breast2 (D134 (horizontal plane)/D062)	-0.126	-0.712	0.011	0.012	0.045	0.219	0.108	-0.076
T028 Inner angle of lower breast	0.375	0.711	-0.106	-0.117	-0.075	0.378	0.240	-0.151
T029 Inner angle of whole breast	-0.352	-0.699	-0.213	0.112	0.084	-0.469	-0.027	-0.072
D112 Angle A of right breast cross-section	-0.171	0.697	0.540	-0.266	0.065	-0.052	-0.075	0.032
T032 Perpendicular distance from bust point to the slanting line of whole breast	0.370	0.648	0.325	0.017	-0.029	0.418	0.168	0.241
D130 Right breast volume	0.377	0.642	0.079	0.293	0.044	-0.114	0.205	0.222
C001 Difference between bust girth and underbast girth (3D)	0.188	0.625	0.300	0.211	-0.021	-0.012	-0.103	0.380
C009 Calculated chubbiness ratio of the breast4 (D136 (slanting plane)/D062)	-0.125	-0.612	-0.091	-0.055	0.062	0.281	0.101	-0.012
D068 Length from front neck point to right bust point (FNP~RBP)	0.524	0.603	-0.150	0.055	0.138	0.152	0.418	-0.019
D104 Length from front neck point to right bust point (FNP~LBP)	0.534	0.562	-0.126	0.042	0.126	0.139	0.393	0.029
D069 Length from side neck point to right bust point (SNP~BP)	0.545	0.558	-0.228	0.078	0.159	0.101	0.437	-0.061
D108 Inner arc length of right breast (slanting plane)	0.508	0.558	0.344	-0.028	-0.062	0.075	0.302	0.095
D122 Area of the breast cross-section	0.522	0.528	0.054	0.268	-0.038	-0.054	0.231	0.050
C008 Calculated chubbiness ratio of the breast3 (D136 (slanting plane)/D110-b)	0.293	0.504	-0.471	-0.209	-0.124	-0.006	0.229	-0.028
D105 Width of the breast_a_inner	0.065	0.202	0.920	0.085	0.084	-0.013	0.036	0.106
D110 Width of the breast_b_inner	-0.052	-0.195	0.907	-0.097	0.087	-0.102	0.046	0.099
D117 Inner length from right breast cross-section	0.097	0.338	0.875	0.099	0.087	-0.079	0.025	0.123
D108 Inner arc length of right breast (horizontal plane)	0.112	0.370	0.853	0.090	0.081	-0.033	0.057	0.154
T021 Angle 1 of the breast triangle	-0.009	-0.290	0.717	-0.200	-0.010	0.108	-0.316	0.035

Appendix I (continued)

D105 Width of the breast_a	0.354	0.091	0.616	0.437	0.039	-0.444	0.040	0.098
T023 Angle 3 of the breast triangle	-0.025	0.227	-0.578	0.139	0.076	0.078	0.296	-0.088
T027 Inner angle of upper breast	0.111	0.294	0.560	-0.038	-0.039	0.354	-0.322	0.391
T022 Angle 2 of the breast triangle	0.038	0.229	-0.551	0.175	-0.058	-0.245	0.203	0.032
D129 Global average radius of curvature of inner breast under curve	0.351	0.061	0.545	0.255	0.063	-0.069	0.151	-0.105
D059 Bust point width	0.534	0.351	0.538	-0.110	0.107	0.228	0.164	0.009
D060 Horizontal plane distance between inner-most point of bust	-0.008	-0.169	-0.234	-0.137	0.218	0.195	-0.181	-0.139
D119 Depth from lower-most point to outer-most point of the breast	0.128	-0.317	-0.074	0.839	0.048	0.107	-0.213	-0.124
D110 Width of the breast_b_outer	0.511	0.164	-0.137	0.782	-0.029	0.129	0.041	-0.004
D116 Outer length from right breast cross-section	0.476	0.437	0.059	0.726	0.000	0.112	0.019	0.018
D107 Outer arc length of right breast (horizontal plane)	0.461	0.464	0.024	0.710	0.014	0.076	0.000	0.037
D110 Width of the breast_b	0.423	0.000	0.577	0.646	0.040	0.038	0.071	0.071
D106 Thinkness of the breast	0.378	0.394	0.150	0.634	0.038	0.443	0.034	0.051
D128 Global average radius of curvature of outer breast under curve	0.097	0.123	-0.085	0.590	-0.023	-0.077	0.207	0.055
D127 Global average radius of curvature of the breast under curve	0.571	0.111	0.383	0.581	-0.017	0.101	0.185	-0.098
D118 perpendicular distance from lower-most point of breast to the base width line of the breast	-0.187	-0.223	0.229	0.579	0.111	-0.185	-0.379	-0.137
D134 Total arc length of right breast (horizontal plane)	0.389	0.525	0.468	0.544	0.050	0.033	0.035	0.111
D001 Whole body height	0.077	-0.033	0.057	0.008	0.932	0.041	0.025	0.032
D010 Chest height	0.045	-0.033	0.075	0.006	0.919	0.040	-0.016	0.033
D012 Underbust height	-0.005	-0.176	0.074	-0.047	0.887	0.015	-0.232	-0.035
D011 Bust height	-0.054	-0.225	0.182	0.007	0.859	-0.002	-0.237	0.086
T010 Length from side neck point to back waist centre	0.223	0.085	-0.034	0.012	0.754	-0.104	0.330	0.030
T011 Length from side neck point to front waist centre	0.521	0.026	0.002	0.085	0.666	-0.029	0.133	0.128
D067 Back waist length over shoulder blade	0.267	-0.029	-0.046	-0.045	0.650	0.091	0.369	-0.027
D066 Front waist length over bust	0.483	0.417	0.051	0.086	0.509	0.017	0.159	0.143
D111 Orientation of the breast (angle)	0.078	-0.168	-0.168	0.280	-0.018	0.876	0.079	-0.043
D106 Thinkness of the breast_1	0.273	-0.135	0.174	0.559	0.009	0.712	0.089	-0.007
D105 Width of the breast_a_outer	0.407	-0.115	-0.254	0.491	-0.047	-0.591	0.014	0.009
T036 Length of whole breast leg of breast triangle (°)	0.307	0.313	-0.064	0.243	0.026	0.057	0.644	0.157
T034 Length of upper breast leg of breast triangle (°)	0.381	0.542	-0.208	0.063	-0.023	0.186	0.562	-0.067
T030 Vertical angle of upper breast	0.221	0.310	0.466	0.177	-0.021	0.123	-0.482	0.372
C011 Calculated chubbiness ratio of the breast6 (D134 (horizontal plane)/M046)	0.148	-0.235	-0.026	0.324	-0.013	0.045	-0.081	-0.767
C012 Calculated chubbiness ratio of the breast7 (D136 (slanting plane)/M046)	0.309	-0.168	-0.374	0.105	-0.111	0.040	0.128	-0.687

Appendix I (continued)

M046 Vertical arc length from right bust point to underbust (BP~UBL)	0.168	0.548	0.355	0.154	0.047	-0.008	0.096	0.639
D083 Centre bridge height	-0.093	-0.273	0.520	0.312	0.096	-0.123	-0.116	0.602
T035 Length of lower breast leg of breast triangle (°)	0.180	0.256	0.534	0.159	0.040	0.243	0.002	0.588

Extraction Method: Principal Components Analysis

Rotation Method: Varimax with Kaiser Normalization

APPENDIX II

Informed Consent

You are being asked to participate in a study investigating the bra fitting feeling on both aspects of compressive and comfort. This study is one part of a PhD thesis being conducted at the Hong Kong Polytechnic University by Rong Zheng under the supervision of Dr. Winnie Yu and Prof. Jintu Fan.

As a participant, you will be asked to attend two parts of investigation: bra fitting objective evaluation and subjective evaluation. In the objective part, you will be asked to wear total 31 pieces of bras, to measure the bra pressure and to scan the body surface when wearing identified bras. In the subjective part, you will be asked to complete various questionnaires about the bra comfort & pressure sensation. Your name will not be on any of the questionnaires and related documents of analysis results. It will take approximately few hours to complete the whole experiment.

I am very appreciative of your kind help and will be happy to answer any questions you may have. Thank you very much for your cooperation. Please answer all questions honestly.

Sincerely,
Rong Zheng

I have read and understand the above information and agree to participate in this project.

Signature______________________

Data__________________________

APPENDIX III

Bra Comfort & Pressure Sensation Evaluation Form

New developed seamless bra style 1 / two commercial seamless bras / two conventional bras Style:

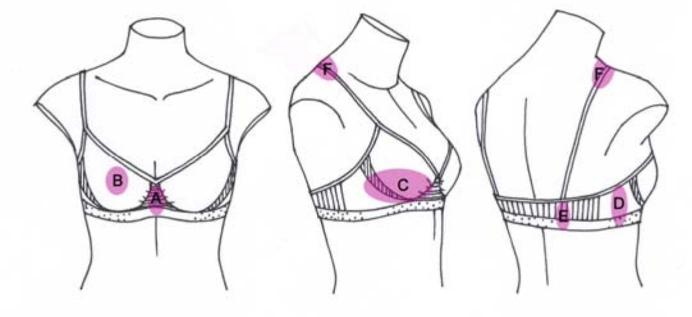

A. Gore

Comfort sensation Very bad Neutral Very good

Score 1 2 3 4 5 6 7

Pressure sensation Very weak Neutral Very strong

Score 1 2 3 4 5 6 7

B. Cup

Comfort sensation Very bad Neutral Very good

Score 1 2 3 4 5 6 7

Pressure sensation Very weak Neutral Very strong

Score 1 2 3 4 5 6 7

C. Wire

Comfort sensation Very bad Neutral Very good

Score 1 2 3 4 5 6 7

Pressure sensation Very weak Neutral Very strong

Score 1 2 3 4 5 6 7

D. Side wire

Comfort sensation Very bad Neutral Very good

Score 1 2 3 4 5 6 7

Pressure sensation Very weak Neutral Very strong

Score 1 2 3 4 5 6 7

E. Back wire

Comfort sensation Very bad Neutral Very good

Score 1 2 3 4 5 6 7

Pressure sensation Very weak Neutral Very strong

Score 1 2 3 4 5 6 7

F. Shoulder strap

Comfort sensation Very bad Neutral Very good

Score 1 2 3 4 5 6 7

Pressure sensation Very weak Neutral Very strong

Score 1 2 3 4 5 6 7

Bra Comfort & Pressure sensation Evaluation Form

Developed seamless bra style 2 Style:

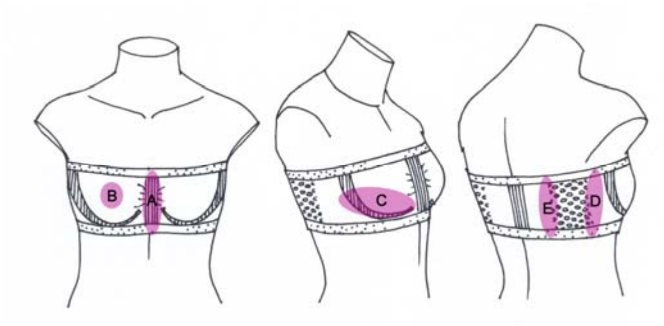

A. Gore

Comfort sensation Very bad Neutral Very good

Score 1 2 3 4 5 6 7

Pressure sensation Very weak Neutral Very strong

Score 1 2 3 4 5 6 7

B. Cup

Comfort sensation Very bad Neutral Very good

Score 1 2 3 4 5 6 7

Pressure sensation Very weak Neutral Very strong

Score 1 2 3 4 5 6 7

C. Wire

Comfort sensation	Very bad			Neutral			Very good
Score	1	2	3	4	5	6	7
Pressure sensation	Very weak			Neutral			Very strong
Score	1	2	3	4	5	6	7

D. Side wire

Comfort sensation	Very bad			Neutral			Very good
Score	1	2	3	4	5	6	7
Pressure sensation	Very weak			Neutral			Very strong
Score	1	2	3	4	5	6	7

E. Back wire

Comfort sensation	Very bad			Neutral			Very good
Score	1	2	3	4	5	6	7
Pressure sensation	Very weak			Neutral			Very strong
Score	1	2	3	4	5	6	7

Bra Comfort & Pressure sensation Evaluation Form

Developed seamless bra style 3 Style:

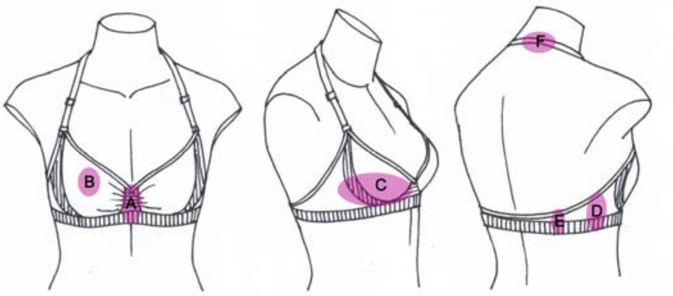

A. Gore

Comfort sensation	Very bad			Neutral			Very good
Score	1	2	3	4	5	6	7
Pressure sensation	Very weak			Neutral			Very strong
Score	1	2	3	4	5	6	7

B. Cup

	Very bad			Neutral			Very good
Comfort sensation							
Score	1	2	3	4	5	6	7

	Very weak			Neutral			Very strong
Pressure sensation							
Score	1	2	3	4	5	6	7

C. Wire

	Very bad			Neutral			Very good
Comfort sensation							
Score	1	2	3	4	5	6	7

	Very weak			Neutral			Very strong
Pressure sensation							
Score	1	2	3	4	5	6	7

D. Side wire

	Very bad			Neutral			Very good
Comfort sensation							
Score	1	2	3	4	5	6	7

	Very weak			Neutral			Very strong
Pressure sensation							
Score	1	2	3	4	5	6	7

E. Back wire

	Very bad			Neutral			Very good
Comfort sensation							
Score	1	2	3	4	5	6	7

	Very weak			Neutral			Very strong
Pressure sensation							
Score	1	2	3	4	5	6	7

F. Shoulder strap

	Very bad			Neutral			Very good
Comfort sensation							
Score	1	2	3	4	5	6	7

	Very weak			Neutral			Very strong
Pressure sensation							
Score	1	2	3	4	5	6	7

APPENDIX IV

Overall Bra Comfort & Pressure Sensation Evaluation Form

No.______

Demographic info

Data of birth (mm / dd / yy)______________

Birth place____________________________

Ethnic place (father)____________________

(Mother)___________________

Growing place_________________________

Current education level___________________

Telephone number_______________________

Have one or more child Yes ( ) No ( )

Numbers of children 1 2 3

Occupation status________________________

1. When you wear developed seamless knitted bras, do you think the fabric handle and comfort sensation are overall better than the conventional bras?

No			Regular			Yes
1	2	3	4	5	6	7

2. When you wear developed seamless knitted bras, do you think your breast shape appears to be natural?

No			Regular			Yes
1	2	3	4	5	6	7

3. When you wear developed seamless knitted bras adding 3D underwires, do you feel they provide better support than before?

No			Regular			Yes
1	2	3	4	5	6	7

APPENDIX V

Paired-sample T Test of Pressure Values between with and without 3D Wires

Appendix V.1 Paired-sample T test results of pressure values of style 1 between with and without 3D wires (arms-down posture)

	With 3D wires vs without 3D wires	Mean	Std. D	Std. Error Mean	95% Confidence Interval of the Difference		t	df	Sig. (2-tailed)
					Lower	Upper			
Pair 1	Point 01: Centre front	0.000	0.052	0.023	-0.065	0.064	-0.017	4	0.987
Pair 2	Point 02: Inner wire	0.080	0.103	0.046	-0.048	0.208	1.729	4	0.159
Pair 3	Point 03: Apex	0.070	0.055	0.024	0.002	0.138	2.875	4	0.045
Pair 4	Point 04: Cup base point	-2.491	1.011	0.452	-3.746	-1.236	-5.510	4	0.005
Pair 5	Point 05: Underarm	0.378	0.069	0.031	0.292	0.464	12.182	4	0.000
Pair 6	Point 06: Outer wire	0.308	0.105	0.047	0.177	0.438	6.538	4	0.003
Pair 7	Point 07: Side underband	-0.085	0.247	0.110	-0.391	0.222	-0.767	4	0.486
Pair 8	Point 08: Side bottomband	-0.388	0.204	0.091	-0.641	-0.134	-4.247	4	0.013
Pair 9	Point 09: Back strap	0.350	0.265	0.119	0.021	0.679	2.954	4	0.042
Pair 10	Point 10: Back strap end	-0.188	0.108	0.048	-0.322	-0.054	-3.904	4	0.017
Pair 11	Point 11: Shoulder point	0.165	0.328	0.147	-0.242	0.572	1.126	4	0.323

Appendix V.2 Paired-sample T test results of pressure values of style 1 between with and without 3D wires (arms-up posture)

	With 3D wires vs without 3D wires	Mean	Std. D	Std. Error Mean	95% Confidence Interval of the Difference		t	df	Sig. (2-tailed)
					Lower	Upper			
Pair 1	Point 01: Centre front	0.000	0.094	0.042	-0.118	0.117	-0.010	4	0.992
Pair 2	Point 02: Inner wire	0.006	0.085	0.038	-0.100	0.111	0.148	4	0.890
Pair 3	Point 03: Apex	-0.002	0.097	0.043	-0.122	0.118	-0.053	4	0.960
Pair 4	Point 04: Cup base point	-0.276	0.604	0.270	-1.026	0.474	-1.022	4	0.365
Pair 5	Point 05: Underarm	0.178	0.223	0.100	-0.099	0.455	1.787	4	0.148
Pair 6	Point 06: Outer wire	0.282	0.211	0.094	0.020	0.543	2.985	4	0.041
Pair 7	Point 07: Side underband	-0.194	0.438	0.196	-0.738	0.349	-0.993	4	0.377
Pair 8	Point 08: Side bottomband	0.184	0.468	0.209	-0.397	0.765	0.880	4	0.429
Pair 9	Point 09: Back strap	0.155	0.271	0.121	-0.183	0.492	1.273	4	0.272
Pair 10	Point 10: Back strap end	-0.068	0.043	0.019	-0.121	-0.014	-3.504	4	0.025
Pair 11	Point 11: Shoulder point	-0.472	0.426	0.190	-1.001	0.057	-2.478	4	0.068

Appendix V.3 Paired-sample T test results of pressure values of style 2 between with and without 3D wires (arms-down posture)

	With 3D wires vs without 3D wires	Mean	Std. D	Std. Error Mean	95% Confidence Interval of the Difference		t	df	Sig. (2-tailed)
					Lower	Upper			
Pair 1	Point 01: Upper centre front	-0.005	0.020	0.009	-0.029	0.019	-0.559	4	0.606
Pair 2	Point 02: Centre front	0.003	0.017	0.007	-0.018	0.023	0.346	4	0.747
Pair 3	Point 03: Inner wire	-0.118	0.121	0.054	-0.268	0.032	-2.180	4	0.095
Pair 4	Point 04: Bust upperband	-0.261	0.487	0.218	-0.866	0.345	-1.196	4	0.298
Pair 5	Point 05: Apex	0.117	0.177	0.079	-0.102	0.337	1.483	4	0.212
Pair 6	Point 06: Cup base point	0.029	0.531	0.237	-0.630	0.688	0.123	4	0.908
Pair 7	Point 07: Underarm upperband	0.045	0.401	0.179	-0.454	0.543	0.249	4	0.815
Pair 8	Point 08: Outer wire	0.094	0.111	0.050	-0.044	0.231	1.888	4	0.132
Pair 9	Point 09: Side underband	-0.027	0.447	0.200	-0.582	0.528	-0.134	4	0.900
Pair 10	Point 10: Side bottomband	0.108	0.384	0.172	-0.369	0.585	0.627	4	0.564
Pair 11	Point 11: Back strap upperband	0.098	0.152	0.068	-0.091	0.287	1.442	4	0.223
Pair 12	Point 10: Back strap bottomband	0.047	0.318	0.142	-0.348	0.442	0.331	4	0.757

Appendix V.4 Paired-sample T test results of pressure values of style 2 between with and without 3D wires (arms-up posture)

	With 3D wires vs without 3D wires	Mean	Std. D	Std. Error Mean	95% Confidence Interval of the Difference		t	df	Sig. (2-tailed)
					Lower	Upper			
Pair 1	Point 01: Upper centre front	-0.006	0.012	0.005	-0.021	0.009	-1.045	4	0.355
Pair 2	Point 02: Centre front	-0.001	0.032	0.014	-0.041	0.039	-0.064	4	0.952
Pair 3	Point 03: Inner wire	-0.075	0.087	0.039	-0.183	0.034	-1.905	4	0.129
Pair 4	Point 04: Bust upperband	-0.025	0.062	0.028	-0.102	0.053	-0.880	4	0.429
Pair 5	Point 05: Apex	0.113	0.062	0.028	0.036	0.189	4.094	4	0.015
Pair 6	Point 06: Cup base point	-0.263	0.416	0.186	-0.779	0.254	-1.413	4	0.231
Pair 7	Point 07: Underarm upperband	0.048	0.377	0.169	-0.420	0.516	0.284	4	0.790
Pair 8	Point 08: Outer wire	0.124	0.145	0.065	-0.056	0.304	1.914	4	0.128
Pair 9	Point 09: Side underband	-0.196	0.524	0.234	-0.847	0.454	-0.837	4	0.450
Pair 10	Point 10: Side bottomband	-0.200	0.109	0.049	-0.336	-0.064	-4.085	4	0.015
Pair 11	Point 11: Back strap upperband	0.116	0.201	0.090	-0.134	0.366	1.288	4	0.267
Pair 12	Point 10: Back strap bottomband	-0.056	0.164	0.073	-0.259	0.148	-0.758	4	0.491

Appendix V.5 Paired-sample T test results of pressure values of style 3 between with and without 3D wires (arms-down posture)

	With 3D wires vs without 3D wires	Mean	Std. D	Std. Error Mean	95% Confidence Interval of the Difference		t	df	Sig. (2-tailed)
					Lower	Upper			
Pair 1	Point 01: Centre front	-0.049	0.055	0.024	-0.116	0.019	-1.988	4	0.118
Pair 3	Point 03: Apex	0.068	0.058	0.026	-0.004	0.139	2.623	4	0.059
Pair 4	Point 04: Cup base point	-0.652	1.208	0.540	-2.151	0.848	-1.206	4	0.294
Pair 5	Point 05: Underarm	0.144	0.145	0.065	-0.036	0.324	2.225	4	0.090
Pair 6	Point 06: Outer wire	0.135	0.060	0.027	0.061	0.209	5.060	4	0.007
Pair 7	Point 07: Side underband	-0.099	0.235	0.105	-0.391	0.193	-0.939	4	0.401
Pair 8	Point 08: Side bottomband	-0.094	0.323	0.144	-0.495	0.306	-0.653	4	0.550
Pair 9	Point 09: Back strap	0.020	0.118	0.053	-0.127	0.166	0.376	4	0.726
Pair 10	Point 10: Back strap end	0.082	0.127	0.057	-0.075	0.240	1.456	4	0.219
Pair 11	Point 11: Shoulder point	0.114	0.276	0.123	-0.228	0.457	0.928	4	0.406

Appendix V.6 Paired-sample T test results of pressure values of style 3 between with and without 3D wires (arms-up posture)

	With 3D wires vs without 3D wires	Mean	Std. D	Std. Error Mean	95% Confidence Interval of the Difference		t	df	Sig. (2-tailed)
					Lower	Upper			
Pair 1	Point 01: Centre front	-0.042	0.038	0.017	-0.088	0.005	-2.485	4	0.068
Pair 3	Point 03: Apex	0.030	0.065	0.029	-0.051	0.110	1.021	4	0.365
Pair 4	Point 04: Cup base point	-0.103	0.343	0.153	-0.528	0.323	-0.670	4	0.540
Pair 5	Point 05: Underarm	0.078	0.114	0.051	-0.064	0.220	1.518	4	0.204
Pair 6	Point 06: Outer wire	0.077	0.179	0.080	-0.145	0.299	0.964	4	0.390
Pair 7	Point 07: Side underband	0.037	0.218	0.097	-0.234	0.308	0.381	4	0.723
Pair 8	Point 08: Side bottomband	-0.028	0.147	0.066	-0.210	0.155	-0.422	4	0.695
Pair 9	Point 09: Back strap	-0.118	0.159	0.071	-0.315	0.080	-1.651	4	0.174
Pair 10	Point 10: Back strap end	0.091	0.090	0.040	-0.021	0.202	2.262	4	0.087
Pair 11	Point 11: Shoulder point	0.000	0.110	0.049	-0.137	0.137	0.004	4	0.997

APPENDIX VI

Paired-sample T Test of Pressure Values between Arms-up and Arms-down Standing Postures

Appendix VI.1 Paired-sample T test results of pressure values of style 1 between arms-up and arms-down postures (without 3D soft wires)

	Arms-up posture Vs arms-down posture	Mean	Std. D	Std. Error Mean	95% Confidence Interval of the Difference		t	df	Sig. (2-tailed)
					Lower	Upper			
Pair 1	Point 01: Centre front	-0.051	0.125	0.056	-0.207	0.104	-0.911	4	0.414
Pair 2	Point 02: Inner wire	-0.070	0.153	0.068	-0.259	0.120	-1.021	4	0.365
Pair 3	Point 03: Apex	-0.154	0.121	0.054	-0.304	-0.004	-2.844	4	0.047
Pair 4	Point 04: Cup base point	-3.232	0.817	0.366	-4.247	-2.217	-8.842	4	0.001
Pair 5	Point 05: Underarm	0.346	0.198	0.088	0.100	0.591	3.906	4	0.017
Pair 6	Point 06: Outer wire	0.064	0.077	0.035	-0.032	0.159	1.843	4	0.139
Pair 7	Point 07: Side underband	0.245	0.355	0.159	-0.196	0.687	1.543	4	0.198
Pair 8	Point 08: Side bottomband	-0.683	0.237	0.106	-0.978	-0.389	-6.436	4	0.003
Pair 9	Point 09: Back strap	0.526	0.301	0.134	0.153	0.900	3.916	4	0.017
Pair 10	Point 10: Back strap end	0.268	0.086	0.038	0.161	0.375	6.961	4	0.002
Pair 11	Point 11: Shoulder point	1.018	0.614	0.275	0.255	1.780	3.705	4	0.021

Appendix VI.2 Paired-sample T test results of pressure values of style 2 between arms-up and arms-down postures (without 3D soft wires)

	Arms-up posture Vs arms-down posture	Mean	Std. D	Std. Error Mean	95% Confidence Interval of the Difference		t	df	Sig. (2-tailed)
					Lower	Upper			
Pair 1	Point 01: Upper centre front	-0.014	0.022	0.010	-0.042	0.013	-1.438	4	0.224
Pair 2	Point 02: Centre front	-0.063	0.081	0.036	-0.163	0.037	-1.744	4	0.156
Pair 3	Point 03: Inner wire	-0.047	0.118	0.053	-0.194	0.100	-0.886	4	0.426
Pair 4	Point 04: Bust upperband	-0.748	0.350	0.156	-1.183	-0.314	-4.785	4	0.009
Pair 5	Point 05: Apex	-0.222	0.170	0.076	-0.433	-0.011	-2.915	4	0.043
Pair 6	Point 06: Cup base point	-0.725	0.184	0.082	-0.953	-0.497	-8.815	4	0.001
Pair 7	Point 07: Underarm upperband	-0.274	0.266	0.119	-0.604	0.056	-2.308	4	0.082
Pair 8	Point 08: Outer wire	0.063	0.055	0.025	-0.005	0.131	2.557	4	0.063
Pair 9	Point 09: Side underband	0.798	0.653	0.292	-0.013	1.608	2.733	4	0.052
Pair 10	Point 10: Side bottomband	-0.293	0.569	0.255	-1.000	0.414	-1.152	4	0.314
Pair 11	Point 11: Back strap upperband	0.307	0.316	0.141	-0.085	0.700	2.177	4	0.095
Pair 12	Point 10: Back strap bottomband	0.165	0.318	0.142	-0.230	0.560	1.160	4	0.310

Appendix VI.3 Paired-sample T test results of pressure values of style 3 between arms-up and arms-down postures (without 3D soft wires)

Arms-up posture Vs arms-down posture		Mean	Std. D	Std. Error Mean	95% Confidence Interval of the Difference		t	df	Sig. (2-tailed)
					Lower	Upper			
Pair 1	Point 01: Centre front	-0.040	0.045	0.020	-0.096	0.015	-2.006	4	0.115
Pair 3	Point 03: Apex	-0.122	0.039	0.017	-0.169	-0.074	-7.045	4	0.002
Pair 4	Point 04: Cup base point	-1.950	0.833	0.373	-2.984	-0.915	-5.232	4	0.006
Pair 5	Point 05: Underarm	0.353	0.077	0.034	0.258	0.448	10.291	4	0.001
Pair 6	Point 06: Outer wire	0.143	0.097	0.043	0.022	0.263	3.279	4	0.031
Pair 7	Point 07: Side underband	0.017	0.248	0.111	-0.291	0.325	0.155	4	0.884
Pair 8	Point 08: Side bottomband	-0.454	0.156	0.070	-0.647	-0.260	-6.516	4	0.003
Pair 9	Point 09: Back strap	0.776	0.222	0.099	0.501	1.052	7.818	4	0.001
Pair 10	Point 10: Back strap end	0.278	0.197	0.088	0.033	0.523	3.149	4	0.035
Pair 11	Point 11: Shoulder point	-1.298	0.360	0.161	-1.744	-0.851	-8.069	4	0.001

APPENDIX VII

Comfort & Pressure Value Comparisons among Newly Developed Seamless Bras (Style 2 & 3) of Different Loop Density & Elastic Yarn Tension

Appendix VII.1 Comfort & pressure values of five seamless bras of style 2 (without 3D soft wires)

Style	Comfort sensation				Pressure sensation			
	Gore	Cup	Side wing	Back wing	Gore	Cup	Side wing	Back wing
ST2L-25Y20N	5.17	4.50	$\boxed{4.33}$	$\boxed{4.33}$	$\boxed{3.00}$	$\boxed{3.83}$	$\boxed{4.17}$	$\boxed{3.83}$
ST2L-25Y12N	$\boxed{5.00}$	$\boxed{4.33}$	4.67	4.83	$\boxed{3.00}$	3.67	3.50	3.17
ST2L0Y16N	**6.17**	5.00	5.17	5.50	***1.83***	3.33	3.00	2.67
ST2L+25Y12N	6.00	**6.00**	**6.00**	**6.00**	2.33	***2.33***	2.33	2.33
ST2L+25Y20N	5.33	5.00	5.83	5.67	2.50	2.67	***2.00***	***2.17***
Average	5.53	4.97	5.20	5.27	2.53	3.17	3.00	2.83

$\boxed{}$ means the lowest comfort & highest pressure sensation

Appendix VII.2 Comfort & pressure values of five seamless bras of style 2 (with 3D soft wires)

Style	Comfort sensation					Pressure sensation				
	Gore	Cup	Wire	Side wing	Back wing	Gore	Cup	Wire	Side wing	Back wing
ST2L-25Y20Y	$\boxed{4.83}$	4.17	5.50	$\boxed{4.00}$	4.50	3.00	4.17	$\boxed{2.67}$	$\boxed{4.33}$	3.67
ST2L-25Y12Y	$\boxed{4.83}$	$\boxed{4.00}$	$\boxed{5.33}$	4.33	$\boxed{3.83}$	$\boxed{3.17}$	$\boxed{4.33}$	$\boxed{2.67}$	4.00	$\boxed{4.00}$
ST2L0Y16Y	$\boxed{4.83}$	5.83	**6.17**	5.00	5.17	***2.17***	3.67	***1.83***	3.17	3.00
ST2L+25Y12Y	**5.67**	**6.00**	6.00	5.67	**5.67**	2.33	***2.33***	2.00	2.33	***2.33***
ST2L+25Y20Y	5.17	4.83	5.83	**5.83**	**5.67**	2.33	2.83	2.00	***2.00***	3.83
Average	5.07	4.97	5.77	4.97	4.97	2.60	3.47	2.23	3.17	3.37

$\boxed{}$ means the lowest comfort & highest pressure sensation

Appendix VII.3 Means of comfort & pressure values of five seamless bras of style 3 (without 3D soft wires)

Style	Comfort sensation					Pressure sensation				
	Gore	Cup	Side wing	Back wing	Strap	Gore	Cup	Side wing	Back wing	Strap
ST3L-25Y20N	5.00	$\boxed{3.00}$	$\boxed{3.17}$	$\boxed{3.33}$	4.50	$\boxed{3.00}$	5.50	$\boxed{4.67}$	$\boxed{4.83}$	3.50
ST3L-25Y12N	$\boxed{4.83}$	$\boxed{3.00}$	3.50	3.83	$\boxed{4.33}$	2.83	$\boxed{5.67}$	4.33	4.17	$\boxed{3.67}$
ST3L0Y16N	5.67	5.33	4.50	5.17	5.00	2.83	3.50	3.67	3.83	3.17
ST3L+25Y12N	**6.83**	**6.50**	5.67	5.67	**5.83**	***1.17***	***1.50***	2.33	2.33	***2.17***
ST3L+25Y20N	6.00	5.50	**6.00**	**5.83**	5.33	1.67	2.67	***2.17***	***2.17***	2.67
Average	5.67	4.67	4.57	4.77	5.00	2.30	3.77	3.43	3.47	3.04

$\boxed{}$ means the lowest comfort & highest pressure sensation

Appendix VII.4 Means of comfort & pressure values of five seamless bras of style 3 (with 3D soft wires)

Style	Comfort sensation						Pressure sensation					
	Gore	Cup	Wire	Side wing	Back wing	Strap	Gore	Cup	Wire	Side wing	Back wing	Strap
ST3L-25Y20Y	$\boxed{4.67}$	$\boxed{2.83}$	5.17	$\boxed{3.33}$	$\boxed{3.17}$	4.50	$\boxed{\textit{2.83}}$	5.50	$\boxed{\textit{3.50}}$	$\boxed{\textit{4.50}}$	$\boxed{\textit{4.67}}$	3.50
ST3L-25Y12Y	5.17	$\boxed{2.83}$	$\boxed{4.83}$	3.50	3.83	$\boxed{4.17}$	2.33	$\boxed{\textit{5.67}}$	3.17	$\boxed{\textit{4.50}}$	4.33	$\boxed{\textit{3.83}}$
ST3L0Y16Y	6.00	4.83	5.33	5.17	5.50	5.00	2.00	3.33	2.50	3.33	3.00	3.00
ST3L+25Y12Y	**6.83**	**6.50**	5.83	5.83	5.67	**6.00**	***1.17***	***1.50***	2.17	2.17	2.33	***2.00***
ST3L+25Y20Y	6.17	5.83	**6.00**	**6.00**	**6.00**	5.50	2.00	2.83	***2.00***	***2.00***	***2.00***	2.67
Average	5.77	4.56	5.43	4.77	4.83	5.03	2.07	3.77	2.67	3.30	3.27	3.00

$\boxed{}$ means the lowest comfort & highest pressure sensation

APPENDIX VIII

One-way ANOVA of Push-up & Push-in Effects among 3 New Seamless Styles

Appendix VIII.1 One-way ANOVA of push-up & push-in effects among 3 new seamless styles (with 3D wires)

		Sum of Squares	df	Mean Square	F	Sig.
Bust height	Between Groups	0.087	2	0.044	1.836	0.202
	Within Groups	0.285	12	0.024		
	Total	0.372	14			
Bust girth	Between Groups	5.538	2	2.769	2.782	0.102
	Within Groups	11.943	12	0.995		
	Total	17.481	14			
Bust point width	Between Groups	0.309	2	0.155	0.613	0.558
	Within Groups	3.023	12	0.252		
	Total	3.332	14			
FNP~RBP	Between Groups	0.889	2	0.444	8.057	0.006
	Within Groups	0.662	12	0.055		
	Total	1.551	14			
FNP~LBP	Between Groups	0.234	2	0.117	2.808	0.100
	Within Groups	0.501	12	0.042		
	Total	0.735	14			

Appendix VIII.2 One-way ANOVA of push-up & push-in effects among 3 new seamless styles (without 3D wires)

		Sum of Squares	df	Mean Square	F	Sig.
Bust height	Between Groups	0.196	2	0.098	6.857	0.010
	Within Groups	0.171	12	0.014		
	Total	0.367	14			
Bust girth	Between Groups	10.239	2	5.119	8.984	0.004
	Within Groups	6.838	12	0.570		
	Total	17.076	14			
Bust point width	Between Groups	0.591	2	0.296	2.102	0.165
	Within Groups	1.688	12	0.141		
	Total	2.279	14			
FNP~RBP	Between Groups	0.875	2	0.437	3.089	0.083
	Within Groups	1.699	12	0.142		
	Total	2.573	14			
FNP~LBP	Between Groups	0.383	2	0.192	11.550	0.002
	Within Groups	0.199	12	0.017		
	Total	0.582	14			

REFERENCES

Abdali, O., Viktor, H., Paquet, E., & Rioux, M. (2004). Exploring anthropometric data through cluster analysis. *2004 SAE digital human modeling for design and engineering symposium*. Oakland University, Rochester, Michigan, June 15-17.

Aimer Human Engineering Research Centre of Beijing Institute of Clothing Technology. (2004). *The reference document of establishing database of Chinese body shape for apparel industry*. Unpublished Internal Document.

Albright, D., & Rockingham, N. D., inventor, The Russell Group, Ltd., Rockingham, N. D., assignee. (1998). *Knitted brassiere blank having integral seamless elasticated contours defining bra cup borders*. U.S. Patent Publication Number 5850745.

Alexander, M., Connell, L. J., & Presley, A. B. (2005). Clothing fit preferences of young female adult consumers. *International Journal of Clothing Science and Technology*, **17**(1), 52-64.

American Standards for Testing and Materials (ASTM, 1995a). *Standard table of body measurements for adult female misses figure type, sizes 2-20*, 7(2). Designation: D5585-95, West Conshohocken, PA: ASTM.

American Standards for Testing and Materials (ASTM, 1995b). *Standard table of body measurements for women aged 55 and older (All figure type)*, 7(2). Designation: D5586-95, West Conshohocken, PA: ASTM.

American Standards for Testing and Materials (ASTM, 1999). *Standard terminology relating to body dimensions for apparel sizing*, **7**(2). Designation: D5219-99, West Conshohocken, PA: ASTM.

American Standards for Testing and Materials (ASTM, 1996/2004). *Standard test* *method for tension and elongation of elastic fabrics (constant-rate-of-extension type tensile testing machine)*. Designation: D4964-96 (2004), West Conshohocken, PA: ASTM.

Anon. (1994). 1589 and all that and birth of the stocking frame. *Knitting International*, 66-68.

Armstrong, H. J. (1987). *Pattern Marking for Fashion Designer*. New York: Harper Collins.

Asahikasei AGMS Corporation. (2005). *The pattern making, grading and marking maker system of the AGMS garment CAD system*. Available online at: http://www.agms.co.jp/ag3d1.html

Ashdown, S. P. (1998). An investigation of structure of sizing systems: A comparison of three multidimensional optimized sizing systems generated from anthropometric data with the ASTM standard D5585-94. *International Journal of Clothing Science and Technology*, **10**(5), 324-341.

Ashdown, S. P. (2003). Sizing up the apparel industry. *Cornell's Newsletter for the New York State Apparel and Sewn Products Industry*.

Barron, E. R., Scribano, F., & Burns, M. (1970). *Design , development and fabrication of a personnel armor load profile analyzer*. U.S. Army Natick Laboratories, Report No. 70-65CE.

Bennett, K. A., & Osborne, R. H. (1986). Interobserver measurement reliability in anthropometry. *Human Biology*, **39**, 124-130.

Black, S. (2002). *Knitwear in Fashion*. New York: Thames & Hudson.

Bouman, F. G. (1970). Volumetric measurement of the human breast and breast tissue before and during mammaplasty. *British Journal of Plastic Surgery*, **23**, 263.

Boyes, K. (1996). Buying the perfect bra. *Good Housekeeping*, **8**, 50.

Bray, G. A., Greenway, F. L., & Molitch, M. E. (1978). Use of anthropometric measures to assess weight loss. *American Journal of Clinical Nutrition*, **31**, 769-773.

Bremner, N. (2005). Seamless bodysize technology round-up. *Knitting International*, **112**, 26-29.

Bressler, K., Newman, K., & Proctor, G. (1998). *A Century of Style: Lingerie*. London: Quarto Publishing Plc.

Brinson, E. G. (1977). *Pattern alterations predicted and quantified using angle measurements*. Unpublished master's thesis, Auburn University, Auburn, AL.

Browder, Jr., inventor. (2000). *Brassiere, brassiere blank and methods of making same*. U.S. Patent Publication Number 6125664.

Bulstrode, N., Bellamy, E., & Shrotria, S. (2001). Breast volume assessment: comparing five different techniques. *The Breast*, **10**, 117-123.

Cajah Corporation. (2005). *Why would a customer chose to purchase a seamless garment?* Available online at: http://www.cajahcorp.com/nat_advantage.htm

Campaigne, B. N., Katch, V. L., Freedson, P. et al. (1979). Measurement of breast volume in females: Description of a reliable method. *Annals of Human Biology*, **6**, 363-367.

Chan, C., Yu, W., & Newton, E. (2001). Evaluation and analysis of bra design. *The Design Journal*, **4**(3), 33-40.

Choi, W., & Powell, N. B. (2005). Three dimensional seamless garment knitting on V-bed flat knitting machines. *Journal of Textile and Apparel, Technology and Management*, **4**(3), 1-33.

Costantakos, A. V. & Watkins, S. M. (1982). Pressure analysis as a design research technique for increasing the comfort of nursing brassieres. *Home Economics Research Journal*, **10**(3), 271-278.

Cox, D. B., Owens, R. A., & Hartmann, P. E. (1998). *Studies on human lactation: The development of the computerized breast measurement system*. Available online at: http://www.asklenore.info/breastfeeding/additional_reading/breast_measurement.html

Designing the perfect bra? (2002). *Autospeed*. Available online at: http://autospeed.drive.com.au/cms/A_1260/article.html

Devarajan, P., & Istook, C. S. (2004). Validation of 'female figure identification technique (FFIT) for apparel©' Software. *Journal of Textile and Apparel, Technology and Management*, **4**(1), 1-23.

Douty, H. (1968). Visual somatometry in health related research. *Journal of the Alabama Academy of Science*, **39**(1), 21-34.

Edsander-Nord, A., Wickman, M., & Jurell, G. (1996). Measurement of breast volume with thermoplastic casts. *Scandinavian Journal of Plastic and Reconstructive Surgery and Hand Surgery*, **30**(2), 129-132.

Elam, C. (1997). The bra dilemma – Solved. *Threads*, **71**, 36-40.

Ellenbogen, R. (1978). A new device to assist in sizing breasts. *Annals of Plastic Surgery*, **1**(3), 333.

Fan, J., Liu, F., Wu, J., & Dai, W. (2004a). Visual perception of female physical attractiveness. *Proceedings of the Royal Society of London-B-Biological Sciences*, **271,** 347-352.

Fan, J., Liu, F., Wu, J., & Dai, W. (2004b). An equation for attraction. *Nature*, URL: http://www.nature.com/nsu/040112/040112-5.html

Farrell-Beck, J. A., & Pouliot, C. J. (1983). Pants alteration by graphic somatometry techniques, *Home Economics Research Journal*, **12**(1), 95-105.

Fildan, G., & Wanzenbock, K. (2001). Fildan Accessories Corporation, assignee. *Spoon underwire*. U.S. Patent application number 6346028-B1.

Fontanel, B. (1997). *Support and Seduction: the History of Corsets and Bras* (W. Wood, Trans.). New York, N.Y.: Abrams. (Original work published 1992)

Foster, T. A., Webber, L. S., & Sathanur, R. (1980). Measurement error of risk factor variables in an oeidemiologic study of children: The bugalusa heart study. *Journal of Chronic Disease*, **33**, 661-672.

Fowler, P. A., Casey, C. E., Cameron, G. G., Foster, M. A., & Knight, C. H. (1990). Cyclic changes in composition and volume of the breast during the menstrual cycle, measured by magnetic resonance imaging. *British Journal of Obstetrics and Gynaecology*, **97**, 595-602.

FZ/T 73012-2004. (2004). *Brassiere*. Chinese Textile Industrial Standard.

Gain, G. (1950). *The American Way of Designing*. New York: Fairchild Publications.

Gazzuolo, E., Delong, M., Lohr, S., Labat, K. & Bye, E. (1992). Predicting garment pattern dimensions from photographic and anthropometric data. *Applied Ergonomics*, **23**(3), 161-171.

Gehlsen, G., & Stoner, LJ. (1987). The female's breast in sport and exercise. In: MJ. Adrian (Eds.), *Sports Women* (pp. 13-22). Basel: Karger.

GERBER Technology. (2005). *AccuMark V-Stitcher*. Available online at: http://www.gerbertechnology.com/default.asp?contentID=56

Gittelson, B., inventor, Triumph-Universa G.m.b.H., assignee. (1960). *Bust measuring device*. U.S. Patent 2,946,125.

Global seamless market round-up. (2004a). *Knitting-International*, **7**, p. 18-19.

Gordon, C. C., Bradtmiller, B., Churchill, T., Clauser, C. E., McConville, J. T., Tebbetts, I. O., et al. (1989). *Anthropometric survey of U.S. army personnel: Methods and summary statistics*. Technical Report NATICK/TR-89/044, Natick, MA: U.S. Army Natick Research, Development and Engineering Centre.

Gordon, C. C., & Bradtmiller, B. (1992). Interobserver error in a large scale anthropometric survey. *American Journal of Human Biology*, **4**, 253-263.

Gordon, C. C., & Friedl, K. E. (1994). Anthropometry in the US Armed force. In S. J. Ulijaszek & C. G. N. Mascie-Taylor (Eds.), *Anthropometry: The Individual and the Population* (pp. 178-210). Cambridge: Cambridge University press.

Gray, D. S., & Fujioka, K. (1991). Use of relative weight and body mass index for the determination of adiposity. *Journal of Clinical Epidemiology*, **44**, 545-550.

Greenbaum, A. R., Heslop, T., Morris, J., & Dunn, K. W. (2003). An investigation of suitability of bra fit in women referred for reduction mammaplasty. *British Journal of Plastic Surgery*, **56**(3), 230-236.

Grossman, A. J., & Roudner, L. A. (1980). A simple means for accurate breast volume determination. *Plastic & Reconstructive Surgery*, **66**, 851.

Haggar, A. (2004). *Pattern Cutting for Lingerie, Beachwear and Leisurewear*. Oxford : Blackwell Pub. ; Ames, Iowa : Iowa State Press. (Original book published 1990).

Hardaker, C. H. M., & Fozzard, G. J. W. (1997). The bra design process: A study of professional practice. *International Journal of Clothing Science and Technology*, **9**(4), 311-325.

Hatakeyama, K., & Aoki, M. (1990). The clothing pressure of the brassiere. *Journal of Clothing Structure of Tokyo Women University*, **35**(1), 79-84.

Himes, J. H. (1989). Reliability of anthropometric methods and replicate measurements. *American Journal of Physical Anthropology*, **40**, 197-203.

Hong Kong Productivity Council. (2006). *Product development – stereolithography (SLA)*. Available online at http://www.hkpc.org/html/eng/webcast/latest_tech_demo/landing.jsp

Hsu, C. H., & Wang, M-J. J. (2004). Using decision tree-based data mining to establish a sizing system for the manufacture of garments. *International Journal of Advanced Manufacturing Technology*, **26**(5/6), 669-674.

Instruction manual of SM8-Top2, revision 3.1. (2001). Santoni group.

Intimate apparel and shapewear. (1997). *Apparel Industry Magazine*, **3**, p. 66-67.

ISO 4416. (1981). *Size designation of clothes – women's and girl's underwear, nightwear, foundation garments and shirts*. The International Organization for Standardization.

ISO 8559. (1989). *Garment construction and anthropometric surveys - body dimensions*. The International Organization for Standardization.

ISO 7250. (1996). *Basic human body measurements for technological design*. The International Organization for Standardization.

ISO15535. (2003). *General requirements for establishing anthropometric databases*. The International Organization for Standardization.

ISO/DIS 20685. (2004). *3D scanning methodologies for internationally compatible anthropometric databases*. The International Organization for Standardization.

Istook, C. L., & Hwang, S. J. (2000). 3D body scanning systems with application to the apparel industry. *Journal of Fashion Marketing and Management*, **5**(2), 120-132.

Ito, N., Ogihara, C., & Horino, T. (1986). Estimation of clothing pressure on the uniaxial tensile deformation of clothing materials. *Japan Research Association Textile End-Uses*, **27**(6), 257-262.

Jamison, P. L., & Zegura, S. L. (1974). A univariate and multivariate examination of measurement error in anthropometry. *American Journal of Physical Anthropology*, **40**, 197-203.

Japanese body size data 1992-1994. (1997). Research Institute of Human Engineering for Quality Life, Osaka.

Jiao, X. N., Leung, P. P. K., Tao, X. M., Qian, X. M., & Yu, W. (2001). Fabric tensile performance under large deformation. *Proceeding of the 6th Asian Textile Conference*, 22-24 August.

Johnston, F. E., & Martorell, R. (1988). Population surveys. In T.G. Lohman, A.F. Roche, & R. Martorell (Eds.): *Anthropometric Standardization Reference Manual* (pp. 107-110). Champaign, Ill.: Human Kinetics Books.

Johnson, D. E. (1998). *Applied Multivariate Methods for Data Analysts*. Pacific Grove, Calif.: Duxbury Press.

Johnson, R. A., & Wichern, D. W. (2002). *Applied Multivariate Statistical Analysis*. Upper Saddle River, N.J.: Prentice Hall. (Original work published 1982)

Jones, F. W. (1929). *Measurements and Landmarks in Physical Anthropology*. Honolulu, Hawaii: Bernice P Bishop Museum.

Jones, P. R. M., & Rioux, M. (1997). Three-dimensional surface anthropometry: Application to the human body. *Optics and Lasers in Engineering*, **28**, 89-117.

Kanhai, R. C. J., & Hage, J. J. (1999). Bra cup size depends on band size. *Plastic & Reconstructive Surgery*, **104**(1), 300.

Katariya, R., Forrest, A., & Gravelle, I. (1974). Breast volume in cancer of the breast. *British Journal of Cancer*, **29**, 270-273.

Kim, J. W., Lee, S. Y., & Hong, K. H. (2000). Development of sensible brassiere for middle aged women. *Journal of Korean Society of Clothing and Textiles*, **24**(5), 714-723.

Kirianoff, T. G. (1975). *Method and apparatus for measuring the volume of asymmetrical breasts*. U.S. Patent Office Application, 627,126.

Kopell, M. (2005). What next for seamless bodysize clothing? *Knitting International*, **112**, 23-25.

Kouchi, M., Mochimaru, M., Tsuzuki, K., & Yokoi, T. (1996). Random error in anthropometry, *Journal of Human Ergonomic*, **25**, 155-166.

Laing, R. M., Holland, E. J., Wilson, C. A., & Niven, B. E. (1999). Development of sizing systems for protective clothing for the adult male. *Ergonomics*, **42**(10), 1249-1257.

Laing, R. M., & Sleivert, G. G. (2000). Clothing, textiles and human performance. *The Textile Institute*, 3**2**(2), 1-14.

Lam, C. (2005). Seamless technology: Trend and market. *Journal for Asia on Textile and Apparel*, **16**(4) 32-34.

Lamarque, JL. (1981). *An Atlas and Text of the Breast: Clinical Radiodiagnosis*. London: Wolfe Medical.

Lawrence, RA. (1980). *Breast-Feeding: A Guide for the Medical Profession*. St Louis (MO): The C. V. Mosby Company.

Lee, H. Y., & Hong, K. (2007). Optimal brassiere wire based on the 3D anthropometric measurements of under breast curve. *Applied Ergonomics*, **38**(3), 377-384.

Lee, H. Y., Hong, K., & Kim, E. A. (2004). Measurement protocol of women's nude breasts using a 3D scanning technique. *Applied Ergonomics*, **35**, 353-359.

Lee, H.Y., Hong, K.H., Kim, J.W., & Lee, S.Y. (2001). Development of design parameters of brassiere: Part 1. Three dimensional shape of the breast and under-wire of the brassiere. *Proceedings of Joint World Conference; Korea Society of Clothing and Textiles/International Textile and Apparel Association*, pp. 90.

Lee, L., Stickland, V., Wilson, R., & Evans, A. (2003). *Fundamentals of Mammography*. Edinburgh: Churchill Livingstone. (Original work published 1995)

Li, Y., Zhang, X., & Yueng, K. W. (2003). A 3D bio-mechanical model for numerical simulation of dynamic mechanical interactions of bra and breast during wear. *Sen-I Gakkaishi*, **59**, 12–21.

Liang, J. (2001). The dyeing processes of seamless knitted garments with Lycra. *Knitting industry*, **3**, 66-69.

Lim, N. Y.,Yu, W., Fan, J. & Yip, J. (2006). Innovation of girdles, Chapter 5. In W. Yu, J. Fan, S. C. Harlock & S. P. Ng (Eds.), *Innovation and Technology of Women's Intimate Apparel* (pp. 114-131). Boca Raton, Fla: CRC press; Cambridge: Woodhead Publishing.

Lipton, B. (1996). Are you wearing the wrong size bra? *Ladies Home Journal*, **3**, 46.

Loker, S., Ashdown, S. P., Cowie, L., & Schoenfelder, K. A. (2004). Consumer interest in commercial applications of body scan data. *Journal of Textile and Apparel Technology and Management*, **4**(1), 55-67.

Loker, S., Ashdown, S., & Schoenfelder, K. (2005). Size-specific analysis of body scan data to improve apparel fit. *Journal of Textile and Apparel, Technology and Management*, **4**(3), 1-15.

Lonati, F., Lonati, E., Lonati, F., & Lonati, T., inventor. (2000). *Method for* *manufacturing knitted items with a passage for the insertion of support elements, and item obtained with the method*. U.S. Patent Publication Number 6082145.

Loughry, C. W., Sheffer, D. B., Price, T. E. Jr., et al. (1987). Breast volume measurement of 248 women using biostereometric analysis. *Plastic & Reconstructive Surgery*, **80**, 553-558.

Loughry, C. W., Sheffer, D. B., Price, T. E. Jr., et al. (1989). Breast volume measurement of 598 women using biostereometric analysis. *Annals of Plastic Surgery*, **22**, 380.

Makabe, H. (1977). An application of principal component analysis to the posture and the figure of adult women. *Journal of Domestic Science, Japan*, **28**(3) 223-229.

Makabe, H., Momota, H., Missuno, T. & Ueda, K. (1991). A study of clothing pressure developed by brassiere. *Journal of the Japan Research Association for Textile End-Uses*, **32**(9), 416-423.

Malini, S., Smith, E. O., & Goldzieher, J. W. (1985). Measurement of breast volume by ultrasound during normal menstrual cycles and with oral contraceptive use. *Obstetrics & Gynecology*, **66**(4), 538-541.

Marks, G. C., Habicht, J. P., & Mueller, W. H. (1989). Reliability, dependability, and precision of anthropometric measurements. *American Journal of Epidemiology*, **130**(3), 578-587.

Marples, G., (2004). *The history of the bra–An uplifting story*. Available online at: http://www.online-shopping-webmall.com/lingerie.htm

Martin, R. (1957). *Lehrbuch der Anthropologie*. Third edition, Fischer: Jena.

Martorell, R., Habicht, J. P., & Yarbrough, C. (1975). The identification and evaluation of measurment variability in the antropometry of preschool children. *American Journal of Physical Antrhopology*, **43**, 347-352.

McConville, J. T. (1979). *Anthropometric source book volume I: Anthropometry for designers*. NASA Reference Publication No. 1024, Scientific and Technical

Information Office.

McCulloch, C. E., Paal, B., & Ashdown, S. P. (1998). An optimization approach to apparel sizing. *Journal of the Operational Research Society,* **49**, 492-499.

McIntyre J. E., & Daniels, P. L. (1997). Textile terms and definitions. *The Textile Institute,* **10**.

McKinnon, L., & Istook, C. (2001). Comparative analysis of the image twin system and the 3T6 body scanner. *Journal of Textile and Apparel Technology and Management*, **1**(2), 1-7.

Mellian, S. A., Erwin, C. A., & Robinette, K. M. (1990). Sizing evaluation of Navy women's uniforms. *Technical Report NCTRF 182*. Navy Clothing and Textiles Research Facility: Natick, MA.

Merriam-Webster Online Dictionary. (2005). Available online at: http://www.m-w.com/

Milligan, G. W. (1980). An examination of effect of six types of error perturbation of fifteen clustering algorithms. *Psychometrika*, **45**, 325-342.

Minitab Inc. (2003). Design of experiments, help-to-go.

Minott, J. (1978). *Fitting Commercial Patterns: The Minott Method*. Minnesota: Burgess Publishing Company.

Mitchell, J., & Waitz, S. A., inventor. (2004). *Circular knit bra having different areas of strengthability and method of making the same*. U. S. Patent Publication Number 6,790,122 B2.

Mitchell, J. C., inventor. (2005). *Seamless circular knit garment with differential tightness areas and method of making same*. U.S. Patent Publication Number 6899591 B2.

Mitchell, J. C., Ratcliffe, A. & Williamson, C., inventor. (2005). *Circular knitted garments having seamless shaped bands*. U.S. Patent Publication Number 6886367 B2.

Miyoshi, M. (1970). A study on the clothing construction, part Ⅰ: The anthropometry of women's cross-section and cross-shape. *Journal of Bukan Women's University*, 1970, **2,** 22-43.

Miyoshi, M., & Nakahon, Y. (1983). Classification of women's side silhouettes, partⅡ. *Journal of Bukan Women's University*, **14**.

Miyoshi, M. (2001). *Clothing Construction*. Tokyo: Bunka Publishing Bureau.

Monget, K. (1999). Seamless: The next generation. *WWD*, October 18.

Montgomery, D. C. (2001). *Introduction to Statistical Quality Control* (4th Edition). New York: John Wiley & Sons.

Montgomery, D. C. (2005). *Design and Analysis of Experiments* (6th Edition). Hoboken, N.J.: Wiley.

Morooka, H., Fukuda, R., Nakahashi, M., Morooka, H., & Sasaki, H. (2005). Clothing pressure and wear feeling at under-bust part on a push-up type brassiere. *Sen-I Gakkaishi*, **61**(2), 55-60.

Morris, D. (2003). *World Markets for Knitted Textiles and Apparel: Forecasts to 2010*. Wilmslow: Textile Intelligence Electronic Publishing.

Morris, D., Mee, J., & Salt, H. (2002). The calibration of female breast size by modeling. *International Foundation of Fashion Technology Institutes Conference*, Hong Kong.

Mueller, W. H., & Martorell, R. (1988). Reliability and accuracy of measurement. In T.G. Lohman, A. F. Roche & R. Martorell (Eds.): *Anthropometric Standardization Reference Manual* (pp. 83-86). Champaign, Ill.: Human Kinetics Books.

Nakai, K., & Makabe, H. (1976). A Study of body measurements by principal component analysis. *Journal of Ergonomics, Japan*, **12**(2), 41-47.

New Product Development Report (1998). What's driving category growth for bras? New York: Port Washington. 8th September.

Ng, S. F., & Hui, C. L. (2001). Pressure model of elastic fabric for producing pressure garment. *Textile Research Journal*, **71**(3), 275-279.

Norušis, M. J. (2004). *SPSS 12.0 Guide to Data Analysis*. Upper Saddle River, N.J. : Prentice Hall.

O'Brien, R., & Shelton, W. C. (1941). *Women's measurements for garment and pattern construction*. Miscellaneous Publication No. 454, Washington D C: Government Printing Office.

Osborne, H. G., & Boomer, N. C., inventor, Alba-Waldensian, Inc., Valdese, N. C., assignee. (1999). *Seamless circular knit brassiere and method of making same*. U.S. Patent Publication Number 5946944.

Oxford dictionary & thesaurus. (2001). Oxford : Oxford University Press.

Paal, B. (1997). *Creating efficient apparel sizing systems: an optimization approach*. Unpublished master's thesis, Cornell University, US.

Page, KA., & Steele, J. R. (1999). Breast motion and sports brassiere design: Implications for future research. *Sports Medicine*, **27**(4), 205-211.

Paquette, S. (1996). 3D scanning in apparel design and human engineering. *IEEE Computer Graphics and Application*, **16**(5), 11-15.

Pechoux, B. L., & Ghosh, T. K. (2002). *Apparel sizing and fit: A critical appreciation of current developments in clothing size*. Manchester, England: Textile Institute.

Pechter, E. A. (1998). A new method for determining bra size and predicting postaugmentation breast size. *Plastic & Reconstructive Surgery*, **102**(4), 1259-1265.

Pederson, S. (2004). *Bra: A Thousand Years of Style, Support and Seduction*. UK: David & Charles.

Penn, J. (1955). Breast reduction. *British Journal of Plastic Surgery*, **7**, 357-371.

Powell, D., & Seymour, R., inventor, Charnos PLC, assignee. (2002). *Brassiere including breast-supporting inserts*. U.S. Patent Publication Number 6447365 B1.

Powell, N. B. (2003). Design: Italian style. *Journal of Textile and Apparel, Technology and Management*, **3**(1), 1-9.

Read, C. (1993). *A Woman's Breast*. Melbourne (VIC): Ashwood Medical House.

Revicki, D. A., & Israel, R. G. (1986). Relationship between body mass indices and measures of body adiposity. *American Journal of Public Health*, **76**, 992-994.

Revolution in seamless underwear and outerwear manufacture. (2000). *African Textiles*, **2/3**, p. 22-23.

Richards, M. S., inventor. (1985). *Methods of knitting brassiere blank, manufacturing brassiere, and products*. U.S. Patent Publication Number 4531525.

Richards, A. (2001). *Bra's and breast size*. Available online at: http://transwoman.tripod.com/breastsize.htm

Robinette, K. M., & Daanen, H. A. M. (2003). Lessons learned from CAESAR: a 3-D anthropometric survey. *International Ergonomics Association 2003 Conference Proceedings.*

Roebuck, Jr. J. A. (1995). *Anthropometric methods: designing to fit the human body*. Santa Monica, CA: Human Factors & Ergonomics Society.

Roedel, H., Deussen, A., & Haase, E. (2002). Fundamental investigations for the construction of compressive clothing and their effect on the blood circulation of human extremities. Project founded by German research council.

Salusso, D. C. J., DeLong, M. R., Martin, F. B., & Krohn, K. R. (1985-86). A multivariate method of classifying body form variation for sizing women's apparel. *Clothing and Textiles Research Journal*, **4**(1), 38-45.

Santoni group marketing department. (2005). *The Santoni seamless innovation stage*, Santoni Private Show, Hong Kong.

Schwabe, C. (1989). Thoughts on the history of the circular knitting machine. *Knitting Technology*, **11**(3), 186-189.

Seamless finishing routes. (2005). *Knitting International*, **7**. Available online at: http://www.inteletex.com/FeatureDetail.asp?PubId=4&NewsId=4047

Seamless revolution: An Italian knitting machine builder offers a technique for the future. (2000). *Textile Asia*, **8**, p. 76-77.

Sharma, S. (1996). *Applied Multivariate Techniques*. New York; Chichester: John Wiley & Sons, Inc..

Shiraiwa, N., inventor, WACOAL CORP., assignee. (1994). *Breasts measuring device*. Japan Patent U06-069227.

Shiraiwa, N., & Kusakabe, T., inventor, WACOAL CORP., assignee. (1996). *Instrument for measuring breast shape*. US Patent U.S. 005485855.

Simmons, K. P. (2001). *Body measurement techniques: A comparison of three-dimensional body scanning and physical anthropometric methods*. Unpublished PhD Thesis, College of Textiles, North Carolina State University, North Carolina, USA.

Simmons, K. P., & Istook, C. L. (2003). Body measurement techniques: Comparing 3D body-scanning and anthropometric methods for apparel applications. *Journal of Fashion Marketing and Management*, **7**(3), 306-332.

Smith, D. J. Jr., Palin, W. E. Jr., Katch, V. L., & Bennett, J. E. (1986). Breast volume and anthropomorphic measurements: Normal values. *Plastic & Reconstructive Surgery*, **78**(3), 331-335.

Spencer, D. (2001). *Knitting Technology, a Comprehensive Handbook and Practical Guide* (3rd edition). Woodhead Publishing Limited, Cambridge, England. (Original work published 1983)

Starr, C., Branson, D., Shehab, R., Farr, C., Ownbey, S., & Swinney, J. (2005). Biomechanical analysis of a prototype sports bra. *Journal of Textile and Apparel, Technical and Management*, **4**(3), 1-14.

Technology spurs seamless growth. (2004b). *Knitting International*, **9**. Available online at: http://www.inteletex.com/FeatureDetail.asp?NewsId=3324

Thakur, A., & Horta, J., inventor, S&S Industries, Inc., assignee. (2002). *Underwire for brassiere*. U.S. Patent Publication Number 6468130 B1.

The human science research center of Wacoal. (2000). *Spiral Ageing*, Wacoal Crop.

Thomas, D. (1995). The quest for the perfect bra. *SELF*, **3**, 146-155.

Tryfos, P. (1986). An integer programming approach to the apparel sizing problem. *Journal of the Operational Research Society*, **37** (10), 1001–1006.

Utermohle, C. J., & Zegura, S. L. (1982). Intra- and interobserver error in craniometry: A cautionary tale. *American Journal of Physical Anthropology*, **57**, 303-310.

Utermohle, C. J., Zegura, S. L., & Heathcote, G. M. (1983). Multiple observers, humidity, and choice of precision of statistics: Factors influencing craniometric data quality. *American Journal of Physical Anthropology*, **61**, 85-95.

Van Graf, F. (1949). *Sanitary breast measuring device*. U.S. Patent Office Application, 86,876.

Van Graf, F. (1953). *Sanitary breast measuring device*. U.S. Patent Office Application, 373,212.

Wacoal Corp., assignee. (1993). *Curve underwire*. Japan Patent U05-022506.

Wacoal Corp., (1995). *Golden canon*, Unpublished internal document, Japan.

Wacoal Crop., assignee. (2001). *Curve underwire and its using material*. Japan Patent U2001-131807.

Wacoal Crop., assignee. (2003). *Curve padding material to be used for lady's wear*. Japan Patent U2003-328210.

Wacoal Corp,. (2005). *The human science research center*. Available online at: http://www.wacoal.co.jp/company/aboutcom/ningen/index.html

Werner, L. M., inventor. (2000). *Brassiere with helical underwire*. U.S. Patent Publication Number 6106363.

Westreich, M. M. D. (1997). Anthropomorphic breast measurement: Protocol and results in 50 women with aesthetically perfect breasts and clinical application', *Plastic & Reconstructive Surgery*, **100**(2), 468-479.

Williamson, R. (2000). Seamless sails in southwest. *WWD*, October 16.

Winks, J. M. (1997) *Clothing Sizes International Standardization*. Manchester UK: The Textile Institute International Headquarters.

Wohleber, C. (2003). *The bra: It uses structural mechanics and materials science to counteract the law of gravity*. Available online at: http://www.inventionandtechnology.com/xml/2003/4/it_2003_4_dept_objlessons.xml

Wright, M. C. M. (2002). Graphical analysis of bra size calculation procedures. *International Journal of Clothing Science and Technology*, **14**(1), 41-45.

Yeung, A. P., Ca, S. D., & Levinson, M. S., Inventor. (2002). *Dual-layered seamless sports bra and camisole*. U.S. Patent Publication Number 20020022433A1.

Yoshimura, H., & Ishikawa, K. (1983). Some measurements of garment compression on the body. *Sen-I Gakkaishi*, **39**(12), 525-531.

Young, V. L. (1995). The efficacy of breast augmentation: Breast size increase, patient satisfaction, and psychological effects (Letter) (Reply). *Plastic & Reconstructive Surgery*, **96**, 1237.

Yu, W. M. (2004). 3-D body scanning. In J. Fan, W. M. Yu, & L. Hunter: *Clothing Appearance and Fit: Science and Technology* (pp. 135-168). Cambridge England: Woodhead Publishing Limited.

Yu, W. (2006). *Teaching Notes: Bra Fitting Checklist*. Ace Style Institute of Intimate Apparel (ASIIA), Institute of Textiles & Clothing, the Hong Kong Polytechnic University.

Zheng, R. (2002). *A study on the method of drafting a basic pattern of upper torso for chinese young women's clothing design*. Unpublished MPhil thesis, Beijing Institute of Clothing Technology.

Zheng, R., Zhang, H., Huang, H., Hu, X., Duan, X., & Li, J. (2004). *Shape anthropometric system.* Aimer Human Engineering Research Center of Beijing Institute of Clothing Technology.

Zheng, R., Yu, W., & Fan, J. (2006). Breast Measurement and Sizing, Chapter 2. In W. Yu, J. Fan, S. C. Harlock & S. P. Ng (Eds.), *Innovation and Technology of Women's Intimate Apparel* (pp. 28-58). Boca Raton, Fla: CRC press; Cambridge: Woodhead Publishing.

Zhou, J., Feng, S., Xiao, H., Xia, T., Xu, Y., Yan, X. et al. (1992). *The Application and Interpretation of Clothing Sizing Systems*. Beijing: Standard Publications.

http://www.voxelan.co.jp/index-en.html

http://www.santoni.com/english/home.htm